

---

# **POTENTIAL AND SIGNIFICANCE OF LEAF TRAIT CHANGES OF LONG LIVED SPECIES DURING THE PALEOGENE**

**DISSERTATION**  
Zur Erlangung des akademischen Grades  
**Doctor rerum naturalium**  
(Dr. rer. nat.)

Vorgelegt  
Der Fakultät Mathematik und Naturwissenschaften  
der Technischen Universität Dresden  
von Frau

**Diplom-Geographin Karolin Moraweck**

Geboren am 11.11.1986 in Zittau

Die Dissertation wurde in der Zeit von 07 / 2013 bis  
02/2017 am Institut für Botanik angefertigt.

Erster Gutachter: Prof. Dr. Christoph Neinhuis (Lehrstuhl für Botanik, Fakultät  
Mathematik und Naturwissenschaften, Technische Universität  
Dresden)

Zweiter Gutachter: Associate Prof. Tao Su (Xishuangbanna Tropical Botanical Garden,  
Chinese Academy of Sciences, Menglun, Mengla, 666303 Yunnan,  
China)

Tag der Verteidigung: 15.08.2017

---

# Table of Contents

<b>Acknowledgments .....</b>	<b>vi</b>
<b>1. General Introduction .....</b>	<b>4</b>
1.1. Eocene to Miocene paleogeography and climate evolution.....	7
1.2. Floristics and vegetation dynamics.....	14
1.3. Current knowledge on correlation of leaf traits with climate and ecology .....	18
1.4. Scientific questions.....	20
1.5. Hypothesis to test.....	22
<b>2. Site characteristics and plant assemblages .....</b>	<b>24</b>
2.1. Paleobiogeographical settings.....	24
2.2. Depositional settings and paleoenvironment .....	26
2.2.1. Marine depositional settings.....	26
2.2.2. Coastal plain and floodplain depositional facies types .....	28
2.2.3. Volcanic depositional facies types.....	30
2.3. Site characteristics.....	32
<b>3. Selection of taxa and brief characteristics .....</b>	<b>48</b>
3.1. Fossil plant material.....	48
3.1.1. <i>Rhodomyrtophyllum reticulosum</i> (Myrtaceae).....	48
3.1.2. <i>Platanus neptuni</i> (Platanaceae) .....	51

---

3.2. Extant plant material .....	55
3.2.1. <i>Platanus kerrii</i> (Platanaceae) .....	55
3.2.3. <i>Syzygium samarangense</i> (Myrtaceae) .....	57
<b>4. Methods .....</b>	<b>59</b>
4.1. Paleoclimate reconstruction .....	59
4.1.1. Coexistence Approach .....	59
4.1.2. Climate Leaf Analyses Multivariate Program .....	61
4.2. Morphological and morphometric parameters .....	63
4.3. Cuticular derived parameters .....	66
4.4. Paleoatmospheric reconstruction .....	69
4.4.1. Determination of input parameters .....	72
4.4.1.1. Determination of $d_{asPP}$ , $d_{st}$ and $p_{wst}$ .....	73
4.4.1.2. Carbon isotope measurements .....	74
4.4.1.3. Determination of climate input parameters .....	75
4.4.2. Systematic parameter variation .....	76
<b>5. Results .....</b>	<b>78</b>
5.1. Paleoclimate reconstruction .....	78
5.1.1. Coexistence Approach .....	78
5.1.2. Climate Leaf Analyses Multivariate Program .....	80
5.2. Morphometric parameters .....	84

---

5.2.2. <i>Rhodomyrtophyllum reticulosum</i> .....	84
5.2.1. <i>Platanus neptuni</i> .....	86
5.3. Cuticular derived parameters.....	91
5.3.2. <i>Rhodomyrtophyllum reticulosum</i> .....	91
5.3.1. <i>Platanus neptuni</i> .....	95
5.4. Paleoatmospheric reconstruction.....	100
5.4.1. <i>Rhodomyrtophyllum reticulosum</i> .....	100
5.4.2. <i>Platanus neptuni</i> .....	103
5.5. Synthesis.....	106
<b>6. Interpretation .....</b>	<b>110</b>
6.1. Paleoclimate reconstruction .....	110
6.1.1. Uncertainties and outliers .....	110
6.1.2. Paleoclimate signals.....	114
6.2. Morphological and morphometric parameters .....	118
6.2.1. Uncertainties and outliers .....	118
6.2.2. Morphological and morphometric interpretation .....	120
6.2. Cuticular parameters .....	127
6.2.1. Uncertainties and outliers .....	127
6.2.2. Interpretation of cuticular-based parameters.....	128
6.3. Paleoatmospheric reconstruction.....	131

---

6.3.1. Uncertainties and outliers .....	131
6.3.2. Interpretation of paleoatmospheric parameters.....	131
<b>7. Conclusion .....</b>	<b>134</b>
<b>8. Perspectives.....</b>	<b>136</b>
<b>List of Figures.....</b>	<b>137</b>
<b>List of Tables .....</b>	<b>140</b>
<b>Supplementary Data.....</b>	<b>142</b>
<b>Bibliography.....</b>	<b>143</b>
<b>Publications and presentations.....</b>	<b>162</b>
<b>Eigenständigkeitserklärung.....</b>	<b>165</b>

## Acknowledgments

This thesis has been written with the help of numerous people, who I would like to acknowledge here.

First of all, I thank Dr. Lutz Kunzmann, who shares the same fascination for paleobiodiversity and the potential of fossil plant assemblages to determine ancient both climate and environmental conditions. He provided new insights and changes in mind during various fruitful discussions and motivated and supported me during the whole working and writing process. I am especially thankful to Prof Dr. Christoph Neinhuis, who gave me the opportunity to be a doctorate at the Institute of Botany of the Technical University Dresden. The study of Geography and the doctorate in the field of Botany wonderfully connects the main subject of my main working interest, geobiodiversity in ancient times.

I am grateful to my colleagues at the Senckenberg Natural History Collections in Dresden: Carola Kunzmann for macro preparation and preparation of cuticle slides. I especially thank her for her patience in preparing partly difficult material and her endurance during numerous changes in the working procedure. I thank Denise Hennig, Susann Stiller and Madeleine Streubig for digitizing and polygonization of hundreds of fossil leaves. They also had to face changes in methodical progresses and I appreciate their participation and motivation. I thank all colleagues and Franziska Ferdani for further methodical help. Thanks go to the graduate students Babette Jurke, Jana Böttger and Christian Müller for taxonomic investigation and data collection of considered sites and relevant topics for this thesis, in their respective Bachelor- or Master theses. I would like to thank Dorothea Bräutigam for critical reading of parts of the thesis. These people and even more have a great part on the success of this thesis. I would like to thank the whole section Paleobotany, whose members did not only support me during my working processes, but gave me always self-confidence and a sympathetic ear, whenever necessary.

Additionally, I thank all collaborators of the VW project; Prof. Dr. Johanna Kovar-Eder, PD Dr. Anita Roth-Nebelsick, Dr. Michaela Grein and RNDr. Dr. Jiří Kvaček for their input and helpful comments during the preparation of the *Platanus* manuscript. I am grateful to Dr. Dr. Wilfried Konrad for his help with the gas exchange model and the model application, as

well as Anita and Michaela did during various visits in Dresden and Stuttgart. Thanks go to Christopher Traiser, collaborating in the project as well as the head of the MORPHYLL database for his good will in managing data coming from the Dresden collections and their implementation into the database.

Special thanks go to all colleagues of the Palaeoecology Research Group at the Xishuangbanna Tropical Botanical Garden, especially Prof. Dr. Zhou Zhe-Kun, Prof. Dr. Su Tao and Huang Jian, for their hospitality, help with the equipment and support during measurements and sampling. I thank the whole working group for a pleasant stay and a fruitful working atmosphere.

I am thankful to the VW foundation for further employment after the regular end of the contract and to the Graduate Academy of the Technical University of Dresden for a 4 month lasting grant during the final phase of my writing phase. Many thanks go to the International Organization of Paleobotany for financial support and the employees of the Senckenberg administration in Frankfurt/Main for their intensive examination with contractual matters.

I am grateful to many colleagues I met at various meetings and conferences, who gave me support and positive feedback, whenever possible. I am thankful to be a member of this small community of Paleobotanists.

Finally, I would like to thank my family and friends, who supported me mentally and with confidence and encouragement. I shared with them many hours and evenings of pleasure with discussions, in activities like climbing, hiking, travelling, running, swimming, cycling or skiing. Especially these times in nature, during long walks through forests, sitting on mountains after a strenuous climbing tour, or a cycling tour providing wonderful views helped me to calm down, relax and broad my view during work. I am thankful to my husband and my daughter, who gave me always the time I needed for work but also demanded time, which forced me to relax and to keep in mind what is substantial in life as well.

# 1. General Introduction

Fossil plants are regarded to be excellent proxies to trace paleoclimatic and paleoatmospheric changes. The vegetational response to changing paleoclimate and paleoatmospheric conditions has already been known for a long time and is well documented for the Paleogene of central Europe (Mai, 1981, 1995; Kvaček, 2010; Kunzmann et al., 2016). Methods such as the Coexistence Approach (CA) first introduced by Mosbrugger and Utescher (1997) and the Climate Leaf Analyses Multivariate Program (CLAMP) (Wolfe, 1993; Wolfe and Spicer, 1999) analyze the composition of fossil plant assemblages. CA therefore uses taxonomic and ecological relationships with assumed nearest living relatives and their climatic niches, whereas CLAMP tracks paleoclimate conditions by morphological comparison of fossil plant assemblages with extant plant assemblages under a given climate. Changes in paleoclimate and CO<sub>2</sub> through time can be tracked also via changes in morphometric parameters such as leaf area, leaf size and leaf shape (Peppe et al., 2011; Royer, 2012) or epidermal (cuticular) parameters as for instance stomata density (SD), stomata index (SI) and stomata size (Roth-Nebelsick et al., 2004, 2012; Steinhorsdottir et al., 2016). The multivariate gas exchange model, first introduced by Konrad et al. (2008), combines morphometric and cuticular parameters, together with assumed paleoclimate conditions and physiological data of nearest living equivalents to determine paleo-CO<sub>2</sub> (Grein et al., 2011a; Grein et al., 2013; Roth-Nebelsick et al., 2014). Plants show differences in morphological, morphometric and cuticular parameters, not only in response to overall changes in CO<sub>2</sub> and climate, but also due to their immobility and dependency on light intensity, water availability and soil conditions at the respective site.

The long-lived fossil taxa *Rhodomyrtophyllum reticulosum* and *Platanus neptuni* were used to reconstruct the response of vegetation to paleoclimatic and paleoatmospheric changes through considerable parts of the Paleogene (Figure 1) and to distinguish between overall trends therein and site-specific traits. *Rhodomyrtophyllum reticulosum* was an, in northern central Europe widely distributed, subtropical evergreen Myrtaceae (Glinka and Walther, 2003) predominantly occurring in riparian environments during the early to late Eocene. Its presence covers a time span of globally decreasing mean annual temperature (MAT) and carbon dioxide (CO<sub>2</sub>) and distinct climatic events (Figure 1). These are the end of the Early Eocene Climatic Optimum (EECO; 52-50 Ma) (Greenwood and Wing, 1995; Hyland and Sheldon, 2013), the Mid-Eocene Climatic Optimum (MECO; ca. 40 Ma) (Zachos et al.,



2008; Bijl et al., 2010) and the Eocene-Oligocene turnover (EOT; 34-33.5 Ma) (Coxall et al., 2005; Zachos et al., 2008; Hren et al., 2013). Afterwards *Rhodomyrtophyllum reticulosum* was not present anymore in any central European azonal plant assemblage. *Platanus neptuni* was a deciduous thermophilic warm-temperate species (Kvaček and Manchester, 2004), occurred from the middle Eocene to the early Miocene in central Europe and covers a period of substantial climatic change. Those are for instance the EOT with a remarkable decrease in temperature and CO<sub>2</sub> (Coxall et al., 2005), the Oi-1 cooling event in the earliest Oligocene (Coxall et al., 2005; Zachos et al., 2008; Hren et al., 2013) and progressing glaciation of the Antarctic. The ongoing cooling process was only intermitted by a short globally recognizable increase in temperature during the late Oligocene (Late Oligocene Warming) (Kürschner et al., 2008; Zhang et al., 2013).

The exclusive distribution of *Rhodomyrtophyllum reticulosum* leaves in riparian environments, the high abundance in the studied leaf assemblages, together with the mostly excellent preservation allow for first assumptions on both morphological/morphometric adaptation strategies and changes in epidermal characteristics, such as SD, SI, trichome density (TD) and stomata size bound to the globally recorded decrease in temperature and CO<sub>2</sub>. In distinction from *Rhodomyrtophyllum reticulosum*, *Platanus neptuni* leaves are relatively highly abundant in taphocoenoses from different depositional settings (fluvial, lacustrine, estuarine and sublittoral-pelagial sediments). Its presence in the late Eocene until the early Miocene in central Europe together with the abundance in different depositional facies types, which might also reflect different environmental settings, allows for first assumptions on site-related dependencies of epidermal parameters and morphological and morphometric correlations.

In this study leaf traits of both *Rhodomyrtophyllum reticulosum* and *Platanus neptuni* from 23 sites in Germany, Austria and the Czech Republic covering a time span from the late early Eocene to the early Miocene (Figure 1) of central Europe are investigated. Alongside the stratigraphic range of the data set, which allows for tracing long-term variations in the respective parameters, I also incorporated sites of different depositional facies types (maar deposits, marine deposits and fluvial-lacustrine deposits). During my investigations I consider different leaf traits in accordance with their own trends in time and depending on site-related characteristics.

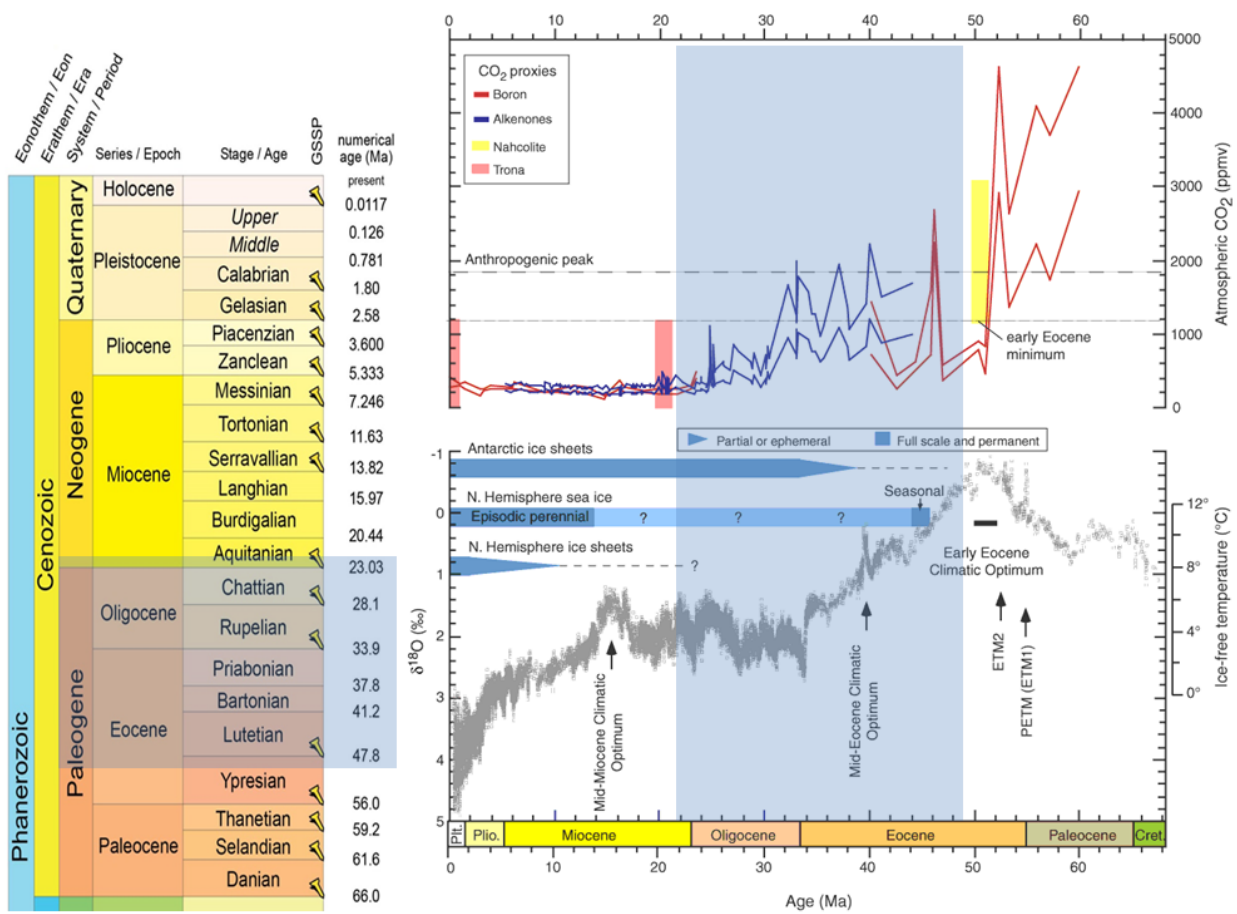


FIGURE 1. Cenozoic chronostratigraphic chart and global climate history (left: excerpt of the International Chronostratigraphic Chart v2016/12; the light blue colored frame marks the stratigraphic range of the investigated sites, modified from Cohen et al. (2013, updated); right: Cenozoic climate history during the Paleogene, upper panel: atmospheric CO<sub>2</sub>, lower panel: ice-free temperature in °C and δ<sup>18</sup>O from benthic foraminifera; the light blue colored frame marks the stratigraphic range of the investigated sites, modified from Zachos et al. (2008)).

## 1.1. Eocene to Miocene paleogeography and climate evolution

In the following chapter, both the global and regional paleogeographic situation and changes are delineated together with global changes in paleoclimate. Figure 2 illustrates the position of the main considered geological and topographic units.

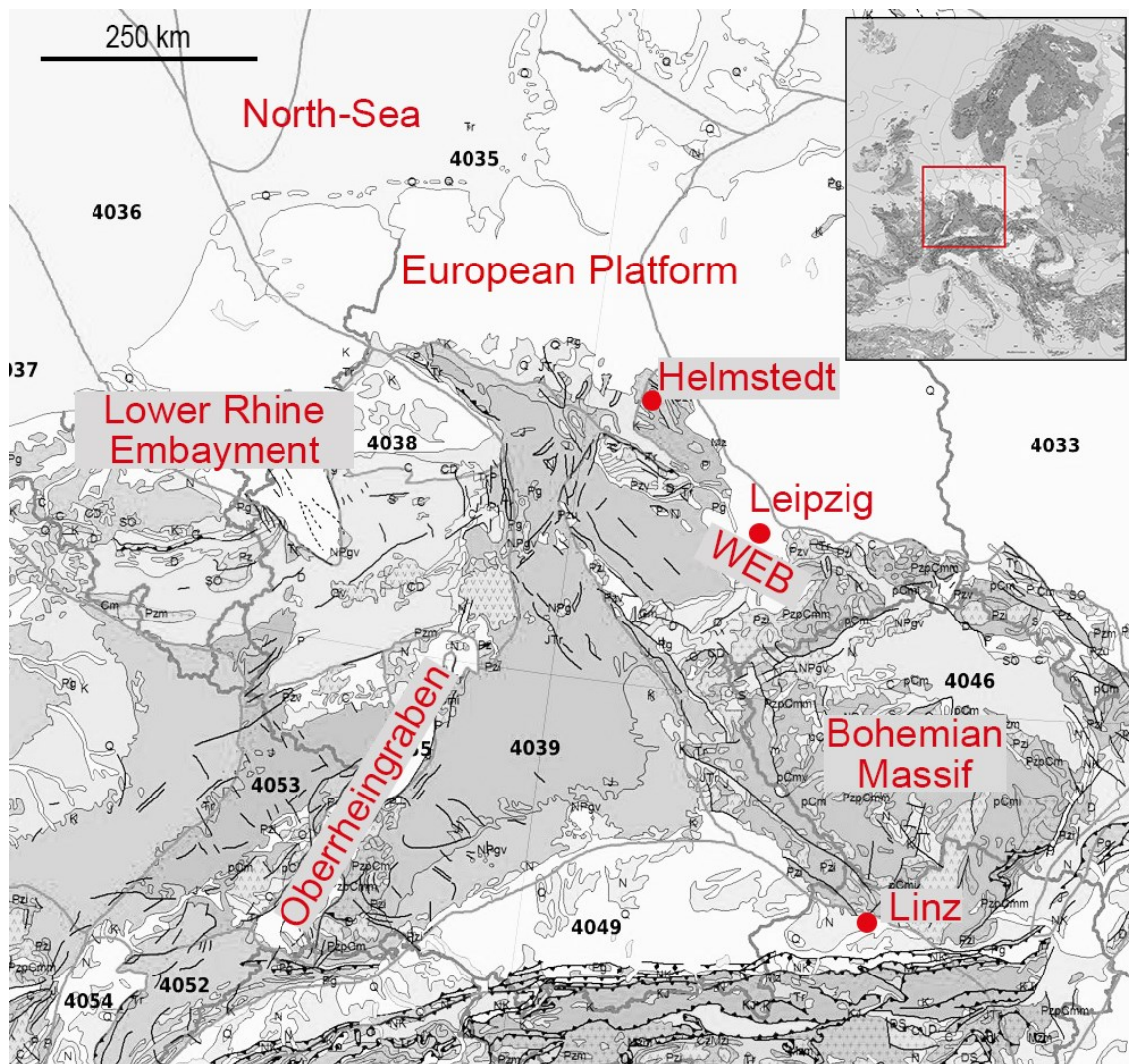


FIGURE 2. Geological map of central Europe and selected geological units and topographic landmarks (abbreviation: WEB – Weiße Elster Basin; modified from Gaertner et al. (1971)).

The Paleogene is a time of extraordinary paleoclimatic changes with the transition from the “last greenhouse world” in the Eocene towards the onset of Antarctic glaciation and global cooling, leading to the onset of the Pleistocene glacial-interglacial cycles (Zachos et al., 2001, 2008; Beerling and Royer, 2011; Hren et al., 2013).

Changes in paleoclimate were forced primarily by earth’s orbital geometry (eccentricity, obliquity, precession) and plate tectonics (Zachos et al., 2001). Oscillations in climate therefore respond both, to orbitally related rhythms and gradual changes in the earth’s boundary conditions, namely continental geography and topography, opening and closing of oceanic gateways and the concentration of atmospheric greenhouse gases (Zachos et al., 2001) which are controlled by plate tectonics.

**Eocene.** During the Paleocene and Eocene the splitting of Pangaea continued, resulting, for instance, in the northwards drift of India towards Asia, the segregation of Antarctica and Australia (Walter, 2014) and the separation of Greenland apart from Europe (Boenigk et al., 2015), which was accompanied by the opening of the North Atlantic Ocean basin (Gibbard and Lewin, 2016). The northwards drifting Indian plate led to the stepwise closing of the Tethys Ocean and the segregation into the western and the eastern Neotethys (Oschmann, 2016). During the Eocene Europe was still an archipelago with intercontinental seas covering large areas of the European platform (Figure 2). An important seaway connection (Turgai Strait) existed between the western Neotethys and the northern sea (Rögl, 1999; Walter, 2014), which provided warm water exchange and may have caused the warm climate during the Eocene in Europe (Rögl, 1999).

In central Europe the subsidence of the North-West-European Basin resulted in the foray of the paleo-North Sea towards the South until central Germany (Figure 3; Standke et al., 2010; Gibbard and Lewin, 2016) and led to the deposition of marine sediments in northern central Germany (Helmstedt area; Figure 2; Standke, 2008). The area south of Leipzig (Leipzig Embayment, Weißelster Basin; Figure 2), situated far away from the ancient coastline, defeated erosional processes. Following alternations of transgression and regression processes led to the deposition and intercalation of marine, fluvial, lacustrine, terrestrial and brackish sediments in northern Germany (Standke et al., 2010; Krutzsch, 2011). In the middle Eocene mainly terrestrial sediments were deposited in the Weißelster Basin and rivers transported sand, clay and marl into the sea near Helmstedt although first transgressions already reached the Leipzig Embayment and led to the deposition of marine sediments as well (Standke et al., 2010). Eissmann (1994) describes the deposition of huge fluvial sediment series, with locally intercalated plant macrofossil assemblages (Standke

et al., 2010). During the late Bartonian the coastline of the paleo-North Sea reached the Weißelster Basin and led to the formation of paralic lignites (lignite seam 1; Rascher et al., 2008) and the deposition of estuarine sediments (Standke et al. 2010). The alternating deposition of terrestrial, estuarine and fluviatile sediments continued until the late Priabonian (Standke et al., 2010), visible in the main lignite seam 2/3 (Standke et al., 2010) which is intercalated by several horizons containing fluvial sediments. The marine influence in the southern Leipzig Embayment is characterized by the Domsen member (Standke et al., 2010). In the late Eocene the Oberrheingraben developed (Figures 2, 3) due to southwest-northeast oriented tectonic movement (Walter, 2014). These first orogenic activities are caused by the northwards drift of the African plate and were accompanied by increased volcanic activity (Grimm and Hottenrott, 2011). The Oberrheingraben was connected as well with the southern valley systems (e.g. Bresse and Rhône valley). In southern Europe the formation of the Paratethys started around the Eocene-Oligocene turnover (Rögl, 1999). Volcanic activities are known since the late Eocene in central Europe (Suhr, 2003).

The Paleocene was a time of overall warmer climate, compared to all younger stages in earth history. It culminated in the Paleocene-Eocene Thermal Maximum with a rise of global temperatures by mean 5°C in less than 10.000 years (Zachos et al., 2001, 2008) about 55 Ma ago (PETM) (Röhl et al., 2007; Zachos et al., 2008; McInerney and Wing, 2011) and approximately 2.000 Gt carbon entered the atmosphere and oceans. The short-term hyperthermal PETM (Figure 1) was followed by another peak in temperature and CO<sub>2</sub>, the EECO (52-50 Ma) (Greenwood and Wing, 1995; Hyland and Sheldon, 2013). The EECO in continental (central) Europe tentatively occurred in the early middle Eocene mirrored by quasitropical vegetation (Kvaček, 2010) whereas (on a global scale) in marine environments, it is placed into the early Eocene (Figure 1). After the EECO an approximately 17-myr-long trend in decreasing CO<sub>2</sub> and temperature is reported (Zachos et al., 2001), intermitted by a short warming peak, the MECO. Deep-sea temperature declined from the EECO towards the EOT roughly 7°C (Zachos et al., 2001). During the middle and late Eocene, it has been demonstrated that no mountain glaciers were present. Smaller ice sheets developed during the late Eocene in Arctic regions (Eldrett et al., 2004) and on Antarctica (Kennett, 1977; Zachos et al., 2001; DeConto and Pollard, 2003; Coxall et al., 2005). *Nothofagus*-forests have been present until the late Eocene in Antarctica (Francis et al., 2009). In contrast to the reconstructed sharp decline in temperature and CO<sub>2</sub>, estimated with marine proxy data, central European vegetation in the Atlantic Boreal phytoprovince (sensu Mai, 1995) underwent only minor (e.g. Kvaček et al., 2014;

Kunzmann et al., 2016) or almost no detectable changes throughout the late middle and late Eocene, indicating that there was presumably no significant climate change.

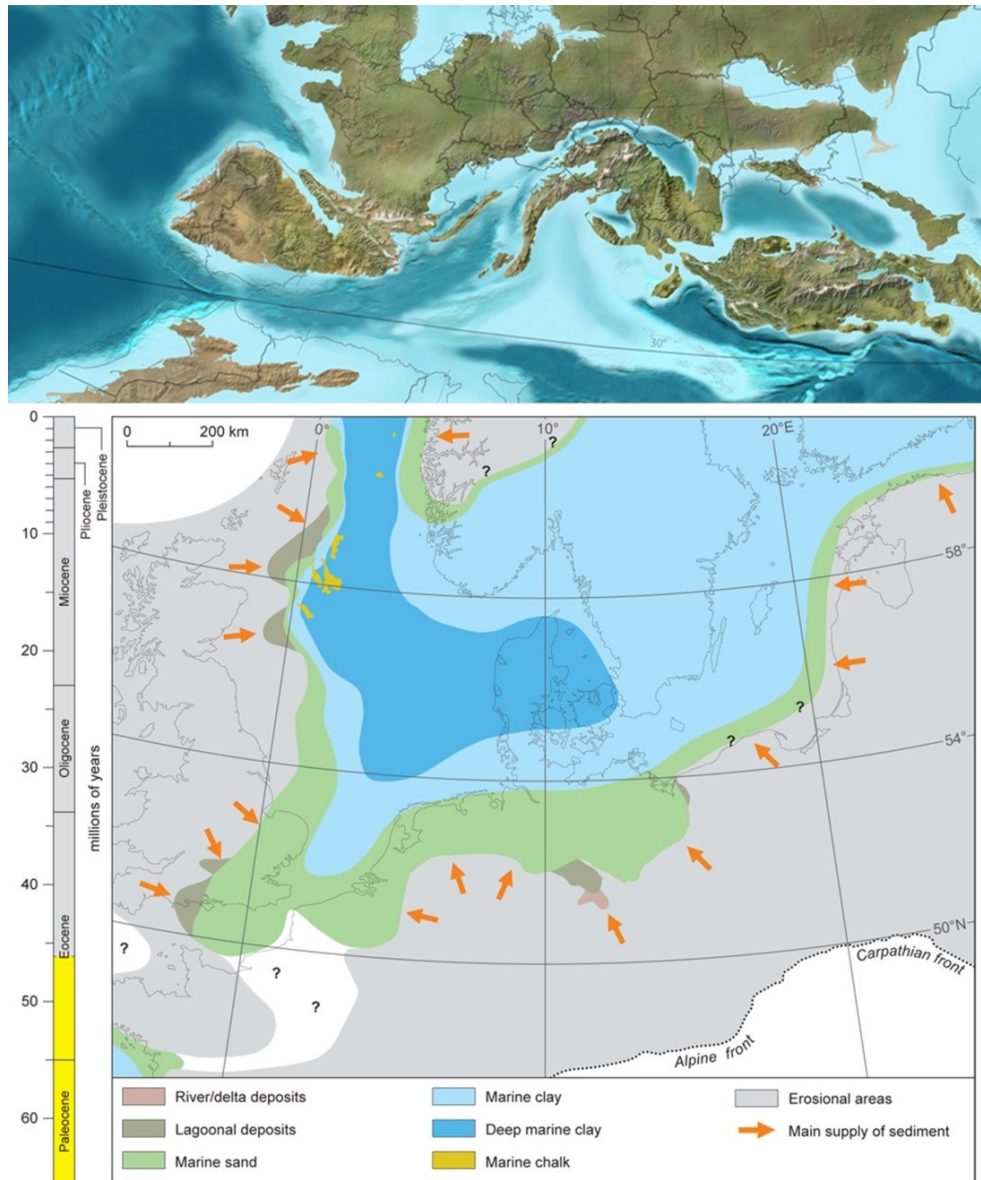


FIGURE 3. Paleogeographic situation of Europe during the Eocene (upper map: paleogeography of Europe at 50 Ma (DeepTime Maps Inc.™) and lower map, showing the distribution of the paleo-North Sea during the late Ypresian (Gibbard and Lewin, 2016)).

**Oligocene.** During the Oligocene the drifting continents approached their extant position, which includes the northwards drift of Australia, increasing isolation of Antarctica and the opening of the Southern Ocean accompanied with the development of the Tasmanian gateway and the northwards drift of South America and thereby the opening of the Drake Passage (Heydt and Dijkstra, 2006). The establishment of these gateways led to the strengthening of the Antarctic Circumpolar Current (Heydt and Dijkstra, 2006; Grimm and Hottenrott, 2011) and the ongoing cooling process, which accelerated ice growths in the Northern Hemisphere (Figure 1). The opening of oceanic gateways in the Southern Hemisphere and therein the global cooling (Coxall et al., 2005; Zachos et al., 2001, 2008) together with enabled mammal migration due to the closing of the Bering Bridge (Rögl, 1999) caused a mass extinction at the Eocene/Oligocene boundary (Ivany et al., 2000), commonly called the 'Grand Coupure' of vertebrates (Prothero, 1994; Grimm and Hottenrott, 2011). Tectonic activities along the Alpine front together with the ongoing drift of the Indian plate to the north led to the development of the intercontinental Paratethys (Rögl, 1999) and the Mediterranean Sea in the south. During the Oligocene the continentalization of Europe increased, the Turgai Strait closed and a newly established sea way (Danish-Polish Strait) supplied water from the paleo-North Sea to the Paratethys (Figure 4; Rögl, 1999).

The EOT in northern Europe was characterized by the regression of the paleo-North Sea and the repeatedly transgression in the early Oligocene in central Germany (deposition of Rupelian clay in the Weißelster Basin, "Rupelton"; Standke et al., 2010; Walther, 2014). During the late Oligocene several transgressions and shifts in the coastline are proven in the Weißelster Basin (Standke et al., 2010). Main sedimentation in the Lower Rhine Embayment started in the Oberrheingraben (Figure 1, 4), which underwent complex tectonic development during the Oligocene (Maxwell et al., 2016). Both, marine-lagoonal and river deposits can be found (Gibbard and Lewin, 2016; Kovar-Eder, 2016; Maxwell et al., 2016). During the Oligocene the seaways providing fresh water for the Paratethys steadily narrowed and culminated in the middle Rupelian (nannoplankton zonation (NP) 23; Rögl, 1999) in the first closure. This short closure ended with the repeatedly opening in the early Chattian (Rögl, 1999).

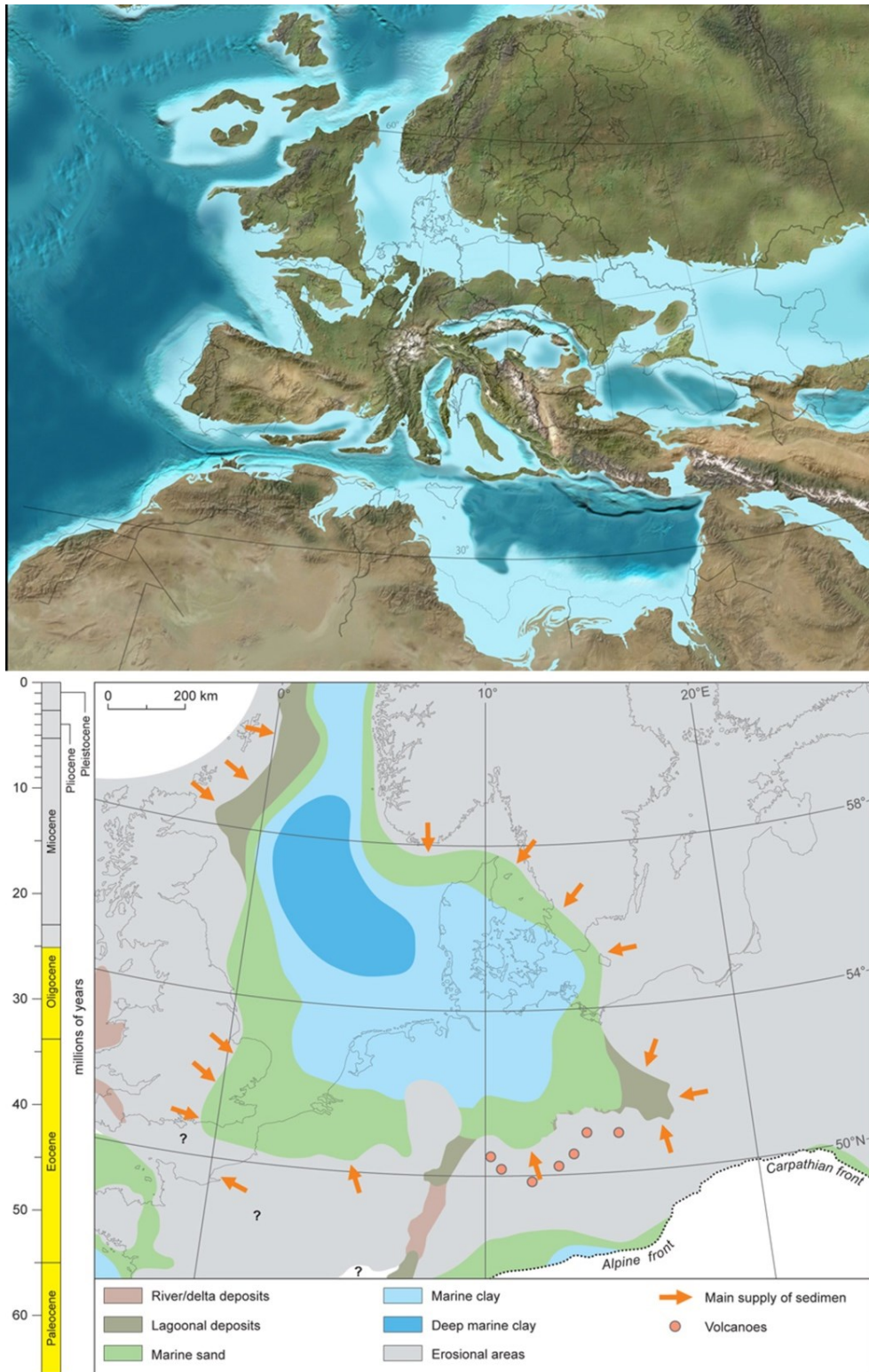


FIGURE 4. Paleogeographic situation of Europe during the Oligocene (upper map: paleogeography of Europe at 25 Ma (DeepTime Maps Inc.<sup>TM</sup>) and lower map, showing the distribution of the paleo-North Sea during the Chattian (Gibbard and Lewin, 2016)).



The rapid decrease in  $\delta^{18}\text{O}$  at the EOT of more than 1‰, seen in Figure 1, has to be interpreted carefully, as half of the signal reflects the changing  $^{17}\text{O}/^{18}\text{O}$  ratio due to the onset of Antarctic glaciation and therefore an increased ice volume (Zachos et al., 2001, 2008). Nevertheless, a drop in temperature is noticeable at the EOT (Zachos et al., 2001, 2008; Lear et al., 2008; Kvaček et al., 2014). Antarctic ice sheets expanded rapidly during the early Oligocene and had an area of around 50% of the today's ice sheets expansion (Zachos et al., 2001). These ice sheets persisted in size until the late Oligocene, before another warming trend (Late Oligocene Warming; Zachos et al., 2001) caused a reduction of the ice mass, which remained stable afterwards until the middle Miocene (~15 Ma). During the late Oligocene the circumequatorial current weakened which caused a cooling of the equatorial ocean water (Heydt and Dijkstra, 2006).

**Miocene.** The Miocene is characterized by the global intensification of orogenic and other tectonic movements, especially the uplift of the Tibetan Plateau (Bruch et al., 2007) and the spreading of the Red Sea Rift. The Tethys Seaway closed in the early Miocene when the African and Eurasian plate collided (Heydt and Dijkstra, 2006).

There is evidence for widespread uplift and tectonic movement around the northern Atlantic (Gibbard and Lewin, 2016) with uplift of Scandinavia and the Bohemian Massif (Figure 2). The latter caused the closure of the Oberrheingraben connection (Rögl, 1999; Gibbard and Lewin, 2016). Thick fluvial and associated sequences are known from the Lower Rhine Basin and the Weißeelster Basin (Standke et al., 2010; Gibbard and Lewin, 2016), with intercalated fluvial sands, gravels and clays indicating the presence of meandering river systems. Within the Paratethys, the circulation from the Indian towards the Atlantic Ocean remained open and the spreading of the Balearic Sea in the west started (Rögl, 1999). During the early Miocene, rapid changes in the opening and closing of seaways led to a mosaic pattern of terrestrial and marine facies, which ended with the counterclockwise rotation of Africa and the closing of the Indo-Pacific connections (Rögl, 1999). Another short opening occurred during the middle Miocene.

During the early Miocene  $\delta^{18}\text{O}$  remained as stable as in the late Oligocene (Figure 1) with the exception of several, smaller periods of glaciation (Mi-events). A steadily ongoing warming trend peaked in the Mid-Miocene Climatic Optimum (17-15 Ma; Figure 1; Zachos et al., 2008) and was followed by a rapid decrease in temperature and the reestablishment of a major Antarctic ice sheet at 10 Ma. Cooling went on during the late Miocene and Pliocene and led to the establishment of ice sheets in the Arctic.

## 1.2. Floristics and vegetation dynamics

Fortunately, central Europe exhibits a long and dense record of intensively studied Paleogene fossil plant assemblages. Changes in the composition of these plant assemblages through time are long known and have been described by various authors. Mainly, due to an enormous record of collected material from the Weißelster Basin, Mai and Walther (e.g. Mai and Walther, 1978, 1983, 1985, 1991, 2000) made first attempts to unify these plant assemblages to establish a phytosociological and phytostratigraphic concept, the 'Florenkomplex' (floristic complex, afterwards abbreviated FC) which was later on further refined by Mai (1995) and e.g. Walther (1999), Kvaček (2004) and Walther and Kvaček (2007). By definition the FC is characterized to represent a temporary stage in the floristic evolution of regional vegetation independently from the respective sedimentary facies type and type of plant community (Mai and Walther, 1983; Mai, 1995; Kunzmann et al., 2016) and therefore represents a kind of step in evolutionary history. Within the FC plant assemblages from similar stratigraphic positions as far as known but different paleogeographic and paleoenvironmental settings were unified. The FC concept presented in Kvaček and Walther (2001) is based on a latitudinal gradient (Boreal Province in northern Europe and Paratethys Province in southern Europe), but comparisons of floras from different paleogeographical settings imply that the influence of regional climate patterns and therefore also marine influences induce a much more complex vegetation pattern (Kovar-Eder, 2016). The recently published work of Kunzmann et al. (2016) points out the necessity to reconsider the FC concept and to leave the idea of evolutionary steps in the migration of species and composition of vegetation behind in favour of reported more gradually changes in vegetation which are not supposed to fit into categories (Figure 5).

During the Paleogene central European vegetation changes from being mainly subtropical in the early and middle Eocene up to the late Eocene with the stepwise immigration of warm-temperate taxa, recognized in many plant assemblages from the Oligocene towards the establishment of a nearly Neogene vegetation similar to the ones present nowadays in Europe in the early Miocene.

The paratropical to subtropical evergreen-broadleaved, basically zonal vegetation of site Messel (Wilde, 1989; Mai, 1995; Collinson et al., 2012), which is dated to early Eocene (Lenz et al., 2014) is bound to a time interval with tropical to subtropical climate after the

EECO (Figure 1). Most of the occurring taxa are not determinable to species level (Wilde, 1989; Collinson et al., 2012) and therefore not equally comparable with recent taxa but Collinson et al. (2012) described the distribution of a tropical to subtropical inland forest in a state of a climax community (Lenz et al., 2011) surrounding the Messel lake.

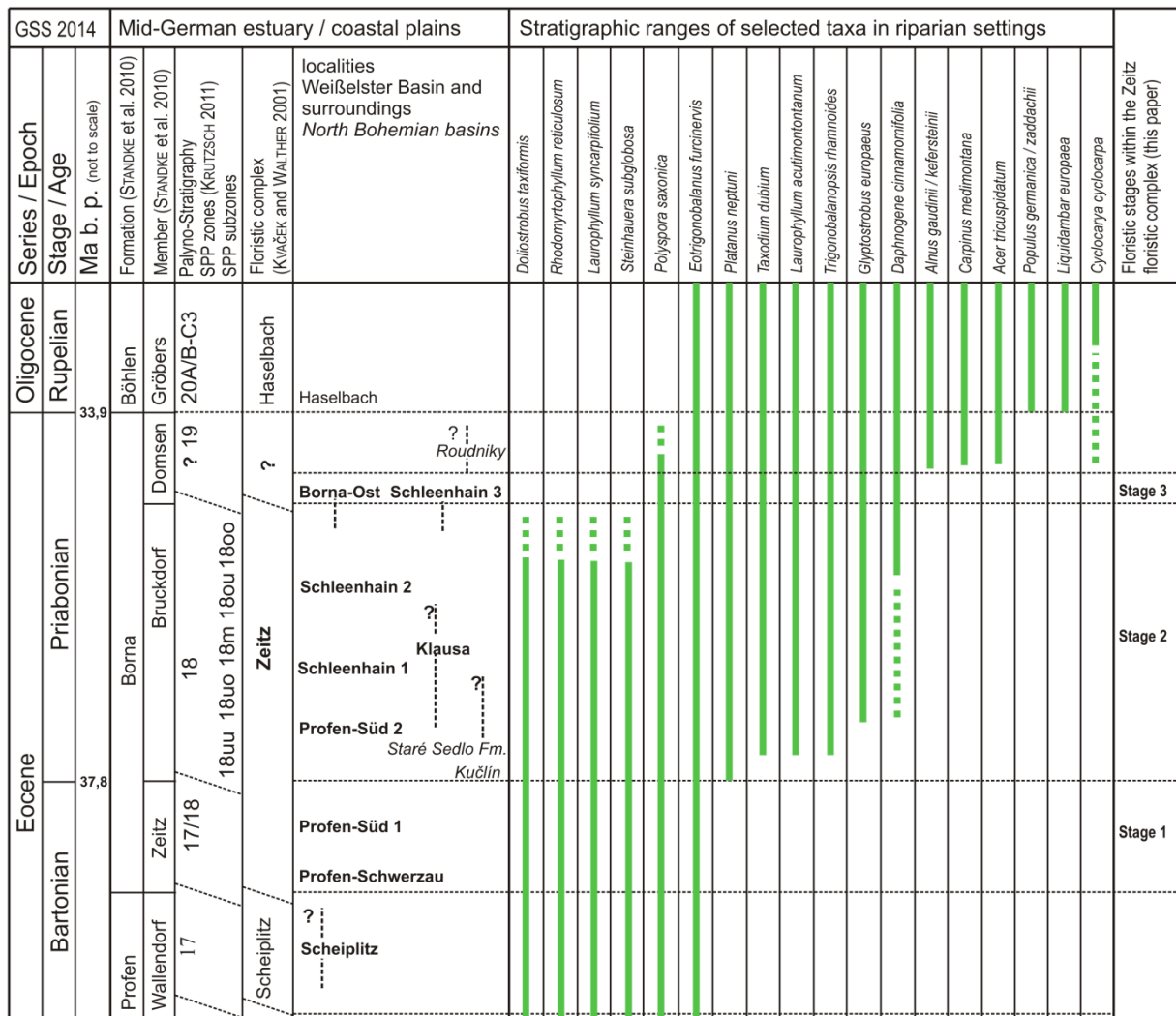


FIGURE 5. Vegetation dynamics of riparian forests in Europe during the Eocene until the early Oligocene; the stratigraphic ranges of selected taxa (green lines) indicate a stepwise change in vegetation in at least three stages, reported from several sites; Kunzmann et al. (2016).

A dense record of studied plant assemblages comes from the central German Weißelster Basin, where the 'Florenkomplex' concept (e.g. Mai and Walther, 1983, 1985, 1991; Mai, 1995) was developed and further elaborated. The floras mainly represent azonal or intrazonal vegetation (Kvaček, 2010). The middle Eocene vegetation, represented by various sites (e.g. Scheiplitz; Fischer (1990) and Profen-Schwerzau 1u (unpublished material)), is characterized as being subtropical with dominating species of Fagaceae (*Dryophyllum*, *Eotrigonobalanus*), Lauraceae (*Actinodaphne*, *Laurophyllum*, *Daphnogene*), Myrtaceae (*Rhodomyrtophyllum*), Theaceae (*Polyspora*, *Ternstroemites*) and others (Mai and Walther, 2000). Palms were common (e.g. *Phoenix*, *Sabal*). The physiognomic characters of the respective floras are very different, ranging from broad-leaved assemblages (e.g. Profen-Schwerzau 1u) to subxerophytic small-leaved plant assemblages (Scheiplitz). Kvaček (2010) defined the vegetation as 'Mixed *Doliosrobis* (and/or *Quasisequoia*) and broad-leaved evergreen swamp forest'. The distribution of *Quasisequoia* trees dominated the coal-forming vegetation (Kunzmann and Walther, 2012).

Ongoing decrease in MAT and the establishment of more seasonal variations led to the disappearance of subtropical species in the macrofossil plant record. The late Bartonian to early Priabonian sites (e.g. Profen-Schwerzau ZC) are characterized by the persistence of broad-leaved notophyllous vegetation (grouped together in the Zeitz FC; Mai, 1995), consisting of mainly evergreen, subtropical to warm-temperate elements (Mai and Walther, 2000), whose diversity is already lowered compared to the Scheiplitz FC (Kvaček, 2010). The vegetation is characterized by the key elements *Steinhauera subglobosa* and *Rhodomyrtophyllum reticulosum*, associated with diverse Lauraceae and palms (Kunzmann et al., 2016). Kvaček (2010) proposed the term 'Broad-leaved evergreen riparian gallery forest with palms' for this type of intrazonal vegetation, which covered essential parts of the Weißelster Basin. Zonal vegetation was, if present, rich in mastixioids. This interpretation partly differs from phytosociological interpretations proposed by Mai and Walther (2000) who reconstructed several intrazonal types such as the *Steinhauera-Rhodomyrtophyllum* riparian forest, Lauraceae-conifer swamp forests and zonal vegetation types including *Eotrigonobalanus*-oak-Lauraceae forests partly with conifers. However, the flora of the Zeitz FC was dominated by characteristic evergreen species including *Eotrigonobalanus furcinervis*, *Rhodomyrtophyllum reticulosum*, *Symplocos kirstei*, *Sterculia labrusca*, *Retinomastixia glandulosa*, *Doliosrobis taxiformis* and others (Figure 5; Mai and Walther, 2000). Several deciduous taxa such as *Platanus neptuni*, *Taxodium dubium* and *Rubus* spp. are recorded amongst new immigrants (Mai and Walther, 2000). Recent taxonomic studies and the dense macrofossil plant record in the late Eocene gave rise to

the assumption that the Zeitz FC, which covers a considerably time period of approximately 3 myr from 38.5 to 35 Ma (Moraweck et al., 2015), comprises different stages in the composition of regional vegetation (Kunzmann et al., 2016), responding to paleoclimatic changes. Within the Zeitz FC gradually changes in the distribution of taxa can be recognized (Figure 5). The continuously migration of deciduous and evergreen, warm-temperate and thermophilic species (e.g. *Taxodium dubium*, *Laurophyllum acutimontanum*, *Trigonobalanopsis rhamnoides* and *Glyptostrobus europaeus*) co-occur with the common species *Doliosstrobos taxiformis*, *Eotrigonobalanus furcinervis*, *Rhodomyrtophyllum reticulosum* and *Steinhauera subglobosa*. The late Priabonian site Borna-Ost DC lacks the typical species *Doliosstrobos taxiformis*, *Rhodomyrtophyllum reticulosum* and *Steinhauera subglobosa* (Müller, 2014; Kunzmann et al., 2016) and underlines the ongoing cooling process in central Europe. The Oligocene plant assemblages are characterized by the existence of both laurophyllous, paleo-tropical and deciduous, arcto-tertiary elements (Mai, 1995) whereby the latter dominate in comparison to the slightly older Zeitz FC (Mai, 1995; Kunzmann and Walther, 2012). Index species for the early to middle Oligocene vegetation (Haselbach FC; Mai and Walther, 1991, Mai, 1995) are e.g. *Ampelopsis hibschii*, *Mastixia meyeri*, *Matudaea menzelii*, *Meliosma reticulata*, *Myrica altenburgensis*, *Ottelia minutissima* and *Pinus eophylla*. Species such as *Acer haselbachense*, *Carpinus medimontana*, *Carya quadrangula*, *Populus germanica* or *Rosa lignitum* occur the first time in the central European fossil record and can be interpreted as typical Eocene-Oligocene turnover immigrants (Kvaček and Walther, 2001; Kunzmann and Walther, 2012), whose first appearances are recorded already in the late Eocene (Roudníky, Czech Republic; Figure 5; Kvaček et al., 2014). The zonal vegetation outside of the lignite basins indicates the distribution of mixed-mesophytic forests with a high proportion of 'modern' arcto-tertiary elements (Seifhennersdorf FC; Kvaček and Walther, 1998). First occurrences of e.g. *Ostrya atlantidis*, *Celtis*, *Zelkova*, *Liriodendron*, *Quercus lonchtis*, *Tilia gigantea* and *Vitis stricta* can be as recognized as the low representation of paleosubtropical elements, such as *Engelhardia* (Kvaček and Walther, 1998). Towards the Oligocene-Miocene boundary the receding of *Eotrigonobalanus furcinervis* as dominating species and the more frequent occurrence of *Trigonobalanopsis rhamnoides* instead in the plant communities (Mai, 1995) can be recognized. The very diverse mixed mesophytic forests firstly show a dominance of arcto-tertiary elements. Dominating species are *Carpinus cordataeformis*, *Cyclocarya cyclocarpa*, *Fagus saxonica*, *Laurophyllum medimontanum* and *Populus germanica* (Mai, 1995). Conspicuously new immigrants, which are typical Miocene elements, first occur in the Thierbach FC, e.g. different species of *Acer*, *Catalpa microsperma*, *Cathaya bergeri*, *Dombeyopsis lobata* or *Tilia praegrandidifolia*. The late Oligocene/early Miocene flora of

Witznitz WC reflects the effect of the late Oligocene Warming (Zachos et al., 2001) and inhibits thermophilic, often also evergreen laurophyllous elements (Mai, 1995). Typical representatives were for instance *Quercus rhenana*, *Daphnogene cinnamomifolia*, *Cunninghamia*, different Lauraceae and *Magnolia kristinae* (Mai, 1995; unpublished data J. Hammer).

### 1.3. Current knowledge on correlation of leaf traits with climate and ecology

Most of these above described remarkable temperature excursions and changes as well as global carbon dioxide levels for the Paleogene have so far been estimated based on marine proxies. Maximum ocean water temperature curves calculated from oxygen isotopes of benthic foraminifera (Zachos et al., 2001, 2008) are often correlated with global climate evolution (Mosbrugger et al., 2005; Favre et al., 2014; McInerney and Wing, 2011) and global atmospheric CO<sub>2</sub> changes (Mosbrugger et al., 2005; McInerney and Wing, 2011). The terrestrial record, however, is not so well understood and indicates partly distinct and different developments (Mai, 1995) which means that averaged global ocean water temperature values and changes may not necessarily faithfully mirror continental paleoclimate especially on a regional scale (Grein et al., 2013; Hyland and Sheldon, 2013; Kvaček et al., 2014; Kunzmann et al., 2016).

Plants are ideal proxies to trace paleoclimatic, paleoatmospheric and paleoecological variations both on a global and a regional scale. The connection between climate, atmosphere and leaf morphology and anatomy is already long known and has been object of various publications (e.g. Woodward and Bazzaz, 1988; Royer, 2001; Roth-Nebelsick, 2005; Royer et al., 2005; Uhl et al., 2007; Doria et al., 2011; Blonder and Enquist, 2014). Most publications focus on single leaf traits, but to date only little is known about the dependencies between leaf morphology and cuticle parameters together with paleoclimatic and paleoatmospheric conditions in multidimensional approaches taking different leaf traits and their interrelationships into account.

Morphological and morphometric studies concentrate on the one hand on single leaf traits, such as variation in leaf size and shape (Dolph and Dilcher, 1980; Greenwood and Wing, 1995; Nicotra et al., 2011; Peppe et al., 2011; Royer, 2012), length and width (Uhl, 2014), leaf mass per area (LM<sub>A</sub>; Wright et al., 2004; Royer et al., 2007; Villar et al., 2013), venation

(Sack and Scoffoni, 2013; Blonder and Enquist, 2014) or on the other hand on multivariate changes in leaf trait combinations (Green and Hickey, 2005; Royer et al., 2005; Traiser et al., 2005; Roth-Nebelsick et al., 2017) regarding changes in morphometric features. Most prominent climate and leaf trait relationships are known from changing leaf size patterns depending on moisture conditions (Wilf et al., 1998; Royer, 2012) and MAT (Givnish, 1979) and from the long known correlation of toothness and MAT (Bailey and Sinnott, 1915), which led to the establishment of the Leaf Margin Analysis (LMA; Wolfe, 1979; Wing and Greenwood, 1993; Wilf, 1997; Su et al., 2010). The occurrence of a high proportion of leaves with drip-tips within a sample gives further information on precipitation patterns in the respective site (Ellenberg, 1975; Mosbrugger and Schilling, 1992; Mai, 1995). Mai and Walther (1985) used these correlations to characterize the fossil assemblages from the Weißelster Basin and to reconstruct changes in climate referring to changes in leaf physiognomy. The correlation of leaf physiognomic characters with climate led to the establishment of various methods, such as the already mentioned LMA, CLAMP and DiLP (Digital Leaf Physiognomy; Royer et al., 2005; Peppe et al., 2011). Especially LMA and CLAMP were widely used for climate reconstructions on Paleogene European plant assemblages (Uhl et al., 2003, 2007; Kvaček, 2004; Mosbrugger et al., 2005, Grein et al., 2011b; Teodoridis and Kvaček, 2015).

In Grein et al. (2013) SD determination and CO<sub>2</sub> reconstruction was performed using five different fossil species (*Quercus praerhenana*, *Eotrigonobalanus furcinervis*, *Platanus neptuni*, *Laurophyllum acutimontanum*, *Laurophyllum pseudoprinceps*) derived from five different fossil sites (in Germany and Austria) from the late Oligocene to early Miocene. They found that co-occurring species in one site reveal very different CO<sub>2</sub> signals. The Lauraceae yielded partially extreme high values compared to the other taxa, although other studies used Lauraceae species for stomata-based CO<sub>2</sub> reconstruction successfully (Greenwood et al., 2003; Kürschner et al., 2008). This fact points out, that the solely consideration of cuticular derived parameters may not sufficiently mirror paleoatmospheric conditions, although all other considered taxa revealed similar estimates in coherence to published CO<sub>2</sub> estimates derived by different proxies (Grein et al., 2013). The results of Grein et al. (2011a) and Grein et al. (2013) point out the necessity to couple CO<sub>2</sub> estimations derived by different taxa and to overlay the data to create an interval of coincidence and therefore more reliable results. Roth-Nebelsick et al. (2014) used *Platanus neptuni* leaves and enriched the existing dataset of Grein et al. (2013) to evaluate SD and SI data for the Oligocene and to obtain a CO<sub>2</sub> signal on terrestrial implications for Cenozoic CO<sub>2</sub> records. Roth-Nebelsick et al. (2014) found that raw SD and SI data revealed partially

conflicting results, with SD data indicating a decrease in CO<sub>2</sub> and SI data showing an increase in CO<sub>2</sub> from the early to late Oligocene. Interestingly, site Kleinsaubernitz, representing an ancient maar fill (Walther, 1999), the only non-fluvial deposit, revealed the highest SD and lowest SI value (Roth-Nebelsick et al., 2014) compared to the other stratigraphically older and younger sites which gives rise to the assumption that the depositional setting and thus ancient habitat type could influence the results as well. CO<sub>2</sub> calculated with the gas exchange model (Konrad et al., 2008) indicate relatively stable CO<sub>2</sub> for the considered time intervals. CO<sub>2</sub> reconstructions were performed also using other long-lived fossil taxa, such as *Eotrigonobalanus furcinervis* in Steinthorsdottir et al. (2016) who reconstructed CO<sub>2</sub> from the middle late Eocene towards the late Oligocene and found decreasing CO<sub>2</sub> values prior to the EOT which is in accordance to vegetational shifts in central Europe (Kunzmann et al., 2016) and paleoclimate reconstructions (Mosbrugger et al., 2005). In general, stomata proxy-based CO<sub>2</sub> values tend to report significantly lower CO<sub>2</sub> estimates (Royer et al., 2001 using *Ginkgo biloba* and *Metasequoia glyptostroboides*) than alkenone- or boron-based proxies (DeConto et al., 2009; Pearson et al., 2009; Zhang et al., 2013). These differences are currently not well understood but stomata based proxies reveal the same overall trend compared to other proxy data.

#### 1.4. Scientific questions

The response of vegetation to overall changes in climate and atmospheric conditions is widely known, whereas the response of single taxa to changing boundary conditions and climate-atmosphere-biosphere relationships were not considered at all. Morphological, morphometric and cuticular investigations and the interpretation of shift in those traits of *Rhodomyrtophyllum reticulosum* and *Platanus neptuni* will suit to answer the following questions:

I. Do *Rhodomyrtophyllum reticulosum* and *Platanus neptuni* leaf traits deliver suitable proxies to trace global climate and CO<sub>2</sub> shifts?



The widely distribution of *Rhodomyrtophyllum reticulosum* in northern central Europe during the early to late Eocene provides the basis to trace shifts in the respective leaf traits during times of globally decreasing MAT and CO<sub>2</sub> prior to the EOT (see chapter 1.1.). The coriaceous leaves are mostly very good preserved and are thus suitable for the application of different methods (see chapter 4). The solely distribution of *Rhodomyrtophyllum reticulosum* in riparian environments allows for proper comparison of the results, almost neglecting differences in these proxy data due to habitat related conditions.

The occurrence of *Platanus neptuni* in plant assemblages from the late Eocene to early Miocene in central Europe allows for the investigation of morphological, morphometric and cuticular leaf traits and shifts therein for a longer time span of approximately 16 Ma, from the Bartonian/Priabonian to the early Aquitanian with overall decreasing MAT and CO<sub>2</sub>, covering different thermal and cooling events, such as the EOT, the Oligocene cooling and Late Oligocene Warming.

Both taxa and revealed morphological, morphometric and cuticular shifts will be interpreted in terms of accordance to global and regional known shifts in climate and atmospheric CO<sub>2</sub>.

## II. Do *Rhodomyrtophyllum reticulosum* and *Platanus neptuni* reveal a CO<sub>2</sub> signal that is correlated with the global curves?

In Grein et al. (2011a, 2013) and Roth-Nebelsick et al. (2014) the 2008 published gas exchange model of Konrad et al. was applied to determine paleo-CO<sub>2</sub> using measured cuticular and morphological parameters of certain long-lived taxa, climate and isotope data of the respective sites and time intervals to estimate ancient atmospheric CO<sub>2</sub>. Estimated CO<sub>2</sub> indicate partly conflicting results, depending on both, the considered time interval and the respective taxon, which served for CO<sub>2</sub> reconstructions. CO<sub>2</sub> reconstructed for the early Oligocene (Roth-Nebelsick et al., 2014) delivered lower results than other proxy data, whereas late Oligocene CO<sub>2</sub> reconstructions indicate estimates comparable to the global CO<sub>2</sub> trend (Grein et al., 2013; Roth-Nebelsick et al., 2014). In Grein et al. (2011a) and Grein et al. (2013) gas exchange modelling was applied for different taxa and reconstructed CO<sub>2</sub> differs partly greatly for the same considered time intervals.

In this study gas exchange reconstructions will be performed to both enrich the known dataset of Roth-Nebelsick et al. (2014) using *Platanus neptuni* for paleo-CO<sub>2</sub> reconstructions and to determine CO<sub>2</sub> also for the Eocene sites, represented by leaves of *Rhodomyrtophyllum reticulosum*. The long stratigraphic record together with already published data delivered by the respective taxa and others (Grein et al., 2013) serve as ideal base to enrich the stomata based CO<sub>2</sub> record for the Paleogene.

III. Is it possible to distinguish between *Platanus neptuni* leaf traits corresponding to globally driven changes in climate and CO<sub>2</sub> and site specific traits corresponding to the respective depositional setting?

The distribution of *Platanus neptuni* in both northern central Europe and at the shores of the Paratethys suit for investigations of paleogeographical influences (see chapter 2.1.) as the paleo-North Sea is a cold ocean compared to the Paratethys were warm water affects regional climate and therefore vegetation. Additionally, *Platanus neptuni* leaves can be found in different depositional settings correlated with different habitat types. These differences may be most likely mirrored in the respective leaf traits. Their investigation helps to distinguish between site related features or even taphonomically biased parameter variation and leaf traits corresponding to global changes in paleoclimate and CO<sub>2</sub>.

## 1.5. Hypothesis to test

1. The long-lived species *Rhodomyrtophyllum reticulosum* and *Platanus neptuni* are suitable to trace global and regional paleoclimatic and paleoatmospheric conditions and changes.
2. Changes in leaf morphology/morphometry are coupled with changes in cuticular morphology. Both are bound to paleoclimatic and paleoatmospheric changes.

3. Leaf morphology/morphometry and cuticular parameters differ in respect to the depositional setting and thus habitat.
4. The CO<sub>2</sub> signal derived from *Rhodomyrtophyllum reticulosum* and *Platanus neptuni* leaf traits neglects regional paleoclimate and habitat related conditions in favor of global correspondence.

## 2. Site characteristics and plant assemblages

To answer the scientific questions the chosen fossil sites and assemblages containing *Rhodomyrtophyllum reticulosum* or *Platanus neptuni* leaves come from several stratigraphic levels, paleogeographical and environmental settings and depositional facies type. Selection was made in terms of

- frequency of available leaf remains in the respective collections (Senckenberg Naturhistorische Sammlungen in Dresden (Germany), Senckenberg Gesellschaft für Naturforschung in Frankfurt/Main (Germany), Naturkundemuseum in Berlin (Germany), Staatliches Museum für Naturkunde in Stuttgart (Germany), Naturhistorisches Museum in Vienna (Austria) and Národní Muzeum Prague (Czech Republic))
- sufficiently well preserved compressions (to obtain leaf cuticles) and
- clarity of the geoscientific background (stratigraphy, facies).

The selected fossil sites cover the time span from the late early Eocene (Messel) to the earliest Miocene (Linz).

### 2.1. Paleobiogeographical settings

The investigated plant assemblages come from different phytoprovinces. The definition of the single European phytoprovinces and regions is explicitly outlined in Mai (1995) and further elaborated in Kvaček (2010). The majority of plant assemblages come from the Atlantic Boreal Province (e.g. Mai and Walther, 1978, 1985; Mai, 1995; Hennig and Kunzmann, 2013; Ferdani, 2014) and covers the European Arctic and western and central Europe (Figure 6; Kvaček, 2010). The flora of Linz in Austria (Kovar, 1982) belongs to the Transeuropean Paratethys Bioprovince (Mai, 1995; Kvaček, 2010) which is characterized by a very distinct composition of vegetation in comparison to the floras of central and

western Germany (Mai, 1995) due to the influence of the warm Paratethys (Figure 6; Kovar, 1982; Kvaček et al., 2006). This is mirrored by the lower proportion of deciduous, arcto-tertiary elements in the floras from this province in comparison to the Atlantic-Boreal Province (Mai, 1995). As outlined in Kovar-Eder (2016), pointing out the differences in vegetation patterns not only in dependency on the latitudinal gradient, but also on regional effects, like the influence of oceans and has to be kept in mind while interpreting the results.



FIGURE 6. Paleogeographical map of Europe during the latest Oligocene (25 Ma) und distribution of study sites (1 – Weißelster and Geiseltal Basin, Germany; 2 – Northern Bohemia, Czech Republic; 3 – Oberrheingraben, Germany; 4 – Western Central Paratethys, Austria; modified from Deep Time Maps Inc.<sup>TM</sup>).

## 2.2. Depositional settings and paleoenvironment

The preservation of plant organs and the formation of fossil plant assemblages is bound to special environmental conditions, most important are anaerobic conditions, which prevent decaying and coverage by sediments (Taylor et al., 2009). This usually involves deposition in fluvial, lacustrine or marine environments. The respective sites investigated in this study come from different depositional settings, which will be described briefly.

### 2.2.1. Marine depositional settings

Characteristically marine sites comprise both marine and terrestrial elements widely scattered within the sediments (Figure 7; Kovar-Eder, 2016). Obviously the taphocoenoses are characterized by both, sorting and selection mechanisms and on the other hand by a mixture of plant remains from very different habitats (Kovar-Eder, 2016). The highly allochthonous taphocoenoses comprise a high degree of incomplete leaves (Kovar-Eder, 2016) due to longer transport distances compared to par-/autochthonous plant assemblages and the degree of specimen with fungal infection is higher than recorded from other depositional settings caused by the longer transport distance from the plant to the burial place (Kovar, 1982). Typically, these plant assemblages derived from marine sediments are very diverse but many species are only represented by a few specimens (Kvaček, 2004; Kovar-Eder, 2016). Generally, in marine sites, deciduous taxa are under-represented due to their lower resilience against bacterial and fungal infection and therefore a lower probability of fossilization and mechanical stress during transport. This effect is for instance emphasized by the scarcity of deciduous woody taxa in the flora of Rauenberg (Kovar-Eder, 2016), whereas evergreen coriaceous Lauraceae are predominant in the plant assemblage of Flörsheim (Kvaček, 2004). Regarding the carpological remains, the common elements can be found within families with floatable fruits and seeds, as documented e.g. in the flora of Flörsheim where pine cones and nuts of *Carya* are common and floated for longer distances (Kvaček, 2004). The dominance of evergreen, woody taxa in the fossil record is often taphonomically biased and has to be taken into account when interpreting the results of vegetational and paleoclimate reconstructions. Within the marine taphocoenoses different vegetation types can be reconstructed, comprising both azonal and zonal vegetation types (Kvaček, 2004; Kovar-Eder, 2016). For sites Flörsheim,

Rauenberg and Linz mainly three different vegetation types can be distinguished: the vegetation along the coast, mainly composed of pine forests with palms on sandy soils, riparian forests along streams and zonal vegetation (Kovar, 1982; Kvaček, 2004; Kovar-Eder, 2016).

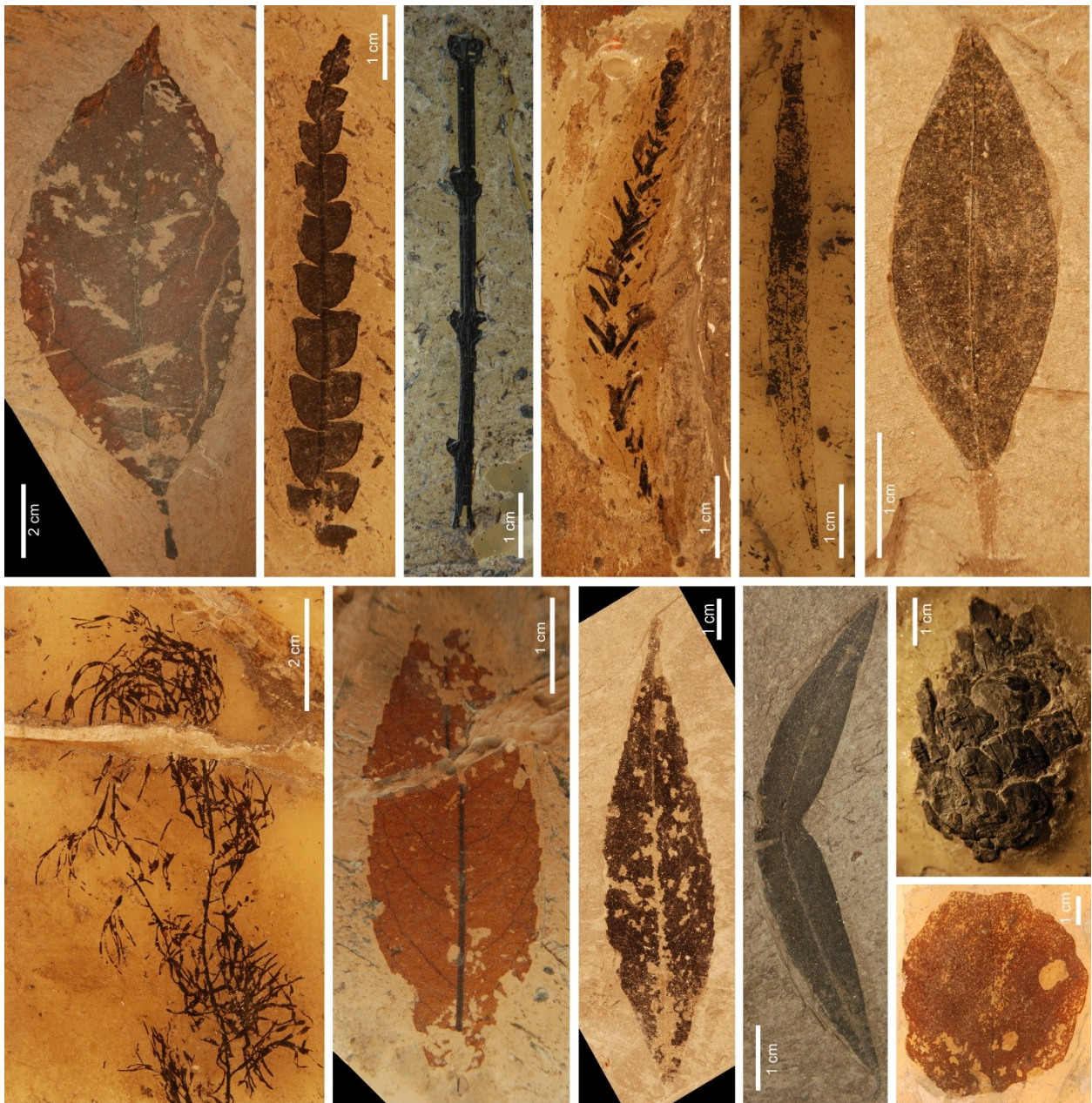


FIGURE 7. Typical preservation of different plant organs in marine depositional settings (Rauenberg; collection SMNS; photos provided by J. Eder, Staatliches Museum für Naturkunde Stuttgart, Germany).

### 2.2.2. Coastal plain and floodplain depositional facies types

The Weißelster Basin, the southern part of the Leipzig Embayment, belonging to the North German Depression (Standke, 2008) bears a variety of fossil plant assemblages. This embayment is characterized by intercalation of marine, brackish-marine (tidal), estuarine and fluvial sediments including lignites (e.g. Kunzmann, 2012). As diverse as the sediments, are also the sites, with either abandoned channels filled with litter, clay or silt lenses or sandbars where plant material got buried within the stream, swamps or little pounds (Greenwood, 1991). The respective plant assemblages therefore can be assumed to show very small-scale differences in the vegetation but are all in all assigned to be parautochthonous (Kunzmann and Walther, 2012), which means that the plant organs floated for a certain distance but became buried in the original habitat of this particular plant (Kunzmann and Walther, 2012). These plant assemblages mainly mirror the azonal riparian vegetation and only to a minor degree the more zonal 'hinterland' vegetation (Gastaldo et al., 1996; Kunzmann, 2012). The floating distance is controlled either by the e.g. turbulence and speed of the respective channel or the morphological traits and weight of the plant organ (Spicer, 1981; Greenwood, 1991; Gastaldo et al., 1996; Gastaldo et al., 1998). Sorting, fragmentation and bacterial or fungal decay have to be considered while interpreting the composition of the floras and the abundance of different species. Fruit and seed assemblages can be either allochthonous to parautochthonous, which is the most common case. Autochthonous assemblages are uncommon and the fruit and seeds in these colluvia stem mainly from water plants (Kunzmann and Walther, 2012). Parautochthonous carpological assemblages often show co-occurrence with leaves and are both valuable indicators for whole-plant reconstructions (Kvaček, 2008) and contribute to the reconstruction of vegetation, when leaves of these respective taxa are missing. The leaves are distributed mostly in packages, one overlying another with no or only a thin sediment layer in between and were embedded close to each other (Figure 8; Gastaldo et al., 1996). This is different from the marine sites, where the single plant organs often occur in bigger distances to each other. Mass occurrences of special taxa, both fruits or seeds (Gee, 2005) and leaves, can be recognized from fluvial plant assemblages as well and are documented from different Weißelster Basin sites with, for instance, mass occurrences of *Eotrigonobalanus furcinervis*, *Rhodomyrtophyllum reticulosum* (e.g. Walther, 1976) or *Zingiberoideophyllum liblarensense* (Kunzmann, 2012). Gastaldo et al. (1996) showed on different examples that leaves in fluvial deposits often show a log-normal distribution of



leaf sizes (length:width ratio), which points out that sorting processes appear to be more taxon-related in terms of preservation ability than dependent on the respective leaf size. If the respective sample is assumed to be a fluvial deposit, one would find most of the leaves directionally orientated (Gastaldo et al., 1996). The more calm the water conditions have been, the lesser developed should be the leaves orientation.

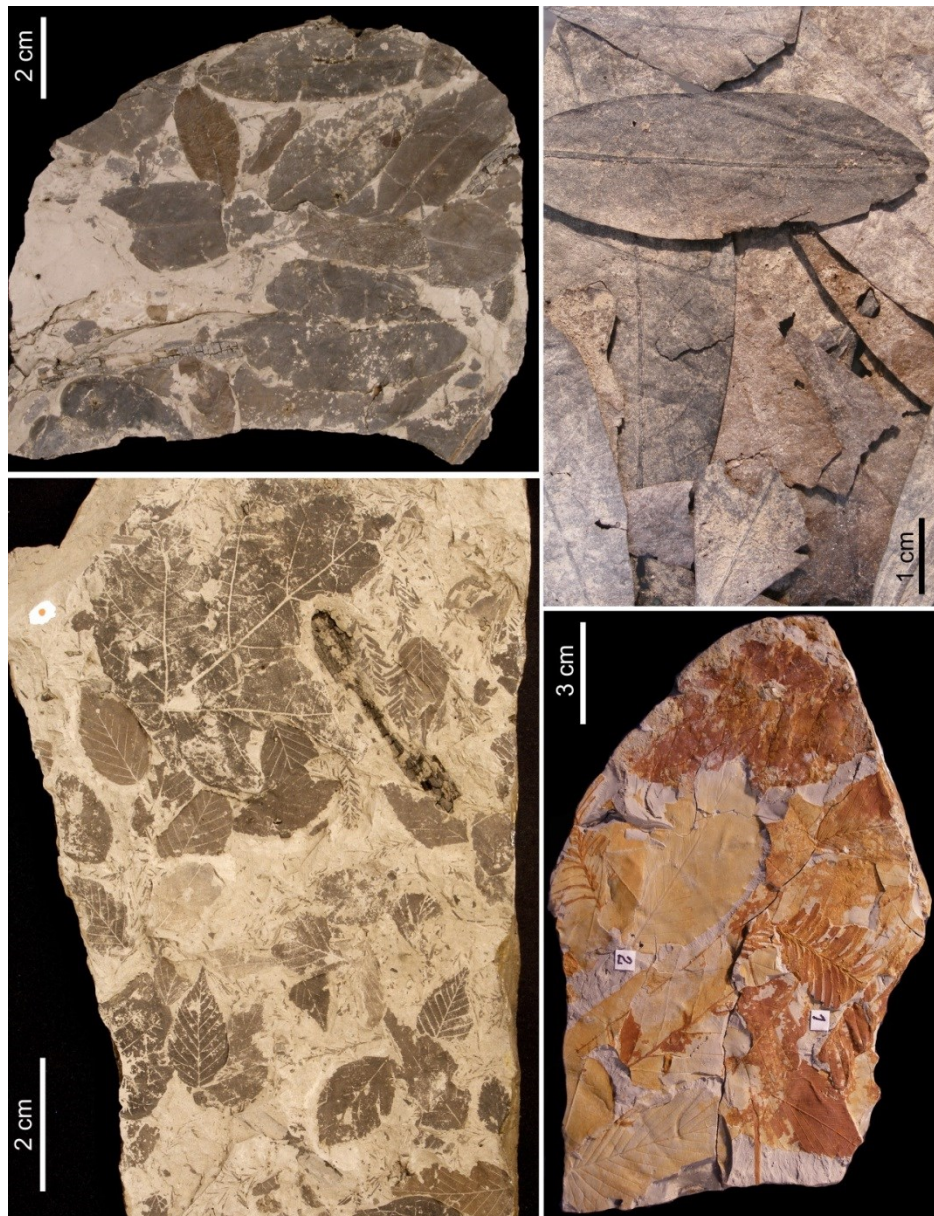


FIGURE 8. Typical coastal plain and fluvial plant assemblages with mass occurrences of special taxa, overlying each other forming packages of plant remains (collection material SNSD Dresden).

Coastal plain deposits allow for insights into the composition of the azonal vegetation. The lignite basins, where sedimentation and accumulation of plant material took part for a long time, are perfect sites to study vegetational succession processes and changes in the occurrence of taxa and thus vegetation dynamics, as documented in various publications (e.g. Mai and Walther, 1983, 1985, 1991, 2000; Kunzmann et al., 2016).

### 2.2.3. Volcanic depositional facies types

Volcanic floras developed under the influence of volcanic activity and the sites of deposition are for instance depressions or fault basins, maar and crater lakes (Kvaček and Walther, 1998; Akhmetiev et al., 2009). Plant assemblages are mainly preserved in diatomites, tuffites or oil shales. Diverse plant taphocoenoses can be found in e.g. Kundračice (Kvaček and Walther, 1998), Kleinsaubernitz (Walther, 1999), Bechlechovice (Kvaček and Walther, 2004), Seifhennersdorf (Walther and Kvaček, 2007), Kučlín (Kvaček and Teodoridis, 2011) and Messel (Wilde, 1989). The formation of the taphocoenoses occurred in calm standing water of, valid for some sites, meromictic (Walther, 1999) lakes. The fossil plant assemblages typically mirror the composition of the lake surrounding zonal vegetation (Figure 9; Walther, 1999; Akhmetiev et al., 2009) whereby azonal elements are underrepresented (Kvaček and Walther, 1998). Incoming streams may transport plant material from sites some hundreds of meters away, but the main proportion of the fossil material is parautochthonous to nearly allochthonous (Kvaček and Walther, 1998; Walther, 1999; Akhmetiev et al., 2009). If deposited in the center of a deep meromictic maar lake where mixing does not reach the ground and therefore anaerobic conditions inhibit decaying of leaves one can find nearly undisturbed layers of both sediment and plant material and track vegetational and paleoclimatic changes. This was possible for site Kleinsaubernitz, where drill cores existed and allowed for systematic studies of the flora (Walther, 1999). In contrast to marine and fluvial deposits, leaves found in maar lakes are mostly complete because short transport distances prevent fragmentation. Also sorting processes play a subordinate role, which leads to very diverse plant assemblages in which also fragile plant remains, e.g. flowers (Messel) were able to get preserved. The accumulation of special taxa, leading to mass occurrences in distinct strata, could mirror the seasonal leaf fall of deciduous taxa (e.g. *Acer haselbachense*, *Betula kleinsaubernitzensis*, *Fagus saxonica*; Walther, 1999) or the less often leaf shedding of evergreens. Depending on

the steepness of the slope, surrounding the maar, a swamp vegetation belt with elements of azonal associations could have been developed and thus preserved in the fossil record. The existence of pioneer vegetation, which occupied the slopes right after the eruption event is not resolved (Walther, 1999) but imaginable (Akhmetiev et al., 2009).

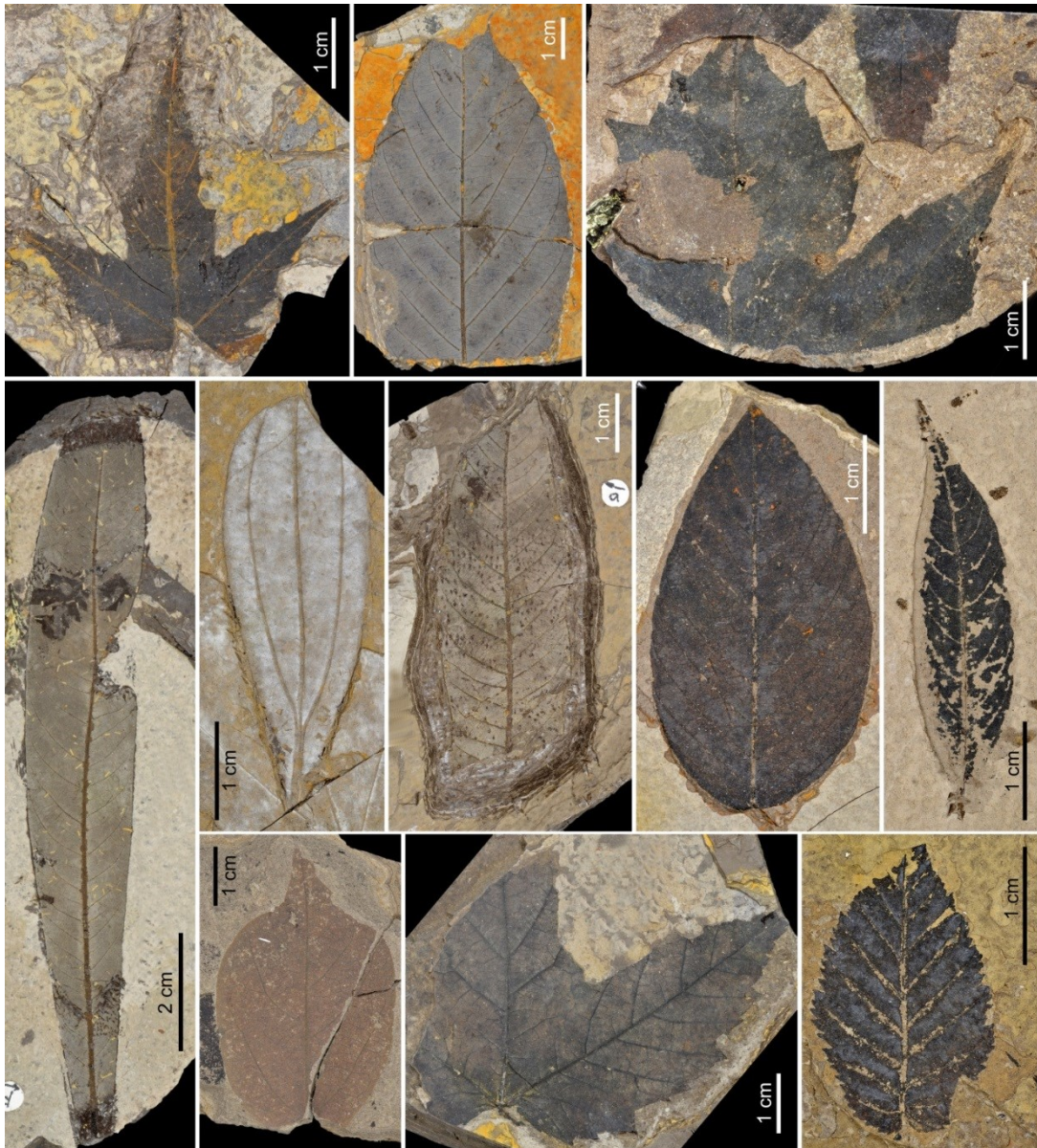


FIGURE 9. Typical association of plant organs derived from volcanic deposits with high diversity and predominantly very good preservation (example from site Kleinsaubernitz (collection SNSD\_MMG\_Pb Ks and LA\_Ks) illustrating a variety of morphotypes and species).

### 2.3. Site characteristics

The investigated sites cover a time span of approximately 26 myr, whereof site Messel is considered to be the oldest site at the Ypresian/Lutetian boundary in the early Eocene and site Linz represents the youngest site from the early Aquitanian (see chronostratigraphical chart in Figure 1 and Figure 11). Tables 1 and 2 list stratigraphic information and age determination for the single sites containing *Rhodomyrtophyllum reticulosum* (Table 1) and *Platanus neptuni* (Table 2) leaf remains.

The floral lists of all investigated sites can be found in the supplementary information (Appendix A).

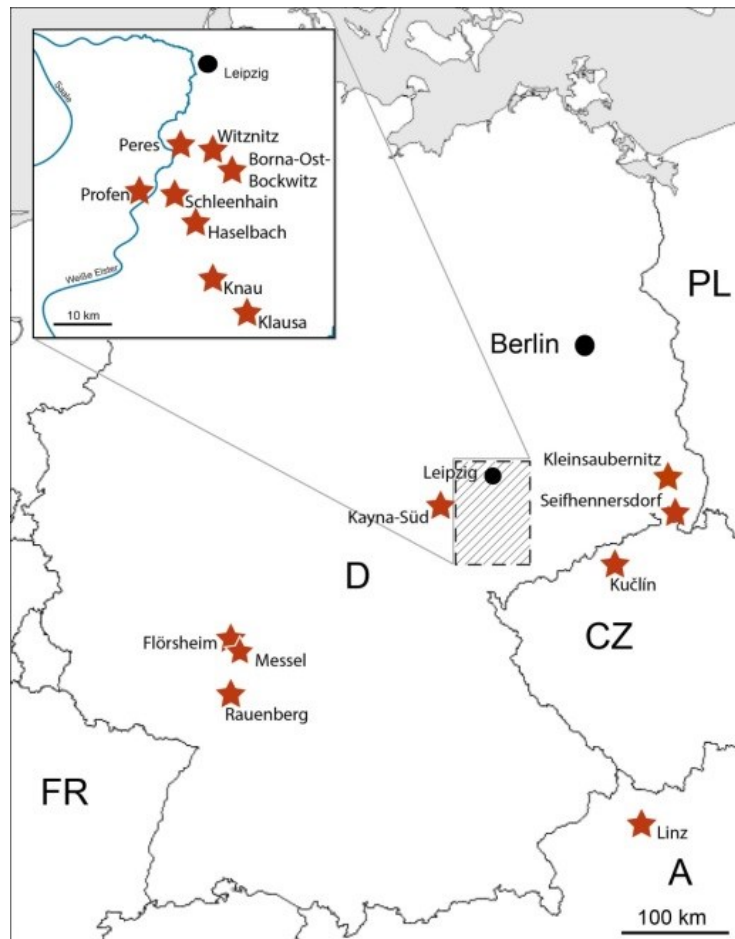


FIGURE 10. Location of investigated sites in Germany, Austria and the Czech Republic (the sites within the striped frame represent the Weiße Elster Basin sites).

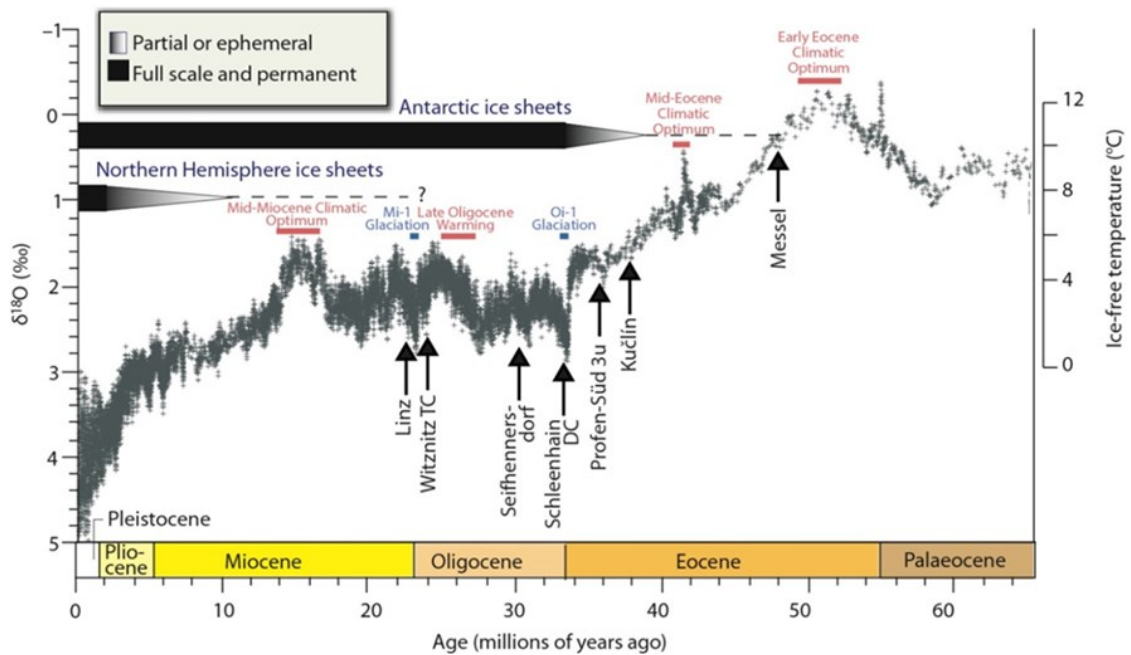


FIGURE 11. Stratigraphic position of selected sites and their correspondence to the Cenozoic paleoclimate evolution, modified from Zachos et al. (2008).

**Messel.** The Messel pit (Sprendlingen Horst, Hesse, Germany) belongs to one of the best known and studied fossil sites in the Eocene. The laminated oilshale of the Middle Messel Formation (Felder and Harms, 2004) formed through the sedimentary infilling of a maar lake which lasted for approximately one myr (Mertz and Renne, 2005). Based on a drilling in 2001 the fossil bearing sediments were dated to 48.27 to 48.11 myr (Lenz et al., 2014) which places the formation of the maar lake due to phreatomagmatic activity into the early Eocene. During mining and later scientific excavations the fossil flora and fauna was studied intensively. In terms of excellent preservation, the fossil leaves were systematically studied (Engelhardt, 1922; Sturm, 1971; Wilde, 1989; Wilde, 2004). Also studies on fossil fruits and seeds, wood, flowers and palynomorphs enhanced the knowledge of evolutionary, climatic and environmental processes. The flora was systematical treated regarding the leaf remains by Wilde (1989) and Collinson et al. (2012) for carpological remains. Dominating taxa, represented by leaves can be found within the Juglandaceae, Theaceae, Lauraceae and Leguminosae (Wilde, 1989). Collinson et al. (2012) found most carpological remains within the families of Menispermaceae, Icacinaceae, Vitaceae and Mastixiaceae. Paleoecological and taphonomical studies stated the plant assemblage as mainly autochthonous. The vegetation surrounding the Messel lake can be interpreted as a

subtropical inland forest (e.g. Engelhardt, 1922; Wilde, 1989) with trees like *Ailanthus*, *Meliosma*, diverse mastixioids, *Sloanea*, *Anacardium* and others as parts of a multiple canopy forest (Collinson et al. 2012). Palms grew near the lake shore on wet ground or swamp conditions and the fossil record indicates the presence of a variety of lianas, which framed the forest vegetation (Collinson et al. 2012).

**Kučlín.** The northern Bohemian site Kučlín (Czech Republic), bearing a fossiliferous diatomite, represents a classical European paleontological site (Kvaček and Teodoridis, 2011) providing a diverse flora and fauna with fishes and insects (Mach and Dvořák, 2011). The origin of the Kučlín lake is probably connected with tectonic movements in the Ohře graben zone which formed a basin in the late Eocene (Kvaček and Teodoridis, 2011; Mach and Dvořák, 2011). Alluvial and lacustrine sediments as well as eroded material of the underlying Cretaceous rocks are accumulated. The sedimentation took place in a presumably, in early stages of lake development, endorheic and salty basin and continued in a calmer, probably fresh-water lake. Ongoing sedimentation gradually transitioned to diatomitic deposits (Mach and Dvořák, 2011), which was interrupted either by landslide or mudflow deposits or by occasional drying out of the basin. Radiometric dating (Bellon et al., 1998) revealed an age estimate for the sediment overlying basaltoid rock of  $38.3 \pm 0.9$  Myr which is late middle Eocene (Bartonian) to early late Eocene (Priabonian) according to the most recent International Chronostratigraphic Chart (ISC v2016/12; Cohen et al., 2013, updated). These diatomites (‘Papierschiefer’) and silicified diatomites bear plant impressions (Kvaček and Teodoridis, 2011; Mach and Dvořák, 2011). Most of the plant macrofossils are preserved as leaf impressions. As almost no coalified material is available, the cuticle is not preserved. Morphological features and even fine details of the venation are often clearly visible and taxonomic determination was done, regarding leaf morphology. Main focus had lain on the paleoenvironmental studies (Kvaček and Teodoridis, 2011). Beside leaves, also fruits and seeds are available. The diverse flora of Kučlín is interpreted by Kvaček and Teodoridis (2011) as mainly derived from the zonal vegetation, i.e. notophyllous evergreen broadleaved forests, and to very minor extend from azonal associations growing in the littoral zone of the ancient lake. Comprising the composition of the fossil plant assemblage, the landscape can be described as being flat with surrounding moderate uplands (Kvaček and Teodoridis, 2011). A high proportion of recovered woody plants include mesophytic elements of Lauraceae, Juglandaceae, Elaeocarpaceae and even subxerophytic elements such as *Cedrelospermum* and *Ziziphus* (Kvaček and Teodoridis, 2011) which could be linked to the vegetation on the slopes. *Tetraclinis salicornioides*, *Platanus neptuni*, *Sterculia labrusca* and other deciduous

elements accompany evergreen forests. Aquatic and helophytic plants such as species of the Nymphaeaceae and Araceae are present and most common, whereas elsewhere common trees in basins and alluvial sandy facies such as *Eotrigonobalanus*, *Steinhauera* or *Sabal* are rare or even absent.

**Kayna-Süd.** The abandoned lignite opencast mine Kayna-Süd is situated in the eastern part of the Geiseltal Basin (Krumbiegel et al., 1976). The *Lagerstätte* was built during the middle Eocene until the late Eocene and was associated with subsrosion processes which deepened the basin and promoted the development of thick lignite seam complexes (Krumbiegel et al., 1976). The limnic-fluviatile sediments, overlying the lignite seams, were built in the late Eocene and contain rich floras, whereof the flora of Kayna-Süd (Ks 14 sensu Krumbiegel et al., 1976) is one of the most diverse and was collected between 1961 and 1964 (Mai and Walther, 2000). Krutzsch et al. (1992) date this flora into SPP zone 17/18. The Janus-cauldron (Januskessel; Krumbiegel et al., 1976), located in the Kayna-Süd basin is a 56 meter thick sediment profile consisting of an intercalation of (a) both gravel and sand, with preserved cones, conifer twigs, fruit and seed remains and leaves of dicots, e.g. *Steinhauera subglobosa*, *Rhodomyrtophyllum reticulosum*, Lauraceae, *Sterculia labrusca* and *Schisandra europaea* at the bottom of the profile, (b) a fine sand and silt layer with a similar paleobotanical facies (Krumbiegel et al., 1976) and (c) overlying thin rooted lignite layers (first and second Farnflöz) in nearly pure kaolonitic clays. Within this profile paleogeographical developments and changes in vegetation can be observed. Both leaf remains as carpological remains are incorporated into the analyses. The flora of (a) stems from a broad valley associated with a braided river system, where plant accumulation occurred in calm water. The flora of (b) does not refer to a fluviatile formation, but depicts the filling of little lakes and ponds whereas (c) shows both limnic and fluviatile facies. The flora was extensively studied by e.g. Barthel and Rüffle (1970), Barthel (1976a, b), Mai and Walther (1985), Rüffle and Litke (2000). As the single sites within the Janus-cauldron are not always documented, the flora summarizes the findings of the above described single, plant-bearing layers (Mai and Walther, 2000). Unless uncertainties in the origin of some specimen, it is possible to describe different vegetation types, present in the late Eocene of the Geiseltal with an evergreen forest dominated by *Doliosstrobos* and *Quasisequoia* for site (a) (*Trigonobalanus*-oak-Lauraceae forest; (Mai, 1967)). Limnic and swamp conditions which led to the development of site (c) are characterized by different fern communities (*Ruffordia subcretacea*, *Blechnum dentatum* and *Osmunda lignitum*). Representatives of water plants are *Eichhornia*, *Monochoria*, *Ottelia* and *Vallisneria* (Mai and Walther, 2000). Accessory elements in this evergreen flora are deciduous holarctical elements such as

*Asimina germanica*, *Decodon gibbosus* and *Glyptostrobus borysthenica* (Mai and Walther, 2000).

**Profen-Schwerzau ZC.** The material was recovered by L. Kunzmann, J. Dietrich and D. Hennig in 2010 and 2011 in the Weißelster Basins opencast mine Profen in Sachsen-Anhalt and comes from the lower part of the Zeitz Sand Complex (Zeitz Member; Borna Formation) representing the lower part of SPP zone 17/18 (Krutzsch, 2011; Moraweck et al., 2015) and comprises mainly leaves, but also fossil wood, seeds and fruits (Dietrich, 2012). The leaves are present either coalified or as impression. Dominant species are *Rhodomyrtophyllum reticulosum*, cf. *Phoenicites borealis* and *Toddalia hofmannii* accompanied by the fossil fruit *Steinhauera subglobosa* (Altingiaceae) (Dietrich, 2012). The flora has been reconstructed representing a *Steinhauera-Rhodomyrtophyllum* riparian forest and is typically developed in sites with high and fluctuating ground water conditions (Mai and Walther, 1985; Glinka and Walther, 2003) which are typically developed in coastal and floodplain environments. The abundance of palms is conspicuously high and could be interpreted with either taphonomic processes or with habitat related features (Dietrich, 2012), as palms are pioneers and may mirror erosion and depositional settings in these highly disturbed environments. A preliminary analysis of the respective pollen spectra from this site additionally found at least 5 different palm taxa (e.g. *Calamus*), which is more than the macrofossil record attains (Kunzmann et al., 2016).

**Profen-Süd LC.** The fossil material was collected in 1999 in the opencast mine Profen (Sachsen-Anhalt) and comes from the underbedding layer of the main lignite seam (Kunzmann et al., 2016) which lithostratigraphically corresponds to the uppermost part of the Zeitz Member, consisting of alluvial braidplain sediments (Luckenau Clay complex) of the Borna Formation (Standke et al., 2010; Kunzmann et al., 2016). The position of the Luckenau Clay complex according to regional Spore-Pollen-Paleogene (SPP) zones is not fully resolved and the complex can be placed into either SPP zone 17/18 (latest Bartonian) or 18 (between 18m and 18o; early to middle Priabonian) according to Krutzsch (2008, 2011) which corresponds to the Zeitz FC. The flora is currently under taxonomic investigation by L. Kunzmann and C. Müller. First results show high abundances of typical riparian elements such as *Rhodomyrtophyllum reticulosum* and *Steinhauera subglobosa*. Fagaceae, Theaceae and conifers are missing and Lauraceae are rare. This is contrary to other Weißelster Basin assemblages from the Zeitz FC. Due to the occurrence of species, until now unknown from the Zeitz FC (Kunzmann et al., 2016), this flora will be of importance for future phytosociological and developmental questions (Kunzmann et al.,



2016). Beside differences in the composition of the flora, also differences in the abundance of leaf forms and morphological varieties are detectable. Additional to taxonomic studies a master thesis dealing with the abundance and diversity of insect folivory was conducted (Müller, 2016).

**Profen-Schwerzau 1u.** The taphocoenoses stems from floodplain deposits beneath the main lignite seam complex of the Borna Formation which is correlated by Krutzsch (2011) to SPP zone 18. This zone is considered by the same author as early to middle Priabonian. The exact lithostratigraphic position of the site is not yet resolved (Wallendorf Member of the Profen Formation vs. Zeitz Member of the Borna Formation) and thus the stratigraphic position ranges from late Bartonian to early Priabonian. The flora is interpreted as notophyllous evergreen broad-leaved (unpubl.; pers. communication with Franziska Ferdani, Dresden) and is currently under taxonomic investigation.

**Schleenhain 2o.** The material of the plant-bearing horizons of the opencast mine Vereinigtes Schleenhain (Weißelster Basin) was collected in 2008 and 2009 and taxonomically investigated and published by Hennig and Kunzmann (2013). The respective flora comes from isolated sediment blocks, which fell down from high-wall during the excavation (Hennig and Kunzmann, 2013). The material was considered to be part of the roof of lignite seam 23u and might belong to SPP subzone 18m (Kunzmann et al., 2016). The clay- and silt-dominated sediment is interpreted to come from an abandoned channel of the meandering river system. The taphocoenoses contains leaves, nicely preserved fruits and seeds, conifer branches, cone scales and wood fragments (Hennig and Kunzmann, 2013). Dominant species are *Eotrigonobalanus furcinervis* (more than 40 %) and *Rhodomyrtophyllum reticulosum* (more than 25 %). Together with the occurrence of the fossil fruit *Steinhauera subglobosa* and *Rhodomyrtophyllum* the distribution of the *Rhodomyrtophyllum-Steinhauera* riparian forest can be stated. Other species, underlining this azonal, swampy character of vegetation are the evergreen subtropical conifer *Quasisequoia couttsia* and *Vaccinioides ovosimilis*. The high abundance of the zonal *Eotrigonobalanus furcinervis* points out the occurrence of Fagaceae-Lauraceae forests, although the Lauraceae are only accessory elements in the taphocoenoses, which are an important vegetational unit in the late Eocene (Mai, 1995).

**Haselbach 2-3 mi.** The plant material of this site comes from the intercalated bed between lignite seam 23u and 23o (SPP zone 18uo; sensu Krutzsch, 2011) from the former opencast mine Haselbach. This diverse flora belongs to one of the richest in species in the Weißelster

Basin and was collected in 1962, 1965 and 1969 (Mai and Walther, 2000). The flora contains conifer twigs, angiosperm leaves and a high proportion of fruits and seeds. Dominant species are *Quasisequoia couttsiae*, *Daphnogene lanceolata*, *Eotrigonobalanus furcinervis*, and *Rhodomyrtophyllum reticulosum* (Mai and Walther, 1985). Mai and Walther (2000) furthermore describe the presence of an *Eotrigonobalanus*-Lauraceae forest with conifers. Lacustrine conditions are proven by the distribution of numerous water- and swamp plants, e.g. *Cladiocarya*, *Ottelia*, *Taxodium*, *Limosella* and *Osmunda* (Mai and Walther, 2000).

**Peres 3u.** From the lignite opencast mine Peres, today part of the opencast mine Vereinigtes Schleenhain, plant-bearing sediments were recovered from the main lignite seam (seam 2/3o after Standke et al., 2010; lignite measure IV in Krutzsch, 2008) in 1970 (Mai and Walther, 2000) which is dated to SPP zone 18ou sensu Krutzsch (2011). The clayey sediments bear a rich carpological flora, complemented by only five species proven by leaves. The composition of the flora leads to the distinction of a zonal *Eotrigonobalanus*-Lauraceae forest and riparian monocot-fern-association (Mai and Walther, 2000). *Ottelia minutissima* and *Aldrovanda ovata* indicate the presence of small lakes and ponds.

**Profen-Süd 3u.** The flora of site Profen-Süd 3u comes from the underburden of the upper part of the main lignite seam (seam 2/3o after Standke et al., 2010; lignite measure IV in Krutzsch, 2008) in the Bruckdorf Member (Mai and Walther, 2000) and was collected in 1975. Krutzsch (2008) classified these lignite measures belonging to SPP zone 18ou. The composition of the flora is similar to the slightly older site Profen-Schwerzau ZC with species of both conifer-Lauraceae forests and waterplant-swamp associations together with Fagaceae-Lauraceae forests (Mai and Walther, 2000). *Broussonetia rugosa* is the only new immigrant.

**Schleenhain 3u.** The investigated flora comes from the underlying bed of the main lignite seam (seam 2/3o after Standke et al., 2010; lignite measure IV in Krutzsch, 2008) in the Bruckdorf Member, Borna formation (Ferdani, 2014), which is dated to SPP zone 18ou sensu Krutzsch (2011). Fossil wood, leaves, fruits and seeds are preserved, whereby only the fruit *Steinhauera subglobosa* beside the leaves is taxonomically determined (Ferdani, 2014). Dominant species are *Eotrigonobalanus furcinervis*, *Quasisequoia couttsiae* and *Rhodomyrtophyllum reticulosum*. The dominance of Lauraceae is conspicuous. The flora covers both elements of zonal vegetation namely a Fagaceae-Lauraceae forest and azonal backswamp and riparian communities (Ferdani, 2014).

site	Stratigraphy and dating				
	Chronostratigraphic unit	lithostratigraphy		Biostratigraphy (SPP-zone)	Age [Ma]
		Formation/Member	Horizon/bed		
Schleenhain 3u	Priabonian	Borna-Formation, Bruckdorf-Member	seam 3, underlying bed	18 ou	35.8-35.4
Profen-Süd 3u	Priabonian	Borna-Formation, Bruckdorf-Member	seam 3, underlying bed	18 ou	35.8-35.4
Peres 3u	Priabonian	Borna-Formation, Bruckdorf-Member	seam 3, underlying bed	18 ou	35.8-35.4
Haselbach 2-3 mi	Priabonian	Borna-Formation, Bruckdorf-Member	main intercalated bed	18 uo	36.7-36.4
Schleenhain 2o	Priabonian	Borna-Formation, Bruckdorf-Member	seam 2, overlying bed	18 m	36.4-36.2
Knau	Priabonian	Borna-Formation, Bruckdorf-Member	Zeitz Sand Complex	18	37.0-34.8
Klausa	Priabonian	Borna-Formation, Bruckdorf-Member	Zeitz Sand Complex	18	37.0-34.8
Profen-Süd LC	Latest Bartonian/ Early or middle Priabonian	Borna-Formation, Zeitz Member	Luckenau Clay Complex	?17/18 to 18	37.5-34.8
Kayna-Süd	Bartonian	Janus-cauldron	56m of sediments of different origin	17/18	38.5-38.0
Profen-Schwerzau ZC	Bartonian	Borna-Formation, Zeitz Member	Zeitz Sand Complex	17/18	38.5-38.0
Messel	Ypresian/ Lutetian	Middle Messel Formation	Layers of laminated oilshale	not determined	48.27 - 48.11

TABLE 1. Characteristics of the study sites containing *Rhodomyrtophyllum reticulosum* leaves, regarding stratigraphy and dating (abbreviations: Ma – million years, SPP-zone – Spore-Pollen Paleogene zone sensu Krutzsch (2011) and Krutzsch et al. (1992)).

**Klausau.** The abandoned Klausau sand pit (community of Nobitz, Thüringen) exposes fluvial sediments of the Zeitz Sand Complex of the Borna Formation, deposited at the southern margin of the Weißelster Basin (Rascher et al., 2005) and collected in 1972. According to Mai and Walther (2000) and Krutzsch (2011) the deposits are an equivalent of the Bruckdorf Member of the Borna Formation and thus are placed in SPP zone 18 generally. The plant taphocoenoses of Klausau was studied by Mai and Walther (1985, 2000) and represents a riparian forest within notophyllous evergreen broad-leaved vegetation. Dominant species are *Eotrigonobalanus furcinervis* and *Rhodomyrtophyllum reticulosum* (Mai and Walther, 1985). *Platanus neptuni*, *Daphnogene cinnamomifolia* f. *lanceolata* and *Polyspora saxonica* are predominant. The vegetation comprised Lauraceae-conifer forests with *Doliosstrobilus taxiformis* as another predominant species in the taphocoenoses. Thermophilic water plants, such as *Vallisneria stylosa* and *Azolla prisca* indicate warm, shallow and eutrophic ponds (Mai and Walther, 2000).

**Knau.** The flora derived from one of several clay lenses in a layer of 20 meters of late Eocene sands and gravel. It was excavated in 1971 (Mai and Walther, 2000). The flora from this abandoned channel fill is similar to that of Klausau with only minor variations. *Doliosstrobilus taxiformis*, *Eotrigonobalanus furcinervis* and *Rhodomyrtophyllum reticulosum* are dominant species.

**Borna-Ost DC.** The Borna-Ost DC assemblage was excavated from estuarine-fluviatile siliciclastics 3-4 meters above seam 2/3 (Standke et al., 2010; lignite measure IV in Krutzsch, 2008) in the lignite opencast mine Borna-Ost (Mai and Walther, 2000). The sediments are regarded as equivalents of the predominantly brackish-marine Domsen Member of the Borna Formation (Standke et al., 2010). Based on regional palynostratigraphy (Krutzsch, 2011) the Domsen Member is placed in SPP zone 19 and parallelized to late Priabonian (Krutzsch, 2011) and thus most likely older than the Eocene-Oligocene boundary. Although sampled in 1971, the leaf assemblage was undetermined until recently (Müller, 2014) while the carpological remains were investigated and published (Mai and Walther, 1985, 2000). The taphocoenoses mainly consists of highly fragmented coalified leaves and scattered seeds (Müller, 2014). Conspicuously *Doliosstrobilus taxiformis*, *Rhodomyrtophyllum reticulosum* and *Steinhauera subglobosa*, type elements of 'subtropical' associations in the late Eocene Zeitz FC, are missing (Müller, 2014; Kunzmann et al., 2016). Dominant species are *Platanus neptuni*, *Polyspora saxonica* and different species of Lauraceae (Müller, 2014). Based on both carpological remains (Mai and Walther,

2000) and leaves (Müller, 2014) the presence of a Lauraceae-monocot forest is proven by *Quasisequoia couttsiae* as the dominant conifer.

**Schleenhain HC.** The Schleenhain HC flora derived from the Haselbach horizon of the Gröbers Member, Böhlen Formation (Standke et al., 2010). According to the palynostratigraphic concept (Krutzsch, 2011) the horizon is called basal most Oligocene based on the first appearance of the regional key element *Boehlensispollis hohlii* (Krutzsch, 2008). However, the stratigraphic position of the Haselbach horizon is not yet resolved (Steinthorsdottir et al., 2016). Earliest Oligocene is probable but conclusive evidence via linkage to the global marine scale is currently not available. Even a correlation to the latest Eocene cannot be excluded. In general, the flora is interpreted as mixed deciduous evergreen (Kunzmann, 2012; Kunzmann and Walther, 2012) and provides the first massive occurrence of 'modern Arcto-tertiary elements' (Kvaček, 1994) into central Germany.

**Rauenberg.** The Rauenberg assemblage, located in the Oberrheingraben originates from the second and third Rupelian transgression (Maxwell et al., 2016) when marine and brackish sediments were deposited in the northern Oberrheingraben. The fossil plant bearing strata were formed during the second Rupelian transgression (Bodenheim Formation) and yield a rich and diverse fauna including mammals, fishes, birds and insects as well (Micklich and Hildebrandt, 2010). Based on the fish fauna the Fische Schiefer Subformation of the Bodenheim Formation is placed into the regional zones MP 22-23 (Frey et al., 2010). The absolute age is therefore about 32.4–30.5 Ma (Grimm et al., 2011). The fossil assemblage comprises both marine and terrestrial elements (Maxwell et al., 2016). The depositional depth of the fossils is still a matter of debate ranging from shallow water (shallow water fish fauna) to 100-200 m depth according to the foraminifera (Grimm et al., 2002; Frey et al., 2010). However, there is almost no reliable information about the distance of the ancient coastline from the burial place of the plant fossils. The terrestrial plant record comprises 66 species, including 14 new species (Kovar-Eder, 2016). Dominant elements are the Lauraceae at the family level, *Pinus* at generic level and *Platanus neptuni* and *Daphnogene cinnamomifolia* at species level (Maxwell et al., 2016). Around 35% of the taxa were presumably trees, the same percentage represents small trees and shrubs. The proportion of woody evergreen angiosperms amounts more than 60% whereby less than 20% are stated as deciduous. The occurrence of *Ceratozamia floersheimensis*, *Laurus abchasica* and *Sloanea* clearly point out the affinity to the Oligocene and even Miocene plant record of central Europe (Maxwell et al., 2016). The composition of this highly allochthonous assemblage hampers the distinction of different forest types and vegetation

units (Maxwell et al., 2016). The predominance of *Pinus* could indicate the presence of coastal pine forests on sandy soils near the coast, together with co-occurring *Daphnogene cinnamomifolia* and *Laurophyllum pseudoprinceps*. *Platanus neptuni* may have grown in both zonal and azonal habitats along streams. The majority of taxa reflect zonal vegetation types which is also supported by comparison of outecological traits of most similar living relatives (Integrated Plant Record Vegetation Analyses (IPR; Kovar-Eder and Kvaček, 2007), pointing out affinities to evergreen sclerophyllous broad-leaved forests (Kovar-Eder, 2016). The Rauenberg flora shows more affinities to floras from the Paratethys region, for example Linz (Kovar, 1982) than to those from the Leipzig Embayment and volcanic floras from Saxony and Czech Republic (Kovar-Eder, 2016).

**Flörsheim.** The fossil plant bearing strata of Flörsheim (Mainz Basin, Hessen, Germany) belong to the Bodenheim Formation and Hochberg Subformation (‘Rupelton’ horizon) which is dated by regional NP zonation as NP 23 (about 31-29.9 Ma, early Oligocene; Grimm et al., 2011) as the Rauenberg assemblage, as derived from the same subformation (Maxwell et al., 2016). The plant assemblage includes a very diverse flora dominated by coriaceous broad-leaved elements (Kvaček, 2004). High diversity is recognized within the Lauraceae and Fagaceae. Most abundant taxa are for instance *Platanus neptuni*, *Tetraclinis salicornioides*, different *Laurophyllum* species, *Daphnogene cinnamomifolia* and cones of *Pinus* (Kvaček, 2004). The Flörsheim assemblage represents the near-shore lowland vegetation outside of lignite basins. This near-shore environment (land in about 4 km distance; pers. comm. K. Grimm, Mainz) is characterized by badly ventilated water and certain water currents that were able to transport relatively large tree trunks (Grimm and Grimm, 2003). The clay-silt sediment was putatively deposited in a water depth of >100 m based on the associated fauna. Although biased by taphonomic processes one can recognize different vegetation types and the composition from the fossil record. Most elements can be assigned to express the composition of the forests along the coastline (*Platanus neptuni*, *Laurophyllum* cf. *villense*) on mesic substrates, whereas riparian elements are present but rare (*Taxodium*, *Chamaecyparites*, *Alnus*, *Carya*) due to longer transport distances (Kvaček, 2004). The flora has been dedicated to the FC Nerchau-Flörsheim, defined by Mai (1995) but has been recently revised by Kovar-Eder (2016).

**Seifhennersdorf.** In Seifhennersdorf the plant bearing deposits come from a natural catchment lake whereby the accumulation of the water body is most likely caused by abandonment of a valley by a lava flow (trap basalt). The basaltoid tuff that covers the sedimentary complex with siliciclastic strata, diatomites, and coal seams has been

radiometrically dated by Bellon et al. (1998) who obtained a K-Ar age of  $30.7 \pm 0.7$  Ma. The richest fossiliferous deposit is found within the laminated diatomite (Walther and Kvaček, 2007). As most leaves are highly coalified, preparation of cuticles was not always possible, which in some cases prevented accurate taxonomic determination, whereby specimen preserved in fine-grained pyroclastics displayed morphological features excellently. Nevertheless, 84 angiosperm species and five conifers were determined (Walther and Kvaček, 2007), which makes the Seifhennersdorf fossil site unique in central European Tertiary research. Alongside the embedded plant remains, namely foliage, leaves and seed, also a diverse vertebrate and insect fauna can be found (Walther and Kvaček, 2007). Most abundant species are *Taxodium dubium*, *Dusembaya seifhennersdorfensis*, *Carpinus roscheri* and *Carpinus grandis*, *Carya fragiliformis*, *Rosa lignitum* and *Acer angustilobum*. Based on autecological correlations several associations have been determined (Walther and Kvaček, 2007), e.g. *Taxodium-Nyssa* swamp forests, diversified mixed mesophytic forests and Hickory-oak flooded riparian forests. After correlation of the Seifhennersdorf assemblage with those Oligocene plant assemblages from central and west Europe, Kvaček and Walther (1998) defined the FC Seifhennersdorf-Kundratice.

**Kleinsaubernitz.** The Kleinsaubernitz maar is part of a Guttau group of maars north of the city of Bautzen (Standke, 2008). There is no evidence that a local volcano range did exist except for two very small slag hills in proximity of the large maar (Suhr and Goth, 2008). The flora and fauna come from lacustrine laminated oil shales and diatomites (Walther, 1999). Unfortunately, all radiometric dating investigations failed in getting a reliable age estimate for the maar eruption. However, palynological studies revealed a correlation with regional SPP zone 20G (Goth et al., 2003) which is supposed to be early late Oligocene (Krutzsch, 2011). The plant assemblage comprises 63 taxa derived from leaf remains and 17 species proven by carpological remains (Mai, 1997; Walther, 1999). 22 of 44 taxonomically unambiguously determined species are deciduous, arcto-tertiary and 22 laurophyllous paleo-subtropical elements. The diversity and high abundance of conifers is conspicuously. Laurophyllous and thermophilic taxa are very abundant both concerning the amount of taxa and in the number of specimens (Walther, 1999). Typical thermophilic elements are *Magnolia maii*, *Kadsura senftenbergensis*, *Ilex knoblochii* and *Matudaea menzelii*. Dominant evergreen species are *Eotrigonobalanus furcinervis* ssp. *haselbachensis* and *Quercus praeherana*, deciduous elements can be found within the Aceraceae, Corylaceae and Betulaceae. Archaic taxa e.g. *Majanthemophyllum petiolatum*, known since the middle Eocene and typical Miocene elements like "*Illicium*" *limburgense* co-occur. The majority of fossil plant species belong to zonal vegetation types (mixed mesophytic forests

with transition to Broadleaved Evergreen Forests (Mai and Walther, 1978), azonal elements growing in the narrow littoral of the maar lake are only accessory.

**Borna-Ost-Bockwitz TC.** The plant assemblage of Borna-Ost-Bockwitz summarizes the findings from the abandoned lignite opencast mine Bockwitz, sampled from 1982 till 1988 and from the abandoned lignite opencast mine Borna-Ost, collected in 1973 and 1974 (Mai and Walther, 1991). Both mines are situated in the Weißelster Basin and the respective plant assemblage comes from the basal part of the fluvial Thierbach Clay Complex of the Thierbach Member, Cottbus Formation (Standke et al., 2010). The Thierbach Clay is correlated by Krutzsch (2011) to SPP zone 20I (early Neochattian, late Oligocene). Dominant species in both sites are *Populus germanica*, *Fagus saxonica*, *Taxodium dubium*, *Carpinus grandis* and *Acer haselbachense* (Mai and Walther, 1991). Arcto-tertiary elements are prevailing with *Fagus saxonica* as most dominant species beside riparian elements as *Liquidamber*, *Ulmus* and *Populus* (Mai and Walther, 1991). As the leaves are not or only to a minor degree fragmented, the flora of Bockwitz is classified as being mainly autochthonous. The flora of Borna-Ost exposes the same character elements as described for Bockwitz with a predominance of deciduous taxa like *Cyclocarya cyclocarpa*, *Platanus neptuni*, *Carpinus grandis*, *Fagus saxonica* and *Liquidamber europaea*.

**Witznitz TC.** The flora of Witznitz TC comes from an abandoned channel of the Thierbach Clay Complex exposed in the former lignite open cast mine Witznitz and was taxonomically determined by J. Hammer (unpubl. material). The plant assemblage is assigned to SPP zone 20I sensu Krutzsch et al. (2011). The flora comprises 37 taxa, described from leaf and carpological remains and shows the typical elements of the Thierbach FC. Dominant species are *Populus germanica*, *Taxodium dubium*, *Daphnogene cinnamomifolia* and *Salix varians*. The distance between sites Borna-Ost-Bockwitz and Witznitz TC is about 7.5 km whereby the latter is located closer to the coastline.

**Witznitz WC.** The considered plant assemblage of Witznitz WC is an aggregation of plant assemblages sampled separately in the abandoned lignite opencast mine Witznitz. Both assemblages derived from estuarine sediments of the Witznitz complex are correlated to SPN zone I/II (Krutzsch, 2011). The chronostratigraphic position is estimated by Krutzsch (2011) as upper Neochattian near the Oligocene-Miocene boundary. One part comes from the same profile as the above described flora of Witznitz TC, representing the upper part of the profile where a change in sedimentation and floristic elements is obviously visible (unpubl. documentation of J. Hammer) which is supposed to be related to the FC



Mockrehna-Witznitz (Mai and Walther, 1991; Mai, 1995) and was studied and taxonomically determined (both leaves and carpological remains) by J. Hammer (unpubl. material). In contrast to Witznitz TC *Acer*, *Alnus*, *Fagus* and *Carpinus* species are rare or even missing. The abundance of thermophilic elements, such as *Cunninghamia miocenica*, *Magnolia kristinae* and *Kadsura senftenbergensis* indicate warmer climate conditions and clearly differs from the lower part of the profile. This flora is of the mixed deciduous evergreen type (Mai and Walther, 1991; Kvaček and Walther, 2001). The other part of the aggregated plant assemblage comes from a 0.1 to 0.2 m thin layer of densely stacked mummified leaves with a predominance of *Laurophyllum acutimontanum* (60%). Other species in this assemblage, which is very poor in species, are *Platanus neptuni*, different *Laurophyllum* and *Daphnogene* species and *Eotrigonobalanus furcinervis*. Some of the mummified leaves are fixed on preparation slides, whereas the main part of this leaf litter bed is not separated and determined.

**Linz.** The taphocoenoses from Linz (Austria; Kovar, 1982) comes from marine sediments of the Puchkirchen Group (Kovar, 1982; Grunert et al., 2010), the formerly so-called Älterer Schlier (Kovar, 1982), which is part of the Ebelsberg Formation and is dated to nannoplankton zone NN 1 (Rupp and Ćorić, 2012) of the Neogene (Aquitanian). Dominant subtropical to temperate species are e.g. *Cunninghamia mioceneica*, *Pinus* sp., *Cephalotaxus* sp., *Laurophyllum pseudoprinceps*, *Fagus* sp., *Myrica lignitum* and *Sabal major* (Kovar, 1982). Both characteristic Eocene and Oligocene elements (*Quasisequoia couttsiae*, *Platanus neptuni*, *Laurophyllum acutimontanum*, *Ulmus* sp.) and Miocene to Pliocene elements (*Castanopsis toscana*, *Buxus* sp.) are preserved (Kovar, 1982). Kovar (1982) reconstructed three plant communities: riparian vegetation units with *Platanus neptuni* as most dominant element, *Taxodium*, *Alnus*, *Acer* and *Ulmus*; pine communities on oligotrophic, acidic and sandy soils with *Pinus* species, *Comptonia acutiloba*, *Engelhardia* and *Sabal major* and mesophytic forests represented by a variety of elements, such as *Cunninghamia miocenica*, *Sequoia abietina*, Lauraceae, *Buxus egeriana*, several temperate deciduous species of *Fagus*, *Quercus*, *Betula*, *Carpinus*, *Ulmus* and *Acer*.

site	Stratigraphy and dating				Sediments		Depositional setting		
	Chronostratigraphic unit	lithostratigraphy	biostratigraphy	age [Ma]	facies type	sediments	marine-offshore	volcanic	coastal/alluvial plain
Linz	Aquitanian	Ebelsberg Formation (Grunert et al., 2010)	NN 1 (Rupp and Ćorić, 2012)	~22-23	pelagial	pelits ('Rupelton')	X		
Witznitz WC	Chattian or Chattian-Aquitanian boundary	Cottbus Formation, Thierbach Member (Standke et al. 2010)	SPN/SPP zone I/II (Krutzsich 2011)	~23-24.5	estuarine	organic-rich silty leaf litter beds (overbank?)			X
Borna-Ost-Bockwitz Witznitz TC	Chattian	Cottbus Formation, Thierbach Member (Standke et al., 2010)	SPP zone 20I (Krutzsich 2011)	~24.5-25.5	fluvial	abandoned channel fill clastics (silty clay)			X
Kleinsaubernitz	Chattian	Gutttau Group (Standke, 2008)	SPP zone 20G (Goth et al., 2003)	~26-27	lacustrine (maar)	'warved' diatomite		X	
Seifhennersdorf	Rupelian	not determined	not determined	30.7 ± 0.7 (Bellon et al., 1998)	lacustrine	diatomitic pelite		X	
Flörsheim	Rupelian	Bodenheim Formation and Hochberg Subformation (Grimm et al., 2011)	NP 23 (Grimm et al. 2011)	31-29.9	(sublitoral)-pelagial	pelits ('Rupelton')	X		
Rauenberg	Rupelian	Fischschiefer Subformation (Grimm et al., 2011)	MP 22-23 (Frey et al., 2010)	32.4-30.5	(sublitoral)-pelagial	pelits ('Rupelton')	X		

site	Stratigraphy and dating				Sediments		Depositional setting		
	Chronostratigraphic unit	lithostratigraphy	biostratigraphy	age [Ma]	facies type	sediments	marine-offshore	volcanic	coastal/alluvial plain
Schleenhain HC	Rupelian	Böhlen Formation, Gröbers Member (Standke et al. 2010)	SPP zone 20 A/B (Krutzsich 2011)	~33-33.9	fluvial	abandoned channel fill clastics (pelits)			X
Borna-Ost DC	Priabonian	Borna Formation, Domsen Member (Standke et al. 2010)	SPP zone 19 (Krutzsich 2011)	34-35 (?)	estuarine	silty leaf litter bed (overbank?)			X
Klausä	Priabonian to Bartonian	Borna Formation, Bruckdorf Member (Standke et al. 2010)	SPP zone 18 (Krutzsich 2011)	~35-37	fluvial	abandoned channel fill clastics (pelits)			X
Profen-Schwerzau 1u	Priabonian to Bartonian	Profen Formation, Wallendorf Member vs. Borna Formation, Zeitz Member (Standke et al. 2010)	SPP zone 17 or 17/18 (Krutzsich 2011)	~37-38	fluvial, alluvial	abandoned channel fills, floodplain deposits			X
Kučlín	Priabonian to Bartonian	not determined	not determined	38.3 ± 0.9 (Bellon et al. 1998)	lacustrine	diatomite, partly 'Papierschiefer' (paper shale)		X	

TABLE 2. Characteristics of the study sites containing *Platanus neptuni* leaves, regarding stratigraphy, sedimentological and depositional setting (abbreviations: Ma – million years, NN – Nannoplankton zone, MP – Mammal Paleogene zone, SPP zone – Spore-Pollen-Palaeogene zone, SPN zone – Spore-Pollen Neogene zone).

### 3. Selection of taxa and brief characteristics

#### 3.1. Fossil plant material

##### 3.1.1. *Rhodomyrtophyllum reticulosum* (Myrtaceae)

Leaves of *Rhodomyrtophyllum reticulosum* are simple, entire and sometimes thickened at the margins. The lamina is leathery, robust, symmetric and only in few specimens asymmetrically shaped (Glinka and Walther, 2003). Leaf size is very variable and leaf length ranges from at least 35 to 135 mm (mean 80 mm) and leaf width varies between 11 and 90 mm with mean leaf width of approximately 40 mm (Glinka and Walther, 2003). Leaves are shaped elliptic (Figure 12A) or obovate (Figure 12B; Knobloch et al., 1996; Glinka and Walther, 2003). The base is widely to narrow cuneate, the apex round or emerginate (Figure 12A, D). The petiole is thicker than the midrib vein (Figure 12C), often 12 to 21 mm long (Glinka and Walther, 2003). The midrib vein is robust and pronounced on the abaxial site. The venation is brachydromous with several, densely disposed secondaries per leaf (Figure 12D), arising from the midrib in an angle of circa 50-60°, running slightly parallel to each other, forming loops towards the margin (Knobloch et al., 1996) and parallel veins along the lamina margin (Glinka and Walther, 2003). Slightly fainter intersecondaries (one) are running on the half distance to the lamina margin towards the lower secondary vein. The tertiary veins go parallel to the midrib vein and form squares (Knobloch et al., 1996).

The adaxial cuticle of *Rhodomyrtophyllum reticulosum* (Figure 12E) is rather thick and robust and often more cutinized than the abaxial cuticle (Knobloch et al., 1996). Epidermal cells are 10-25 µm in diameter, polygonal with very variable undulation of anticlines (Glinka and Walther, 2003). The abaxial cuticle inhibits apertures of glands and features, interpreted as trichome bases (Knobloch et al., 1996; Glinka and Walther, 2003) but no stomata. The abaxial cuticle features larger epidermal cells with 25-50 µm (Glinka and Walther, 2003), or even up to 60 µm in diameter (Knobloch et al., 1996), than present in the adaxial cuticle. The anticlinal walls of the mostly elongated epidermal cells are very variable in the degree of undulation, ranging from nearly straight to Ω-shaped (Figure 12F). Stomata are distributed both randomly within the intercoastal areas and sometimes grouped. The nearly round stomata (Figure 12F) are very variable in size (Knobloch et al.,

1996) ranging from length of 15-29  $\mu\text{m}$  and 15-28- $\mu\text{m}$  width (Glinka and Walther, 2003). The kidney shaped guard cells form the porus with 6-12  $\mu\text{m}$  in length and 5-10  $\mu\text{m}$  width. Stomata are mainly brachyparazytic (Figure 12F). Frequently giant stomata ('Riesenstomata'; sensu Glinka and Walther, 2003) occur, which can be cyclocytic with 4, 6, 8 or 12 subsidiary cells (Glinka and Walther, 2003). Giant stomata (Figure 12G) are present either within the intercoastal areas or on costae, where they can be almost 43  $\mu\text{m}$  long (Glinka and Walther, 2003). Larger pores and comparable smaller guard cells can be recognized. The abaxial cuticle also inhibits glands from 30-65  $\mu\text{m}$  in diameter with straight gland cell walls and a round or elongated porus. Glands are mostly present on costae and seldomly within the intercoastal areas (Glinka and Walther, 2003).

*Rhodomyrtophyllum reticulosum* is a predominant species in the Eocene plant assemblages (FC Scheiplitz and Zeitz) of riparian environments in the Weißelster Basin and only known by its leaves (Glinka and Walther, 2003). It often occurs together with fossil fruits of *Steinhauera subglobosa* (Altingiaceae) and thus defines and dominates the *Steinhauera-Rhodomyrtophyllum* riparian forests (Mai, 1995; Mai and Walther, 2000; Glinka and Walther, 2003). This riparian environment is characterized by ground-water table variations and accompanied by continuously erosion of river banks. *Rhodomyrtophyllum reticulosum* is unexceptional known from azonal environments, either from fluvial assemblages of the hinterland (Stare Sédlo formation; Knobloch et al., 1996) far from the coast or from the fluvial-lacustrine coastal plain assemblages of the Weißelster Basin (e.g. sites Profen and Schleenhain) and its surroundings (site Kayna-Süd). The occurrence of *Rhodomyrtophyllum reticulosum* in the Messel pit (Wilde, 1989) representing an ancient maar lake is also bound to a high water table. The determination of a most similar relative is accurately described in Glinka and Walther (2003), after the taxonomic determination of the fossil *Rhodomyrtophyllum reticulosum* was discussed in e.g. Bandaluska (1931), Ruffle and Jähnichen (1976) and Knobloch et al. (1996) (see Glinka and Walther, 2003 and citations in there). In Glinka and Walther (2003) 38 extant representatives of the Myrtaceae were examined focusing on similarities to the fossil species in morphological and anatomical characteristics. The authors found 16 species with documented accordance with either morphological or anatomical characters. Most species are assigned to the genera *Syzygium* (e.g. *S. aromaticum*, *S. cordatum*, *S. oleosum*, *S. revolutum*), *Eugenia* (*E. chrysantha*, *E. schiedeana*), *Psidium* (*P. littorale*, *P. guajava*) and *Myrica* (*M. citrifolia*, *M. coriacea*).

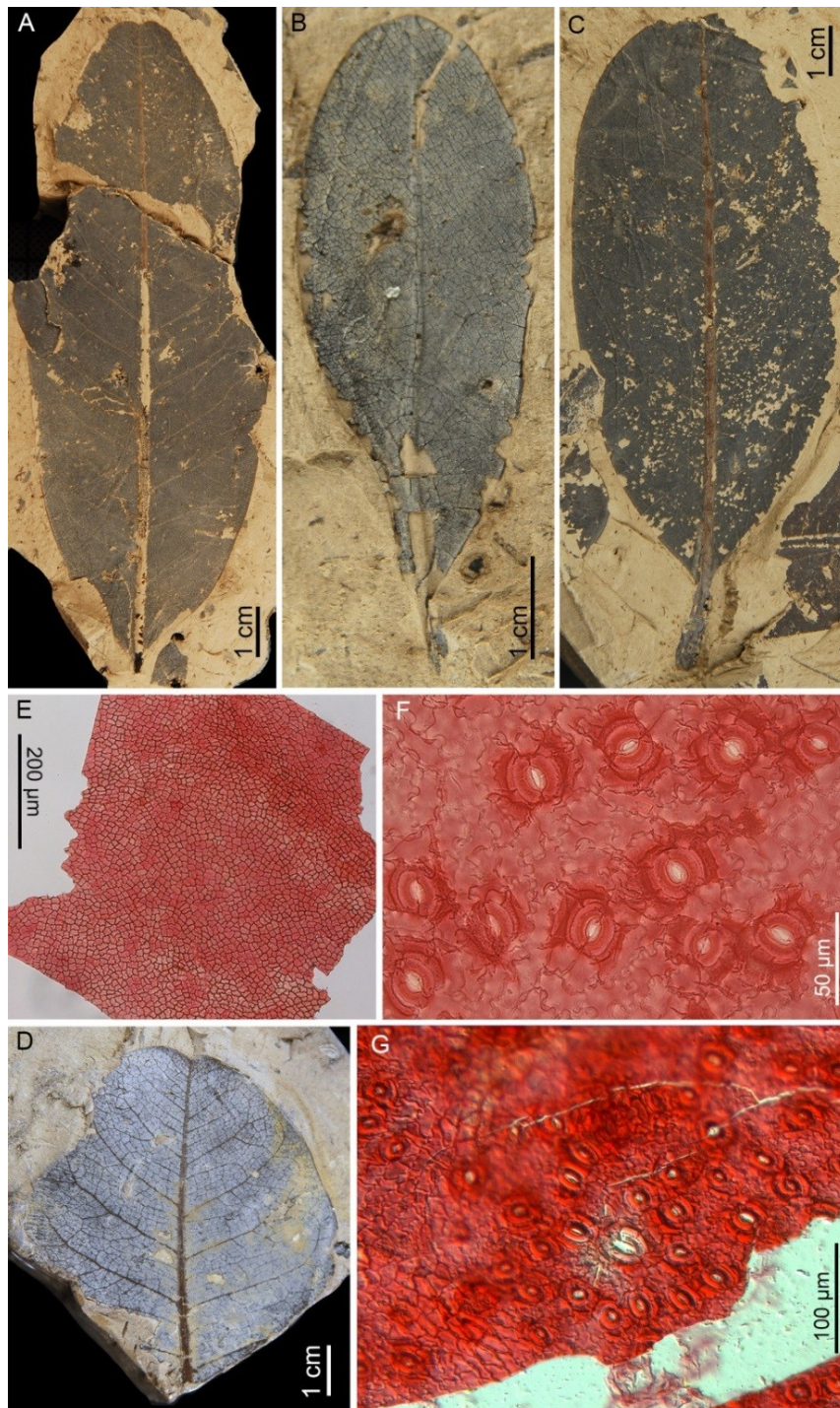


FIGURE 12. Leaf morphology and cuticles of *Rhodomyrtophyllum reticulosum* (A large, elliptic, emerginate leaf (specimen MMG PB Pf 810:2 and 3); B small, obovate leaf (specimen MMG Pb Pf 851); C elliptic leaf with thick petiole (specimen MMG Pb Pf 534); D brachydromous venation and dense tertiary venation (specimen MMG Pb Pe 106); E adaxial cuticle (specimen MMG Pb Schle\_OE 807, prep. 19/15); F abaxial cuticle with deeply undulated anticlines and brachyparazytic stomata and open stomatal pores (specimen MMG Pb Schle\_OE 759:2e, prep. 154/11); G abaxial cuticle with giant stomata within the intercostal area (specimen Schle\_OE 802:3, prep. 1/15).

They are all native in subtropical-tropical climates and therefore endorse the paleoclimatic reconstructions for the late Eocene FC Zeitz reconstructing mean annual temperatures of around 18 °C and mean annual precipitation of more than 1300 mm (Moraweck et al., 2015).

### 3.1.2. *Platanus neptuni* (Platanaceae)

Leaves of *Platanus neptuni* are very variable, ranging from simple (Figure 13A-D) to compound trifoliolate and rarely quinquefoliate (Figure 13F) leaves. Simple leaves and leaflets are either lanceolate or elliptic (Figure 13B-D) to oblanceolate ranging in size from 3 x 10 mm to 50 x 200 mm (Kvaček and Manchester, 2004) and even more. The apex can be both acuminate and narrow to widely acute. The base appears to be narrowly cuneate. The leaf's margin is bluntly toothed in the upper half or third. The teeth are very variable in size, depending on the leaf size, simple and glandular with the basal side being convex and the apical side straight to convex (Figure 13E). Completely toothed leaves are rare but known, e.g. from Flörsheim (Kvaček & Manchester, 2004). Petioles are short to medium in length and widened at the base. The venation is semicraspedodromous to camptodromous with a straight medium thick midrib and approximately regular distributed secondaries arising from the midvein at angles of about 60°, running sub-parallel and slightly curved towards the margin. One or two intersecondaries are present. The tertiary veins proceed partly parallel with the secondaries or irregular, forming reticulate patterns with higher order venation (Kvaček & Manchester, 2004).

The adaxial cuticle is moderately thick and slightly striated along veins (Kvaček & Manchester, 2004). The epidermal cells are 30-50 µm in diameter, polygonal-lobate and anticlines are coarsely undulate. Compound trichome bases are absent or only present dispersed in small laminae (Figure 13G). The epidermal cells of the abaxial cuticle are polygonal-lobate too with diameters between 35 and 50 µm with shallowly to deeply undulated anticlines. Stomata are anomocytic to laterocytic, often elliptic and 35-50 µm long (Figure 13H, I). The outer stomatal aperture appears large-elliptic, whereas the inner aperture looks slit-like. Stomata occur scattered in the laminae. Compound trichome bases, 28-50 µm in diameter rarely up to 65 µm wide, are present (Figure 13H, I) and more sparsely distributed in larger leaves than in smaller leaves. Trichomes are formed by 2 or

more basal cells, with the periphery thickened and surrounded by cutin ridges. Complete glandular trichoms are only rarely preserved (Figure 13 H, I). The terminal, shade-like part is round or broadly elliptic, 65-100 µm in diameter without a detectable internal cell structure and filled with secretory liquid (Figure 13I).

Based on the exclusive abundance of compound leaves in the late Eocene site Klauska (Germany) Walther in Mai & Walther (1985) proposed a separate species *Platanus fraxinifolia* which was reinterpreted by Kvaček and Manchester (2004) as a leaf morphotype of a single species *Platanus neptuni*. This was mainly because the 'fraxinifolia' leaf type co-occurs with the simple 'neptuni' leaf type in several localities and the two types cannot be distinguished by their cuticles. However, the present study is based on the single species concept but we are aware that distinct taxonomic options are conceivable.

First evidences of *Platanus neptuni* in central Europe come from the Eocene of Northern Bohemia, Czech Republic (Kvaček and Teodoridis, 2011) and the Weißelster Basin, Germany (Mai and Walther, 1985) as element of evergreen broadleaved forests and indicate equable subtropical climate with high mean annual precipitation (Kvaček and Manchester, 2004). In Kučlín, the type locality (Kvaček and Manchester, 2004) more than 100 leaves are preserved, together with fruits, seeds and inflorescences. This flora is interpreted as being part of the hinterland with a putative distance to the coast from more than 160 kilometers (Moraweck et al., in review), which corroborates the reconstruction of a zonal notophyllous evergreen broadleaved forest by Kvaček and Teodoridis (2011). Its predominance in the plant assemblage of Klauska, in a clay layer between fluvial sands of the 'Zwickau-Altenburg River', with mainly trifoliate leaves indicate this species being an element of azonal riparian environments, together with other typical Eocene elements of the coastal-alluvial plain, such as *Rhodomырtophyllum reticulosum*, *Sloanea nimrodi*, *Daphnogene cinnamomifolia* or *Doliosrobis taxiformis*, typical elements of the Zeitz FC (Mai and Walther, 2000; Kvaček and Manchester, 2004). In the latest Eocene/earliest Oligocene temperate to warm-temperate species e.g. *Acer* sp., *Alnus* sp., *Betula* sp., *Carpinus* sp. and *Ulmus* sp. occurred the first time in the central European fossil record (Kunzmann et al., 2016), indicate changes in paleoclimate and mirror the global cooling trend (Teodoridis and Kvaček, 2015). The Haselbach and Kundratice FC (early Oligocene) contain mainly deciduous broadleaved elements with only a minor proportion of thermophilic elements. *Platanus neptuni* is present throughout the Oligocene in mixed mesophytic forests and deciduous broadleaved forests (Moraweck et al., in review), both in the coastal plains of the Weißelster Basin (Borna-Ost-Bockwitz), in volcanic maar surrounding plant



assemblages (Kleinsaubernitz) and on the coasts of the Tethys-/Paratethys (Flörsheim, Rauenberg). The composition of the plant assemblages during the Oligocene remains quite stable with only minor changes due to migration and are an indicator for almost stable climate conditions, with lower mean annual temperatures compared to the Eocene. Last evidence from central European fossil assemblages with embedded leaf remains of *Platanus neptuni* is known from site Linz (nannoplankton zone NN 1, Rupp and Ćorić, 2012) in Austria (Kovar, 1982), where this taxon is dominant and interpreted as being part of riparian vegetation. Paleoclimate conditions may have been smoothed due to the influence of the Paratethys with assumed MAT of 11 to 18 °C but distinct differences in summer and winter temperatures, humid conditions and MAP of 1100-2000 mm (Kovar, 1982). Kvaček and Manchester (2004) prove the occurrence of *P. neptuni* in Europe until the late Miocene mainly in south and south-east Europe (e.g. sites Delureni, Valea de Cris, Romania; Cornițel, Romania).

Until now it lacks a modern most similar relative, as the Subgenus *Glandulosa* is extinct and no taxonomic nearest living relative is available. The genus *Platanus* consists of two subgenusses (*Castaneophyllum*, *Platanus*) and associates 7 species and several subspecies (Grimm and Denk, 2010). The monotypic subgenus *Castaneophyllum* inhibits only *Platanus kerrii* (Grimm and Denk, 2010), which is native to Vietnam, unlike most of the species in subgenus *Platanus*, which are native to North- and South-America and *Platanus orientalis*, native to southeastern Asia and Europe (Grimm and Denk, 2010). Because of the very distinct lamina shape from simple to compound and the serrate margin without scalloped sinuses, which both is unlike all present *Platanus* species, the determination of a taxonomic nearest living relative is not possible and underpins the necessity to search for similarities in more habitat related demands and compliances. Mai and Walther (1983) compared the occurrence of different taxa in the Weißelster Basin during the late Eocene in the FC Zeitz, the early Oligocene (FC Haselbach) and during the middle Oligocene (FC Nerchau) both with the southern Chinese evergreen broadleaved forests, vegetation in Laos, Burma and Vietnam and with the notophyllous broadleaved evergreen forests in Mexico for the riparian settings. Kvaček and Manchester (2004) furthermore refer to similarities in leaf morphology of extinct *Platanus neptuni* and extant *Platanus kerrii* and identified similarities in cuticular characteristics and in the inflorescences with species from subgenus *Castaneophyllum*. For this reason *Platanus kerrii* was assigned to serve as nearest ecological equivalent in the present study, in contrast to studies of Grein et al. (2013) and Roth-Nebelsick et al. (2014).

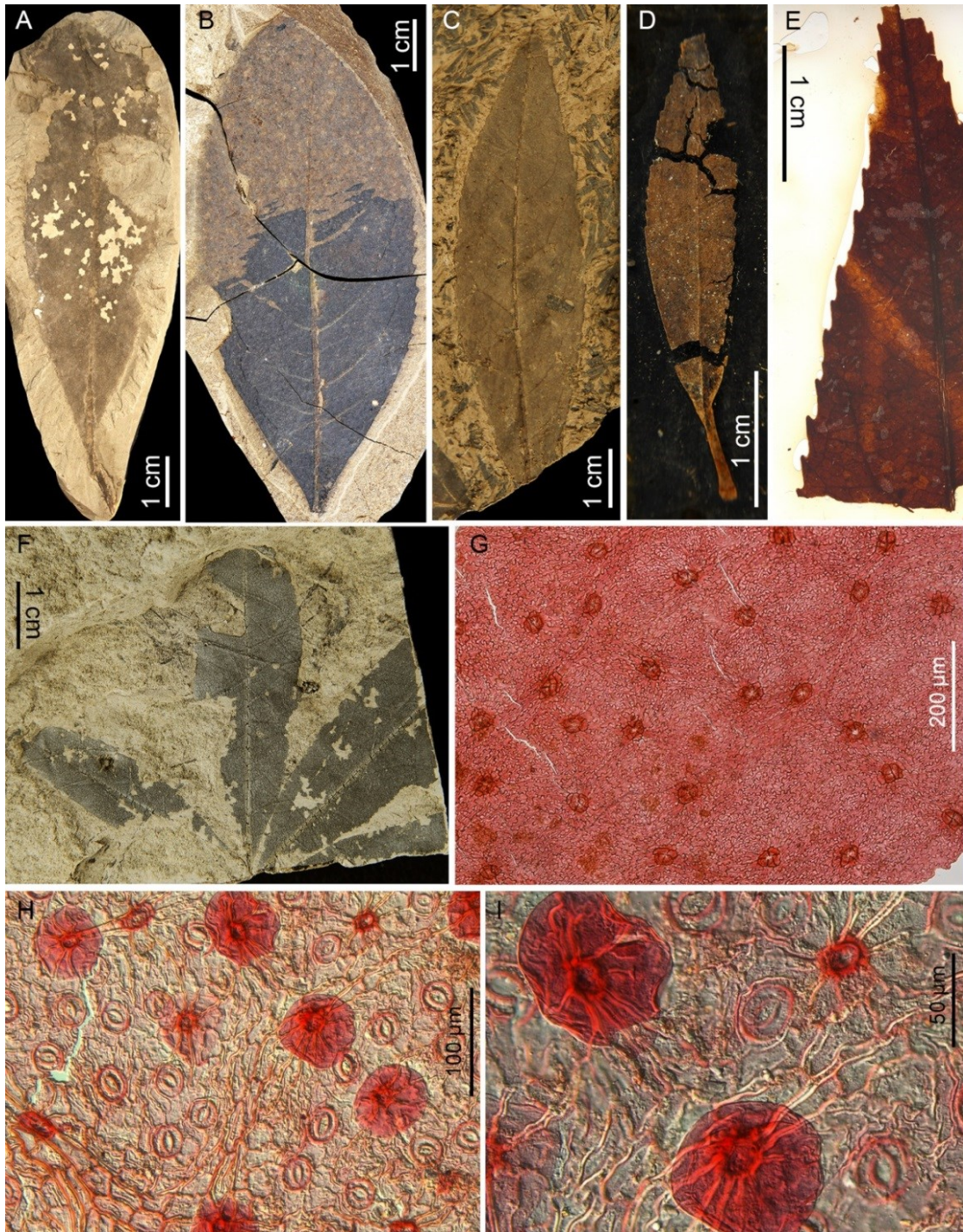


FIGURE 13. Leaf morphology and cuticles of *Platanus neptuni* (A large, elliptic leaf (specimen SM.B. Fh 182); B broad-elliptic leaf with sharp teeth (specimen MMG Pb Ks 66:1a); C typical elliptic leaf (specimen MMG Pb Schle\_MO540); D small leaf with long and thick petiole (specimen MMG Pb WzII 1390); E glandular teeth and acute to acuminate apex (specimen MMG Pb Wz II 1701); F compound, probably quinquefoliate leaf (specimen MMG Pflh 20); G adaxial cuticle with tricome bases (specimen Pflh 24a, prep. 44/15); H abaxial cuticle with stomata and glandular trichomes (specimen MMG Pb Schle\_MO 472a, prep. 22/13); I glandular trichomes and trichome base together with anomocytic stomata (specimen Schle\_MO 472 a, prep. 22/13)).

## 3.2. Extant plant material

### 3.2.1. *Platanus kerrii* (Platanaceae)

Leaves of *Platanus kerrii* are simple, ovate to elliptic (Figure 14A, B) ranging in size from 80 to 155 mm in length and 20 to 45 mm in width, even bigger leaves (180 x 70 mm) are known (Baas, 1969). The apex can be narrow to widely acute or partly acuminate (Figure 14B). The base appears to be narrow to widely cuneate and in some specimen asymmetric. The margin is bluntly toothed in the upper 70 % of the lamina with widely and irregular teeth in the lower third and increasingly denser teeth towards the apex (Figure 14B). Teeth are shaped concave in the basal side of the tooth and convex at the apical side. Petioles are short and maximum 5 mm long. The secondary veins arise from the strong and straight midrib in an angle of 45 to 60°, they form a eucamptodromous to brochodromous vein framework; teeth are innervated by tertiary veins. One or two intersecondaries can be recognized. The tertiary veins form reticulate patterns with higher order venation.

The adaxial cuticle is composed of polygonal epidermal cells 30-50 µm in diameter with straight to slightly undulated anticlines. Trichomes occur less frequently compared to the abaxial cuticle, but are common mainly above veins but also within the intercoastal areas (Figure 14C). Cuticular striations cover the complete cuticular surface, mostly radiating from the trichome bases (Figure 14D; Baas, 1969). The compound trichomes are approximately 20 µm in diameter and appear as a thickened ring with two to eight basal cells (Carpenter et al., 2005). The thin abaxial cuticle (Figure 14E) features a high density of both stomata and trichomes. The epidermal cells are polygonal with straight anticlines, which are less pronounced than on the adaxial cuticle. Cuticular striations are present but less pronounced in comparison to the adaxial cuticle. The numerous stomata are distributed in the intercoastal areas. Stomata are 26 to 30 µm in diameter and only slightly longer than wide. The subsidiary cell arrangement is very variable (Carpenter et al. 2005) ranging from anomocytic to laterocytic types and often not possible to determine as anticlines between subsidiary cells are poorly defined. The guard cells overlie the subsidiary cells (Carpenter et al., 2005) and stronger cutinized rims frame the guard cells (Figure 14F). Trichomes are smaller (10 µm in diameter) than on the adaxial cuticle and bigger trichomes are mainly restricted to the major veins (Carpenter et al., 2005).

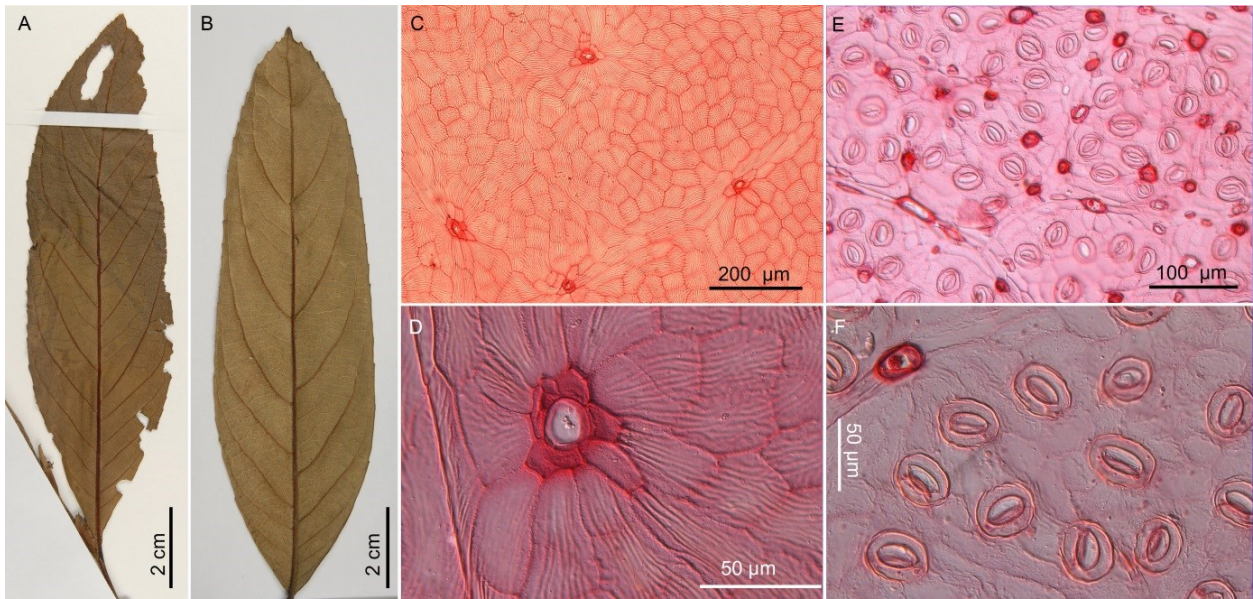


FIGURE 14. Leaf morphology and cuticles of *Platanus kerrii* (A typical, elliptic leaf (specimen MMG Herbarium 4957); B ovate leaf with slightly acuminate apex (specimen MMG Herbarium 4957); C adaxial cuticle with trichome bases (specimen MMG Herbarium 4957, prep. r 27/14); D adaxial cuticle with large, compound trichome base (specimen MMG Herbarium 4957, prep. r 27/14); E abaxial cuticle with numerous stomata and trichomes (specimen MMG Herbarium 4957, prep. r 28/14); F abaxial cuticle with large stomata and small trichome base (specimen MMG Herbarium 4957, prep. r 28/14)).

*Platanus kerrii* is native to northern provinces of Vietnam and Vieng Chan in Laos (World Conservation Monitoring Centre, 1998). It is assigned as vulnerable species listed in the 'IUCN Red List of Threatened Species' since 1998 (World Conservation Monitoring Centre, 1998) due to increasing habitat loss. The large tree is rarely distributed along streams at low latitudes on gravel soils, mud flats or alluvial deposits.

The studied material comprises three twigs with approximately 30 leaves suitable for morphological and cuticular investigations, comes from northern-central Vietnam (Thanh Hou Province, Thuong Xuan District, Yen Nhan Community; unfortunately no GPS data available) and was sampled by Dr. Do Van Truong (Vietnam National Museum of Nature, Hanoi, Vietnam) on April 18, 2014 along a stream (Name not known). The climate is of Cwa type sensu Köppen and Geiger (Köppen, 1936; Peel et al., 2007) with pronounced differences in temperature and precipitation throughout the year. MAT in this region estimates 22.0 °C with MAP of 1510 mm (<http://de.climate-data.org>). WMMT and CMMT estimate 26.7 °C and 15.6 °C respectively. The wet season starts in May and ends in September. Winters are colder and dryer than summers.

### 3.2.3. *Syzygium samarangense* (Myrtaceae)

The thick and leathery leaves of *Syzygium samarangense* are elliptic to elliptic-oblong to obovate (Figure 15A, B), 10 to 22 cm long and 5 to 8 cm in width. The leaves are entire margined. The base is mostly narrowly rounded to slightly cordate and the thick petioles are rather short (maximum 4 mm long) or nearly absent. The apex is very different in shape, ranging from acute to acuminate shapes and even emerginate leaves are common (Figure 15C). The 14 to 19 secondary veins on each side of the midrib arise in an angle of approximately 45°. They unify in a distance of 5 mm from the margin, forming loops. Intersecondary veins occur frequently.

The adaxial cuticle is rather thick and robust (Figure 15D). The polygonal epidermal cells, about 20 µm in diameter feature coarsely to fine undulated anticlines. Trichome bases occur scattered on the cuticle, in intercoastal areas as well as above veins. A dense cuticular striation covers the complete cuticle surface, radiating from trichomes. The trichome bases are 25-35 µm in diameter and occur to be highly cutinized. The cells of the abaxial cuticle are 10 to 20 µm in diameter with less undulated anticlines compared to the adaxial cuticle. Stomata occur often grouped and are densely distributed in the intercoastal areas (Figure 15E). 'Giant stomata' are known from the regions above veins, but also in intercoastal areas, where the distribution of the surrounding stomata clearly follow another pattern compared to regions without occurring 'giant stomata'. Stomata are around 20 µm in diameter, round to slightly elliptic. The guard cells are kidney shaped and highly cutinized. The pore was not clearly visible but should be roughly 5 µm in length. Trichomes occur seldom and are distributed in the intercoastal areas as well as above veins (Figure 15E).

*Syzygium samarangense* trees are up to 15 m tall and prefer heavier soils in tropical regions. They are distributed in low elevations up to 1200 m in Fiji, India, Indonesia and Malaysia. *Syzygium samarangense* tolerates dry summers but no drought conditions. This tree is planted along streams or ponds (pers. communication Huang Jian).

Leaves of this species were sampled in April 2016 in the Xishuangbanna Tropical Botanical Garden, Menglun, Mengla, Yunnan, China by Lutz Kunzmann and myself. Leaves were treated regarding morphology and morphometry, cuticular micromorphology and for thin-sectioning (see chapter 4.4.). Additionally, photosynthesis measurements were conducted.

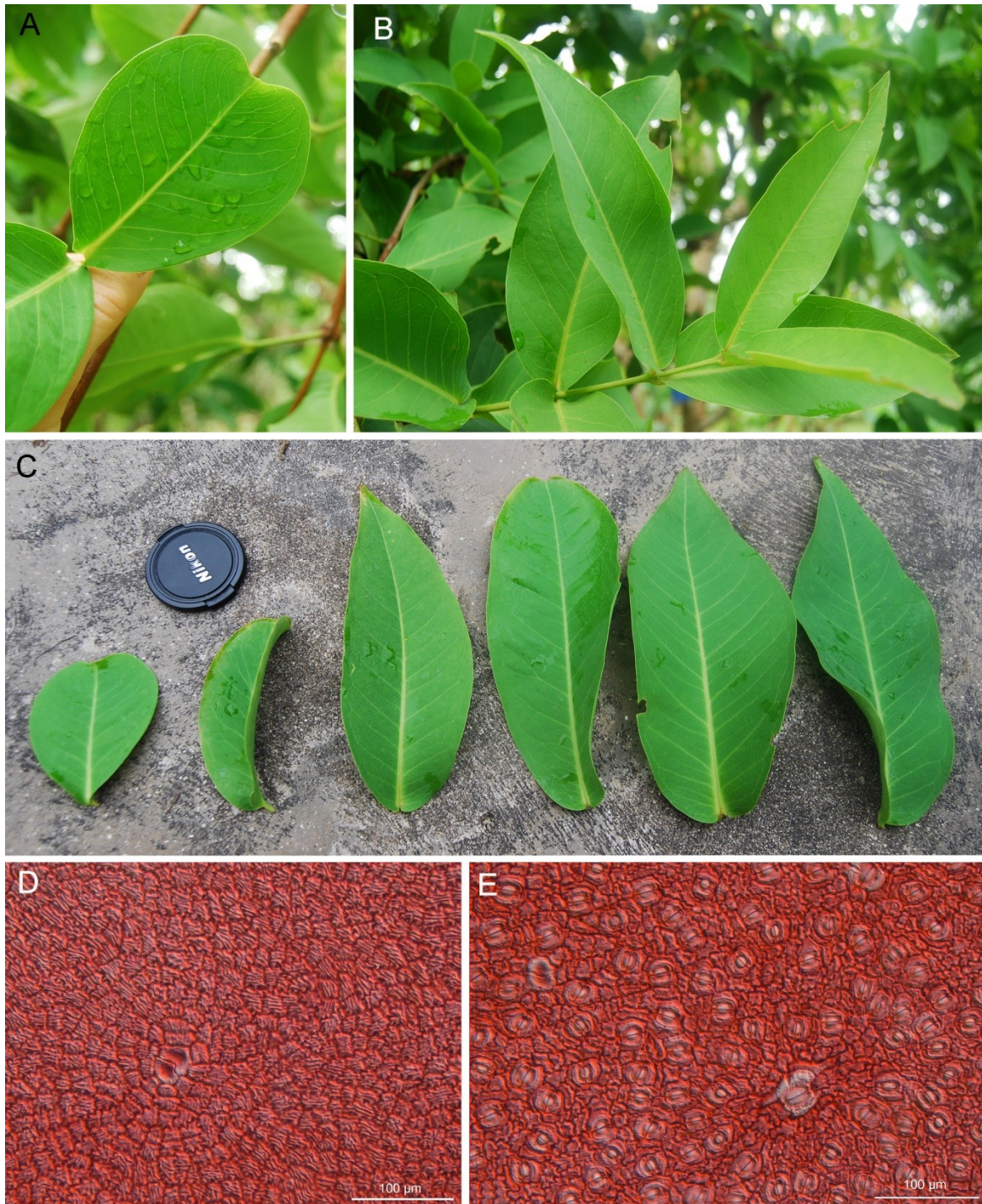


FIGURE 15. Leaf morphology and cuticles of *Syzygium samarangense* (A-C leaves sampled in the Xishuangbanna Tropical Botanical Garden in Menglun, Mengla, Yunnan, China; A emerginate small leaf; B dominating elliptic-oblong leaves with acute apices; C variate of leaf shapes and sizes sampled on one, approximately 8 m high free-standing tree; D adaxial cuticle with polygonal epidermal cells (specimen MMG Herbarium 5007, prep. r13/16) and E abaxial cuticle with dense distribution of stomata (specimen MMG Herbarium 5007, prep. r13/16)).

---

## 4. Methods

### 4.1. Paleoclimate reconstruction

The estimation of paleoclimatic conditions was performed using two quantitative methods providing data for temperature and precipitation: the Coexistence Approach (CA) (Mosbrugger and Utescher, 1997) and the Climate Leaf Analysis Multivariate Program (CLAMP) (Wolfe, 1993; Wolfe and Spicer, 1999). Besides MAT, values for warmest month mean temperatures (WMMT), coldest month mean temperatures (CMMT), mean annual precipitation (MAP) and data determining the distribution of precipitation (seasonality). These are 3WET (precipitation of the three wettest months), 3DRY (precipitation of the three driest months) for CLAMP, MPdry (monthly precipitation of the driest month) and MPwet (monthly precipitation of the wettest month) for CA.

Although for most of the investigated Weißelster Basin sites paleoclimatic methods were already applied, most of the sites have been reinvestigated due to changes in taxonomic determination or added material. Most paleoclimatic reconstructions published by e.g. Teodoridis et al. (2012) or Teodoridis and Kvaček (2015) are based on the publications of Mai and Walther (1985, 1991, 2000). I therefore recalculated the paleoclimatic signal of these sites.

#### 4.1.1. Coexistence Approach

The paleoclimate estimation using the CA is linked with the long known and commonly used Nearest Living Relative concept (Heer, 1855-1859; Wing and Greenwood, 1993; Mosbrugger, 1999; Uhl et al., 2003). The method is supposed to be more independent from taphonomic restrictions and morphological as well as anatomical adaptations of the plants (Uhl, 2006) than physiognomic approaches like Leaf Margin Analysis (LMA) and CLAMP. The CA determines an interval of coexistence of taxa for different climatic parameters (Figure 16), such as MAT, WMMT, CMMT and MAP, based on the actuopaleontological assumption that the fossil taxon and the respective NLR require in most cases comparable

climatic conditions. CA clearly benefits from the opportunity to include all types of fossil plant remains (i.e., diaspores, leaves, wood, palynomorphs; Utescher et al., 2014). The climatic parameters of the NLRs derived from the PALEOFLORA database (supplementary information, Appendix B; Mosbrugger and Utescher, 1997-2016). This database also includes putative NLRs for a number of fossil species. The better these NLRs can be determined (genus level or below) and their climatic and habitat requirements can be investigated, the more reliable is the coexistence interval. In some cases I deflected from given NLRs but using ecological equivalents instead of NLRs that can perhaps better reflect autecological traits of certain fossil species (Moraweck et al., 2015). The CA is a widely used method for quantifying paleoclimatic conditions (Uhl et al., 2003; Mosbrugger and Utescher, 2005; Uhl, 2006; Uhl et al., 2007; Teodoridis et al., 2009; Quan et al., 2012; Teodoridis et al., 2012; Utescher et al., 2015). Advantages and disadvantages are widely discussed in e.g. Mosbrugger and Utescher (1997), Kvaček (2007), Grimm and Denk (2012), Utescher et al. (2014), Grimm et al. (2016), Grimm and Potts (2016).

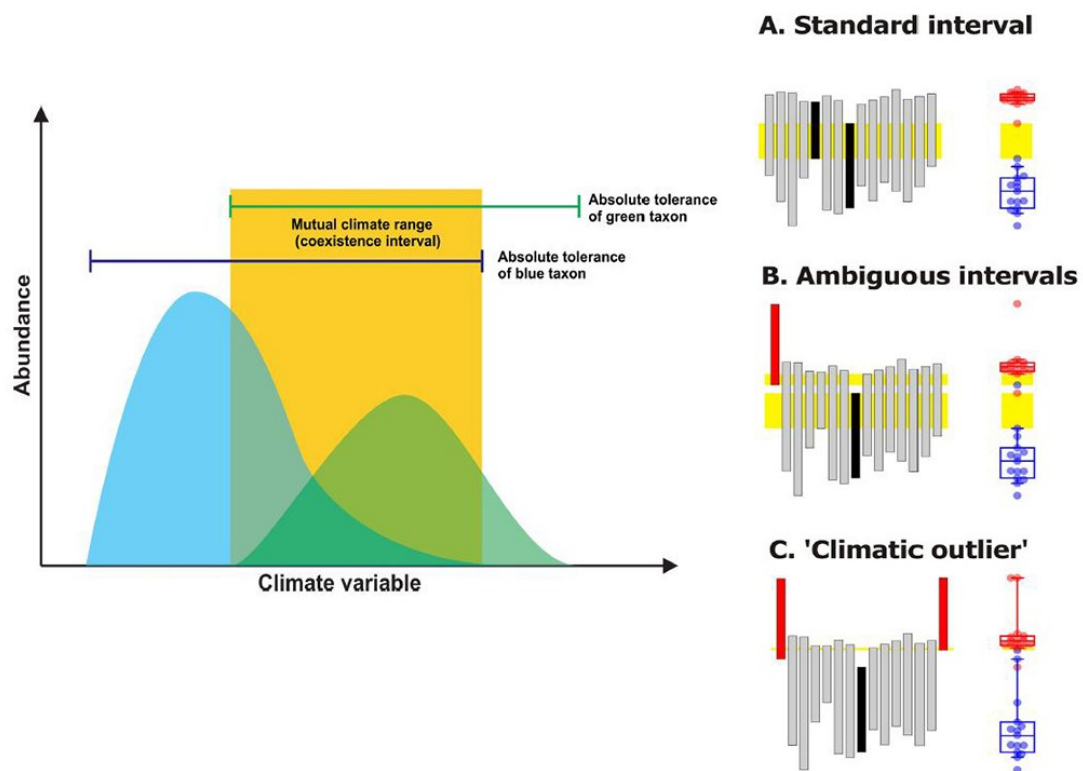


FIGURE 16. Concept and principles of the Coexistence Approach and definition of A standard intervals, B ambiguous intervals (definition of two climate intervals due to wide ranges and missing overlapping of single climate intervals), C definition of a coexistence interval and two outliers with no overlapping in their climatic demands with the other climatic intervals (modified from Grimm and Potts (2016) and Grimm et al. (2016)).



Paleoclimatic reconstruction using CA was performed for all taxonomically determined floras. As the plant assemblages Profen-Schwerzau 1u and Profen-Süd LC are currently under taxonomic investigation CA was not possible to perform.

#### 4.1.2. Climate Leaf Analyses Multivariate Program

CLAMP, introduced by Wolfe (1993) and further developed by various authors (e.g., (Spicer, 2009; Jacques et al., 2011; Teodoridis et al., 2011; Yang et al., 2011), is a multidimensional tool, correlating selected leaf physiognomic traits and climatic parameters. The physiognomic character states of fossil leaves get coupled with datasets from extant plant assemblages and respective meteorological data by Canonical Correspondence Analysis (CCA) (Kovach and Spicer, 1995; Spicer, 2009; Teodoridis et al., 2011; Yang et al., 2011; Kennedy et al., 2014). CLAMP correlates 31 leaf physiognomic states simultaneously (e.g. lobbing, occurrence and form of teeth, leaf shape, length-width ratio, form of apex and base; Figure 17). To score a taxonomically undetermined fossil flora it is possible simply to create morphotypes. As taxonomic determination of the plant assemblages of all study sites is already done (Mai and Walther, 1985, 2000; Dietrich, 2012; Moraweck, 2013; Ferdani, 2014) it was possible to use taxa for this study. There are six calibration datasets (at <http://www.clamp.ibcas.ac.cn>) available online for the morphological correlation (Physg3brcAZ, Physg3arcAZ, PhysgAsia1, PhysgAsia2, PhysgGlobal378, PhysgSH90) with extant plant assemblages from different localities. For the coupling with meteorological data Spicer (2009) introduced, additional to the meteorological data directly derived from local meteorological stations, global gridded data (GRIDMet3arAZ, GRIDMet3brAZ, SH90HiResGridMet, HiResGRIDMetGlobal378). In this study the global gridded data (GRIDMet3brAZ) were used and the selection of the appropriate dataset for morphological data followed the automatic calibrationset test of Teodoridis et al. (2012). Physg3brcAZ, consisting of data from 144 sites from the temperate regions of the northern hemisphere and the calibration dataset PhysgAsia1 with the datasets from Physg3brcAZ with 45 additional sites from China have been used for the correlation of climatic parameters. Recent studies (e.g. Kvaček, 2010; Krutzsch, 2011) contradict assumptions of monsoonal or even monsoonal-like conditions for the Eocene in central Europe. The PhysgAsia2 calibration dataset (Khan et al., 2014) including sites from

southern China, Thailand and India, reflecting (sub-) tropical monsoon climates has therefore been excluded from the analyses.

Species Number	Species / Morphotypes	Lamina		Margin Character States									Size Character States						Apex Character States			Base Character States		Length to Width Character States				Shape Character States																	
		Unlobed	Lobed	No Teeth	Teeth	Teeth Regular	Teeth Irregular	Teeth Close	Teeth Distant	Teeth Round	Teeth Acute	Teeth Compound	Compound<50%	Nanophyll	Leptophyll I	Leptophyll II	Microphyll I	Microphyll II	Microphyll III	Mesophyll I	Mesophyll II	Mesophyll III	Emarginate	Round	Acute	Attenuate	Cordate	Round	Acute	L:W <1:1	L:W 1-2:1	L:W 2-3:1	L:W 3-4:1	L:W >4:1	Obovate	Elliptic	Ovate								
1	rtophyllum re	1		1																			1	1																					
2	obalanus fur	1		1	1	1																																							
3	ogene cinnan	1		1												1	1	1																											
4	loanea nimrod	1			1																																								

FIGURE 17. Example of a CLAMP scoresheet (Scored morphotype or taxon with present (1) leaf physiognomic states).

Wolfe (1993) indicates a minimum sample size of 20 taxa, which unfortunately is not accomplished in all floras, thus these results have to be seen with great care. Especially the plant assemblages from the coastal plain deposits did not reach the minimum sample size. Also, the scoresheet completeness of 0.66 (Spicer et al., 2011) was never reached in the coastal plain assemblages. The calculations for CLAMP were performed with the software-package CANOCO 4.02 for Windows (for sites Profen-Schwerzau ZC, Profen-Süd 2, Profen-Süd 3u, Klaus and Schleenhain 3u published in Moraweck et al. (2015), before PhysgAsia1 was available for online analysis) and with scoresheets provided on the CLAMP website (<http://www.clamp.ibcas.ac.cn>) for the calculation with the PhysgAsia1 calibration files. The online calculation was performed for sites, which required the calibration file Physg3brcaZ, and PhysgAsia1 for all sites investigated in recent times. The leaf physiognomic states of the species (as defined by Wolfe, 1993 and at the CLAMP website) of the study sites are given in the supplementary data (Appendix C lists all scoresheet of investigated plant assemblages and Appendix D shows the respective percentages of derived leaf physiognomic states).

## 4.2. Morphological and morphometric parameters

Morphometric data were gathered following different steps, starting with image acquisition of suitable fossil leaves, followed by image processing, extraction of leaf shape, the implementation into a database collecting morphometric data of fossil leaves (MORPHYLL; Traiser et al., 2015) and the calculation of morphometric parameters. If the preservation status of the fossils was suitable the leaves were scanned (*Canon CanoScan-5600F*) or photographed (*Nikon-D5100*). The images were calibrated with respect to scale by using Photoshop (CS 6; Adobe Systems, San Jose, California, USA) and ImageJ (U. S. National Institutes of Health, Bethesda, Maryland, USA), later rotated in order to align the main parts of the primary (central) leaf vein vertically. After contrast adaptation the images were resized to real object size with the help of the scale bar. In order to measure morphometric traits the leaf outlines have been digitized in QGIS (version 2.0 – 2.10). After georeferencing the lamina base in QGIS, shape layers of the leaves were compiled. Owing to the fact that nearly all fossil leaves are fragmented and thus some parts of the lamina are not preserved, for each leaf two versions of outlines were generated – both a minimum outline representing unequivocally parts of the fragmented lamina and a maximum outline representing the assumed complete replenished lamina. To ensure the reliability of measured morphometric traits of reconstructed leaves, only specimens were included showing an approximate ratio between minimum and maximum outline of 0.7 (preservation index). The calculation of leaf morphometric parameters such as leaf area, leaf length and width were performed by spatial SQL-queries. The shapefiles of leaf outlines were imported to an object-relational PostgreSQL-database with PostGIS extension adding support for spatial queries to be run in SQL.

Morphometric data of *Rhodomyrtophyllum reticulosum* are restricted to measurements of leaf length and width using the produced maximum shapes. But due to the fact that these shapes have not been integrated in the MORPHYLL database yet, not all morphometric data are available in the moment. Their integration into the database, which is maintained by C. Traiser and M. Grein (both partly employed at Staatliches Museum für Naturkunde Stuttgart, Germany), is currently in progress. The missing implication SQL-queries for reconstructed leaves unfortunately induce missing control of the preservation index. As *Rhodomyrtophyllum reticulosum* is predominant in most of the azonal plant assemblages

and their lamina is most robust against decay, all of the specimen are supposed to reach the minimum preservation of 0.7.

*Platanus neptuni* leaves are mostly simple, but trifoliate or quinquefoliate leaves are known from sites Kučlín (rare), Klauska (several), Borna Ost DC (n01), Profen-Süd 1u (n=3), Flörsheim (n=1) and Borna-Ost-Bockwitz (n=1). The digitization, calibration and further treatment in QGIS was done for every leaflet, which allowed for reconstruction regarding the minimum preservation index.

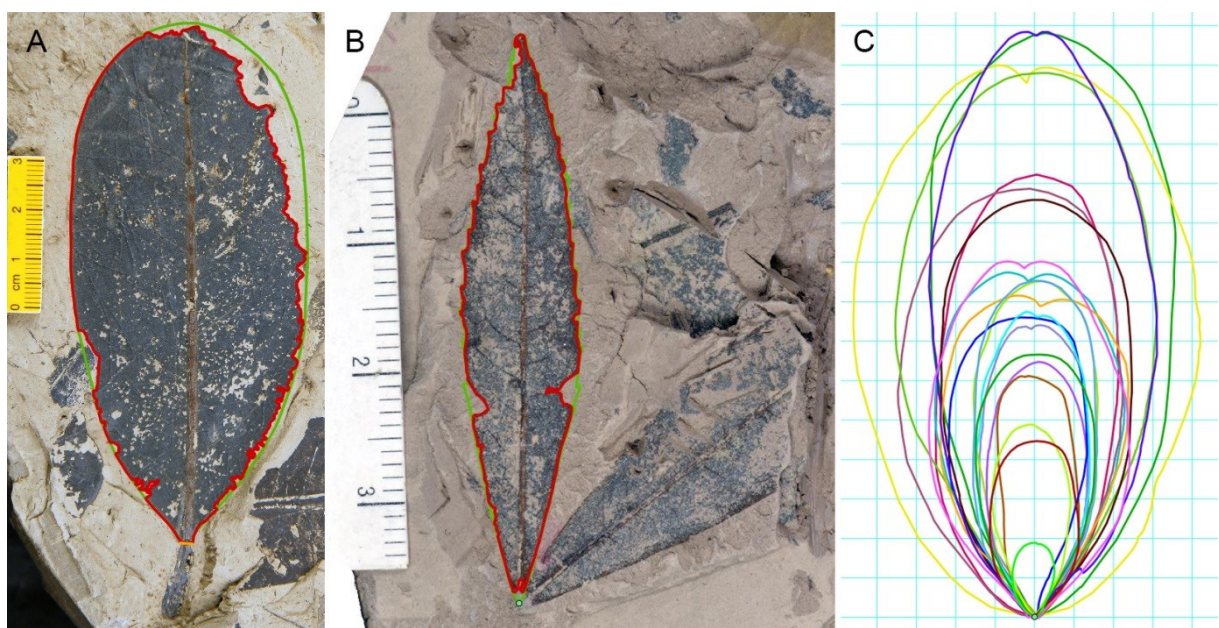


FIGURE 18. Leaf morphometric traits (A and B: Minimum- (red) and Maximum (green) shape of A *Rhodomyrtophyllum reticulosum* (specimen MMG Pb Pf 534) and B a leaflet of *Platanus neptuni* (specimen MMG Pb Kl 136); C: Maximum shapes of *Rhodomyrtophyllum reticulosum* specimens and recognized leaf size variability from site Profen-Süd LC, one grid corresponds to 1x1 cm).

Leaf mass per area ( $LM_A$ ) in  $[g/m^2]$  according to Royer et al. (2007) was determined for *Platanus neptuni* leaves with,

$\text{Log}(M_A) = a + b * \log(PW^2/A)$ , where

a is a factor of 3.070, b is 0.382, PW is the petiole width in [mm] and A represents the leaf area of the replenished leaves in  $[mm^2]$ .

Species, which invest in high  $LM_A$  are supposed to have lower photosynthetic rates based on leaf mass but tend to have a longer leaf lifetime. These species are able to compensate the lower rate of fixed carbon with a longer-lasting carbon gain (Westoby et al., 2002; Wright et al., 2004). Species with a higher expense in leaf construction maximizing their resource retention are called 'slow-return' species (Grubb, 1998). In contrast, deciduous species with shorter life spans and the need of high carbon gain rates within the vegetation period are called 'fast-return' species (Grubb, 1998). Calculation of  $LM_A$  thus allows for appraising whether a species is regarded to be deciduous ( $LM_A < 87 \text{ g/m}^3$ ) or evergreen ( $LM_A > 129 \text{ g/m}^3$ ).

Digitization and replenishment of *Rhodomyrtophyllum reticulosum* leaves was done regarding the respective stratigraphic age in order to obtain as much information of leaf trait changes through time. Therefore site Klaus, Schleenhain 2o and Profen-Süd 3u have been skipped from the analysis due to either broad ranges in relative age determination (see Table 1) or due to similar stratigraphic positions compared to other investigated assemblages (see site Profen-Süd 3u, Table 1).

Highest amount of *Platanus neptuni* leaves suitable for morphometric studies were derived from sites Kučlín, Rauenberg, Flörsheim and Linz (Table 3), where 13 to 38 leaflets were incorporated into the analyses, due to their high abundance and low fragmentation rates. For the fluvial Weißelster sites maximum 10 leaves got digitized and replenished while not a single leaf in Kleinsaubernitz and Borna-Ost DC yielded a preservation index of minimum 0.7. As for sites Seifhennersdorf and Profen-Schwerzau 1u no petioles were preserved,  $LM_A$  estimation was not possible.

All quantitative as well as qualitative data for *Platanus neptuni* leaf traits and partly *Rhodomyrtophyllum reticulosum* data compiled for this study, are stored in the database MORPHYLL (Traiser et al., 2015; Traiser et al., in review) hosted by State Museum of Natural History, Stuttgart. Morphometric data gathered from *Rhodomyrtophyllum reticulosum* are listed in the supplements (see Appendix E).

site	number of leaves	
	digitized and replenished	LM <sub>A</sub> [g/m <sup>2</sup> ]
<i>Platanus neptuni</i>		
Linz	17	12
Witznitz WC	4	3
Witznitz TC	10	2
Borna-Ost-Bockwitz	2	1
Kleinsaubernitz	-	-
Seifhennersdorf	5	-
Flörsheim	13	4
Rauenberg	38	17
Schleenhain HC	7	2
Borna-Ost DC	-	-
Klausä	8	2
Profen-Schwerzau 1u	4	-
Kučlín	18	14
<i>Rhodomyrtophyllum reticulosum</i>		
Schleenhain 3u	10	-
Profen-Süd 3u	-	-
Peres 3u	11	-
Haselbach 2-3 mi	15	-
Schleenhain 2o	-	-
Knau	15	-
Klausä	-	-
Profen-Süd LC	21	-
Kayna-Süd	13	-
Profen-Schwerzau ZC	25	-
Messel	15	-

TABLE 3. Number of digitized and replenished leaves of *Rhodomyrtophyllum reticulosum* and *Platanus neptuni* for the single sites and appropriate leaves for LM<sub>A</sub> determination (abbreviation: LM<sub>A</sub> – leaf mass per area)

### 4.3. Cuticular derived parameters

To obtain leaf cuticles small fragments of the coalified material were removed and macerated for one to four minutes in Schultze solution. Cuticles with adhered sediment got washed in HF before maceration. Afterwards, the cuticles were cleaned with NH<sub>4</sub>OH or KOH

to dissolve the mesophyll, rinsed with distilled water and subsequently stained with safranin, affixed to slides with glycerol or glycerol jelly, and studied using a Leica DM 5500B microscope with a DFC 420 digital camera. Images were processed with the Leica QWin software.

As micromorphological patterns may vary over the leaves surface, cuticle samples were produced from the upper (apex), middle and lower (base) parts of the leaf, if enough material was available allowing for the exclusive involvement of non- or less fragmented leaves. In this study both, already existing cuticle slides were incorporated together with additionally prepared cuticle material. In sites Kučlín and Klauska no cuticles are preserved.

Stomata density (SD), stomata index (SI), stoma width ( $w_{st}$ ) and pore length ( $h_{st}$ ) as well as trichome density (TD; for *Platanus neptuni*) were measured on microscopic images of cuticle preparation slides. The number of counts for each site and parameter is specified in Table 4.

Stomata density (SD), which is defined as the number of stomata per  $\text{mm}^2$  (McElwain and Chaloner, 1996; Poole and Kürschner, 1999) was determined on areas of at least  $0.03 \text{ mm}^2$  within the intercoastal areas or in areas with only minor order venation. As SD shows considerably variation among different leaves and also within one leaf the minimum sample size has been determined by utilization of the cumulative mean (Poole and Kürschner, 1999; Beerling and Royer, 2002). For *Rhodomyrtophyllum reticulosum* at least 11 leaves were investigated (beside site Schleenhain 2o, with only 5 leaves were available for cuticle preparation), whereas for *Platanus neptuni* a minimum sample size of 6 leaves for most sites delivered adequate results, which corroborates the advice of Grein et al. (2013). At least 3 counts per leaf in the respective leaf areas were conducted. If the chosen areas for SD determination also contain fragmented stoma on its margin, those on the upper and right margin were counted and those stomata on the lower and left frame margin were excluded to get reliable results. Data of Grein et al. (2011a) and Roth-Nebelsick et al. (2014) were included as well.

Trichome density (TD) was determined on the same slides and areas as SD for leaves of *Platanus neptuni*, allowing for comparison of both. TD is defined as number of trichomes per  $\text{mm}^2$ . Trichomes were counted only within the intercoastal areas and on minor order venation. The incorporation of fragmented trichomes on the margin of the chosen area follows the same rules as for SD determination.

site	number of cuticle counts			
	SD [1/mm <sup>2</sup> ]	SI [%]	TD [1/mm <sup>2</sup> ]	h <sub>St</sub> /w <sub>St</sub> [μm]
<i>Platanus neptuni</i>				
Linz	19	-	22	-
Witznitz WC	27	13	21	109
Witznitz TC	27	18	27	116
Borna-Ost-Bockwitz	36	13	33	164
Kleinsaubernitz	16	-	15	36
Seifhennersdorf	25	2	25	76
Flörsheim	25	-	22	90
Rauenberg	21	-	21	60
Schleenhain HC	45	9	40	212
Borna-Ost DC	16	8	16	78
Klaus	-	-	-	-
Profen-Schwerzau 1u	35	-	36	108
Kučlín	-	-	-	-
<i>Rhodomyrtophyllum reticulosum</i>				
Schleenhain 3u	36	14	-	161
Profen-Süd 3u	20	12	-	139
Peres 3u	46	23	-	453
Haselbach 2-3 mi	30	14	-	141
Schleenhain 2o	27	14	-	175
Knau	40	12	-	197
Klaus	-	-	-	-
Profen-Süd LC	20	12	-	128
Kayna-Süd	31	13	-	274
Profen-Schwerzau ZC	48	34	-	456

TABLE 4. Number of cuticle counts for SD, SI, TD and h<sub>St</sub> and w<sub>St</sub> determination for *Rhodomyrtophyllum reticulosum* and *Platanus neptuni* (abbreviations: SD – stomata density, SI – stomata index, TD – trichome density, h<sub>St</sub> – stomata pore length and w<sub>St</sub> – stomata width).

Stomata index (SI) data were obtained on those cuticles, which allowed for clear identification of epidermal cell walls. SI [%] was calculated as

$$\frac{\text{total number of stomata}}{\text{total number of stomata} + \text{total number of epidermal cells}} * 100$$



following Poole and Kürschner (1999). Data of Roth-Nebelsick et al. (2014) were included in this study. The incorporation of fragmented cells on the margin of the framed area followed the same rules as for SD and TD determination.

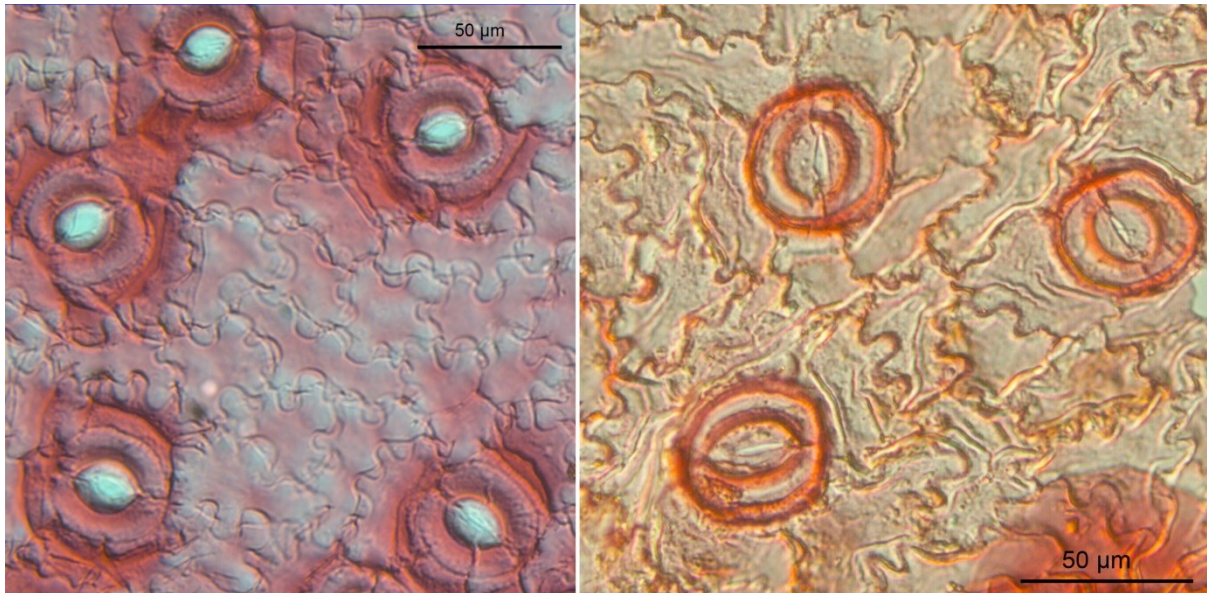


FIGURE 19. Stomata with open stomatal pore (left: *Rhodomyrtophyllum reticulosum* (specimen MMG Schle\_OE 779a, prep. 154/11); right: *Platanus neptuni* (specimen MMG Pb Schle\_MO 472a, prep. 23/13)).

Stoma width ( $w_{st}$ ) and stoma pore length ( $h_{st}$ ) data were obtained only from stomata with clearly identifiable cell walls and open pores (Figure 19). Those stomata where the thin and fragile inner pore diameter is preserved were used to measure pore length ( $h_{st}$ ), allowing for identifying of the effective gas exchange channel.

#### 4.4. Paleoatmospheric reconstruction

SD and SI have been widely used to determine atmospheric  $CO_2$  (further abbreviated  $C_{atm}$ ) in numerous publications (Woodward, 1987; Woodward and Bazzaz, 1988; Royer, 2001;

Royer et al., 2001; Beerling and Royer, 2002; Kouwenberg et al., 2003; Kürschner et al., 2008; Haworth et al., 2010; Doria et al., 2011; Steinthorsdottir et al., 2016). Leaves are the main photosynthesis organs and stomata therefore represent the gateway for gas exchange (Konrad et al., 2008). If  $C_{atm}$  increases, stomata are supposed to respond to these changes. Hence, SD is widely used to determine changes in the ancient atmospheric  $CO_2$  record. But SD is not only varying in dependence on available  $C_{atm}$ , but reacts also to changes in environmental parameters, such as water availability, insolation or soil conditions (Hetherington and Woodward, 2003; Galmés et al., 2007). Konrad et al. (2008) denotes also the possibility of an increased  $CO_2$  flux into the leaf if external  $C_{atm}$  increases under a given stomatal conductance and  $CO_2$  gradient. The correlation of SD and  $C_{atm}$  is nonlinear and its gradient is decreasing with increasing  $CO_2$  (McElwain et al., 2016). This indicates that plants are able to maintain the required  $CO_2$  influx while SD decreases (Konrad et al., 2008). Hence, SD is not always sensitive to changing  $C_{atm}$  and the response of SD to  $C_{atm}$  is species specific. Therefore, calibration functions derived from data of extant species are necessary to evaluate reasonable  $C_{atm}$  values (Konrad et al., 2008; Grein et al., 2011a). This approach becomes increasingly difficult with increased distance in time and hence evolutionary processes between the fossil and the extant species. Only a few species can be tracked back this far in time, such as *Gingko biloba* and *Metasequoia glyptostroboides* (Royer et al., 2001; Doria et al., 2011). Due to these methodical constraints a mathematical model developed by Konrad et al. (2008), coupling photosynthesis data, anatomical and morphometric data and paleoclimate was applied to the respective sites. The model is based on the coupling of  $CO_2$  diffusion into the leaf (leading to a certain  $CO_2$  concentration in the interior leaf  $c_i$ ) driven by photosynthesis ( $A$ ) and water vapour diffusion out of the leaf (transpiration,  $E$ ) which is depending on the water potential gradient between the atmosphere and the leaf interior (Konrad et al., 2008; Roth-Nebelsick et al., 2014). Parameters  $A$  and  $E$  are therefore coupled via the leaf permeability ( $g_{leaf}$ ):

$$A = g_{leaf}(C_{atm} - C_i)$$

$$E = a g_{leaf}(w_{sat} - w_a)$$

with  $a = 1.6$ ,  $w_{sat}$  = leaf internal air humidity, which is defined as saturation value of the water vapour concentration in the air and  $w_a$  as measured air humidity in the atmosphere (Roth-Nebelsick et al., 2014). As  $g_{leaf}$  is influenced by SD it appears that  $C_a$  can be derived by stomata-based methods, such as the above described method of using transfer functions for  $CO_2$  determination. The following briefly outlined premises and abundancies show that

this simple method is not applicable. Most prominently,  $g_{leaf}$  is not only coupled with SD, as the area of the stomatal pore ( $a_{st}$ ) and its depth ( $d_{st}$ ) together with characters characterizing leaf morphology influence gas exchange (Grein et al., 2011a):

$$g_{leaf} = \frac{SD * a_{st} D_{CO_2}}{\left[ d_{bl} + d_{asPP} \frac{\tau_{as}^2}{\eta_{as}} \right] SD * a_{st} + d_{st}}$$

$d_{st}$ ,  $\tau_{as}$  and  $\eta_{as}$  denote thickness, tortuosity and porosity of the assimilation mesophyll ( $d_{asPP}$ ).  $D_{CO_2}$  characterizes the diffusional constant of  $CO_2$  and  $d_{bl}$  stands for the atmospheric boundary layer at the leaf surface. Due to changing photosynthetic activity throughout the day,  $a_{st}$  is not fixed but dynamically controlled by the plant itself. Additionally,  $C_i$  is coupled with  $A$  not only depending on anatomical and morphometrical boundary conditions, but also with biochemical parameters, such as  $q$  (carboxylation limited by Rubisco),  $K$  (a parameter containing the Michaelis-Menten constant for carboxylation and oxygenation),  $\Gamma$  ( $CO_2$  compensation point) and the mitochondrial respiration rate in daylight abbreviated  $R_d$  (Farquhar et al., 1980; Konrad et al., 2008; Grein et al., 2011a).

The gas exchange model, described in Konrad et al. (2008) is designated as optimization model, because it involves the trade-offs between  $CO_2$  uptake and hence photosynthesis and coincident transpiration water loss while stomata pores remain open. Plants which are able to gain a maximum of carbon with a minimum of transpiration and water loss should be favoured by natural selection processes (Givnish, 1986). Plants in most environments have to balance stomatal conductance (opening and closing of stomatal pores) therefore as water is mostly a limiting factor during a certain time in the vegetation period. This is expressed with  $\lambda$ , the 'cost of water'. Plants growing in arid to semihumid environments where water is a limiting factor in plant life, need to be highly adapted and hence, optimized. A very low stomatal conductance for example, would result in a very low water loss due to transpiration but only a minimum of carbon gain (Grein et al., 2011a). Plants therefore need to adapt an optimization strategy. Two obvious strategies among a variety of others include firstly, the change of stomata density, which needs longer time, at least one leaf fall or even longer and secondly, the change in pore area ( $a_{st}$ ) which is possible to realize within minutes (Grein et al., 2011a).

Due to these complex processes the gas exchange model has been developed to at least partly involve the above described constraints and abundancies. For a detailed outline see Konrad et al. (2008), Grein et al. (2011a, 2013) and Roth-Nebelsick et al. (2014). The

model, which is supplied as a MAPLE (Maplesoft, Ontario, Waterloo, Canada) sheet was allocated from one of the author of the initial publication Wilfried Konrad (Universität Tübingen; Technische Universität Dresden, Germany). An example of a MAPLE sheet for one site and parameter combination is given in the supplementary information (see Appendix G).

#### 4.4.1. Determination of input parameters

The model requires a variety of input parameters, of whose some were derived from literature and others were measured or/and calculated during studies on both, fossil and extant leaves. These are listed in Table 5 for a better overview.

Parameter	Symbol	Source
Mean wind velocity	$V_{wind}$	Literature <sup>1</sup>
mean relative air humidity	RH	Paleoclimate approach (CA)
mean temperature	T	Paleoclimate approach (CA)
water availability "cost of water"	$\lambda$	derived from $c_i/c_a$
Depth of assimilation tissue	$d_{asPP}$	measurements on extant leaves
mean depth of stomatal pore	$d_{st}$	measurements on extant leaves
mean length of stomatal pore	$h_{st}$	measurements on fossil leaves
maximum width of stomatal opening	$pw_{st}$	constructed from $h_{st}/2$
mean leaf width	$l$	measurements on fossil leaves
Porosity of the assimilation tissue	$\eta_{as}$	Literature <sup>2</sup>
Tortuosity of the assimilation tissue	$\tau_{as}$	Literature <sup>2</sup>
Stomatal density	SD	measurements on fossil leaves
Maximum RuBP-saturated rate of carboxylation at 25 °C	$q_{25}$	Literature <sup>3</sup>
Mitochondrial respiration rate in the light at 25 °C	$R_{d25}$	Literature <sup>3</sup>
Factor used to calculate Michaelis-Menten constants at 25 °C	$\kappa_{25}$	Literature <sup>4</sup>
Factor used to calculate the CO <sub>2</sub> -compensation point in the absence of dark respiration at 25 °C	$\Gamma_{25}$	Literature <sup>4</sup>
Ratio of leaf-internal to ambient CO <sub>2</sub>	$c_i/c_a$	derived from $\delta^{13}C$

TABLE 5. List of all parameters that are required for gas exchange model application (1 Nobel (1999); <sup>2</sup> Konrad et al. (2008); <sup>3</sup> Bowden and Bauerle (2008); <sup>4</sup> Bernacchi et al. (2003)).

All parameters which have been measured during this study will be briefly described in the following, with exception of the input parameters  $l$  and  $SD$ . Their determination has been already described in chapters 4.2. and 4.3.

It has to be stated that, in former publications (Grein et al., 2011a, 2013; Roth-Nebelsick et al., 2014), leaf length served as input parameter and not, as correctly, the respective mean leaf width of the leaves. As the wind is not supposed to sweep over the full length of the leaf lamina without turbulences developing due to surface friction and thus beginning flapping of the leaf, leaf length seems to overestimate indirectly coupled boundary layer thickness (see Konrad et al., 2008) between the leaf and the atmosphere. Therefore, leaf width serves as a more reliable input parameter to evaluate the boundary layer thickness (pers. communication, Anita Roth-Nebelsick, Staatliches Museum für Naturkunde, Stuttgart).

#### 4.4.1.1. Determination of $d_{asPP}$ , $d_{st}$ and $pw_{st}$

For thin-sectioning small parts of fresh leaf material from *Platanus kerrii* and *Syzygium samarangense* were infiltrated with Leica HistoResin™. Afterwards the leaf samples were embedded in a two-component Leica HistoResin Embedding kit™ and Mounting medium™ and cut with a Leica rotation microtome RM2155. Thin sections (~4 µm thick) are stained with Safranin and mounted on glass slides according to the procedure for leaf cuticles described above.

$d_{asPP}$  measurements were done on cross-sections of leaves from *Platanus kerrii* and *Syzygium samarangense*.

The reconstruction of ancient  $CO_2$  levels additionally requires data of the pore depth and pore width. As the depth of a stoma ( $d_{st}$ ) is not measurable on cuticle slides,  $d_{st}$  was determined using half of the stoma width, following Roth-Nebelsick et al. (2014). The width of the stomata pore ( $pw_{st}$ ) was reconstructed as the half of the individual pore length of the stomata pore ( $h_{st}$ ) (see Grein et al. 2013).

#### 4.4.1.2. Carbon isotope measurements

Isotope data of plant material and particularly the resultant  $c_i/c_a$  from atmospheric carbon dioxide provide information on ecophysiological and thus environmental conditions (Grein et al., 2010) serving as input parameters into the gas exchange model.

For carbon isotope measurements mainly non-fragmented fossil *Rhodomyrtophyllum reticulosum* and *Platanus neptuni* leaves have been chosen. Samples of at least 1 cm<sup>2</sup> were cut out of the leaf lamina on various regions (apex, center, base). The samples have been washed with water to separate leaf material and sediment. The shredded samples were sent to the geochemical laboratory of the Institute Geosciences (Department of Geochemistry), University of Tübingen. The measurements of  $\delta^{13}\text{C}$  isotopes on the fossil leaf material were conducted using a Carlo Erba NC2500 Elemental Analyzer connected to a Thermo Quest Delta Plus XL mass spectrometer. The samples were calibrated to  $\delta^{13}\text{C}$  values of USGS 24 with  $\delta^{13}\text{C}$  values of  $-16\text{‰}$ , relative to VPDB. The reproducibility for  $\delta^{13}\text{C}$  measurements was  $\pm 0.1\text{‰}$ .

Since  $\delta^{13}\text{C}_{\text{atm}}$  values varied throughout earth history the benthic records of foraminifera (Zachos et al., 2001) was used to derive  $\delta^{13}\text{C}_{\text{atm, CO}_2}$  from  $\delta^{13}\text{C}_{\text{CaCO}_3}$  of marine carbonates based on the assumption that  $\delta^{13}\text{C}_{\text{atm, CO}_2}$  is about 7‰ more negative (Beerling et al., 1998; Grein et al., 2010).

site	$\delta^{13}\text{C}_{\text{leaf}} [\text{‰}]$	$\delta^{13}\text{C}_{\text{atm}} [\text{‰}]$	$c_i/c_a$
Schleenhain-3u	-26.85 (0.98)	6.16	0.75 (0.04)
Peres 3u	-27.37 (0.08)	6.16	0.77 (0.004)
Haselbach-2-3-mi	-26.91 (0.39)	6.26	0.74 (0.02)
Knau	-26.66 (0.39)	6.21	0.73 (0.02)
Profen-Süd-LC	-26.77 (0.61)	6.21	0.74 (0.03)
Kayna-Süd	-26.83 (0.42)	6.27	0.76 (0.02)
Profen-Schwerzau ZC	-26.69 (0.88)	6.27	0.73 (0.04)

TABLE 6. Carbon isotope data gathered from *Rhodomyrtophyllum reticulosum* leaves (abbreviations:  $\delta^{13}\text{C}_{\text{leaf}}$  – leaf internal  $^{13}\text{C}/^{12}\text{C}$  ratio of carbon,  $\delta^{13}\text{C}_{\text{atm}}$  – atmospheric  $^{13}\text{C}/^{12}\text{C}$  ratio of carbon, estimated from the Zachos et al. (2001) curve,  $c_i/c_a$  – ratio of leaf internal ( $c_i$ ) and leaf external ( $c_a$ )).

The ratio of leaf internal ( $C_i$ ) to atmospheric ( $C_a$ ) carbon dioxide concentration ( $C_i/C_a$ ) was calculated with the equation, suitable for  $C_3$  plants, according to (Farquhar et al., 1982; Farquhar et al., 1989). Table 6 and Table 7 list the respective  $\delta^{13}C$  values and calculated  $c_i/c_a$  ratios.

site	$\delta^{13}C_{leaf}$ [‰]	$\delta^{13}C_{atm}$ [‰]	$C_i/C_a$
Witznitz WC	- 27.72 (0.72)	- 6.105	0.79 (0.03)
Witznitz TC	- 26.68 (0.42)	- 6.21	0.75 (0.03)
Borna-Ost-Bockwitz	- 26.95 (0.72)	- 6.21	0.75 (0.03)
Seifhennersdorf	- 26.44 (1.60)	- 6.17	0.73 (0.07)
Flörsheim	- 26.35 (0.74)	- 6.26	0.72 (0.03)
Rauenberg	- 25.33 (0.69)	- 6.02	0.72 (0.05)
Schleenhain HC	- 25.78 (0.65)	- 6.00	0.71 (0.04)
Borna-Ost DC	- 26.33 (0.90)	- 5.965	0.73 (0.04)
Profen-Schwerzau 1u	- 25.87 (0.38)	- 6.15	0.70 (0.02)

TABLE 7. Carbon isotope data gathered from *Platanus neptuni* leaves (abbreviations:  $\delta^{13}C_{leaf}$  – leaf internal  $^{13}C/^{12}C$  ratio of carbon,  $\delta^{13}C_{atm}$  – atmospheric  $^{13}C/^{12}C$  ratio of carbon, estimated from the Zachos et al. (2001) curve,  $c_i/c_a$  – ratio of leaf internal ( $c_i$ ) and leaf external ( $c_a$ )).

#### 4.4.1.3. Determination of climate input parameters

Based on MAT the mean temperature of the vegetation period ( $T_{veg}$ ) was calculated following the course of a sine function,

$$T_{veg} = A * \sin \frac{(M + 8) * \pi}{6} + MAT$$

with A as the half distance between WMMT and CMMT, M = number of month (+8 to place the maximum value in July) (Grein et al., 2013). If  $T_{veg} \neq MAT$ , seasonality in climate, regarding temperature can be assumed. As temperature is one of the parameters to be varied during gas exchange modelling,  $T_{min}$  (calculated MAT using  $C_a$ ),  $T_{fixed}$  (mean  $T_{veg}$ ) and  $T_{max}$  (mean temperature from April to October, when mean monthly temperatures  $>10$  °C) were determined. The beginning of the growing season in humid zones is defined by a mean monthly temperature and differs between 5 and 10 °C in the literature (Grein et al.,

2013 and citations therein) and due to various studies and differences in the definition of the minimum growing season temperatures  $T_{veg} \geq 10 \text{ }^\circ\text{C}$  was fixed.

#### 4.4.2. Systematic parameter variation

The influence of the respective input parameters (see Table 5) was described in detail in Konrad et al. (2008). Parameters, that have only a limited influence on the accuracy of the results are for instance,  $v_{wind}$ ,  $l$ ,  $\eta_{as}$  and the biochemical parameters  $R_{d25}$ ,  $\kappa_{25}$  and  $\Gamma$ .

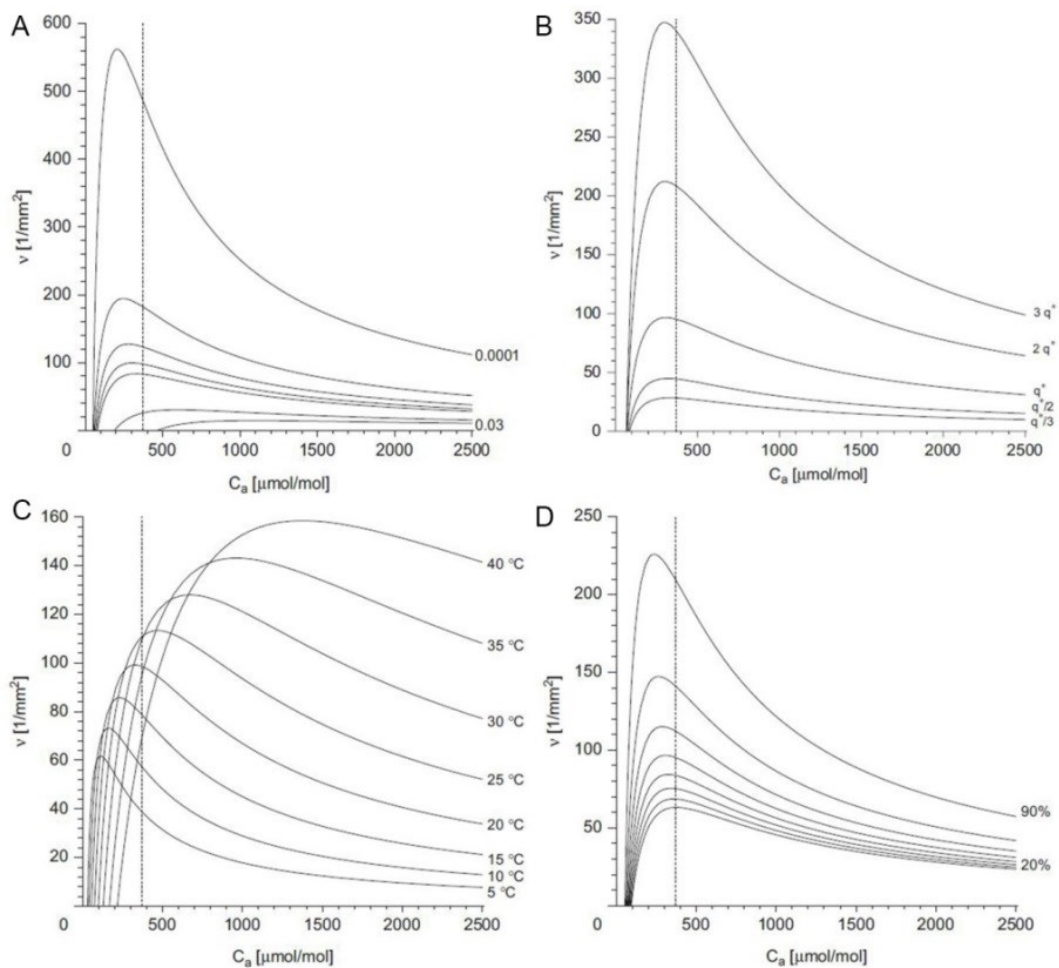


FIGURE 20. Dependencies between SD(Ca) and most critical parameters which have been varied during gas exchange reconstruction (SD herein abbreviated with  $v$ ; sensitivity of changes in A:  $\lambda$  'the cost of water', B:  $q$ ; C: temperature and D: RH under given  $v$ ); modified from Konrad et al. (2008).



Most critical parameters are illustrated in Figure 20 and systematic parameter variation was therefore applied for the input parameters  $c_i/c_a$ ,  $q$ , temperature and relative humidity. As  $\lambda$  is mostly not determinable directly, at least not for fossil material, changes in  $c_i/c_a$  were used to indirectly measure water availability (Grein et al., 2011a). The  $c_i/c_a$  ratio, reflecting the ratio of leaf internal and external carbon and thus photosynthetic activity which is likely driven by  $\lambda$ , allows for inferring this critical parameter.

## 5. Results

### 5.1. Paleoclimate reconstruction

#### 5.1.1. Coexistence Approach

CA estimates comprise data from both leaf assemblages and leaf assemblages with taxonomically determined carpological remains. Paleoclimatic reconstruction includes published CA data from Teodoridis and Kvaček (2015) for Kučlín and Grein et al. (2011b) for site Messel. Highest MAT was reconstructed from the oldest site Messel (20.3 °C; Table 8, Figure 21). CA data for the Bartonian site Kučlín (SPP-Zone 17, sensu Krutzsch et al., 2011), containing both leaf remains, fossil fruits and seeds indicate MAT of 15.7-17.6 °C (Teodoridis and Kvaček, 2015), whereas for the slightly younger site Profen-Schwerzau ZC (SPP-Zone 17/18), an almost solely leaf assemblage with known fruit remains of *Steinhauera subglobosa* MAT of 15.9-21.3 °C where estimated. Sites Schleenhain 2o and Haselbach-2-3 mi (both SPP-Zone 18uo sensu Krutzsch et al., 2011) reveal similar MAT estimates with 15.7-21.1 °C and 16.5-20.8 °C respectively. MAT for sites Profen-Süd 3u and Schleenhain 3u, coming from the underlying bed of lignite seam 3 and site Peres 3u (all SPP-zone 18ou) are in great accordance to each other and indicate MAT of 15.6 °C (Peres 3u) to 20.8 °C. MAT reconstructed using the plant assemblage Borna-Ost DC, situated at the Eocene-Oligocene boundary and comprising mainly leaves support the paleoclimatic estimates derived by the slightly older sites Profen-Süd 3u, Schleenhain 3u and Peres 3u with MAT of 16.0-20.8 °C. Site Schleenhain HC indicates a drop in MAT (15.7-16.1 °C), as already stated in Roth-Nebelsick et al. (2014), although the flora has been taxonomically revised, in contrast to the younger sites Rauenberg (MAT 17.2-20.5 °C) and Flörsheim (15.9-21.3 °C). The Chattian sites Kleinsaubernitz, Borna-Ost-Bockwitz and Witznitz TC point out another slight drop in MAT (e.g. Kleinsaubernitz, 15.2-16.1 °C) before temperature rises again towards the early Miocene. For the plant assemblages Witznitz WC, located at the Oligocene-Miocene transition and Linz (dated to NN 1, Rupp and Córíc (2012)) broad intervals were reconstructed due to missing species richness for site Witznitz WC (MAT 13.8-20.5 °C) and NLR determination mainly on genus and family level for site Linz (MAT 16.5-21.9 °C).

Coexistence Approach (CA)						
site	MAT [°C]	WMMT [°C]	CMMT [°C]	MAP [mm]	MPwet	MPdry
<i>Platanus neptuni</i> sites						
Linz	16.5 - 21.9	25.6 - 27.9	9.0 - 13.6	748 - 1322	170 - 217	42 - 43
Witznitz WC	13.8 - 20.5	25.6 - 27.5	9.0 - 13.6	979 - 1297	178 - 191	42 - 52
Witznitz TC	16.0 - 16.1	25.6	9.0 - 13.3	1096 - 1297	178 - 191	43 - 52
Borna-Ost-Bockwitz	15.7 - 16.1	25.4 - 25.6	5.0 - 6.2	1231 - 1355	?	?
Kleinsaubernitz	15.2 - 16.1	25.7 - 28.7	4.3 - 7.8	867 - 1613	148 - 195	42 - 63
Seifhennersdorf	16.5 - 18.3	25.6 - 25.9	9.0 - 10.9	1231 - 1333	180 - 191	43 - 51
Flörsheim	15.9 - 21.3	25.6 - 28.1	12.2 - 13.6	979 - 1352	180 - 237	42 - 55
Rauenberg	17.2 - 20.5	25.0 - 25.9	12.6 - 13.6	1217 - 1322	204 - 349	21 - 27
Schleenhain-HC	15.7 - 16.1	25.6	4.3 - 7.8	979 - 1189	178 - 185	42 - 66
Borna-Ost-DC	16.0 - 20.8	23.6 - 26.4	9.6 - 9.7	1090 - 1520	180 - 187	41 - 51
Klausau	16.5 - 21.3	25.6 - 27.9	9.6 - 13.3	1096 - 1520	180 - 241	42 - 51
Profen-Schwerzau 1u	-	-	-	-	-	-
Kučlín *	15.7 - 17.6	24.7 - 27.1	7.7 - 10.0	1003 - 1613	-	-
<i>Rhodomyrtophyllum reticulosum</i> sites						
Schleenhain 3u	16.5 - 20.8	26.0 - 27.9	4.8 - 13.3	1090 - 1520	180 - 241	5 - 59
Profen-Süd 3u	15.9 - 20.8	24.7 - 28.1	12.2 - 13.3	1096 - 1355	175 - 195	7 - 38
Peres 3u	15.6 - 20.8	23.6 - 28.1	5.0 - 13.3	1135 - 1520	180 - 187	41 - 59
Haselbach-2-3 mi	16.5 - 20.8	26.0 - 27.8	12.2 - 13.3	1096 - 1355	195 - 241	42 - 53
Schleenhain 2o	15.7 - 21.1	24.9 - 28.1	3.4 - 17.3	1090 - 1335	180 - 195	7 - 59
Knau	18.0 - 18.6	24.7 - 25.0	8.1	1135 - 1355	182 - 195	33 - 38
Klausau	16.5 - 21.3	26.0 - 27.9	12.2 - 13.3	1308 - 1520	180 - 241	42 - 51
Profen-Süd LC	-	-	-	-	-	-
Kayna-Süd	16.5 - 18.8	26.0 - 27.7	4.8 - 13.3	1135 - 1347	180 - 187	43 - 59
Profen-Schwerzau ZC	15.9 - 21.3	24.4 - 28.1	12.2 - 13.3	1090 - 1520	182 - 195	22 - 67
Messel **	16.8 - 23.9	24.7 - 27.9	10.6 - 19.4	803 - 2540	175 - 329	9 - 56

TABLE 8. Paleoclimate estimates derived from CA

(comprising also published data of \* Teodoridis and Kvaček (2015) and \*\* Grein et al. (2011b); abbreviations: MAT – mean annual temperature, WMMT – warm month mean temperature, CMMT – cold month mean temperature, MPwet – mean precipitation of the wettest month, MPdry – mean precipitation of the driest month); question marks indicate assemblages where no interval of coexistence (more than three outliers) was identifiable for the respective climate parameter; sites with – mark assemblages where taxonomic determination has not been done yet or missing data in recent publications (see site Kučlín).

WMMT and CMMT of all sites give indication that seasonal changes in temperature were present already during the Eocene (Table 8, Figure 21). They generally follow the already described trend of MAT. WMMT ranges between 23.6 °C (Peres 3u, Borna-Ost DC) and 28.7 °C (Kleinsaubernitz). CMMT amounts at least 3.4 °C and indicate that during the Eocene as well as the Oligocene freezing could likely have been occurred only occasionally and slightly

beneath 0 °C. This is corroborated by the occurrence of thermophilic water plants as *Vallisneria stylosa*, *Azolla prisca* and *Ottelia minutissima* in many plant assemblages (Mai and Walther, 2000).

MAP consistently amounts mean values of circa 1000 mm (Table 8). The highest interval for reconstructed MAP is given for site Messel with 803-2540 mm. Lowest MAP (979-1189 mm) was reconstructed for site Schleenhain HC, accompanied by lower MAT, WMMT and relatively low CMMT.

MP<sub>wet</sub> and MP<sub>dry</sub>, gathered as well, clearly indicate differences in the distribution of precipitation throughout the year. As intervals of coexistence were only drawn for sites where less than three NLR were defined as outliers, for site Borna-Ost-Bockwitz no interval for MP<sub>wet</sub> and MP<sub>dry</sub> got estimated.

### 5.1.2. Climate Leaf Analyses Multivariate Program

The CLAMP data set comprise both data from own measurements and in a few cases published data (Kučlín: Teodoridis and Kvaček, 2015; Messel: Teodoridis et al., 2012). The respective calibration dataset was chosen using the statistical tool published by Teodoridis et al. (2012) using the percentages of foliar physiognomics of the studied floras, which are listed in Appendix D. As the validity of paleoclimate estimates derived by CLAMP are dependent on sample size with at least 20 morphotypes (Wolfe, 1993) and a scoresheet completeness of 0.66 (Spicer et al., 2011) most of the fluvial sites were not investigable or led to ambiguous results. Sites with a scoresheet completeness of less than 0.4 were skipped from the analysis.

MAT for the oldest site Messel, which represents the paleoclimate conditions close to the EECO amounts 16.5 °C, which is comparable with the younger site Kučlín (MAT 16.8 °C). MAT shows no consistent pattern during the Priabonian (Table 9, Figure 21). Site Profen-Schwerzau 1u delivers MAT of 18.0 °C while the slightly younger site Profen-Süd LC reveals MAT of 15.7 °C. The high scoresheet completeness of 0.7 (Profen-Schwerzau 1u) and 0.78 (Profen-Süd LC) underpins the reliability of MAT reconstruction. Beside site Haselbach-2-3 mi, for no other Priabonian site the minimum scoresheet completeness was reached. MAT

decreases towards the EOT, indicated in MAT of only 14.2 °C for site Schleenhain HC. Considering the small number of morphotypes and the low scoresheet completeness and MAT for the younger sites Rauenberg (18.0 °C) and Flörsheim (17.6 °C) situated in the Oberrheingraben region in southern central Germany, this value has to be interpreted regarding the paleogeographic position. Otherwise the Oligocene sites Seifhennersdorf (MAT 10.0 °C), Kleinsaubernitz (13.4 °C), Borna-Ost-Bockwitz (10.1 °C) and Witznitz TC (11.0 °C) located at, or not far away from the shore of the paleo-North Sea reveal lower MAT. MAT increases towards the Oligocene-Miocene transition and during the early Miocene, indicated by sites Witznitz WC and Linz with 13.8 °C and 16.0 °C respectively.

WMMT and CMMT (Table 9, Figure 21) follow the same trends as MAT. WMMT of at least 22.6 °C for the Chattian site Borna-Ost-Bockwitz to 26.7 °C for Klausä (Priabonian) and CMMT between -1.6 °C (Seifhennersdorf) and 13.6 °C in Schleenhain 2o and Schleenhain 3u imply seasonal changes in temperature throughout the year. CMMT below 0 °C indicate occasionally freezing. CMMT for the Priabonian sites range between 8.8 °C (Profen-Süd LC) and 13.6 °C (Schleenhain 2o, Schleenhain 3u) respectively and decrease towards the Oligocene, except for sites Rauenberg and Flörsheim. CMMT increases at the Oligocene-Miocene boundary. WMMT slightly decreases from the Priabonian (23.4-26.7 °C) towards the Oligocene-Miocene boundary (22.9-25.5°C, except for sites Rauenberg and Flörsheim) and slightly increases in the early Miocene site Linz with WMMT of 25.2 °C.

Regarding precipitation patterns, only low GSP was reconstructed for site Messel (Teodoridis et al., 2012) with mean 991.0 mm. The Bartonian and Priabonian sites deliver a mean precipitation of 1267.0-2403.1 mm during the growing season except for site Klausä with 700.0 mm. GSP considerably decreases in the Oligocene (654.5-945.4 mm) except for sites Rauenberg and Flörsheim with 1323.0 mm and 1805.7 mm respectively. 3\_wet and 3\_dry estimation indicates seasonality in the distribution of precipitation.

TABLE 9 (next page). Paleoclimate estimates derived from CLAMP (comprising also published data of \* Teodoridis and Kvaček (2015) and \*\* Teodoridis et al. (2012); abbreviations: ScoreCom. – scoresheet completeness, Cal.set – chosen calibration dataset (defined using the automatic CLAMP test published by Teodoridis et al. (2012)), MAT – mean annual temperature, WMMT – warm month mean temperature, CMMT – cold month mean temperature, GSP – growing season precipitation, 3\_wet – mean precipitation of the three wettest months, 3\_dry – mean precipitation of the three driest months; sites with – mark assemblages with a scoresheet completeness of less than 0.4 or missing data in recent publications (see site Messel and Kučlín).

Climate Leaf Analyses Multivariate Program (CLAMP)								
site	ScoreCom.	Cal.set	MAT [°C]	WMMT [°C]	CMMT [°C]	GSP [mm]	3_wet [mm]	3_dry [mm]
<i>Platanus neptuni</i> sites								
Linz	0.8	189	16.0 (1.3)	25.2 (1.7)	6.8 (2.6)	1147.5 (497)	617.9 (239)	127.6 (104)
Witznitz WC	0.7	189	13.8 (1.3)	24.2 (1.7)	3.7 (2.6)	791.4 (497)	571.4 (239)	94.6 (104)
Witznitz TC	0.69	189	11.0 (1.3)	23.2 (1.7)	0.2 (2.6)	945.4 (497)	590.0 (239)	144.0 (104)
Borna-Ost- Bockwitz	0.7	189	10.1 (1.3)	22.6 (1.7)	-1.8 (2.6)	878.4 (497)	591.8 (239)	134.7 (104)
Kleinsaubernitz	0.43	189	13.4 (1.3)	25.5 (1.7)	2.5 (2.6)	850.4 (497)	527.9 (239)	112.5 (104)
Seifhennersdorf	0.64	189	10.0 (1.3)	22.9 (1.7)	-1.6 (2.6)	849.4 (497)	559.2 (239)	140.4 (104)
Flörsheim	0.78	189	17.6 (1.3)	26.3 (1.7)	9.4 (2.6)	1805.7 (497)	879.7 (239)	187.9 (104)
Rauenberg	0.66	189	18.0 (1.3)	25.8 (1.7)	9.5 (2.6)	1323.0 (497)	658.2 (239)	140.4 (104)
Schleenhain HC	0.48	189	14.2 (1.3)	25.0 (1.7)	3.6 (2.6)	654.5 (497)	445.7 (239)	76.4 (104)
Borna-Ost DC	-	-	-	-	-	-	-	-
Klausä	0.54	189	18.6 (1.3)	24.7 (1.7)	10.6 (2.6)	700.0 (497)	466.3 (239)	61.0 (104)
Profen- Schwerzau 1u	0.7	144	18.0 (2.1)	24.8 (2.5)	11.8 (3.4)	2106.3 (317)	1040.0 (229)	204.0 (59)
Kučlín *	-	189	16.8 (1.3)	26.1 (1.7)	8.1 (2.6)	1267.0 (497)	638.0 (239)	142.0 (104)
<i>Rhodomyrtophyllum reticulosum</i> sites								
Schleenhain 3u	0.46	144	19.7 (2.1)	26.3 (2.5)	13.6 (3.4)	1902.5 (317)	917.0 (229)	172.0 (59)
Profen-Süd 3u	-	-	-	-	-	-	-	-
Peres 3u	-	-	-	-	-	-	-	-
Haselbach-2-3 mi	0.69	144	17.9 (2.1)	25.5 (2.5)	10.8 (3.4)	2403.1 (317)	1226.6 (229)	187.7 (59)
Schleenhain 2o	0.54	144	19.4 (2.1)	25.7 (2.5)	13.6 (3.4)	2200.7 (317)	1049.7 (229)	202.4
Knau	0.53	189	16.2 (1.3)	26.5 (1.5)	10.4 (2.6)	1590.2 (497)	729.89	152.24
Profen-Süd LC	0.78	144	15.7 (2.1)	23.4 (2.5)	8.8 (3.4)	1584.3 (317)	918.6 (229)	140.5 (59)
Kayna-Süd	-	-	-	-	-	-	-	-
Profen- Schwerzau ZC	-	-	-	-	-	-	-	-
Messel **	-	189	16.5 (1.3)	25.1 (1.5)	7.8 (2.6)	991 (218)	551 (139)	115 (41)

Summarizing the temperature estimations derived by CA and CLAMP (Figure 21) one can recognize the accordance of MAT, WMMT and CMMT estimations until the middle to end of the Rupelian. Estimates derived by both methods mirror a plateau phase in temperature. Since the middle Rupelian (site Seifhennersdorf) temperatures derived from CLAMP consequently deliver lower temperatures than CA based temperatures, but both methods indicate a distinct drop in MAT, WMMT and CMMT at the end of the Rupelian and stable climate conditions until the Oligocene-Miocene boundary.

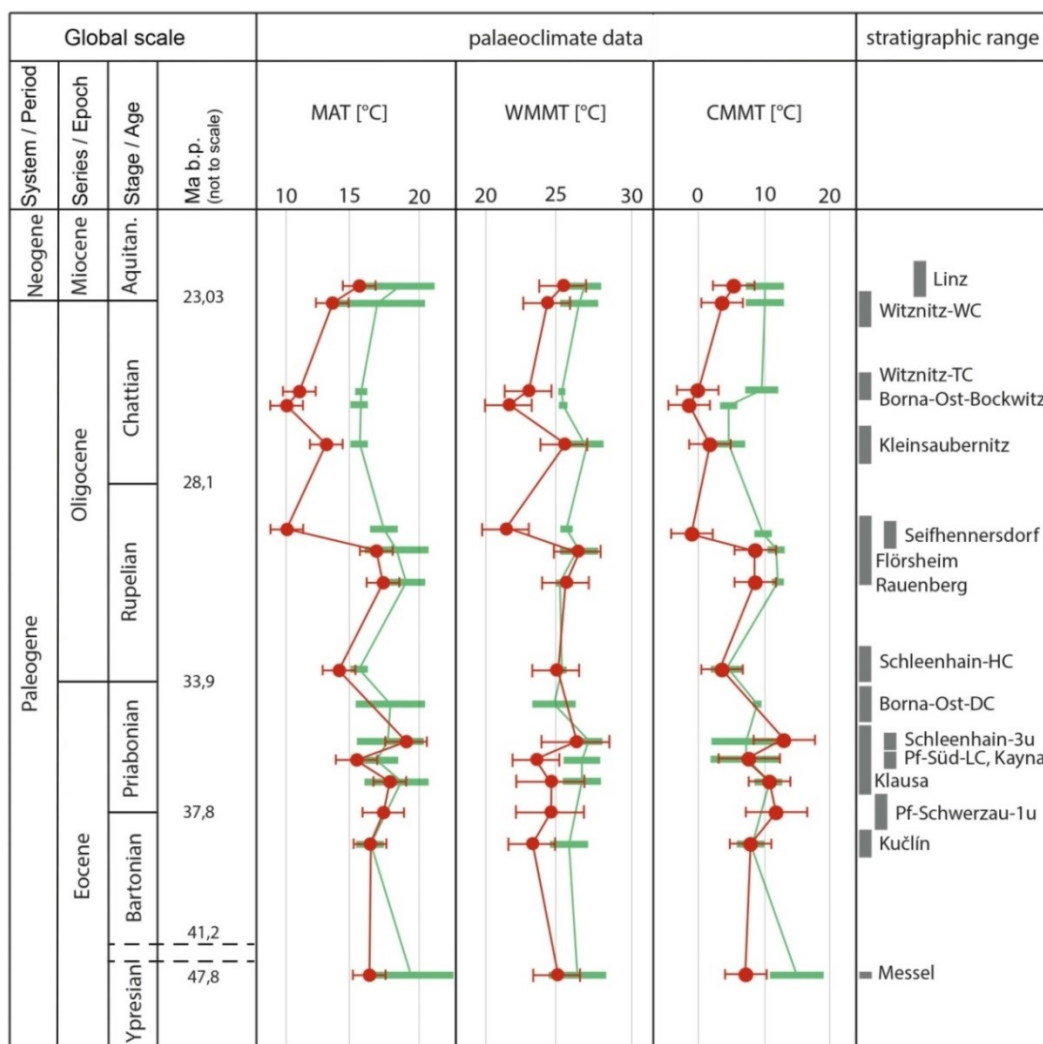


FIGURE 21. Early Eocene to early Miocene temperature trend derived from CA and CLAMP for selected sites (some sites and delivered paleoclimate estimates are not shown due to better readability; based on age determination sensu International Chronostratigraphic Chart v2016/12).

## 5.2. Morphometric parameters

### 5.2.2. *Rhodomyrtophyllum reticulosum*

For morphometric analyses the parameters leaf length and leaf width were observed from certain sites together with the calculated length/width ratio for eight localities (Table 10; Figure 22). As no data of leaf area were available, unfortunately leaf mass per area ( $LM_A$ ) was not estimated.

site	n	length [mm]	width [mm]	l/w ratio
Peres 3u	11	69.45 (16.26)	37.21 (10.15)	1.90 (0.33)
Schleenhain 3u	10	74.90 (20.11)	35.14 (12.48)	2.21 (0.43)
Haselbach 2-3 mi	15	69.24 (20.72)	30.29 (11.01)	2.41 (0.71)
Knau	15	83.17 (27.44)	40.65 (17.59)	1.99 (0.33)
Profen-Süd LC	21	88.68 (34.88)	40.65 (18.81)	2.26 (0.42)
Profen-Schwerzau ZC	24	78.12 (32.02)	33.76 (12.60)	2.31 (0.37)
Kayna-Süd	13	80.22 (25.33)	35.70 (13.18)	2.29 (0.20)
Messel	15	67.76 (15.63)	24.07 (5.65)	2.86 (0.56)

TABLE 10. Leaf morphometric data of *Rhodomyrtophyllum reticulosum* (abbreviations: n – number of polygonised specimens, l/w ratio – length/width ratio).

Leaf length is smallest for site Messel, which is the oldest site in age (67.76 mm). Sites Kayna-Süd, Profen-Schwerzau ZC, Profen-Süd LC and Knau reveal higher leaf lengths (Table 10, Figure 22A). The youngest sites Haselbach 2-3 mi, Schleenhain 3u and Peres 3u delivered lower mean leaf length. Variability in leaf length is most distinct in sites Kayna-Süd, Profen-Schwerzau ZC, Profen-Süd LC and Knau (Figure 22A). Leaf width data reveals a different pattern. Lowest leaf width is proven from site Messel (24.07 mm). In the other sites no trend in time, as seen in leaf length, is evident. Knau and Profen-Süd LC deliver as highest mean leaf width (40.65 mm) as leaf length and also highest variability in leaf widths. Highest length/width ratio is apparent from site Messel with 2.86 accompanied by highest variability (minimum 1.72 to 4.05; Figure 22B). Length/width ratio is slightly decreasing from the Ypresian/Lutetian towards the late Priabonian. Site Peres 3u delivers



the lowest length/width ratio with 1.90. The other sites, in between deliver similar, slightly alternating estimations.

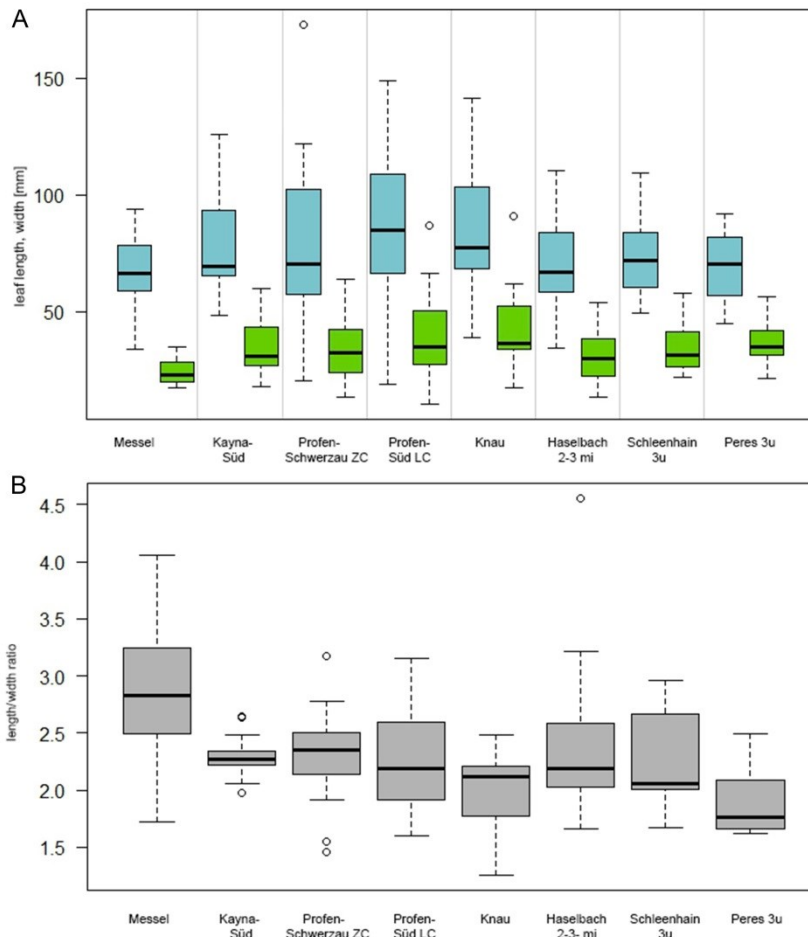


FIGURE 22. Leaf morphometric data plotted against time for *Rhodomyrtophyllum reticulosum* leaf traits (A: length (blue bars) and width (green bars) estimated from the late Ypresian/early Lutetian site Messel to the late Priabonian site Peres 3u; B: length/width ratio of the respective sites).

Site Messel represents the only record in an azonal assemblage in a non-fluvial system. Estimates derived from Messel are featuring morphometric parameters of both the oldest site and a slightly different depositional setting.

5.2.1. *Platanus neptuni*

The average leaf area, length, width, and length/width ratio of individual leaves or leaflets and estimated  $LM_A$  show considerable variation between the different sites (Table 11). Results have to be considered regarding the respective sample size, which is rather different for single sites, ranging from two to 38 leaves which were suitable for reconstruction (Table 3). Only specimens which yielded a preservation index of more than 0.7 were integrated into the analyses. That's why, no results have been derived from sites Borna-Ost DC and Kleinsaubernitz.

site	n	area [mm <sup>2</sup> ]	length [mm]	width [mm]	l/w ratio	n	$LM_A$ [g/m <sup>2</sup> ]
Linz	17	1697.1 (878.2)	95.1 (22.1)	25.7 (7.5)	3.8 (0.7)	12	87.0 (15.8)
Witznitz WC	4	336.9 (138.9)	40.7 (9.8)	12.2 (4.1)	3.6 (1.2)	3	148.2 (11.5)
Witznitz TC	2	704.1 (57.6)	64.8 (1.3)	15.5 (1.3)	4.2 (0.3)	1	108.0
Borna-Ost-Bockwitz	10	830.6 (508.0)	65.2 (22.7)	17.8 (6.6)	3.8 (0.7)	2	65.0 (9.8)
Kleinsaubernitz	-	-	-	-	-	-	-
Seifhennersdorf	5	860.2 (366.6)	71.9 (19.0)	18.8 (2.8)	3.8 (0.6)	-	-
Flörsheim	13	1150.0 (1083.3)	68.9 (33.5)	20.8 (10.7)	3.5 (0.8)	4	130.1 (43.3)
Rauenberg	38	1101.9 (663.8)	74.6 (26.4)	21.7 (6.6)	3.4 (0.7)	17	83.3 (18.5)
Schleenhain HC	7	781.2 (410.2)	65.3 (18.5)	17.2 (4.3)	3.8 (0.6)	2	104.0 (11.9)
Borna-Ost DC	-	-	-	-	-	-	-
Klausa	8	419.1 (102.0)	52.3 (6.2)	12.6 (1.7)	4.2 (0.3)	2	92.1 (10.8)
Profen-Schwerzau 1u	4	426.5 (174.6)	49.5 (6.5)	13.2 (3.3)	3.8 (0.4)	-	-
Kučlín	18	901.1 ( $\pm$ 488.4)	64.0 ( $\pm$ 19.1)	21.2 ( $\pm$ 6)	3.1 ( $\pm$ 0.5)	14	98.4 (18.1)

TABLE 11. Leaf morphometric data of *Platanus neptuni* (abbreviations: n – number of specimens, l/w ratio – length/width ratio, LMA – leaf mass per area).

A coupling of leaf morphometric data with the stratigraphic position is not evident (Figure 23 and Figure 24). Changes in mean leaf length, width or area are strongly coupled with the number of integrated specimen, as sites Kučlín, Rauenberg and Flörsheim reveal a greater variability in leaf sizes.

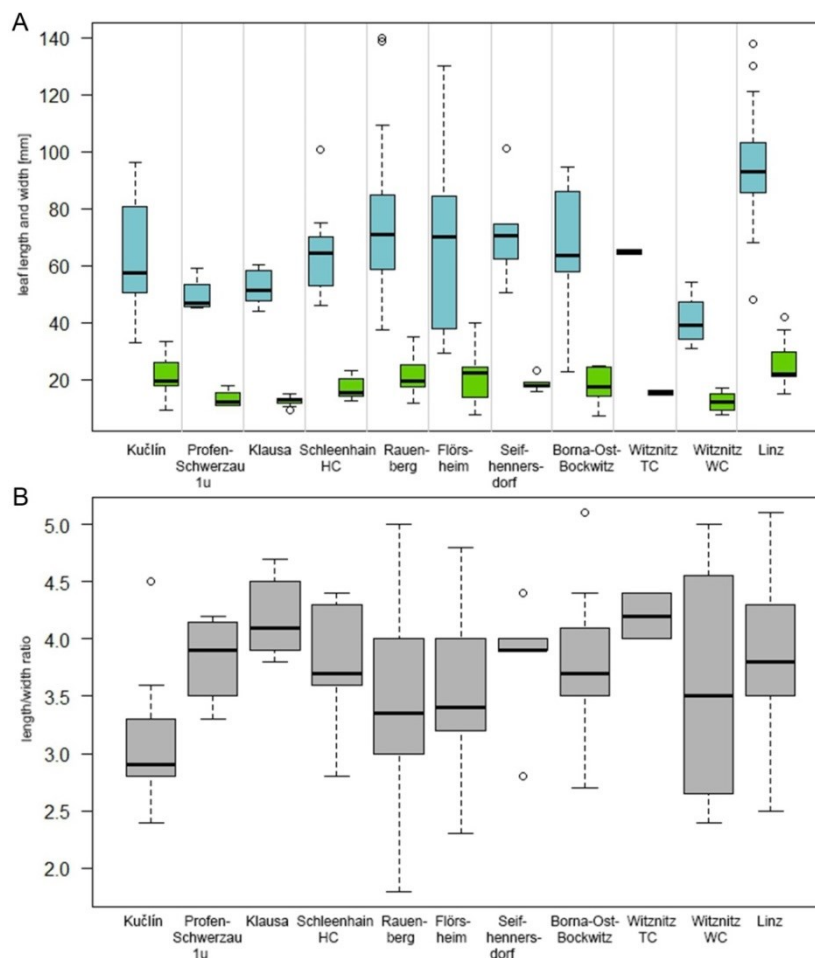


FIGURE 23. Leaf length and width and length/width ratio of *Platanus neptuni* plotted for the single sites in a stratigraphic order (A leaf length (blue bars) and width (green bars) estimated from the Bartonian site Kučlín to the Aquitanian site Linz and B length/width ratio of the respective sites).

Changes in the length/width ratio of 3.1 to 4.2 are coupled neither with the stratigraphic position (Figure 23B), nor with site characteristics. Leaf area for site Rauenberg for instance ranges between 286 and 2704 mm<sup>2</sup> (Figure 24A).  $LM_A$  varies largely between the different sites (Figure 24B) but a coupling with stratigraphic age is not evident.

The difference in leaf area for sites Profen-Schwerzau 1u, Klausau and Witznitz WC (Figure 24A) with significantly smaller leaves, compared to sites Rauenberg, Flörsheim and Linz, characterized by larger leaves, is obvious. Mean leaf area for sites where compound leaves occur frequently (Profen-Schwerzau 1u, Klausau) is significantly lower, than for other sites. Site Witznitz WC delivers similar leaf area estimates (Figure 24A). From this site no tri- or

quinquefoliate leaf is known, but the simple leaves are often asymmetrically shaped, which could indicate them being leaflets of previously compound leaves.

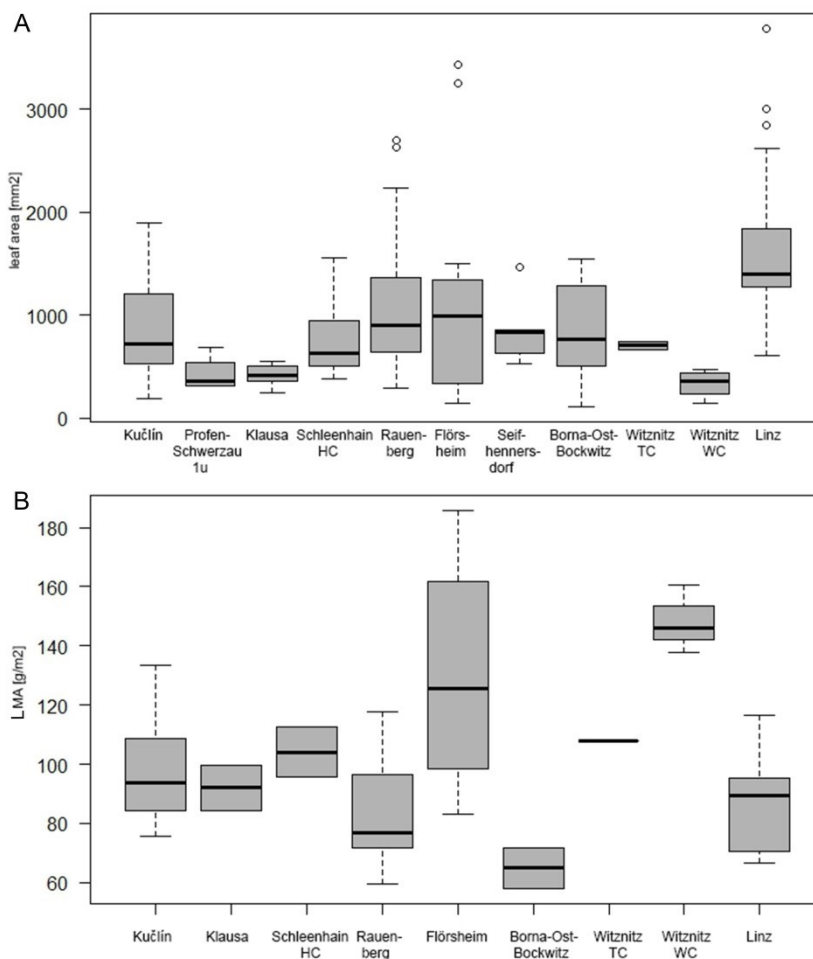


FIGURE 24. Leaf area and LM<sub>A</sub> of *Platanus neptuni* plotted for the single sites in a stratigraphic order (A Leaf area estimated from the Bartonian site Kučlín to the Aquitanian site Linz and B LM<sub>A</sub> for the respective sites).

Leaf size (leaf length and width) is highest in marine depositional settings (Figure 25A). Leaves from coastal-alluvial plains and volcanic environments tend to be smaller in average. Interestingly the length/width ratio of the investigated specimen is highest in leaves from coastal-alluvial plain settings. Leaves are more narrow elongated, than leaves from volcanic depositional settings (Figure 25B).

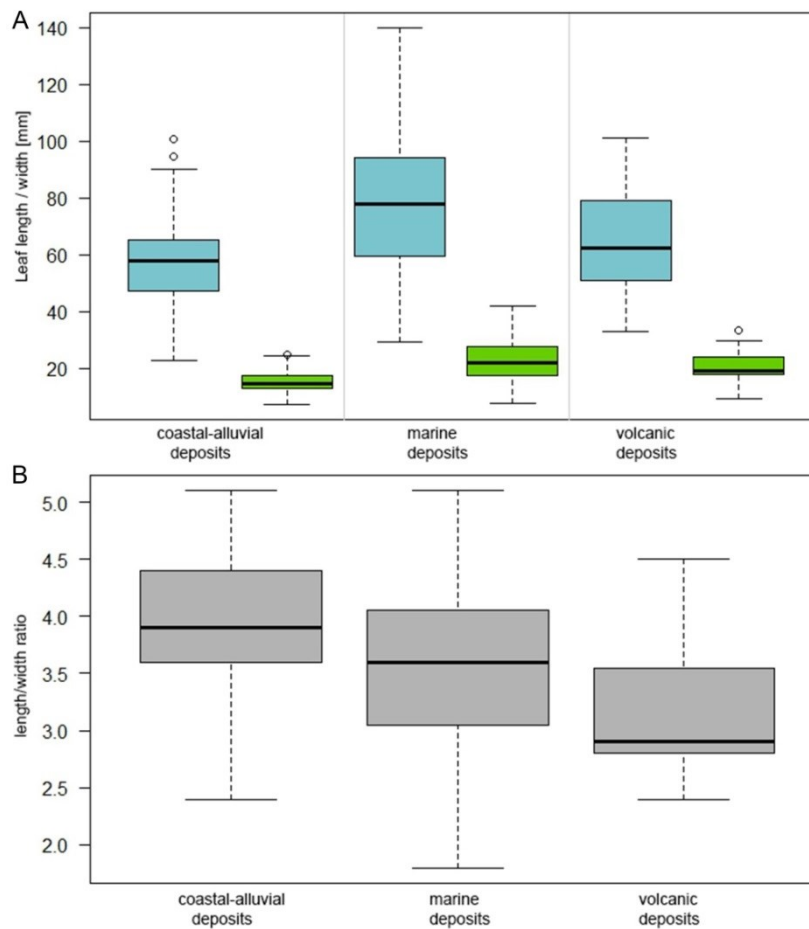


FIGURE 25. Leaf morphometric data of *Platanus neptuni* plotted against depositional setting (A length (blue bars) and width (green bars) estimated for coastal-alluvial deposits, marine and volcanic depositional settings; B length/width ratio for the respective depositional settings).

The average leaf area of *Platanus neptuni* from coastal-alluvial depositional settings (n=35) is significantly lower with 616.8 mm<sup>2</sup>, then for volcanic deposits with 892.2 mm<sup>2</sup> (n=23) and 1259.9 mm<sup>2</sup> for marine deposits (n=68) (Figure 26A). Interestingly, LM<sub>A</sub> is highest for coastal-alluvial plain depositional settings (Figure 26B). Therefore, *Platanus neptuni* leaves from coastal-alluvial depositional settings are smaller with a higher leaf mass per area (LM<sub>A</sub>) in contrast to leaves from marine depositional settings which are overall larger with significantly lower LM<sub>A</sub>.

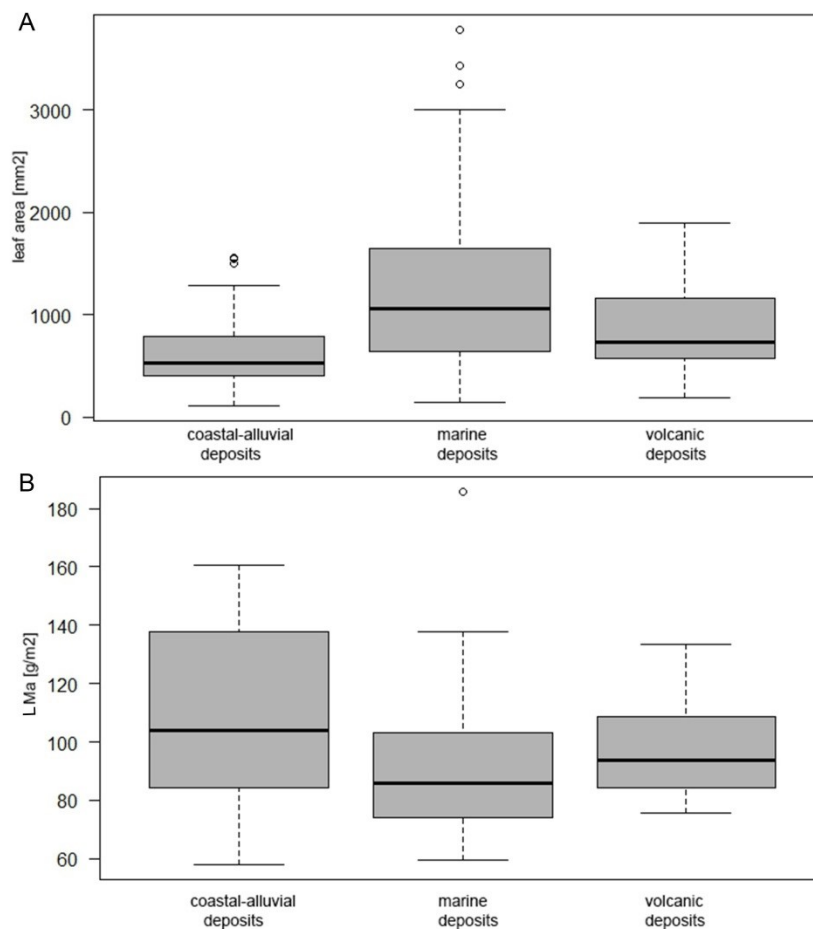


FIGURE 26. Leaf area and LM<sub>A</sub> for *Platanus neptuni* leaves derived from different depositional settings with A highest leaf area and B lowest LM<sub>A</sub> (leaf mass per area) in marine depositional settings.

Royer et al. (2007) define LM<sub>A</sub> of < 87 g/m<sup>2</sup> to be a threshold value of deciduousness and thus a life span of these species of less than 12 months (‘fast-return’ species). LM<sub>A</sub> of > 129 g/m<sup>2</sup> is regarded as a threshold for longer leaf life span and thus ‘slow return’. 40 % of the analysed leaves got LM<sub>A</sub> of less than 87 g/m<sup>2</sup>, 11 % show LM<sub>A</sub> of more than 129 g/m<sup>2</sup> and 48 % deliver LM<sub>A</sub> between (Table 11). If arranged according to the depositional setting leaves from floodplain assemblages delivered slightly higher mean LM<sub>A</sub> (107 g/m<sup>2</sup>) than leaves from marine (90 g/m<sup>2</sup>) and volcanic deposits (98 g/m<sup>2</sup>).

The investigated *Platanus neptuni* leaf traits vary conspicuously in dependence on the depositional setting and correspond more to regional effects than globally induced changes

in paleoclimate and paleoatmospheric conditions. This fact and possible correlations with taphonomical constraints will be further elaborated in chapter 6.2.

### 5.3. Cuticular derived parameters

#### 5.3.2. *Rhodomyrtophyllum reticulosum*

SD measurements were performed for all sites, except Messel (Table 12) because unfortunately no material was available for cuticular studies. Therefore, published data of Grein et al. (2011a) were incorporated. The cumulative mean served as proxy to obtain a statistically meaningful result in SD variations within one site. As SD shows considerable variations more than 10 leaves per site were investigated, except for sites where material was limited or cuticle preparation failed (sites Profen-Süd 3u and Schleenhain 3u). SD counts ranged between 20 and 55. SI was determined on 12 to 34 cuticles per site.

site	SD [1/mm <sup>2</sup> ]	SI [%]	Stomata width [μm]	Pore length h <sub>st</sub> [μm]
Schleenhain-3u	299 (96)	9.57 (2.63)	22.05 (2.65)	6.83 (1.28)
Profen-Süd-3u	290 (80)	10.07 (1.29)	20.75 (2.22)	5.00 (1.14)
Peres 3u	259 (110)	13.33 (1.82)	23.37 (2.90)	7.49 (1.69)
Haselbach-2-3-mi	291 (99)	9.95 (2.80)	20.59 (2.87)	6.81 (1.29)
Schleenhain-2o	384 (85)	9.83 (1.33)	21.65 (1.91)	5.60 (1.36)
Knau	252 (64)	10.63 (2.23)	21.98 (2.21)	6.40 (1.58)
Profen-Süd-LC	274 (90)	10.2 (3.73)	21.63 (2.33)	6.40 (1.23)
Kayna-Süd	212 (52)	9.66 (1.68)	23.40 (2.89)	6.53 (1.41)
Profen-Schwerzau ZC	220 (42)	10.46 (2.58)	23.90 (2.82)	7.60 (1.57)
Messel*	282 (59)	-	-	7.56 (2.00)

TABLE 12. Cuticular data of *Rhodomyrtophyllum reticulosum* (abbreviations: SD – stomata density, SI – stomata index; \* Grein et al. (2011a), - no data available).

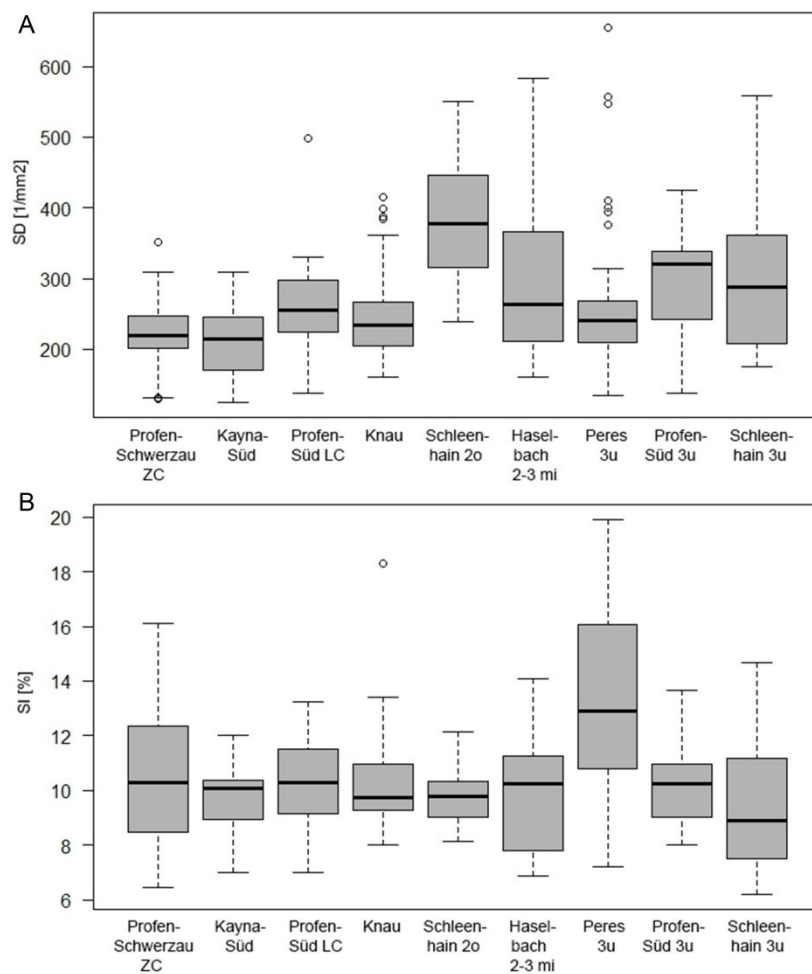


FIGURE 27. Cuticular data (SD, SI) from *Rhodomyrtophyllum reticulosum* in a stratigraphical order with A: SD from the Bartonian/Priabonian site Profen-Schwerzau ZC to the late Priabonian site Schleenhain 3u and B: SI for the respective sites.

Changes in SD do not correspond to global changes in climate and atmospheric conditions if SD is assumed to be negatively correlated to CO<sub>2</sub> (Roth-Nebelsick et al., 2014; Figure 27A). Sites Profen-Schwerzau ZC and Kayna-Süd deliver similar comparably low SD with 220 mm<sup>-2</sup> and 212 mm<sup>-2</sup> respectively. Highest SD was measured for sites Schleenhain 2o (384 mm<sup>-2</sup>). SD ranges greatly in some sites. For site Peres SD of 136 mm<sup>-2</sup> to 655 mm<sup>-2</sup> were measured. Leaves from sites Profen-Süd 3u and Schleenhain 3u, situated in a similar lithostratigraphic position, reveal comparable estimates, whereas SD for site Peres 3u, also coming from the underburden of lignite seam 3, delivers lower mean SD (259 mm<sup>-2</sup>).



SD for *Rhodomyrtophyllum reticulosum* is varying greatly both within one site and within a single specimen. Due to scattered and grouped stomata arrangements (Glinka and Walther, 2003) SD was gathered from cuticle samples from three regions: near the apex, the middle part of the leaf and the lower part near the base (Jurke, 2016; see Figure 28). This procedure allowed for determination of patterns for SD distribution. SD is not coupled with the sampling position on the leaf. Conspicuously high or low SD can be obtained from all sampling positions within a leaf (high SD from the base (MMG Pb Pe 110), highest SD from the middle part (MMG Pb Pe 202:2a) and highest SD at the apex (MMG Pb Pe 142)). To ensure the reliability of the results the minimum sample size (0.03 mm<sup>2</sup>; Poole and Kürschner, 1999) was enlarged to at least 0.7 mm<sup>2</sup> whenever cuticle size allowed for application of this new standard routine.

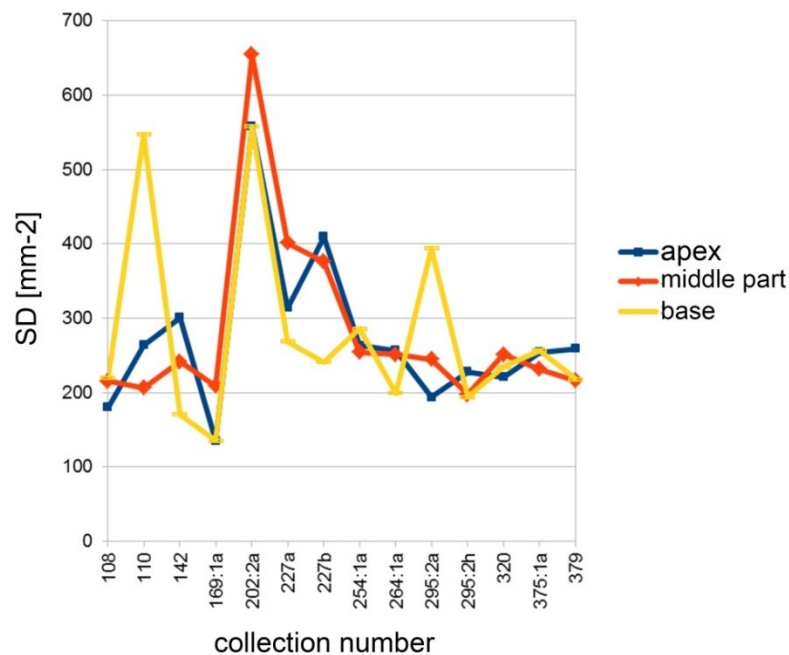


FIGURE 28. SD counts coupled with sampling position on respective specimen of *Rhodomyrtophyllum reticulosum* for site Peres 3u (modified from Jurke, 2016).

SI data deliver wide ranges and alternate greatly in the respective sites (Figure 27B), similar to SD. Grestest differences have been recognized from site Peres, with minimum SI of 7.21 % and a maximum value of 19.00 %. Due to these big variations within one site and

even a single specimen, no trend in SI changes was recognized. Mean SI ranges between 9.57 % (Schleenhain 3u) and 13.33 % (Peres 3u). Interestingly, sites Peres 3u, Profen-Süd 3u and Schleenhain 3u, coming from the similar lithostratigraphic position yield both the minimum and maximum SI (Table 12). SD and SI changes through time do not correspond to global changes in climate and CO<sub>2</sub>. Due to observed great differences in SD and SI it can be stated that these parameters are not sensitive to climatic and environmental processes. Detected ranges in SI variations are greatest in sites with most counts (Profen-Schwerzau 1u, Peres 3u). Differences in SI can be observed between cuticles where the epidermal cells are undulated. They depict bigger epidermal cells than cuticles where straight anticlines dominate.

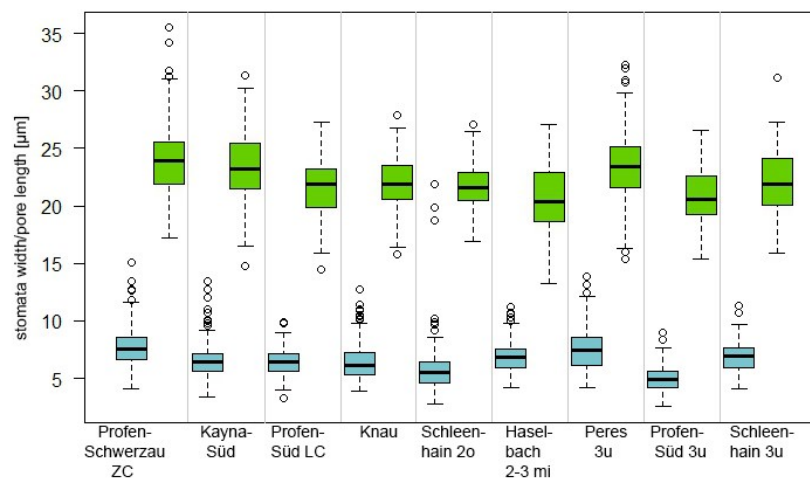


FIGURE 29. Stomata width (green bars) and pore length (blue bars) estimated from *Rhodomyrtoptyllum reticulosum* for the single sites.

Stomata width (Figure 29) varies between 20.75 µm (Profen-Süd 3u) and 23.90 µm (Profen-Schwerzau ZC). Values vary slightly between the different sites but do not change with stratigraphic age if taken standard deviations into account. Interestingly a weak correlation of SD and stomata width can be recognized, though low SD of sites Profen-Schwerzau ZC and Kayna-Süd are bound to greatest stomata width (Table 12, Figure 27A and Figure 29). Sites Profen-Schwerzau ZC and Peres 3u deliver the biggest dataset for stomata width and pore length measurements and show, at the same time, the longest range in measured stomata width variations (Figure 29), which pints out the diversity in

stomata sizes and the necessity of incorporation of a sufficient amount of material. Pore length is also not changing significantly from the Bartonian to the late Priabonian (Figure 29).

### 5.3.1. *Platanus neptuni*

SD measurements were conducted for all sites with cuticle preservation, whereas SI, stomata width and pore length data were only gathered from sites with proper cuticle preservation (Table 13).

site	SD [1/mm <sup>2</sup> ]	SI [%]	TD [1/mm <sup>2</sup> ]	Stomata width [μm]	Pore length [μm]
Linz	73 (24)	-	16 (11)	-	-
Witznitz-WC	89 (28)	11.82 (2.29)	12 (6)	35.07 (3.89)	13.76 (3.18)
Witznit-TC	104 (25)	12.56 (1.76)	11 (6)	30.76 (3.35)	11.25 (2.28)
Borna-Ost-Bockwitz	105 (24)	12.65 (1.90)	7 (4)	33.00 (3.30)	12.66 (2.27)
Kleinsaubernitz	109 (25)	-	6 (4)	30.32 (3.81)	13.29 (2.07)
Seifhennersdorf	112 (30)	13.07 (1.54)	5 (6)	32.73 (3.88)	13.41 (2.47)
Flörsheim	78 (9)	-	10 (7)	35.66 (4.35)	12.87 (2.63)
Rauenberg	69 (11)	-	8 (4)	37.85 (3.65)	14.29 (3.15)
Schleenhain-HC	96 (26)	11.00 (2.77)	16 (11)	34.38 (3.19)	13.16 (2.68)
Borna-Ost-DC	137 (33)	12.44 (1.62)	40 (29)	32.04 (3.50)	12.34 (2.29)
Klausa	-	-	-	-	-
Profen-Schwerzau-1u	150 (21)	-	35 (16)	27.67 (2.69)	10.97 (1.98)
Kučlín	-	-	-	-	-

TABLE 13. Cuticular data of *Platanus neptuni* (abbreviations: SD – stomata density, SI – stomata index, TD – trichome density; - no data available).

Mean SD of the oldest sites that revealed reliable SD datasets, i.e. Profen-Schwerzau 1u (150 mm<sup>-2</sup>) and Borna-Ost DC (137 mm<sup>-2</sup>) is significantly higher if compared to the younger sites (Table 13, Figure 30). SD values decrease towards the Oligocene plant assemblage of

Schleenhain HC ( $96 \text{ mm}^{-2}$ ). The Rupelian sites Rauenberg and Flörsheim show similar and slightly lower SD values ( $69 \text{ mm}^{-2}$  and  $78 \text{ mm}^{-2}$ ) while site Seifhennersdorf, similar in age, indicates higher SD ( $112 \text{ mm}^{-2}$ ) (Figure 30A). The Weißelster sites Borna-Ost-Bockwitz and Witznitz TC, both derived from the Chattian (Thierbach clay horizon) yield similar SD values with mean  $105 \text{ mm}^{-2}$ . Site Witznitz-WC, representing a flora near the Oligocene-Miocene boundary and site Linz from the early Miocene show a decrease in SD.

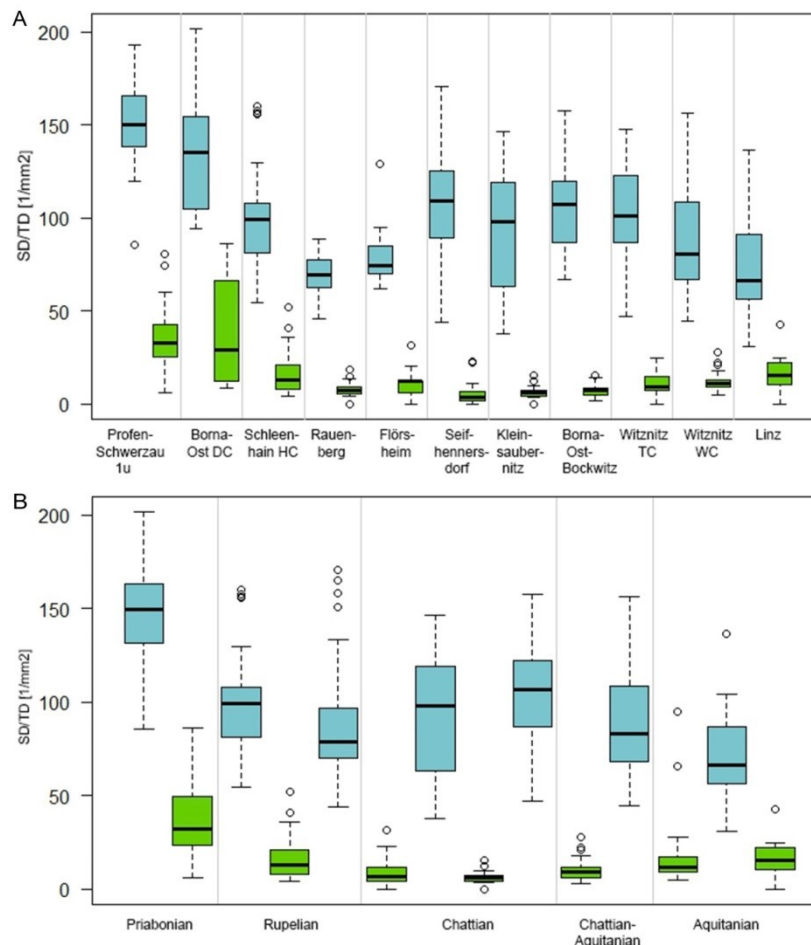


FIGURE 30. SD and TD of *Platanus neptuni* plotted for the single sites and regarding stratigraphy (sites are arranged due to age with Profen-Schwerzau representing the oldest and Linz as youngest site; A: SD (blue bars) and TD (green bars) for the single sites and B: SD, TD grouped and plotted against stratigraphic age.

Considering the data of TD measurements, similar trends comparing to SD are visible (Figure 30) from the Bartonian/Priabonian towards the early Rupelian. The younger sites indicate a slight rise in TD accompanied by a drop in mean SD. Highest TD values were observed from the Bartonian/Priabonian site Profen-Schwerzau-1u ( $35 \text{ mm}^{-2}$ ) and the Priabonian site Borna-Ost-DC ( $40 \text{ mm}^{-2}$ ). In the Rupelian site Schleenhain-HC TD drops to a mean value of  $15 \text{ mm}^{-2}$ . The younger sites deliver similar low TD. The decrease of TD from the Priabonian towards the Rupelian in the coastal-alluvial plain sites Borna-Ost-DC and Profen-Schwerzau-1u comparing to Schleenhain-HC is just as conspicuous as the remarkable reverse trend in SD and TD from the Chattian towards the early Aquitanian with decreasing SD and increasing TD.

SI measurements were performed only for sites Borna-Ost-DC, Schleenhain-HC, Seifhennersdorf, Borna-Ost-Bockwitz, Witznitz-TC and Witznitz-WC, because at all other sites, the cuticles did not allow proper identification of the epidermal cells (Table 3, Figure 31A). The Priabonian site Borna-Ost-DC delivers mean SI of 8.13 %, which is the lowest value, in contrast to the younger sites, where SI values increase towards the Oligocene-Miocene boundary with SI of 9.65 %. Only site Borna-Ost-Bockwitz delivers a higher SI with 9.92 %. SI reveals its own trend regarding time which does not correspond to the trend given by SD data.

Stomata pore length ( $h_{st}$ ) and stomata width show a weak correlation (Table 13, Figure 31B). Stomata width is varying between the Bartonian/Priabonian and the early Aquitanian in the negative correlated to SD, with an increase in stomata width during the Priabonian and early Rupelian. Highest stomata width was estimated from site Rauenberg with  $37.85 \mu\text{m}$  and lowest SD with  $69 \text{ mm}^{-2}$ . Stomata width is decreasing during the Rupelian and early Chattian, before another stepwise rise occurred in the late Chattian to the early Aquitanian (Figure 31B), also corresponding to the reverse trend in SD. For the Priabonian and early Rupelian sites a correlation of TD and stomata width can be recognized, which weakens during the late Rupelian, Chattian and early Aquitanian. In the Priabonian sites TD and stomata width are negatively correlated and indicate the interdependency of stomata size and trichome frequency on cuticles. As Stomata pore length ( $h_{st}$ ) does not vary significantly between the single sites and through time only a weak correlation of SD and  $h_{st}$  was recognized, with high SD values bound to small  $h_{st}$ .

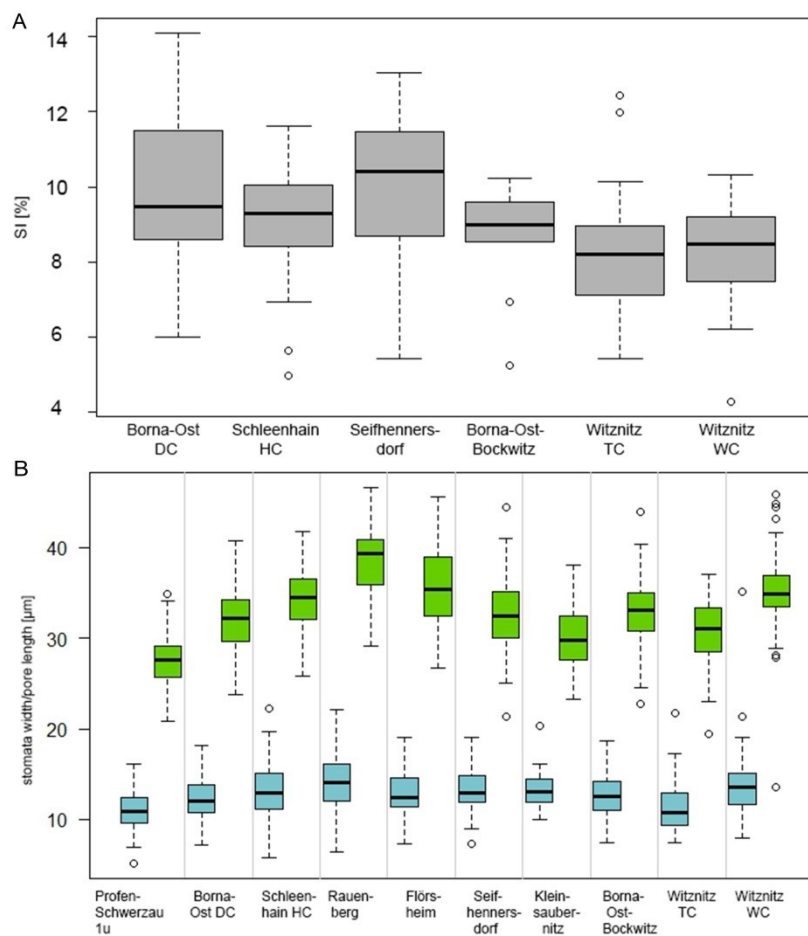


FIGURE 31. SI and stomata width and pore length data of *Platanus neptuni* plotted for the single sites and regarding stratigraphy (sites are arranged due to age with Profen-Schwerzau 1u as oldest and Witznitz WC as youngest site; A: SI for respective sites and B: stomata width (green bars) and pore length (blue bars) for the single sites).

With respect to the depositional setting, SD values show considerable variations (Figure 32A). A mean SD of  $103 \text{ mm}^{-2}$  from coastal-alluvial deposits is similar to the results of SD measurements from volcanic depositional environments, delivering a mean SD of  $106 \text{ mm}^{-2}$ . Leaves from marine deposits deliver significantly lower mean SD of  $77 \text{ mm}^{-2}$  (Flörsheim),  $69 \text{ mm}^{-2}$  (Rauenberg) and  $73 \text{ mm}^{-2}$  (Linz), respectively. This pattern in SD variation is not mirrored in TD values. Mean TD of the volcanic deposits are significantly lower ( $5.6 \text{ mm}^{-2}$ ) than TD of coastal-alluvial depositional settings ( $15.7 \text{ mm}^{-2}$ ). Leaves from marine deposits deliver TD of  $9.3 \text{ mm}^{-2}$ . Remarkably, leaves derived from the coastal-alluvial deposits, with 127 samples plotted together, deliver TD from  $0 \text{ mm}^{-2}$  to  $86 \text{ mm}^{-2}$  (Figure 32A).

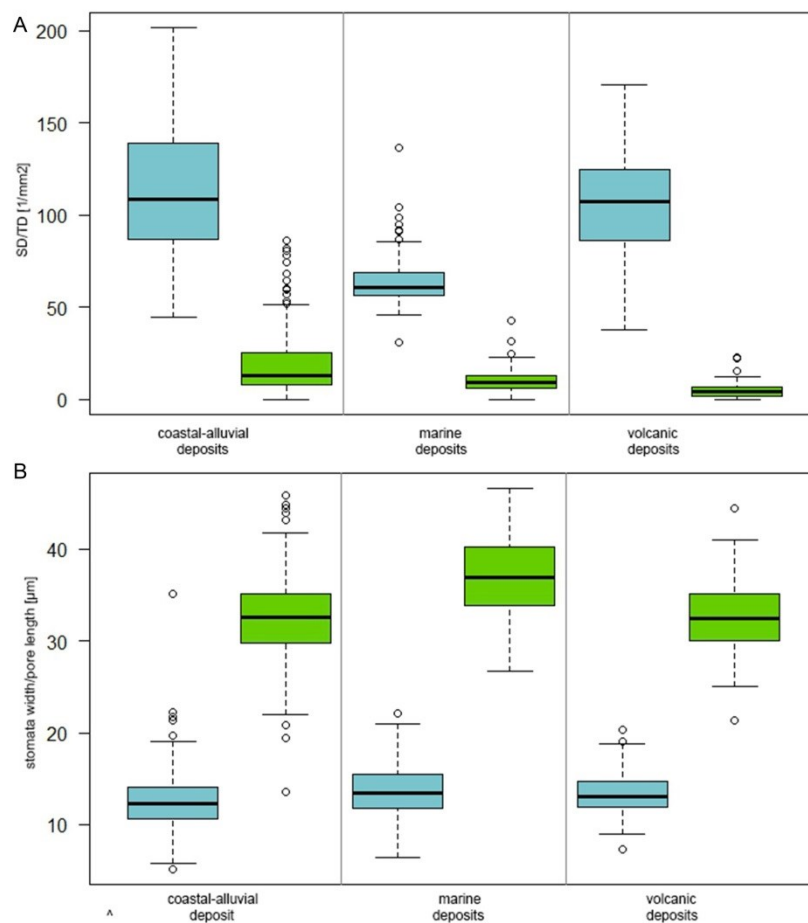


FIGURE 32. SD, TD, stomata width and pore length of *Platanus neptuni* leaves plotted against depositional setting (A SD and TD plotted for coastal-alluvial plain deposits, marine and volcanic deposits; B stomata width (green bars) and pore length (blue bars) plotted for the depositional environment).

If stomata size and pore length plotted for the different depositional settings, one can recognize highest stomata width estimates in marine depositional settings (Figure 32B), which is revealed also in lower SD from leaves derived from marine settings (Figure 32A). Differences in stomata width between leaves from coastal-alluvial settings and volcanic settings are comparatively small. A coupling of  $h_{st}$  with depositional setting is only recognized to a minor degree with highest  $h_{st}$  in marine settings and lowest values derived from coastal-alluvial plain settings.

## 5.4. Paleoatmospheric reconstruction

### 5.4.1. *Rhodomyrtophyllum reticulosum*

Paleoatmospheric reconstructions could obviously only be conducted for those sites delivering all input parameters (Table 14A and 14B). As sufficient morphometric data were not available for all sites (Klausau, Schleenhain 2o, Profen-Süd 3u), these have been excluded from the analyses. For site Messel no cuticular data were ascertained, because no collection material was available for cuticular studies. Included sites were chosen regarding their stratigraphic position and their covering of a long stratigraphic range to trace possible changes in CO<sub>2</sub>. For every sites certain input data for the application of the gas exchange model (Konrad et al., 2008) were gathered, comprising both morphometric and anatomical data (Table 14A) and site related carbon and paleoclimate data together with biochemical parameters (Table 14B). SD,  $d_{st}$ ,  $h_{st}$ ,  $w_{st}$ , leaf length and  $d_{asPP}$  (Table 14A) serve as direct input parameters, whereas  $c_i/c_a$ ,  $q$ ,  $T$  and  $RH$  are indirect critical parameters in whose ranges the respective direct parameters have been varied between the respective minimum and maximum value. The mean value of each critical indirect parameter served as fixed value for all parameter variations. Parameters were shifted towards the mean and maximum character of a parameter within the respective  $c_i/c_a$ . Therefore, mean and maximum values were not reached in every parameter constellation and variation, which is marked in Table 14B.

site	SD [1/mm <sup>2</sup> ]	$d_{st}$ [μm]	$h_{st}$ [μm]	$pw_{st}$ [μm]	leaf length [mm]	$d_{asPP}$ [μm]
Schleenhain-3u	299 (96)	11.03 (1.33)	6.83 (1.28)	3.40 (0.64)	35.2 (12.3)	128.7
Peres 3u	259 (110)	11.65 (1.50)	7.50 (1.70)	3.75 (0.85)	37.2 (10.2)	128.7
Haselbach-2-3-mi	291 (99)	10.30 (1.40)	6.81 (1.29)	3.40 (0.65)	30.9 (10.4)	128.7
Knau	252 (64)	10.99 (1.11)	6.40 (1.58)	3.20 (0.79)	43.1 (17.6)	128.7
Profen-Süd-LC	274 (90)	10.82 (1.17)	6.40 (1.23)	3.20 (0.62)	41.0 (18.6)	128.7
Kayna-Süd	212 (52)	11.70 (1.45)	6.53 (1.41)	3.27 (0.71)	35.6 (1.3)	128.7
Profen-Schwerzau ZC	220 (42)	12.00 (1.41)	7.60 (1.57)	3.80 (0.79)	33.4 (11.9)	128.7

TABLE 14A. Morphometrical and anatomical input data for CO<sub>2</sub> reconstructions gathered from *Rhodomyrtophyllum reticulosum* (abbreviations: SD – stomata density,  $d_{st}$  - depth of stomatal pore,  $h_{st}$  – pore length,  $pw_{st}$  – pore width,  $d_{asPP}$  – mesophyll thickness, measured on extant *Syzygium samarangense*).



site		$c_i/c_a$	$q$ [ $\mu\text{mol}/\text{m}^2\text{s}$ ] *	$T$ [ $^{\circ}\text{C}$ ]	RH [%]
Schleenhain-3u	min	0.71 (0.74)	33.7 (49.35)	18.7 ( <b>19.0</b> )	70 (74.39)
	mean (fixed)	0.75	50.0	19.5	74.5
	max	0.79	54.3	<b>23.5</b>	79
Peres 3u	min	0.766	33.7 ( <b>45.34</b> )	18.2	72 (73.78)
	mean (fixed)	0.77	50.0	19.0	74.5
	max	0.774	54.3 (52.1)	22.7 (20.5)	77 (75.22)
Haselbach-2-3-mi	min	0.72 (0.73)	33.7 ( <b>53.53</b> )	18.7	72 (73.58)
	mean (fixed)	0.74	50.0	18.7	74
	max	0.76	54.3	<b>22.5</b>	76
Knau	min	0.71	33.7 ( <b>47.65</b> )	18.3	72
	mean (fixed)	0.73	50.0	19.1	74
	max	0.75	54.3	<b>22.8</b>	76
Profen-Süd-LC	min	0.71 (0.72)	33.7 (48.22)	16.1 ( <b>16.5</b> ) <sup>1</sup>	50.4 (56.18) <sup>1</sup>
	mean (fixed)	0.74	50.0	18.3 <sup>1</sup>	59.0 <sup>1</sup>
	max	0.77	54.3	20.0 <sup>1</sup>	<b>67.6</b> <sup>1</sup>
Kayna-Süd	min	0.74	33.7 ( <b>39.94</b> )	17.7	70
	mean (fixed)	0.76	50.0	18.5	73.5
	max	0.78	54.3	22.4	77
Profen-Schwerzau ZC	min	0.71 ( <b>0.73</b> )	33.7 ( <b>49.66</b> )	18.6	75
	mean (fixed)	0.73	50.0	18.6	75
	max	0.75	54.3	<b>22.2</b>	75

TABLE 14B. Carbon, biochemical and climate input parameters for gas exchange modelling using *Rhodoyrtophyllum reticulosum* (minimum, mean and maximum parameter variation; red frame: limitation in parameter variation (minimum and/or maximum value not reached) and set minimum in ()); bold values: Minimum or maximum value defining the minimum and maximum  $\text{CO}_2$  for the respective site; abbreviations:  $c_i/c_a$  – ratio of leaf internal ( $c_i$ ) and external ( $c_a$ ) carbon,  $T$  – temperature with  $T_{\text{min}}$  – MAT,  $T_{\text{fixed}}$  – mean temperature of the vegetation period (month with temperature  $\geq 10$   $^{\circ}\text{C}$ ,  $T_{\text{max}}$  – mean temperature between April and October when mean monthly temperature  $\geq 10$   $^{\circ}\text{C}$ , RH – relative humidity; \* value gathered from literature (Grein et al., 2011a and citations in there), <sup>1</sup> paleoclimate data derived by CLAMP due to unavailable taxonomic determination so far).

$\text{CO}_2$  values calculated for 7 Bartonian/Priabonian sites (Table 15) range between mean 397 ppm (Profen-Süd LC) and 656 ppm (Kayna-Süd). Most minimum and maximum boundaries for  $\text{CO}_2$  were defined by parameter variation of the maximum carboxylation rate ( $q$ ) and  $T$ . Calculation of  $\text{CO}_2$  using the gas exchange model (Konrad et al., 2008) and systematic parameter variation, as done in e.g. Grein et al. (2011a, 2013) and Roth-Nebelsick et al. (2014), led to the definition of wide ranges in atmospheric  $\text{CO}_2$ . Site Kayna-Süd delivers minimum and maximum  $\text{CO}_2$  of 284 ppm and 1028 ppm respectively. As parameter variation was done within the ranges of possible  $c_i/c_a$  site Peres 3u delivered the smallest range in  $\text{CO}_2$  as, beside  $T_{\text{max}}$ , all other parameter never reached the possible minimum trait variation (Table 15, Figure 33).

site	CO <sub>2</sub> min [ppm]	CO <sub>2</sub> max [ppm]	CO <sub>2</sub> mean [ppm]
Schleenhain 3u	281	662	471.5
Peres 3u	280	587	433.5
Haselbach 2-3 mi	282	610	446.0
Knau	305	728	516.5
Profen-Süd LC	246	548	397.0
Kayna-Süd	284	1028	656.0
Profen-Schwerzau ZC	287	615	451.0

TABLE 15. Estimated minimum, mean and maximum CO<sub>2</sub> using the gas exchange model (Konrad et al., 2008) for *Rhodomyrtophyllum reticulosum*.

Lowest mean CO<sub>2</sub> was estimated from site Profen-Süd LC. Minimum and maximum CO<sub>2</sub> were defined by both T and RH. Paleoclimate data were gathered from CLAMP estimations, as the flora is currently under taxonomic investigation and CA is not applicable yet. The comparably lower temperature and humidity as input parameters caused the lower CO<sub>2</sub> values. Interestingly, sites Peres 3u and Schleenhain 3u, situated in a similar stratigraphic position deliver comparable minimum and maximum CO<sub>2</sub> (Table 15).

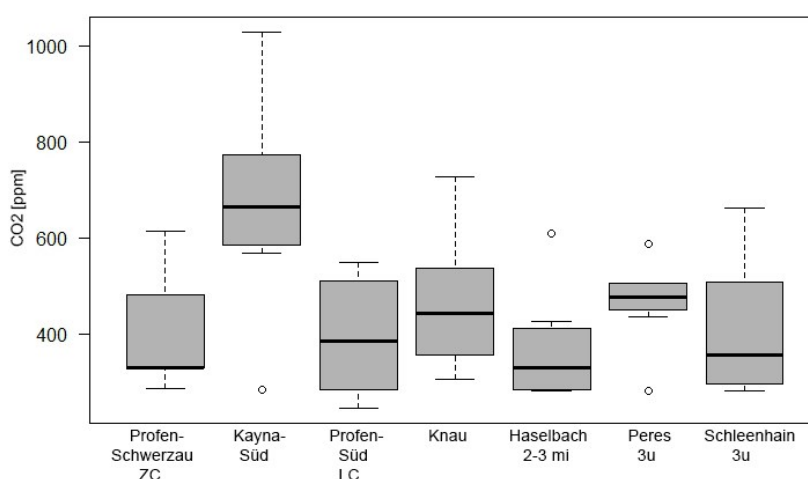


FIGURE 33. Bartonian and Priabonian CO<sub>2</sub> reconstructed using the gas exchange model and *Rhodomyrtophyllum reticulosum* leaf traits, biochemical, carbon and climate data.

5.4.2. *Platanus neptuni*

Paleoatmospheric reconstructions were not feasible for all sites, either because of missing input parameters (no SD for sites Kučlín and Klausau, no  $h_{st}$  data for Linz), or because of conflicting input parameters (Bartonian/Priabonian sites Borna-Ost DC and Profen-Schwerzau 1u and site Kleinsaubernitz). In addition to the studies of Grein et al. (2013) and Roth-Nebelsick et al. (2014) sites Flörsheim, Seifhennersdorf, Borna-Ost-Bockwitz and Witznitz TC have been investigated. Furthermore, sites Schleenhain and Witznitz WC were revisited due to updated input parameters. Table 16A lists the respective sites and morphometric and cuticular input parameters.

site	SD [1/mm <sup>2</sup> ]	$d_{st}$ [μm]	$h_{st}$ [μm]	$pw_{st}$ [μm]	leaf length [mm]	$d_{asPP}$ [μm]
Witznitz WC	89 (28)	17.54 (1.94)	13.76 (3.18)	6.88 (1.59)	12.2 (4.1)	99.6
Witznitz TC	104 (25)	15.38 (1.67)	11.25 (2.28)	5.63 (1.14)	15.5 (1.3)	99.6
Borna-Ost-Bockwitz	105 (28)	15.01 (1.75)	12.66 (2.29)	6.33 (1.15)	17.8 (6.6)	99.6
Seifhennersdorf	112 (30)	16.37 (1.94)	13.41 (2.47)	6.71 (1.24)	18.8 (2.8)	99.6
Flörsheim	78 (9)	17.97 (2.17)	12.87 (2.63)	6.44 (1.32)	20.8 (10.7)	99.6
Rauenberg	69 (11)	18.93 (1.82)	14.29 (3.15)	7.15 (1.58)	21.8 (6.6)	99.6
Schleenhain HC	96 (26)	17.19 (1.60)	13.16 (2.68)	6.58 (1.34)	17.2 (4.3)	99.6
Borna-Ost DC	137 (33)	16.02 (1.75)	12.34 (2.29)	6.17 (1.15)	14.0 (4.1)	99.6
Pofen-Schwerzau 1u	150 (21)	13.84 (1.35)	10.97 (1.98)	5.49 (0.99)	13.2 (3.3)	99.6

TABLE 16A. Morphometrical and anatomical input data for CO<sub>2</sub> reconstructions gathered from *Platanus neptuni*

(abbreviations: SD – stomata density,  $d_{st}$  – depth of stomatal pore,  $h_{st}$  – pore length,  $pw_{st}$  – pore width,  $d_{asPP}$  – mesophyll thickness, measured on extant *Platanus kerrii*).

Critical input parameters which have been shifted through modelling are listed in Table 16B. Notably, in most sites variation of  $q$  and  $T$  defined the minimum and maximum value of atmospheric CO<sub>2</sub>.

site		$c_i/c_a$	$q$ [ $\mu\text{mol}/\text{m}^2\text{s}$ ] *	$T$ [ $^{\circ}\text{C}$ ]	RH [%]
Witznitz WC	min	0.76	23.6 (40.22)	19.8	74
	mean (fixed)	0.79	50.0	19.8	74.5
	max	0.81	56.25	23.9	75
Witznitz TC	min	0.72	23.6 (45.43)	16.1	72
	mean (fixed)	0.75	50.0	18.2	74
	max	0.78	56.25	19.9	76
Borna-Ost-Bockwitz	min	0.72 (0.73)	23.6 (48.1)	15.9	72 (74)
	mean (fixed)	0.75	50.0	18.9	74
	max	0.78	56.25	21.2	76
Seifhennersdorf	min	0.64 (0.75)	23.6 (50)	17.4 (18.1)	75 (76)
	mean (fixed)	0.73 (0.75)	50.0	18.1	76
	max	0.80	56.25	21.6	77
Flörsheim	min	0.69 (0.70)	23.6 (43.84)	18.6	75
	mean (fixed)	0.72	50.0	18.6	75.5
	max	0.75	56.25	22.2	76
Rauenberg	min	0.67 (0.68)	23.6 (46.20)	18.9	75
	mean (fixed)	0.72	50.0	18.9	76
	max	0.77	56.25	22.2	77
Schleenhain HC	min	0.67 (0.70)	23.6 (53.91)	15.9 (18.8)	77
	mean (fixed)	0.71	50.0	18.9	77
	max	0.75	56.25	21.1	77
Borna-Ost DC	min	0.69	23.6	18.4	72
	mean (fixed)	0.73	50.0	18.4	73
	max	0.77	56.25	22.5	74
Profen-Schwerzau 1u	min	0.68	23.6	18.0 <sup>1</sup>	61.2 <sup>1</sup>
	mean (fixed)	0.70	50.0	18.0 <sup>1</sup>	69.8 <sup>1</sup>
	max	0.72	56.25	21.5 <sup>1</sup>	78.4 <sup>1</sup>

TABLE 16B: Carbon, biochemical and climate input parameters for gas exchange modelling using *Platanus neptuni*

(minimum, mean and maximum parameter variation; red frame: limitation in parameter variation (minimum and/or maximum value not reached) and set minimum in ()); bold values: Minimum or maximum value defining the minimum and maximum  $\text{CO}_2$  for the respective site; grey filling: sites where model running was not successful; abbreviations:  $c_i/c_a$  – ratio of leaf internal ( $c_i$ ) and external ( $c_a$ ) carbon,  $T$  – temperature with  $T_{\text{min}}$  – MAT,  $T_{\text{fixed}}$  – mean temperature of the vegetation period (month with temperature  $\geq 10$   $^{\circ}\text{C}$ ,  $T_{\text{max}}$  – mean temperature between April and October when mean monthly temperature  $\geq 10$   $^{\circ}\text{C}$ , RH – relative humidity; \* value gathered from literature (Roth-Nebelsick et al., 2014 and citations in there), 1 paleoclimate data derived by CLAMP due to unavailable taxonomic determination so far.

Estimated  $\text{CO}_2$  for the Oligocene indicates almost stable conditions around 400 ppm (Table 17, Figure 34). For the early Rupelian site Schleenhain HC mean  $\text{CO}_2$  of 407 ppm (301-512 ppm) was calculated. Sites Rauenberg and Flörsheim deliver higher results with mean 538 ppm respectively 515 ppm.  $\text{CO}_2$  drops as estimated for site Seifhennersdorf (393 ppm) and increases steadily towards the Oligocene-Miocene transition (Borna-Ost-Bockwitz (413

ppm), Witznitz TC (454 ppm) and Witznitz WC (566 ppm)), whereby minimum and maximum calculated CO<sub>2</sub> for site Witznitz WC ranges between 252 ppm and 879 ppm.

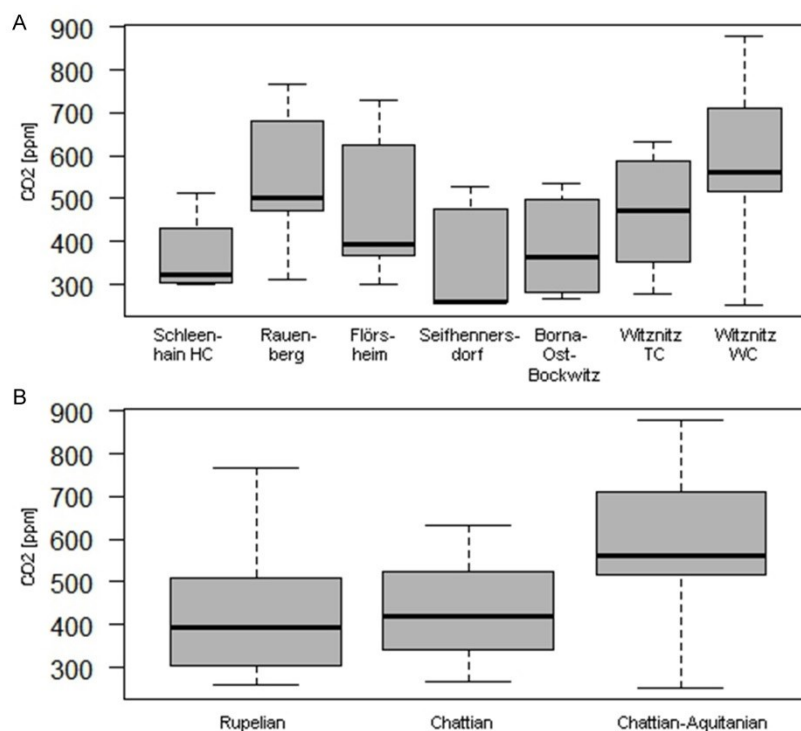


FIGURE 34. Rupelian to Aquitanian CO<sub>2</sub> reconstructed using the gas exchange model and *Platanus neptuni* leaf traits, biochemical, carbon and climate data (A: CO<sub>2</sub> estimated for the single sites through time with Schleenhain HC from the Rupelian to Witznitz WC at the Chattian/Aquitainian boundary and B: CO<sub>2</sub> plotted for single time slices with grouped CO<sub>2</sub> data of the respective sites).

site	CO <sub>2</sub> min [ppm]	CO <sub>2</sub> max [ppm]	CO <sub>2</sub> mean [ppm]
Witznitz WC	252	879	565,5
Witznitz TC	276	632	454
Borna-Ost-Bockwitz	268	536	413
Seifhennersdorf	259	526	393
Flörsheim	299	731	515
Rauenberg	311	765	538
Schleenhain HC	301	512	407
Borna-Ost DC	-	-	-
Profen-Schwerzau 1u	-	-	-

TABLE 17. Estimated minimum, mean and maximum CO<sub>2</sub> using the gas exchange model (Konrad et al., 2008) for *Platanus neptuni*.

Sites providing all necessary input parameters delivering no results are denoted (-).

## 5.5. Synthesis

Due to the longevity, predominance in the examined floras and partly excellent preservation of *Rhodomyrtophyllum reticulosum* and *Platanus neptuni*, covering a time span of approximately 26 Ma, a variety of morphometric, cuticular, palaeoclimatic and CO<sub>2</sub> data from 23 sites were gathered.

*Rhodomyrtophyllum reticulosum* leaf traits were investigated from the Ypresian/Lutetian flora of Messel (Wilde, 1989; Lenz et al., 2014), whose dating marks the end of the EECO to the likely latest Priabonian sites Profen-Süd 3u., Peres 3u and Schleenhain 3u, dated to SPP zone 18ou sensu Krutzsch et al. (2011) from the Weißelster Basin. The azonal, predominantly occurring tree was native to coastal-alluvial environments or, regarding its occurrence in Messel, to lake-shore environments revealed similar and only slightly changing morphological characteristics and morphometric trait variations. The mostly elliptic or obovate leaves, approximately 78 mm long and 32 mm wide (Table 10) do not reveal significant changes in leaf size through time in the Weißelster Basin floras and in the flora derived from Kayna-Süd. Regarding the leaves from Messel one can recognize them being generally smaller and narrow-elliptic which is expressed in a comparable small l/w ratio of 1.9. As diverse as leaf size, are also stomata distribution on the thick and robust cuticles. Their distribution pattern was analysed on leaves of sites Profen-Schwerzau ZC and Peres 3u (Jurke, 2016) to figure out, if (1) the chosen area for SD determination is influencing the results, as enormous differences in either SD and/or SI exist within one leaf and within the single sites or if (2) SD and SI are changing in dependency on the sampling site, namely between the basal part of the leaf, the middle and the apical part. Neither differences between the different sampling positions on the leaves lamina and calculated SD/SI nor the enlargement of the respective counting area resolved the problem of highly fluctuating SD and SI. As constant through time and variable within one site are  $w_{St}$  and  $h_{St}$ . If coupled with paleoclimatic data (Tables 8 and 9, Figure 21), which show almost no substantial changes in MAT, WMMT and CMMT during the late Eocene, both morphometric and cuticular data, indicate consistent and stable environmental and climatic conditions. CO<sub>2</sub> reconstruction was performed for seven sites, of which Profen-Schwerzau ZC is regarded to be the oldest, linked to SPP zone 17/18 by Krutzsch et al. (2011) and therefore Bartonian/Priabonian in age. All sites deliver similar mean atmospheric CO<sub>2</sub> values of 397 ppm to 517 ppm (Table 15). Differences can be seen in estimated CO<sub>2</sub> ranges due to

systematic parameter variation, with site Kayna-Süd revealing a possible atmospheric CO<sub>2</sub> between 284 ppm and 1028 ppm. Paleoclimate data and CO<sub>2</sub> reconstruction yield consistent estimates and underline the stability in leaf traits of *Rhodomyrtophyllum reticulosum* (Figure 35).

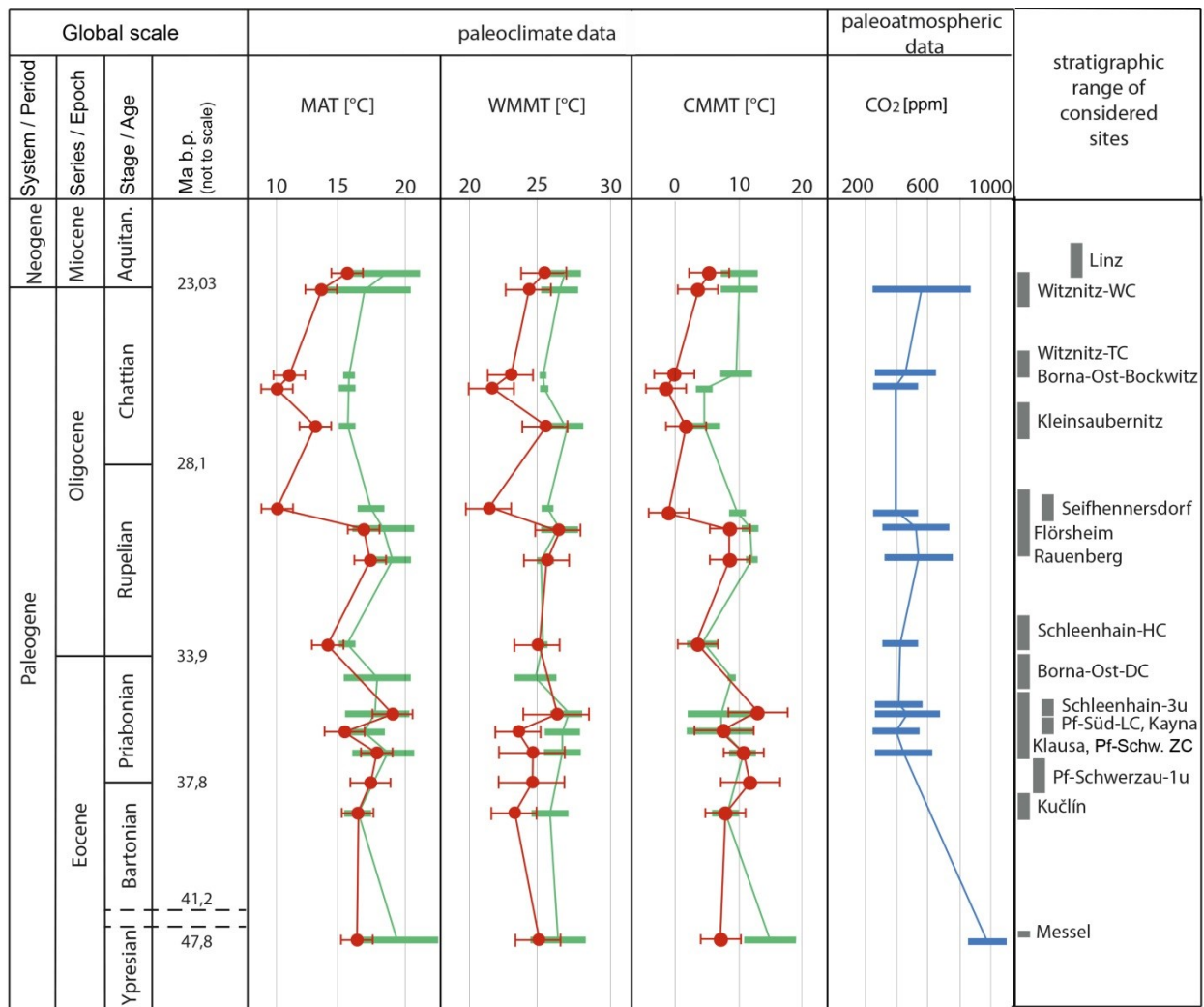


FIGURE 35. Paleoclimate and CO<sub>2</sub> summarized from the Ypresian/Lutetian boundary to the early Aquitanian.

Unfortunately, preservation of leaves in sites Klausa and Borna-Ost DC, where *Rhodomyrtophyllum reticulosum* and *Platanus neptuni* co-occur and therefore deliver a stratigraphic overlap, did not suit for the application of the same methods. Site Borna-Ost

with its highly fragmented leaves did not yield sufficient material for morphometric studies, whereas site Klauska did not yield cuticles and hence, has been skipped from the cuticular analyses.

The record of investigated *Platanus neptuni* leaves ranges from site Kučlín, dated to  $38.3 \pm 0.9$  Myr (Bellon et al., 1998) and therefore Bartonian in age, to the early Aquitanian site Linz, dated to nannoplankton zone NN 1 (Rupp and Ćorić, 2012). Morphometric traits were gathered from 11 sites. The total number of suitable leaves for replenishment, defined by a preservation of at least 70% of the leaf lamina, differs greatly between sites (Table 11). Due to the occurrence of simple, tri- and even quinquefoliate leaves, morphometric data differ greatly between (Witznitz WC versus Linz) and within (e.g. Rauenberg) sites and no correlation of changing leaf morphometric data regarding stratigraphic age have been found (Figure 23 and Figure 24). The cuticle, whose anatomical features are similar in the different morphotypes (Kvaček and Manchester, 2004), allows for the coupling of changes in SD through time, with decreasing SD from the Bartonian to the Rupelian and increased and stable SD in the Rupelian und Chattian, before another drop in SD occurs towards the Oligocene–Miocene boundary (Figure 30). TD, firstly gathered for a long-lived species for 11 sites and a time interval of approximately 16 Ma, partly reveals the same trend as SD. SI determination was only possible for distinct sites and few cuticle preparates. Data show conflicting results (Figure 31) compared to SD. Interestingly,  $w_{st}$  corresponds to SD as does  $h_{st}$  which shows only a weak correlation. Alongside the 'stratigraphical' approach, sites were chosen in order to reflect different depositional settings to investigate site-specific parameter variation. Hence, gathered *Platanus neptuni* leaf traits were considered due to correlations with their respective depositional settings, namely coastal-alluvial settings, marine and volcanic settings. Site dependent correlations are conspicuous, both regarding leaf morphology and cuticular data. One of the most prominent gathered results was derived for the marine sites (Flörsheim, Rauenberg and Linz) with highest leaf area coupled with lowest  $LM_A$  (Figure 26), together with lowest SD and highest mean  $w_{st}$  (Figure 32). Additionally, all three sites mirror the vegetation along the shore of warm oceans and seaways, the Oberrheingraben (Flörsheim, Rauenberg) and the Paratethys. In contrast, *Platanus neptuni* leaves from the coastal-alluvial deposits show reverse relations with low mean leaf area, high SD and low  $w_{st}$ . Paleoclimate data reconstructed using CA and CLAMP show similar trends in MAT, WMMT and CMMT during the middle Rupelian (estimated for sites Flörsheim and Rauenberg) and differ greatly in the Chattian, whereby CLAMP delivers lower temperatures but both methods reveal the same overall trend of likely stable temperatures during the Chattian and a gradual warming towards the



---

Oligocene-Miocene boundary (Figure 35). Highest MAT in the Oligocene was derived from the three marine sites. Unfortunately, gas exchange reconstruction using *Platanus neptuni* leaf traits was not feasible for the Priabonian sites and thus, the stratigraphic record of gathered CO<sub>2</sub> data spans the time interval of the early Rupelian (site Schleenhain HC) to the late Oligocene (site Witznitz WC) with no overlapping in the late Priabonian sites with data derived from *Rhodomyrtophyllum reticulosum* and *Platanus neptuni*. Estimated atmospheric CO<sub>2</sub> in the Rupelian ranges between mean 383 ppm (Seifhennersdorf) and 538 ppm (Rauenberg) delivering as stable estimates for the single sites as paleoclimate data (Figure 35). CO<sub>2</sub> in the Chattian is decreasing and increasing again towards the Oligocene-Miocene boundary which is in good agreement with estimated temperature.

Estimated morphometric and cuticular data of the two species, *Rhodomyrtophyllum reticulosum* and *Platanus neptuni* delivered data on both, changes in respective leaf traits through time correlated to global and regional paleoclimate and paleoatmospheric conditions and in dependency on their depositional setting. A coupling of paleogeographic differences in the considered leaf traits has been proven too.

## 6. Interpretation

The interpretation of the results and discussion on the applicability of the used methods follows the same structure as given in chapter 5. Every method and every result will be discussed. Due to the unique character of every investigated plant assemblage regarding differences in

- the sampling strategy of the individual collector (collection biases),
- age determination
- richness and availability of material of the whole flora and abundance of the respective taxa *Rhodomyrtophyllum reticulosum* and *Platanus neptuni*,
- the composition of the flora (composed of only leaf remains or additionally carpological remains) and the taxonomic determination,
- the preservation of the plant assemblage and the respective taxa and suitability for investigation of both morphological/morphometric and cuticular traits,
- the respective depositional setting (coastal-alluvial plain deposits, marine and volcanic deposits),
- taphonomic and methodological biases,
- differences in the paleogeographic settings

each chapter starts with the depiction of uncertainties and outliers concerning the respective method and derived results.

### 6.1. Paleoclimate reconstruction

#### 6.1.1. Uncertainties and outliers

As the composition of the plant litter in a fossil assemblage never reflects the local vegetation to 100 percent (Ferguson, 2005; Spicer et al., 2011), it is obvious that taphonomic processes have a huge impact on the character and composition of the respective taphocoenoses. The leaf components, in particular leaf litter beds, being mostly

parautochthonous in fluvial, alluvial sediments (Gastaldo et al., 1996; Greenwood, 2005; Kunzmann and Walther, 2007) and highly allochthonous in marine sediments (Kovar, 1982; Kvaček, 2004; Kovar-Eder, 2016) do not necessarily mirror the composition of the vegetation in a reasonable way. In contrast, fossil fruits, which are often buoyant, are likely to be partly conveyed from upstream vegetation and thus being partly allochthonous (Gee, 2005; Vassio and Martinetto, 2012). Leaf assemblages, and to a lesser amount carpodeposits, in fluvial and estuarine environments can indeed be considered as litter from the local vegetation. Other studies observed allochthonous leaf accumulations as well (Spicer, 1981). Nevertheless, certain transport mechanisms have to be kept in mind when analyzing fluvial plant assemblages (Burnham, 1989; Gastaldo et al., 1996; Ferguson, 2005; Greenwood, 2005; Royer et al., 2005). In plant assemblages derived from marine sediments, transport processes and their effect of sorting and fragmentation have an enormous influence on the composition of the respective plant assemblages, resulting in missing apices and bases of leaves and overrepresentation of small-leaved taxa (Kovar-Eder, 2016). These highly allochthonous plant assemblages derived from marine sediments feature a high diversity in species accompanied by low abundance of most taxa. The documentation of a massive fungal infection rate on leaves (Kovar, 1982; Kovar-Eder, 2016) corroborates the influence of sorting processes due to differences in the robustness of certain species and is mirrored also in the underrepresentation of deciduous woody taxa in marine plant assemblages (Kvaček, 2004; Kovar-Eder, 2016). Plant assemblages derived from lake deposits in volcanic settings reflect the composition of the vegetation surrounding a maar lake (e.g. site Kleinsaubernitz) and a fast burial and a short transport distance ensures the preservation of almost complete leaves, fruits and seeds. Lake deposits in volcanic settings often bear very diverse plant assemblages (Walther, 1999). More impact, on the other hand, on the composition of the fossil assemblage is represented by the potential of certain plant parts of different taxa for fossilization. Leaves that are more susceptible to any kind of decay are underrepresented in the fossil taphocoenoses in comparison with the relative percentage of their mother plants in the respective vegetational unit and vice versa (Spicer, 1981; Uhl et al., 2003). For example, Lauraceae leaves are among the most robust ones and therefore present in nearly all fossil assemblages, whereas other predominant evergreen woody plants such as Mastixiaceae and Symplocaceae are almost absent in respective leaf litter horizons. Their presence within the sites is almost exclusively known due to the occurrence of their diaspores (e.g. *Symplocos kirstei*, *S. anglica*, *Mastixia cf. boveyana*, *Eomastixia bilocularis*; Mai and Walther, 2000). The preservation and abundance of certain taxa is influenced by their abundance at the time when they enter the fossil record. The overwhelming inflow of leaf litter derived

from deciduous taxa during leaf fall, which is of lower mechanic strength than evergreen leaves, leads to lower fragmentation rates caused by invertebrate feeders, bacteria and fungi (Spicer, 1981). Evergreens, entering the depositional system gradually, can be easily destroyed chemically, but feature higher mechanic strength. For instance, leaves of the deciduous taxon *Platanus neptuni* are frequent in the fluvial deposits of Klaus, which could be due to the high volume of influx of plant material in a depositional system within a short time during leaf fall.

The interpretation of paleoclimatic estimations derived by CA has to be done regarding the above mentioned taphonomic constraints. Due to e.g. sorting processes, differences in the ability of preservation and the overall poorness in species in azonal, alluvial-coastal plant assemblages exhibit a small sample size for CA reconstructions. Due to this small sample size, the similar floral composition and the determination of NLRs mainly on genus or even family level, the calculated MATs are in a similar range. Fossil species, which are assumed to be climatically sensitive by various authors (e.g. Mai, 1995), do not affect the calculated MAT, CMMT and WMMT due to the lack of knowledge of their NLRs or their absence in the fossil record. In some cases the CA was not able to determine an interval of coexistence due to the disparity of climatic data for the individual NLRs. It is obvious that the composition of the fossil plant assemblages is not always transferable to extant floras. Mai (1995) denotes this as 'ecophysiological dissonance' which means that genera co-occurring in a fossil assemblage may have no overlap in their present-day climatic and environmental requirements. The calculation of CA-intervals has to be done by exclusion of critical taxa, such as monotypic NLRs occurring in relic habitats with climate conditions clearly different from the ones assumed for their fossil counterparts (e.g. *Tetraclinis articulata*). Despite the discussion about the choice of NLR (taxonomic vs. ecological NLR) (Kvaček, 2007) the database PALEOFLORA gives good indications of possible NLRs, but undoubtedly needs constant revision and maintenance of data (Grimm and Denk, 2012; Utescher et al., 2014).

The results of CLAMP have to be interpreted carefully considering the formation and composition of the taphocoenoses and the respective depositional setting. Plant assemblages embedded in coastal-alluvial sediments are mostly poor in species and paleoclimatic signals have to be interpreted in terms of the influences of certain taphonomic factors, because these plant assemblages are heavily affected by fragmentation and sorting processes. As seen in Table 9 only a minor proportion of these fluvial plant assemblages were usable for CLAMP, as the minimum scoresheet completeness was only seldom reached. Therefore, to include also these assemblages all estimations of sites with a

scoresheet completeness of at least 0.4 were included into the analysis. Undoubtable, these results have to be considered regarding these taphonomic and methodical constraints. CLAMP estimates for instance CMMT of 13.6 °C for sites Schleenhain 2o and Schleenhain 3u and high MAT of 19.4 °C and 19.7 °C respectively. Both plant assemblages yield a scoresheet completeness of clearly less than 0.66 and for site Schleenhain 2o only 13 morphotypes were identifiable. For site Schleenhain 3u 19 morphotypes were investigated. Fossil leaf remains of the studied material are fragmented mainly because sediment split-off in the lab does not reveal even surfaces with complete leaves but small specimens with uneven surfaces where most leaves are only partly exposed and thus do not show all leaf physiognomic characters used for CLAMP. Highest scoresheet completeness can be recognized in plant assemblages from marine deposits. This could be due to the scattered occurrence of taxa and therefore the better visibility of leaf physiognomic states, whereas in coastal-alluvial plant assemblages leaves are often co-occurring in packages overlying one another, and the overall higher amount of distinct morphotypes.

The influences of taxonomic and nomenclatural changes of taxa in the utilized floral lists with respect to previous climatic estimations based on older determinations have to be considered as well. The shared identity of the leaves of *Eotrigonobalanus furcinervis* and the fossil fruit *Eotrigonobalanus andreanszky* has been demonstrated (Kvaček and Walther, 1989) and thus only one species, i.e., the whole-plant species has to be used. For the fossil leaves of "*Laurophyllum*" *fischkandelii* the relationship to the fossil fruit *Steinhauera subglobosa* is recently assumed (unpubl.; personal communication L. Kunzmann). The taxonomic relation of leaves and diaspores within the family of the Mastixiaceae and the Lythraceae is not known and has to be taken into account while evaluating the results. The diversity of the *Dryophyllum* complex (extinct Fagaceae) has also been discussed (Kvaček, 2007). According to Kvaček (2007) the taxa *D. curticellense* and *D. dewalquei* are assumed to be distinct species whereas *D. knauense* and *D. moselense* are reinterpreted as local varieties.

### 6.1.2. Paleoclimate signals

CA and CLAMP show considerable variation in estimated paleoclimatic conditions for different reasons, which have been repeatedly discussed in detail (Grimm and Denk, 2012; Grimm et al., 2016). The general trend of decreasing MAT from the late Ypresian to the Chattian and a rise in MAT towards the Aquitanian recorded herein (see Figure 21) is in good agreement with other paleoclimatic studies using fossil plants (Mosbrugger and Utescher, 2005; Teodoridis and Kvaček, 2015). The studied floras cover a time span from about 48 Ma (Messel) to approximately 22 Ma (Linz) and thus five globally important climatic events: the end of the Early Eocene Climatic Optimum (EECO), the Mid-Eocene Climatic Optimum (MECO), the Oi-1 Glaciation near the Eocene-Oligocene turnover (EOT), the late Oligocene Warming and the Mi-1 Glaciation at the Oligocene-Miocene boundary (Zachos et al., 2001, 2008). Because of uncertainties in age determination for the respective fossil sites it is difficult to link one of these assemblages to one of the global climatic events for sure. Highest MAT and CMMT derived by CA was estimated by Grein et al. (2011b) for Messel, which marks, due to new dating (Lenz et al., 2014) the end of the EECO. The Bartonian flora of Kučlín seems to underestimate mean MAT. The vegetation is described as being 40% 'broad-leaved evergreen' (BLE; Kvaček and Teodoridis, 2011), which is low in comparison to other late Eocene sites, such as Klaus, Knau or Phönix-Nord delivering a BLE content of 68-92 %. Kvaček and Teodoridis (2011) compare the late Eocene site Kučlín taxonomically with the early Oligocene sites from Czech Republic and Germany, (Kundratice, Seifhennersdorf, Suletice-Berand). The decrease in MAT from the Eocene towards the Oligocene does not occur at the boundary, but even earlier, as shown in Kvaček et al. (2014) and Kunzmann et al. (2016). Both papers document vegetational changes presumably caused by paleoclimatic changes already in the latest Eocene and thus prior to the EOT. CA and CLAMP indicate similar MAT, WMMT and CMMT for the Priabonian sites. Temperature decreases steadily and for the late Eocene plant assemblages nearly equal paleoclimatic conditions for a time interval of approximately 4 myr can be recognized. The Bartonian/Priabonian Weißelster Basin sites, of which Profen-Schwerzau ZC is the oldest and site Schleenhain 3u marks the transition to the Oligocene, reveal slightly similar MAT, WMMT and CMMT (CA). Of course, taphonomical and methodical constraints have to be considered while interpreting the results. Nevertheless, the steady change in the composition of vegetation (Kunzmann et al., 2016) corroborates the paleoclimatic results. The quantitative estimation matches also with the assumptions by Mai and Walther (1983,

2000) based on phytosociological analyses. Discrepancies only appear in MAP calculations as Mai and Walther (1983) postulated MAP of more than 2000 mm for the late Eocene and seasonal variations in the distribution of precipitation; the latter is also estimated using either CA or CLAMP. Krutzsch et al. (1992) postulate a period of seasonal 'aridity' during the summer month, and Krutzsch (2011) reinforces this hypothesis by the recognition of several summer-dry periods during the SPP zone 18 time intervall, coinciding with sea-level lowstands. However, it has repeatedly been stated that the examined Priabonian floras indeed indicate differences in the annual distribution of precipitation, but summer drought or 'aridity' has never been confirmed by any quantitative study (see Tables 8 and 9). The early Oligocene site Schleenhain HC, probably of latest Eocene to early Oligocene age, delivers remarkable low MAT and CMMT with both CA and CLAMP. This flora could be linked to the increase of Antarctic glaciation (Oi-1 cooling event) and is also mirrored by the immigration of broad-leaved deciduous taxa present in the fossil record e.g. *Populus germanica* and *Populus zaddachii* and *Liquidamber europaea* (Teodoridis and Kvaček, 2015; Kunzmann et al. 2016). Most of the Rupelian and Chattian sites deliver quite similar MAT based on CA, indicating after a rise in MAT after the EOT only a slight decrease in MAT. MAT based on CLAMP are rather different and slightly lower. This obvious MAT deviation in dependency on the used method was already shown by Teodoridis and Kvaček (2015) and is interpreted to be partially caused by the so-called 'riparian effect' for the coastal and fluvial environments by overrepresentation of toothed species, resulting in cooler MAT for the respective sites Borna-Ost-Bockwitz and Witznitz TC. The marine site Flörsheim and the volcanic sites Seifhennersdorf and Kleinsaubernitz deliver higher MAT based on CA but all in all the values clearly coincide with the overall trend. The late Oligocene floras of Witznitz WC and Linz indicate an increase in MAT, which can be linked to the effect of the Late Oligocene Warming, whereas it has to be stated again that for the site Witznitz WC only cleared leaves have been used for the CLAMP analyses, so that there is a certain taphonomic and thus taxonomic bias inhibited.

Beside the long-term period investigated and paleoclimatically treated, the broad spatial distribution and differences in the paleogeographic setting allows for interpretation of paleoclimate conditions regarding influences of both latitudinal and land-sea differences. The difference in latitude and longitude might be negligible but considering the climate conditions in the north of Germany at the coast of the North and Baltic Sea and in general warmer and dryer climate conditions in the Oberrheingraben in southern Germany, only 850 kilometers in distance, elucidates the plausibility of these paleogeographical considerations.

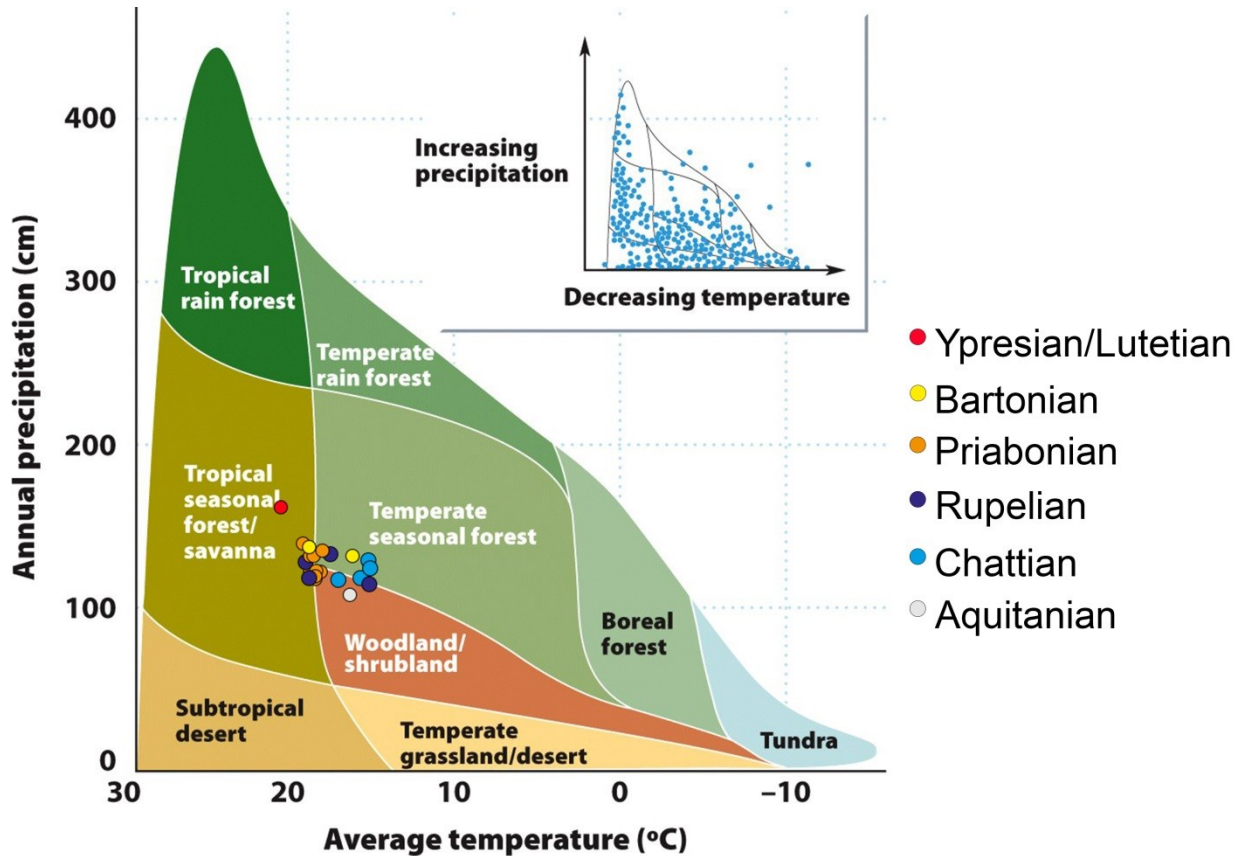


FIGURE 36. Robert Whittaker's Diagram of world biomes and investigated sites ordered following stratigraphy (the plot shows that the Eocene sites plot into the boundary between the biomes of tropical seasonal forests and temperate forests, whereas the Oligocene sites are more related to temperate seasonal forest types; modified from Ricklefs (2008)).

The allocation of land masses and oceans in central Europe during the Paleogene already closely resembled the present distribution (Standke et al., 2010), whereby the north of Saxony has been part of an estuary with connection to the ancient Atlantic (Krutzsch et al., 1992; Standke et al., 2010). The considered plant assemblages derived from the shores of the paleo-North Sea (sites of the Weißeelster Basin, Geiseltal), 100 and more kilometers away to the south (Northern Bohemian site Kučlín representing the 'hinterland' vegetation), from the Oberrheingraben (Rauenberg and Flörsheim) and from the coast of the central Paratethys (Linz) which is the southern-most site. Late Eocene paleoclimate estimates from Northern Bohemia, representing the 'hinterland' vegetation, indicate similar paleoclimate conditions as the coastal plain deposits of the Weißeelster Basin (Kvaček and Teodoridis, 2011; Kvaček et al., 2014; Teodoridis and Kvaček, 2015) with only



minor differences, which are present in the assemblages derived from volcanic deposits (e.g. Kučlín and Roudníky). The flora of the probably coeval Staré Sedlo Formation (late Eocene) indicates a rather wide MAT range of 15.7 – 23.9 °C by CA (Uhl et al., 2007), whereas CLAMP estimates MAT of  $16.2 \pm 1.3$  °C (Teodoridis et al., 2012). Both areas, the coastal-alluvial habitats of the Weißelster Basin as well as the Bohemian ‘hinterland’ including volcanic environments, feature a similar floristic composition, determined by using the integrated plant record vegetation analysis (IPR-vegetation analysis) which indicates the occurrence of broad leaved evergreen forests for both regions (Kvaček et al., 2014). The Bohemian flora of Roudníky (35.4 ± 0.9 Ma) is an exception as it mirrors the gradual change towards mixed mesophytic forests (MMF) by immigration of deciduous, temperate taxa and stepwise extinction of subtropical and tropical plants, and thus the proceeding global cooling trend towards the EOT. The flora of Roudníky shows MAT ranges of 13.6 – 18.0 °C with CA and  $10.0 \pm 1.3$  °C determined by CLAMP (Kvaček et al., 2014). No flora corresponding to Roudníky is currently known from the latest Eocene of the Weißelster Basin. In addition to temperature parameters the determined precipitation parameters for both regions are consistent with each other (Kvaček et al., 2014) regarding the mean annual precipitation calculated by CA, but show similar wide ranges as it is the case for the Weißelster plant assemblages (see Table 8). Differences in the distribution of precipitation throughout the year can be assumed. The amount of precipitation within the three driest and the three wettest months for the Eocene sites are slightly higher in the ‘hinterland’ (sites Roudníky, Staré Sedlo Formation) than determined for the plant assemblages of the Weißelster Basin, but appear to be negligible with relation to similar MAP. Thus, differences in the geographical distribution of the fossil plant assemblages and their influences on the validity of paleoclimate estimates for the terrestrial record, seems to be negligible in the case of the alluvial-coastal plain deposits at or nearby the paleo-North Sea and the ‘hinterland’ vegetation. The floras of sites Rauenberg and Flörsheim, coming from the Oberrheingraben, indicate distinct paleoclimatic conditions. The Oberrheingraben connected the paleo-North Sea with the comparatively warmer Paratethys. This assumes to have an influence on the regional climate, which indeed is mirrored in sites Rauenberg and Flörsheim. The sites, comparable in age, yield similar higher MAT than both, older and younger plant assemblages from the coast of the paleo-North Sea (Table 8, Table 9; Figure 35). As scoresheet completeness for reliable CLAMP estimation amounts at least 0.66 and the minimum amount of scored morphotypes is 28, paleoclimatic consideration can be stated as reliable. For CA, 39 (Rauenberg) and 46 (Flörsheim) NLR were used to calculate an interval of coexistence. MAT of 18.0 °C (Rauenberg) and 17.6 °C for Flörsheim (CLAMP) together with higher amount of precipitation and characterize the regional climate as more

warm-humid (Kovar-Eder, 2016), than delivered from the north-eastern plant assemblages. The plant assemblage of Linz represents the southernmost site on the shore of the central Paratethys and reflects the same patterns in paleoclimate as the considered sites from the Oberrheingarten. MAT, WMMT and CMMT are distinctly higher than for site Witznitz WC, which is already assumed to overestimate temperature and precipitation patterns due to the above described taphonomical and methodical constraints. Although the early Miocene is characterized by a rise in temperature, mirrored also in the composition of vegetation and paleoclimate estimates based on plants (Teodoridis and Kvaček, 2015), these warm-humid conditions can be linked to the same regional effects of the warm Paratethys. Kovar (1982) obtained the same overall climatic pattern for the flora of Linz by comparison of the fossil and assumed analogues in extant vegetation.

All in all, the paleoclimate reconstructions are in rather good agreement with global paleoclimatic trends and observed shifts both from the marine and the terrestrial record. Their origin from different paleogeographical and depositional setting delivers important insights into dependencies on these differences. As most of the paleoclimatic reconstructions using plants were conducted neglecting the influence of these patterns, the studied assemblages and the derived paleoclimatic record sensitize for these influences and possible biases. Alongside these differences regarding the depositional setting, also paleogeographical influences have to be taken into account. Regional effects, therefore, strongly influence the paleoclimatic signal, while the paleo-CO<sub>2</sub> signal is said to be independent of regional effects and indicates global changes in CO<sub>2</sub>.

## 6.2. Morphological and morphometric parameters

### 6.2.1. Uncertainties and outliers

*Rhodomyrtophyllum reticulosum* is predominant in azonal Eocene plant assemblages in central Europe and due to its thick and robust leaves a large amount of leaves was available for digitizing and reconstruction. For all sites 124 leaves were digitized and polygonised. Unfortunately, most of these leaves were not implemented into the MORPHYLL database yet, so that only limited morphometric information are available until now. Leaf length and leaf width were gathered on reconstructions, measured by hand in

QGIS. Deviations from estimated values derived by a SQL query can be assumed but are neglectable in this study, as every leaf from every site experienced the same procedure. The individual error therefore should be the same for all specimens. Sample size is smallest for sites Schleenhain 3u and Peres 3u, which is expressed in lower ranges of the respective parameters and induces, that the range of parameter variation was not gathered in these sites. For sites Schleenhain 3u and Peres 3u, fossil material was limited or for some reasons the majority of specimens were fragmented and not suitable for morphometric studies.

Leaves of *Platanus neptuni* are not as robust against decay as the coriaceous leaves of the evergreen *Rhodomyrtophyllum reticulosum*, but yet they are compared to other deciduous species. Highest amount of *Platanus neptuni* leaves, which were suitable for morphometric measurements, were derived from marine deposits, where assumed transport distances are longest among the floras of the different depositional settings. Fragmentation and sorting processes as main factor of underrepresentation in coastal-alluvial deposits cannot serve as the only evidently reason for these differences in sample size, but clearly they are causing the low abundance of *Platanus neptuni* leaves both in the fossil record and in the samples for morphometric studies. Due to the exclusion of leaves of whose less than 70 % of the lamina is preserved, sample sizes in these depositional settings remain low in comparison to marine depositional settings. Furthermore, the concentration of leaves in lenses within sometimes thick packages where one leaf is overlying another (see Figure 8) leads to unexpected destruction of the delicate leaves during sediment split off either in the field or in the lab. Generally, the leaves are not embedded on even surfaces as the non-consolidated sediment gets deformed during the excavation and rapid drying and shrinking of the sediment blocks leads to the formation of cracks and fissures. As described in chapter 2.3., the investigated material was collected from 1960 onwards, depending on the site and the respective horizon. Therefore, any fragmentation of the material occurred before and not during this study. For site Schleenhain 14 leaves were digitized and polygonised, whereof only 7 yielded a preservation index of more than 70 %. For site Borna-Ost-Bockwitz even 30 leaves were chosen for morphometric studies, whereof only every third leaf was suitable for morphometric measurements, as 20 leaves did not obtain the minimum preservation index, which serves as indicator for reliable reconstructions of the respective leaf. The high fragmentation rate and the tightly packed leaves in site Borna-Ost DC inhibited every attempt to gain leaves suitable for morphometric studies. In contrast, the scattered distribution of leaves in marine depositional settings, lying mainly plain in the sediment, enables for a better reconstruction, as more morphological features are preserved and identifiable. Same holds for most of the volcanic sites. No morphometric data are available

for site Kleinsaubernitz, although 8 leaves were digitized and polygonised. This is caused by the origin of the Kleinsaubernitz material, which comes from a drilling. Every slab therefore has a diameter of around 10 cm to, caused by angular deflection, 25 cm (Walther, 1999). Furthermore, this sampling technique is distinct from the other sites. Only a minor proportion of *Platanus neptuni* leaves were gathered.

The interpretation of leaf trait changes are hampered by the unknown lithostratigraphic position of some sites, e.g. Knau and Klaus, which have to be taken into account while interpreting the results.

### 6.2.2. Morphological and morphometric interpretation

Leaves of *Rhodomyrtophyllum reticulosum* are very variable in leaf size and shape. Narrow-elliptic and broad-obovate leaves are known from all sites and leaf size is varying greatly as well (Table 18). Leaf length and width is smallest in Messel in comparison to the Bartonian/Priabonian sites of the Weielster Basin and the Geiseltal (Kayna-Sud), which deliver rather equal length/width ratios. Leaf morphology is slightly different in Messel, where narrow-elliptic small leaves prevail (Table 18).

Acute apices are known only from sites Messel, Profen-Schwerzau ZC and Profen-Sud LC, although other sites could contain also leaves with acute apices, which are not preserved and therefore were not scored. The occurrence of acute apices could be linked to higher MAP. As CLAMP was not applicable to the assemblage of Profen-Schwerzau ZC (scoresheet completeness below 0.4) and CA estimates are based on 9 NLR only, this interpretation cannot be proofed in detail. The variety of leaf sizes is clearly visible in the broad ranges in Figure 22 and in the scored leaf physiognomic states in Table 18. The overall range in mean width and length does not vary significantly. Although leaf mass per area ( $LM_A$ ) was not determined, a high leaf mass can be assumed for *Rhodomyrtophyllum* leaves due to its thick and robust cuticles and the broad petioles, which are even thicker than the midrib vein. This is typical for 'slow-return species' and is commonly related to evergreen species, which have a longer leaf life span than deciduous species (Wright et al., 2004; Royer et al., 2007). Higher  $LM_A$  is also related to defense against herbivory (Royer et al., 2005; Royer et al., 2007). For site Profen-Sud LC insect-plant interactions have been investigated (Mller,

2016) and results show that the overall proportion of herbivory is related to evergreen species, whereof *Rhodomyrtophyllum reticulosum* was only seldomly affected by insect damage such as feeding, galling and sucking.

Leaf physiognomic states as defined for CLAMP (Wolfe, 1993; Spicer, 2009)	Schleenhain 3u	Profen-Süd-3u	Peres 3u	Haselbach-2-3-mi	Schleenhain-20	Klausa	Knau	Profen-Süd-LC	Kayna-Süd	Profen-Schwerzau ZC	Messel*
Leaf size nanophyll	0	0	0	0	0	0	0	0	0	0	0
Leaf size leptophyll I	0	0	0	0	0	0	0	0	0	0	0
Leaf size leptophyll II	0	0	0	0	0	0	0	0	0	0	0
Leaf size microphyll I	0	0	0	0	0	0	0	0	0	0	0
Leaf size microphyll II	0	0	0,25	0,33	0,25	0,2	0,25	0,2	0,33	0,2	0,5
Leaf size microphyll III	0,5	0,5	0,25	0,33	0,25	0,2	0,25	0,2	0,33	0,2	0,5
Leaf size mesophyll I	0,5	0,5	0,25	0,33	0,25	0,2	0,25	0,2	0,33	0,2	0
Leaf size mesophyll II	0	0	0,25	0	0,25	0,2	0,25	0,2	0	0,2	0
Leaf size mesophyll III	0	0	0	0	0	0,2	0	0,2	0	0,2	0
Apex emarginate	0,5	0,5	0,5	0,5	0,5	0,5	0,5	0,33	0,5	0,33	0,33
Apex round	0,5	0,5	0,5	0,5	0,5	0,5	0,5	0,33	0,5	0,33	0,33
Apex acute	0	0	0	0	0	0	0	0,33	0	0,33	0,33
Apex attenuate	0	0	0	0	0	0	0	0	0	0	0
Base cordate	0	0	0	0	0	0	0	0	0	0	0
Base round	0	0	0	0	0	0,5	0	0	0	0	0,5
Base acute	1	1	1	1	1	0,5	1	1	1	1	0,5
Length/Width <1:1	0	0	0,33	0	0	0	0	0	0	0	0
Length/Width 1-2:1	0,5	0	0,33	0	0	0,5	0	0	0	0	0
Length/Width 2-3:1	0,5	1	0,33	0,5	0,5	0,5	0,5	0,5	0,5	0,33	0
Length/Width 3-4:1	0	0	0,33	0,5	0,5	0	0,5	0,5	0,5	0,33	0,5
Length/Width >4:1	0	0	0	0	0	0	0	0	0	0,33	0,5
Leaf shape obovate	0,5	0,5	0,5	0,5	0	0,5	0	0,5	0	0,5	0,5
Leaf shape elliptic	0,5	0,5	0,5	0,5	1	0,5	1	0,5	1	0,5	0,5
Leaf shape ovate	0	0	0	0	0	0	0	0	0	0	0

TABLE 18. Selected leaf physiognomic characters for *Rhodomyrtophyllum reticulosum* derived from different plant assemblages (0 – character not present, blue marked cells – character present, number – proportion of scored character within a character group)

*Rhodomyrtophyllum reticulosum* represents a typical species of coastal-alluvial plains, which grew along streams, abandoned channels and lake margins (see site Messel) and is exclusively known from azonal environments. These environments are characterized by a high water table and overall humid conditions. Although these braided river systems are characterized by unstable environmental conditions with rapidly changing mosaics of land-water distribution due to flooding events, moderate and rather stable climate conditions can be assumed. Water availability is not a limiting factor in riparian environments, although plants could have been experiences partly drought conditions at sandbars, which should have been affected shallow-rooted plants and can therefore be excluded for *Rhodomyrtophyllum reticulosum*. Seasonality both in precipitation and temperature are buffered. For these reasons *Rhodomyrtophyllum* leaf traits do not vary in a significant way in the considered time interval. In contrast to the global climate curves (Zachos et al., 2001, 2008), the terrestrial realm of central Europe does not display the global trend in gradually decreasing temperature during the late Eocene. Therefore also no profound changes in leaf morphology and morphometry were expected from the Bartonian and Priabonian of central Europe.

Leaves of *Platanus neptuni* are very variable in morphology, being either simple or compound (tri- or quinquefoliate). Compound leaves occur frequently in the Eocene assemblages and their occurrence is known by either a single specimen or even more (Profen-Schwerzau 1u, Klaus). Their occurrence has been also proven in Oligocene assemblages (Kvaček and Manchester, 2004) for instance in sites Flörsheim and Borna-Ost-Bockwitz, which rules out the possibility of being bound to the Eocene. The leaflets of these compound leaves were shed separately and this leads to the assumption, that some of the other investigated leaves were part of formerly compound leaves. The interpretation of morphometric traits therefore should consider these differences. The two Priabonian sites Klaus and Profen-Schwerzau 1u show low leaf area (see Table 11, Table 18, microphyll II).

These 'leaves' are leaflets of compound leaves and are thus not directly comparable to simple leaves with presumably larger leaf area. Leaves from the latest Chattian site Witznitz WC deliver low leaf area too but there is no indication that they are leaflets as well. Mean leaf size of *Platanus neptuni* leaves ranges around 337 mm<sup>2</sup> (n=4!). It has to be taken into account that most leaf remains of the Witznitz WC flora are stored in collections as cleared leaves that are mounted on glass slides. This implicates a sampling and preparation bias because preferentially complete smaller leaves and occasionally small fragments of bigger leaves were prepared and embedded. In short, small leaf area in Witznitz WC is neither

indicative for the abundance of leaflets nor a signal for reliable trait variation. As compound leaves are rarely known from Oligocene assemblages (Mai and Walther, 1991; Kvaček 2004), it is expected that both simple and compound leaves could have been present in these sites and thus leaf area value is slightly influenced by a minor proportion of leaflets. Focusing on Rupelian sites contradicting assertions have been revealed. In Flörsheim and Rauenberg larger leaves with a mean area of 1150 mm<sup>2</sup> and 1101.9 mm<sup>2</sup> respectively are preserved while sites Schleenhain HC and Seifhennersdorf show smaller mean leaf area. These differences between assemblages in a similar stratigraphic position indicate that leaf morphology of *Platanus neptuni* could be likely primarily driven by site-specific dependencies, but not by adaptations to global changes in paleoclimate and paleoatmospheric conditions. A coupling of leaf area through time with global changes in CO<sub>2</sub> and paleoclimate is therefore not evident in the respective samples. Reasons could be differences in sample size and therefore low precision of derived results, if one assumes that the range in morphometric trait variation is not fully captured in small samples. Obviously there are wider ranges in different morphometric patterns for sites with more than 10 sample leaves but smaller ranges for sites where less than 10 leaves were available. By implication, the lower the abundance of *Platanus neptuni* leaves in the fossil assemblage the smaller the range of leaf trait variability.

Obviously changes in leaf morphometric traits, respectively in leaf size, show a distinct pattern, which could not be exclusively linked with distinct lithostratigraphic positions and hence changes of leaf traits through time. Leaves from the floodplain assemblages of the alluvial-coastal plain tend to be much smaller than *Platanus neptuni* leaves from volcanic and marine deposits (Figure 25 and Figure 26). Superficially speaking this could directly dependent on soil characteristics, i.e. less nutrients and waterlogging in the coastal-alluvial plain and rich nutrients under mesic conditions in volcanic settings. Furthermore, the later habitats are less disturbed and favour growing of woody tree species such as *Platanus neptuni*. The original habitats of the marine assemblages are more or less unknown to date. Interestingly, LM<sub>A</sub> indicates a reverse relationship, with mean LM<sub>A</sub> of 107 g/m<sup>3</sup> for leaves from coastal-alluvial plain assemblages and LM<sub>A</sub> of 90 g/m<sup>3</sup> derived from assemblages in marine deposits (Figure 26). These differences in combination with leaf size could be due to sorting processes during transport from growing to burial places. Larger light leaves tend to float for longer distances being predominantly preserved in marine sediments and smaller heavier leaves will sink to the ground after only a short distance as it is the case for the parautochthonous assemblages (e.g. Gastaldo et al. 1998; Kunzmann, 2012) from the Weißelster Basin sites. Otherwise, in parautochthonous assemblages the most complete

range of leaf size and  $LM_A$  should be preserved which is obviously not true for some Weißelster Basin sites (see above). In all marine study sites wide ranges in leaf sizes are recorded which indicate that assumed long distances between growing and burial places did most likely not substantially affect the morphological variability of the respective assemblages in marine depositional environments. Furthermore, a wider range in leaf size in marine assemblages could be dependent on the fact that these assemblages originate from a remarkable larger catchment area than respective assemblages from fluvial settings. Especially for the Weißelster Basin sites Schleenhain, Borna-Ost-Bockwitz and Witznitz TC it has been shown that source vegetation of the fossil leaf assemblages was in the proximity of the burial places that are in most cases abandoned river channels (Gastaldo et al. 1996, 1998; Kunzmann and Walther 2012, Kunzmann 2012). These sites represent rather small catchment areas that could predict the relative low abundance of *Platanus neptuni* leaves in the assemblage as well as the relative abundance of all possibly leaf sizes in the assemblage. Volcanic assemblages preserved in lacustrine series can be called transitional with respect to the catchment area as maar lakes are usually much larger than abandoned river channels.

There are several reasons that could explain comparably small leaf sizes in individual sites. (1) Smaller leaf size in the Bartonian/Priabonian coastal-alluvial plain sites could be an expression of the higher abundance of tri- and quinquefoliate leaves (Profen-Schwerzau 1u, Klaus) and thus presumably reflect an evolutionary aspect of the species independent from the palaeoenvironment. (2) In contrast, differences in leaf size as stated for some Oligocene sites could also indicate possible habitat adaptation strategies, with predominantly smaller leaves in non-favourable habitats in the coastal-alluvial plains, (3) Smaller leaf size otherwise could indicate higher insolation, if we assume the riparian and gallery forests in the Weißelster Basin as being less dense compared to cohere forests. (4) Small leaves reflect unstable environments as described above. In the Weißelster Basin, vegetation is reconstructed as a mosaic of several associations that grew scattered in a braided river system (Kunzmann, 2012) which is characterized by spatial and temporal unstable environmental conditions. Plants needed to be adapted to varying water availability, which includes both waterlogging and 'dry' conditions on sandbars (Roth-Nebelsick et al., 2014), to massive sediment load of all channels, and to rapidly changing topographies in the alluvial plain.



Leaf physiognomic states as defined for CLAMP (Wolfe, 1993; Spicer, 2009)	Linz	Witznitz WC	Witznitz TC	Borna-Ost-Bockwitz	Kleinsaubernitz	Seifhennersdorf	Flörsheim	Rauenberg	Schleenhain HC	Borna-Ost DC	Klausau	Profen-Schwerzau 1u
No teeth	0	0	0	0	0	0	1	0	1	-	0	0
Teeth	1	1	1	1	1	1	1	1	1	-	1	1
Teeth regular	0	0,5	0	0	0	0	0	0	1	-	1	0
Teeth close	0,5	1	1	1	1	1	1	0,5	0	-	1	0
Teeth acute	0,5	0,5	1	1	1	1	1	1	0	-	1	1
Teeth compound	0	0	0	0	0	0	0	0	0	-	0	0
Leaf size nanophyll	0	0	0	0	0	0	0	0	0	-	0	0
Leaf size leptophyll I	0	0	0	0	0	0	0	0	0	-	0	0
Leaf size leptophyll II	0	0	0	0	0	0	0	0	0	-	0	0
Leaf size microphyll I	0	0	0	0	0	0	0,5	0	0	-	0	0
Leaf size microphyll II	0	0,5	0,5	0,5	0,33	0,5	0,5	0	0,5	-	1	1
Leaf size microphyll III	1	0,5	0,5	0,5	0,33	0,5	0	0,5	0,5	-	0	0
Leaf size mesophyll I	0	0	0	0	0,33	0	0	0,5	0	-	0	0
Leaf size mesophyll II	0	0	0	0	0	0	0	0	0	-	0	0
Leaf size mesophyll III	0	0	0	0	0	0	0	0	0	-	0	0
Apex emarginate	0	0	0	0	0	0	0	0	0	-	0	0
Apex round	0	0	0	0	0	0	0	0	0	-	0	0
Apex acute	0,5	1	1	1	1	1	1	1	1	-	1	1
Apex attenuate	0,5	0	0	0	0	0	0	0	0	-	0	0
Base cordate	0	0	0	0	0	0	0	0	0	-	0	0
Base round	0	0	0	0	0,5	0	0,5	0	0	-	0	0
Base acute	1	1	1	1	0,5	1	0,5	1	1	-	1	1
Length/Width <1:1	0	0	0	0	0	0	0	0	0	-	0	0
Length/Width 1-2:1	0	0	0	0	0,5	0	0	0	0	-	0	0
Length/Width 2-3:1	0	0,5	0,5	0	0,5	0,5	0	0,33	0	-	0	0
Length/Width 3-4:1	0,5	0,5	0,5	1	0	0,5	0,5	0,33	0,5	-	1	0,5
Length/Width >4:1	0,5	0	0	0	0	0	0,5	0,33	0,5	-	0	0,5
Leaf shape obovate	0	0	0	0	0	0,5	0	0	0	-	0	0,5
Leaf shape elliptic	0,5	0,5	0,5	1	0,5	0,5	0,5	0,5	1	-	1	0,5
Leaf shape ovate	0,5	0,5	0,5	0	0,5	0	0,5	0,5	0	-	0	0

TABLE 19. Selected leaf physiognomic characters for *Platanus neptuni* derived from the considered plant assemblages for different grouped characters (0 – character not present, blue marked cells – character present, number – proportion of scored character within a character group)

Deciduousness of *Platanus neptuni* was assumed by Kvaček and Manchester (2004) based on morphological features of fossil shoots, i.e. enlarged petiole bases covering the bud, which cannot develop without shedding the leaves and the occurrence of leaves at many fossil sites. However, this character is still a matter of debate, when interpreting our values of  $LM_A$  that are calculated by using of the formula of Royer et al. (2007). Only 40 % of the fossil leaves plotted into the interval that indicates *Platanus neptuni* was a deciduous species but about 48% of the leaves plotted into the transition zone to evergreen. Hence, this result is ambiguous and does not support the morphological interpretation of Kvaček and Manchester (2004). However, these values indicate a rather long leaf life span (Wright et al., 2004) which coincides with the relatively robust leaf cuticles. Such cuticles are unusual for 'true' deciduous woody plants (personal observations). Furthermore,  $LM_A$  results open space for several hypotheses that cannot be resolved at the moment. Was it a semi-evergreen species that shed leaves and spread new leaves within very few weeks? Hints are given by the long reconstructed growing seasons of 9 to 11 months for most of the sites, which indicates a rather long vegetation period. Until now, this hypothesis remains unresolved. Anyway, as *Platanus neptuni* is extinct and no nearest living relative or most similar extant species is available the choice of *Platanus kerrii* as ecological equivalent, as repeatedly proposed (Walther in Mai and Walther 1985; Kovar-Eder, 2016), is in accordance with the  $LM_A$  values.

Based on its relative abundance in Flörsheim and Kučlín respectively Kvaček (2004) and Kvaček and Teodoridis (2011) concluded that *Platanus neptuni* is an element of zonal vegetation whereas Mai and Wather (1985) and Kovar-Eder (2016) propose an alternative and additional azonal aspect for this species, respectively. Relative abundance of leaves in the investigated 13 sites in combination with site characteristics and taphonomic aspects could provide valuable hints for autecological interpretations. Scarcity of *Platanus neptuni* in fluvial and estuarine settings of the northern alluvial-coastal plains could be related to habitat characteristics such as low-nutrients, siliciclastic soils, waterlogging and generally unstable or disturbed environments. Therefore it can be assumed that fluvial and estuarine habitats in these coastal plains are exceptional growing places for *Platanus neptuni* whereas other places in volcanic ranges provide more suitable conditions, e.g. nutrient-rich volcanogenetic soils. Predominance of *Platanus neptuni* leaves in the marine assemblages could be interpreted as a hint of its predominance in the coastal vegetation. Concerning the highly allochthonous aspect of these assemblages it is difficult to conclude on the source vegetation. In case of Flörsheim the coastal vegetation was interpreted as being mainly

zonal (Kvaček 2004), in contrast Rauenberg reveals elements both from azonal and zonal vegetation (Kovar-Eder, 2016).

## 6.2. Cuticular parameters

### 6.2.1. Uncertainties and outliers

Cuticles of *Rhodomyrtophyllum reticulosum* are generally thick and robust. In contrast to thin and fragile cuticles, cuticle sample size of *Rhodomyrtophyllum reticulosum* allows for SD measurements on large areas. This is important, as *Rhodomyrtophyllum* stomata occur both scattered on the leaf lamina or grouped and the cuticle area chosen for SD/SI counting should cover a representative sample of both distribution patterns. Nevertheless, SD is varying greatly in the investigated specimens. One reason is given due to the fact that the dense minor venation (Glinka and Walther, 2003), limits the respective area of stomata counting, as SD determination is bound to the intercostal areas to get reliable results. During measurements two different types of abaxial cuticles have been distinguished; whereof the first type features rather big polygonal to elongate epidermal cells with highly undulated anticlines and bigger distances between stomata. This is expressed in lower SD and SI values. The second type of investigated cuticle shows smaller epidermal cells with rather straight anticlines and a higher amount of stomata, which leads to lower SD and SI values. Big differences in calculated SI and the comparable small number of counts are caused by, firstly, differences in the distribution of stomata as for SD and the high number of fungal infection, visible on the cuticles and covering the anatomical structures. Cuticles oriented with the inner cuticle side facing the microscope exhibit high anticlines, which are sometimes overturned and do not evidently show the cell outlines. This is a problem in cuticles with anticlines that are overwhelmingly densely undulated with high amplitudes. The only weak correlation of  $pw_{St}$  and  $h_{St}$  is caused by uncertainties in  $h_{St}$  measurements due to the partly coverage of the pore by the guard cells, which hampers the unambiguous distinction of the inner pore.

As already described above, cuticles of *Platanus neptuni* are rather robust, as expected for a deciduous species in subtropical environments with a rather long growing season. Comparably large cuticle samples were available for cuticular-based approaches. Stomata in *Platanus neptuni* are considerably bigger than stomata of *Rhodomyrtophyllum*

*reticulosum* and their scarcity in distribution on the leaves lamina required a considerably larger counting area for SD determination. Cuticle preservation was very different for the respective sites. In the coastal-alluvial and marine deposits fungal infection was the main limiting factor for reliable SD and SI determination, whereas in sites Seifhennersdorf and Kleinsaubernitz from volcanic deposits adhered sediment and diatoms caused limitation for sufficient SD and SI measurements. These taphonomically influenced restrictions limited visibility of anticlines of ordinary epidermal cells and thus prevent counting for SI determination in most cases. Adhered sediment in the pores of the stomata hampered and sometimes inhibited  $h_{st}$  measurements (site Linz).

Fortunately, most of the methods were applicable for all sites with cuticle preservation in an adequate extent. For most specimens cuticular parameters were derived from the apical, middle and the basal part of the lamina guaranteeing a significant average of the respective proxy data for individual leaves.

### 6.2.2. Interpretation of cuticular-based parameters

The non-homogeneously and random distribution of stomata on the leaf lamina in *Rhodomyrtophyllum reticulosum* specimens is displayed in SD and SI data. Both, the wide ranges for SD and SI within a site and the big differences in SD and SI within a leaf hamper the interpretation of derived results regarding the influence of paleoclimate and/or paleoatmospheric composition to any changes of these proxies. Generally, SD is said to increase from the leaf base to the apex and from the leaf midrib to the margin (Royer, 2001 and citations in there). These distribution patterns are not identifiable in *Rhodomyrtophyllum reticulosum* cuticles. Within her Bachelor thesis Jurke (2016) investigated nearly the complete cuticles of a half of a single leaf from site Profen-Schwerzau ZC focusing on these differences as possible explanation of SD and SI variations that are ascertained from other samples of this species from the same site. Interestingly, she found no distribution pattern of stomata across the lamina and hence SD and SI. Stomata distribution patterns in cuticles of *Rhodomyrtophyllum reticulosum* still remain unresolved (Jurke, 2016). Royer (2001) proposed that SI, which is said to be more independent from environmental influences (e.g. light intensity, water availability), does not correspond to these SD distribution patterns. This is not evident for

*Rhodomyrtophyllum reticulosum* as seen in Figure 27. Leaving these taxon-specific and methodical constraints aside, one could interpret these rather constant SD and SI as an expression of an plateau phase in regional paleoclimate conditions prior to the EOT, which is proven by paleoclimatic data (Moraweck et al., 2015). Stable SD and SI during times of assumed stable paleoclimate in central Europe is consistent with similar estimates of gathered morphometric data. Taking into account that *Rhodomyrtophyllum reticulosum* was an evergreen tree, native to azonal environments, one can assume that SD and SI may only partly correspond to global changes in paleoclimate and reacts in a different way to these changes compared to deciduous species. It is proven that SD and SI are higher in evergreens compared to deciduous species (Galmés et al., 2007). Unfortunately, publications on SD and SI data and their dependencies on deciduousness are rare to date.

As sample size for SD counting on cuticles of *Platanus neptuni* was not a limiting factor in none of the samples, SD values for the single sites show a valid picture of its variation. The oldest sites Profen-Schwerzau 1u and Borna-Ost DC, both from the late Eocene of the Weißelster Basin, considerably expand the known dataset of *Platanus neptuni* based on SD variation published by (Roth-Nebelsick et al., 2014) and indicate a drop from the Bartonian/Priabonian towards the Rupelian with significantly lower SD in Schleenhain HC, followed by stable SD throughout the Oligocene and a drop towards the early Miocene (Figure 30). This SD trend is remarkably opposed to the global trend in CO<sub>2</sub> (Zachos et al., 2001, 2008; Zhang et al., 2013), if low SD is supposed to correspond to high CO<sub>2</sub>. In conclusion, SD of *Platanus neptuni* leaves do not respond to global CO<sub>2</sub> changes in the usual or expected behavior. This statement nicely fits in general with earlier conclusions by Roth-Nebelsick et al. (2014) derived from a rather limited Oligocene dataset. Unfortunately, SI data (Figure 31), which are assumed to deliver more independent results regarding the influence of environmental factors on stomata amount (Royer, 2001), are rare. Sample sizes and cuticle preservation additionally limit the validity of the results. In the respective samples SI is slightly increasing with age but not adequately reflecting variations in atmospheric CO<sub>2</sub>.

In contrast to Roth-Nebelsick et al. (2014) a weak correlation of changes in SD and pore length through time is detectable in our samples. Correlation between low SD and low stomatal conductance can be cancelled out by pore size changes, as the stomatal pore is an important variable influencing the effective gas exchange (Roth-Nebelsick et al., 2012; Haworth et al., 2013).  $h_{St}$  is varying through time, rising from the late Priabonian towards the early Rupelian, coupled with a drop in SD, and remaining almost stable throughout the

Oligocene. Interestingly,  $w_{St}$  varies considerably through time and displays an inverse trend to SD changes (Figure 30A and Figure 31B). The only weak correspondence of  $h_{St}$  and SD changes and the obviously coupling of SD and stomata width therefore indicates biased  $h_{St}$  measurements, due to difficulties in the visibility of the inner  $h_{St}$ , if stomata size and  $h_{St}$  are assumed to be normally positively correlated.

Interestingly, TD and SD strongly correlate in the Bartonian/Priabonian samples, with decreasing mean TD and SD towards the EOT. Beside low mean SD, estimated for the Rupelian marine sites Rauenberg and Flörsheim, the Oligocene samples delivered similar SD and TD and indicate rather stable conditions. For sites Witznitz WC and Linz a decrease in SD and an increase in TD are documented and thus run contrary to those of the Eocene sites. If coupled with paleoclimatic conditions, one can assume a correlation of SD and TD with temperature. High MAT, WMMT and CMMT and thus a longer vegetation period are accompanied by higher SD and by smaller stomata pore length. However, herein the correlation of paleoclimate conditions, gathered with CA, and micromorphological patterns is rather difficult, as CA potentially is not sensitive enough to display minute changes in paleoclimate (Grimm and Denk, 2012; Grimm et al., 2016). Comparing SD, TD and leaf area estimates (Figures 24 and 30) obviously suggests a correlation between smaller leaves and higher SD and TD and larger leaf area accompanied by lower SD and TD at least for the Eocene and early Oligocene sites. As estimated SD in marine assemblages is lower than SD in coastal and volcanic environments, SD values obviously deliver a mixed signal of globally influenced atmospheric changes and local, site-related dependencies because low mean SD from marine assemblages can be also linked with higher mean leaf area from sites Flörsheim, Rauenberg and Linz.

SD, SI, TD,  $w_{St}$  and  $h_{St}$  deliver enough material and thus reliable results to test the correlations of variations of these parameters with global changes in paleoclimate and  $CO_2$ . SD seems to be coupled with site-specific conditions, as water availability, temperature and insolation affect SD in the same way as the leaves exposition within the canopy. But stomata data are regarded to contain within itself long-term trends in paleoclimate and paleoatmospheric evolution as well.

### 6.3. Paleoatmospheric reconstruction

#### 6.3.1. Uncertainties and outliers

The results derived by gas exchange modelling, when applying systematic parameter variation of the most critical parameters, can be just as precise as the respective input parameters are. The CO<sub>2</sub> data obtained in this study seems to partly display their own trends, which is due to the fact that, in the fossil record, the reliability and validity of each input parameter suffers from methodical and taphonomical constraints. Therefore, the above described uncertainties in paleoclimatic, morphometric and cuticular reconstructions and studies, of course, influence the validity of the results and will not be outlined in detail once again, but should be kept in mind when interpreting the results. Obviously, greatest influence of changing input parameters can be expected in the CO<sub>2</sub> ranges estimated within this study between around 150 and 700 ppm (Figure 35) considering the results of sensitivity studies in Konrad et al. (2008).

#### 6.3.2. Interpretation of paleoatmospheric parameters

The derived CO<sub>2</sub> record, ranging from the late Bartonian (site Profen-Schwerzau ZC) to the latest Chattian (site Witznitz WC) indicates only minor changes in atmospheric CO<sub>2</sub> (Figure 33). CO<sub>2</sub> gathered from *Rhodomyrtophyllum* leaf traits does not show a distinct shift from the Bartonian to the late Priabonian, consistent with paleoclimate data derived from the respective plant assemblages. Estimated wide CO<sub>2</sub> ranges display partly wide ranges in varied critical parameters, such as for instance T for site Schleenhain 3u ranges between 19.0 and 23.5 °C. Sites with highest SD deliver lowest mean CO<sub>2</sub> (sites Haselbach 2-3 mi and Schleenhain 3u) and vice versa (site Kayna-Süd). The effect of SD on the derived results is therefore considerably higher than of all other input parameters which have been shifted during gas exchange modelling. As seen in Tables 14B and 16B, mostly q and T have been the critical input parameters defining the lower and upper CO<sub>2</sub> estimate of the respective site. Ranges of q have been taken from literature, whereas T was estimated using either CA or CLAMP. Grein et al. (2011a) estimated CO<sub>2</sub> for the late/middle Eocene site Messel using

three different taxa (*Laurophyllum lanigeroides*, *Daphnogene crebrigranosa* and *Rhodomyrtophyllum reticulosum*) and estimated an overlap of derived CO<sub>2</sub> ranges of the respective taxa of 853 to 1033 ppm, whereby *Rhodomyrtophyllum reticulosum* delivered the lowest CO<sub>2</sub> values ranging between 347-1033 compared to both other taxa (*Laurophyllum lanigeroides*: 467-1369 ppm; *Daphnogene crebrigranosa*: 853-2151 ppm). This *Rhodomyrtophyllum* based CO<sub>2</sub> range is in accordance with estimated CO<sub>2</sub> of this study. Beside CO<sub>2</sub>, estimated for site Kayna-Süd, all other ranges indicate stable mean CO<sub>2</sub>, which is consistent with paleoclimate data but contrary to the global CO<sub>2</sub> trend, which indicates higher CO<sub>2</sub> for the Eocene, as delineated in Figure 37 (green bars: *Rhodomyrtophyllum reticulosum*), where a variety of CO<sub>2</sub> data derived by different proxies from both, the marine and the terrestrial realm are plotted together. Also stomata-based results indicate higher CO<sub>2</sub> for the Eocene (Royer et al., 2001, 2008).

Estimated CO<sub>2</sub> using *Platanus neptuni* leaf traits deliver comparable results with those derived by other proxies (Figure 37; blue bars: *Platanus neptuni*). Limiting parameters setting the lower and the upper CO<sub>2</sub> boundary for the respective sites have been mostly  $q$  and  $T$ , as for *Rhodomyrtophyllum reticulosum*. Unfortunately, no overlap in CO<sub>2</sub> data gathered from *Rhodomyrtophyllum reticulosum* and *Platanus neptuni* have been derived, due to the fact that SD for Profen-Schwerzau 1u and Borna-Ost DC with 150 mm<sup>-2</sup> and 137 mm<sup>-2</sup> respectively led to no results in gas exchange modelling. The reason is not yet resolved, but it shows that *Platanus neptuni* leaf traits and the respective biochemical and paleoclimatic data together do not provide a consistent data set, appropriate for CO<sub>2</sub> reconstruction. CO<sub>2</sub> modelling for the Oligocene sites showed a decrease in CO<sub>2</sub> until at least ca. 30 ma (site Seifhennersdorf), before another increase in CO<sub>2</sub> occurred towards the late Oligocene, which is in great accordance to results derived by other proxies (Beerling and Royer, 2008). The low CO<sub>2</sub> estimate derived from site Schleenhain HC of mean 407 ppm is similar to the estimate in Roth-Nebelsick et al. (2014) for the same site, indicating mean CO<sub>2</sub> of 383 ppm and could be interpreted as a result of the low  $c_i/c_a$  ratio of 0.71 compared to the other sites. In Roth-Nebelsick et al. (2012, 2014) and Grein et al. (2013) additionally data have been derived from site Kleinsaubernitz, delivering atmospheric CO<sub>2</sub> of mean 431 ppm, which is slightly higher than estimated for the slightly younger site Borna-Ost-Bockwitz (413 ppm) but in agreement with the overall trend in increasing CO<sub>2</sub> prior to the Oligocene-Miocene boundary.



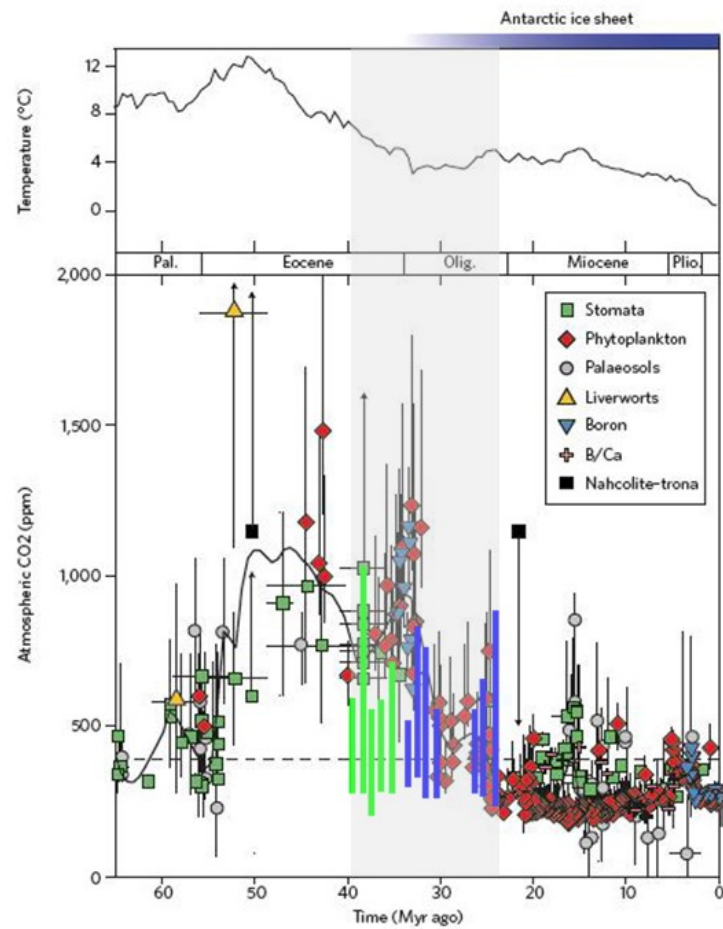


FIGURE 37. Cenozoic atmospheric CO<sub>2</sub> history and derived own estimates using *Rhodomyrtophyllum reticulosum* and *Platanus neptuni* (upper panel: deep-sea temperatures, lower panel: atmospheric CO<sub>2</sub> gathered from terrestrial and marine proxy data, together with plotted CO<sub>2</sub> estimates derived by gas exchange modelling (Konrad et al., 2008) for *Rhodomyrtophyllum reticulosum* (green bars) and *Platanus neptuni* (blue bars) leaf traits); modified from Beerling and Royer (2008).

## 7. Conclusion

The investigation of leaf traits of the long-lived species *Rhodomyrtophyllum reticulosum* and *Platanus neptuni* in favor of tracking global paleoclimatic and paleoatmospheric changes and dependencies of the respective leaf trait changes in correspondence to the considered depositional settings constitutes to be the first multidimensional study in order to obtain critical parameters and the applicability of the respective methods.

Both species respond to global changes in paleoclimate with different leaf traits and in different intensities. *Rhodomyrtophyllum* leaf traits, both morphometric and cuticular, vary greatly within a single leaf and within a site. This intra-site variability outweighs the differences between sites and hence, in stratigraphic ages. These neglectable changes in leaf trait patterns have two possible reasons. The stability of leaf traits in times of slightly decreasing temperature and CO<sub>2</sub> corresponds to a plateau phase with rather stable climate conditions prior to the Eocene-Oligocene turnover. If considered that *Rhodomyrtophyllum reticulosum* was element of riparian vegetation during the Eocene, the stability in derived leaf trait estimates is interpreted due to stable environmental conditions with a rather humid and balanced climate differing from sites with zonal vegetation facing greater variations in precipitation, seasonality in the distribution of preservation and temperature.

The correspondence of leaf trait changes to depositional settings and thus differences in the respective habitat is firstly proven for *Platanus neptuni* leaf trait changes. Leaf size is greatest in marine depositional settings, whereas size is smallest in coastal-alluvial plain deposits. This pattern is also mirrored in stomata density, with smallest stomata density in leaves from marine depositional settings and greatest values in coastal-alluvial plain deposits. If the considered leaf traits change through time one can easily recognize the ambiguity of leaf trait shifts with lowest stomata density reconstructed for the Rupelian. If low stomata density is considered to mirror high CO<sub>2</sub> one would reconstruct highest CO<sub>2</sub> during the Rupelian. This is not true and elucidates the high impact of differences in leaf traits derived from different depositional settings for CO<sub>2</sub> reconstructions, although CO<sub>2</sub> is said to be independent from regional effects reflecting global conditions.

In this study it has been proven that the investigation of single species and their correspondence to global and regional paleoclimatic and paleoatmospheric shifts has to be

done considering differences in the respective depositional setting and thus habitat. Regional effects influence the peculiarity of leaf traits greatly which implies that regional and site related patterns partly overweigh global correspondences. The weak correlation of leaf trait changes to global changes in paleoclimate and CO<sub>2</sub> implies that the long-lived species *Rhodymyrtophyllum reticulosum* and *Platanus neptuni* are not suitable to track these changes due their high plasticity and adaptability. The long stratigraphic range of the investigated species therefore point out the high adaption potential which by implication leads to a lower correspondence to global paleoclimatic changes. The determination of crucial leaf traits and their response to overall changes in paleoclimate and CO<sub>2</sub> hampers the fact that the fossil record bears mainly elements present in azonal vegetation which is caused by predominantly burial of fossils in aquatic bodies. Hence, long-lived species could have been survived these remarkable changes in climate from the end of the Early Eocene Climatic Optimum to the Oligocene icehouse world due to their occurrence in azonal assemblages, buffering global effects in climate variability to a certain degree. The investigation of long-lived fossil species therefore has to be done by coincident consideration of the composition of the whole plant assemblage, which reflects both azonal and partly zonal vegetation of the respective time interval.

---

## 8. Perspectives

As taxon-based studies of vegetational response to global and regional changes in paleoclimate and CO<sub>2</sub> over longer time spans, covering distinct climatic events, with both morphological and cuticular patterns are rare to date, more data and experience is needed to find suitable species to trace these shifts in climate and CO<sub>2</sub> and to develop suitable methods applicable for long-lived species.

Another attempt to deepen the knowledge and experience in the suitability of long-lived fossil species to answer the in this study described scientific questions has been already started in morphometric investigation of *Eotrigonobalanus furcinervis* (Fagaceae) leaf traits. This species is a common element in different depositional settings in central Europe during most parts of the Paleogene and could serve as a kind of control species for already observed relationships between global and regional climate, habitat and leaf macro and micro morphology. Digitization and polygonization of leaves from distinct stratigraphic horizons of the Weißelster Basin has been already started and will proceed coupled with the investigation of cuticular derived results, such as SD, TD and stomata sizes. Together with measured photosynthesis data of assumed nearest living equivalents determined during April and May, 2016 in the Xishuangbanna Tropical Botanical Garden in southwestern Yunnan (China) on species such as *Lithocarpus polystachyus*, *Trigonobalanus doichangensis* and *Castanopsis clarkei*, the already existing CO<sub>2</sub> datasets will be extended.

The same holds true for the upcoming *Rhodomyrtophyllum reticulosum* publication, which is already in preparation and is based on the results illustrated in this thesis and measured photosynthesis data of *Syzygium samarangense* with the focus on the applicability of different methods in azonal riparian environment and their significance for global or even transregional changes in climate and CO<sub>2</sub>.

The collection of the Section Paleobotany at the Senckenberg Natural History Collection in Dresden bears a variety of not yet fully taxonomically determined plant assemblages as well as raw material which gives paleobotanists the rare opportunity to trace vegetational changes and changes in leaf traits of respective taxa through time and only minor differences in the spatial distribution and hence latitude, longitude, oceanity and depositional settings in the Weißelster Basin.

---

## List of Figures

FIGURE 1. Cenozoic chronostratigraphic chart and global climate history.....	6
FIGURE 2. Geological map of central Europe and selected geological units and topographic landmarks.....	7
FIGURE 3. Paleogeographic situation of Europe during the Eocene .....	10
FIGURE 4. Paleogeographic situation of Europe during the Oligocene.....	12
FIGURE 5. Vegetation dynamics of riparian forests in Europe during the Eocene until the early Oligocene .....	15
FIGURE 6. Paleogeographical map of Europe during the latest Oligocene (25 Ma) und distribution of study sites .....	25
FIGURE 7. Typical preservation of different plant organs in marine depositional settings..	27
FIGURE 8. Typical coastal plain and fluvial plant assemblages.....	29
FIGURE 9. Typical association of plant organs derived from volcanic deposits.....	31
FIGURE 10. Location of investigated sites in Germany, Austria and the Czech Republic.....	32
FIGURE 11. Stratigraphic position of selected sites and their correspondence to the Cenozoic paleoclimate evolution.....	33
FIGURE 12. Leaf morphology and cuticles of <i>Rhodomyrtophyllum reticulosum</i> .....	50
FIGURE 13. Leaf morphology and cuticles of <i>Platanus neptuni</i> .....	54
FIGURE 14. Leaf morphology and cuticles of <i>Platanus kerrii</i> .....	56
FIGURE 15. Leaf morphology and cuticles of <i>Syzygium samarangense</i> .....	58
FIGURE 16. Concept and principles of the Coexistence Approach.....	60

---

FIGURE 17. Example of a CLAMP scoresheet .....	62
FIGURE 18. Leaf morphometric traits .....	64
FIGURE 19. Stomata with open stomatal pore.....	69
FIGURE 20. Dependencies between SD(Ca) and most critical parameters which have been varied during gas exchange reconstruction.....	76
FIGURE 21. Early Eocene to early Miocene temperature trend derived from CA and CLAMP for selected sites .....	83
FIGURE 22. Leaf morphometric data plotted against time for <i>Rhodomyrtophyllum reticulosum</i> leaf traits.....	85
FIGURE 23. Leaf length and width and length/width ratio of <i>Platanus neptuni</i> plotted for the single sites in a stratigraphic order.....	87
FIGURE 24. Leaf area and $LM_A$ of <i>Platanus neptuni</i> plotted for the single sites in a stratigraphic order.....	88
FIGURE 25. Leaf morphometric data of <i>Platanus neptuni</i> plotted against depositional setting .....	89
FIGURE 26. Leaf area and $LM_A$ for <i>Platanus neptuni</i> leaves derived from different depositional settings.....	90
FIGURE 27. Cuticular data (SD, SI) from <i>Rhodomyrtophyllum reticulosum</i> in a stratigraphical order .....	92
FIGURE 28. SD counts coupled with sampling position on respective specimen of <i>Rhodomyrtophyllum reticulosum</i> for site Peres 3u.....	93
FIGURE 29. Stomata width (green bars) and pore length (blue bars) estimated from <i>Rhodomyrtopyllum reticulosum</i> for the single sites.....	94
FIGURE 30. SD and TD of <i>Platanus neptuni</i> plotted for the single sites and regarding stratigraphy .....	96

---

FIGURE 31. SI and stomata width and pore length data of <i>Platanus neptuni</i> plotted for the single sites and regarding stratigraphy .....	98
FIGURE 32. SD, TD, stomata width and pore length of <i>Platanus neptuni</i> leaves plotted against depostional setting.....	99
FIGURE 33. Bartonian and Priabonian CO <sub>2</sub> reconstructed using the gas exchange model and <i>Rhodomyrtophyllum reticulosum</i> leaf traits, biochemical, carbon and climate data. ....	102
FIGURE 34. Rupelian to Aquitanian CO <sub>2</sub> reconstructed using the gas exchange model and <i>Platanus neptuni</i> leaf traits, biochemical, carbon and climate data.....	105
FIGURE 35. Paleoclimate and CO <sub>2</sub> summarized from the Ypresian/Lutetian boundary to the early Aquitanian.....	107
FIGURE 36. Robert Whittakers Diagram of world biomes and investigated sites ordered following stratigraphy .....	116
FIGURE 37. Cenozoic atmospheric CO <sub>2</sub> history and derived own estimates using <i>Rhodomyrtophyllum reticulosum</i> and <i>Platanus neptuni</i> .....	133

---

## List of Tables

TABLE 1. Characteristics of the study sites containing <i>Rhodomyrtophyllum reticulosum</i> leaves, regarding stratigraphy and dating.....	39
TABLE 2. Characteristics of the study sites containing <i>Platanus neptuni</i> leaves, regarding stratigraphy, sedimentological and depositional setting.....	47
TABLE 3. Number of digitized and replenished leaves of <i>Rhodomyrtophyllum reticulosum</i> and <i>Platanus neptuni</i> for the single sites and appropriate leaves for LM <sub>A</sub> determination ....	66
TABLE 4. Number of cuticle counts for SD, SI, TD and h <sub>St</sub> and w <sub>St</sub> determination for <i>Rhodomyrtophyllum reticulosum</i> and <i>Platanus neptuni</i> .....	68
TABLE 5. List of all parameters that are required for gas exchange model application .....	72
TABLE 6. Carbon isotope data gathered from <i>Rhodomyrtophyllum reticulosum</i> leaves.....	74
TABLE 7. Carbon isotope data gathered from <i>Platanus neptuni</i> leaves .....	75
TABLE 8. Paleoclimate estimates derived from CA.....	79
TABLE 9 (next page). Paleoclimate estimates derived from CLAMP .....	81
TABLE 10. Leaf morphometric data of <i>Rhodomyrtophyllum reticulosum</i> .....	84
TABLE 11. Leaf morphometric data of <i>Platanus neptuni</i> .....	86
TABLE 12. Cuticular data of <i>Rhodomyrtophyllum reticulosum</i> .....	91
TABLE 13. Cuticular data of <i>Platanus neptuni</i> .....	95
TABLE 14A. Morphometrical and anatomical input data for CO <sub>2</sub> reconstructions gathered from <i>Rhodomyrtophyllum reticulosum</i> .....	100



---

TABLE 14B. Carbon, biochemical and climate input parameters for gas exchange modelling using <i>Rhodomyrtophyllum reticulosum</i> .....	101
TABLE 15. Estimated minimum, mean and maximum CO <sub>2</sub> using the gas exchange model (Konrad et al., 2008) for <i>Rhodomyrtophyllum reticulosum</i> .....	102
TABLE 16A. Morphometrical and anatomical input data for CO <sub>2</sub> reconstructions gathered from <i>Platanus neptuni</i> .....	103
TABLE 16B: Carbon, biochemical and climate input parameters for gas exchange modelling using <i>Platanus neptuni</i> .....	104
TABLE 17. Estimated minimum, mean and maximum CO <sub>2</sub> using the gas exchange model (Konrad et al., 2008) for <i>Platanus neptuni</i> .....	105
TABLE 18. Selected leaf physiognomic characters for <i>Rhodomyrtophyllum reticulosum</i> derived from different plant assemblages.....	121
TABLE 19. Selected leaf physiognomic characters for <i>Platanus neptuni</i> derived from the considered plant assemblages for different grouped characters .....	125

## Supplementary Data

All supplementary data are available upon request ([karolin.moraweck@senckenberg.de](mailto:karolin.moraweck@senckenberg.de) and/or [lutz.kunzmann@senckenberg.de](mailto:lutz.kunzmann@senckenberg.de)).

- Appendix A: Floral lists of all investigated sites
- Appendix B: Climate data of extant nearest living equivalents for paleoclimatic reconstruction using CA
- Appendix C: Scoresheets for CLAMP reconstruction for investigated sites
- Appendix D: Leaf physiognomic states derived by CLAMP for investigated sites
- Appendix E: Morphometric data for *Rhodomyrtophyllum reticulosum*
- Appendix F: Cuticular data for *Rhodomyrtophyllum reticulosum* and *Platanus neptuni* for investigated sites
- Appendix G: Example of gas exchange modelling (MAPLE sheet)
- Appendix H: Input parameters, systematic parameter variation for gas exchange modelling and derived CO<sub>2</sub>

---

## Bibliography

- Akhmetiev, M., Walther, H. and Kvaček, Z., 2009. Palaeogene floras of Eurasia bound to volcanic settings and palaeoclimatic events—experience obtained from the Far East of Russia (Sikhote-Alin') and Central Europe (Bohemian Massif). *Acta Musei Nationalis Pragae, Series B Historia Naturalis*, 65: 61-129.
- Baas, P., 1969. Comparative anatomy of *Platanus kerrii* Gagnep. *Botanical Journal of the Linnean Society*, 62: 413-421.
- Bailey, J.W. and Sinnot, E.W., 1915. A botanical index of Cretaceous and Tertiary climates. *Science*, 41(1066): 831-834.
- Bandaluska, H., 1931. On the cuticles of some recent and fossil Myrtaceae. *Journal of the Linnean Society, Botany*, 48(325): 657-671.
- Barthel, M., 1976a. Die paläobotanische Fazies in den obereozänen Sedimenten des Januskessels (Tagebau Kayna-Süd). In: M. Barthel (Editor), *Eozäne Floren des Geiseltales. Abhandlungen des Zentralen Geologischen Instituts, Berlin*, pp. 31-35.
- Barthel, M., 1976b. Farne und Cycadeen. In: M. Barthel (Editor), *Eozäne Floren des Geiseltales. Abhandlungen des Zentralen Geologischen Instituts, Berlin*, pp. 439-498.
- Barthel, M. and Rüffle, L., 1970. Vegetationsbilder aus dem Alttertiär (Eozän) der Braunkohle des Geiseltales. *Wissenschaftliche Zeitschrift der Humboldt-Universität Berlin*, 19(2-3): 274-283.
- Beerling, D.J., McElwain, J.C. and Osborne, C.P., 1998. Stomatal response of the 'living fossil' *Ginkgo biloba* L. to changes in atmospheric CO<sub>2</sub> concentrations. *Journal of Experimental Botany*, 49(326): 1603-1607.
- Beerling, D.J. and Royer, D.L., 2002. Fossil plants as indicators of the Phanerozoic global carbon cycle. *Annual Review of Earth and Planetary Sciences*, 30(1): 527-556.
- Beerling, D.J. and Royer, D.L., 2011. Convergent Cenozoic CO<sub>2</sub> history. *Nature Geoscience*, 4(7): 418-420.
- Bellon, H., Buzek, C., Gaudant, J., Kvaček, Z. and Walther, H., 1998. The České Stredohorí magmatic complex in Northern Bohemia 40K-40Ar ages for volcanism and biostratigraphy of the Cenozoic freshwater formations. *Newsletters on Stratigraphy*: 77-103.

- Bernacchi, C.J., Pimentel, C. and Long, S.P., 2003. In vivo temperature response functions of parameters required to model RUBP-limited photosynthesis. *Plant Cell and Environment*, 26(9): 1419-1430.
- Bijl, P.K., Houben, A.J.P., Schouten, S., Bohaty, S.M., Sluijs, A., Reichart, G.-J., Damsté, J.S.S. and Brinkhuis, H., 2010. Transient Middle Eocene Atmospheric CO<sub>2</sub> and Temperature Variations. *Science*, 330(6005): 819-821.
- Blonder, B. and Enquist, B.J., 2014. Inferring climate from angiosperm leaf venation networks. *New Phytologist*, 204(1): 1-11.
- Boenigk, J., Wodnick, S. and Glücksman, E., 2015. *Biodiversity and Earth History* Springer, Berlin, 1-401 pp.
- Bowden, J.D. and Bauerle, W.L., 2008. Measuring and modeling the variation in species-specific transpiration in temperate deciduous hardwoods. *Tree Physiology*, 28(11): 1675-1683.
- Bruch, A.A., Uhl, D. and Mosbrugger, V., 2007. Miocene climate in Europe - Patterns and evolution. A first synthesis of NECLIME. *Palaeogeography, Palaeoclimatology, Palaeoecology*, 253: 1-7.
- Burnham, R.J., 1989. Relationships between standing vegetation and leaf litter in a paratropical forest: implications for paleobotany. *Review of Palaeobotany and Palynology*, 58: 5-32.
- Carpenter, R.J., Hill, R.S. and Jordan, G.J., 2005. Leaf cuticular morphology links Platanaceae and Proteaceae. *International Journal of Plant Sciences*, 166(5): 843-855.
- Cohen, K.M., Finney, S.C., Gibbard, P.L. and Fan, J.-X., 2013, updated. The ISC International Chronostratigraphic Chart. *International Commission on Stratigraphy*, 36: 199-204.
- Collinson, M.E., Manchester, S.R. and Wilde, V., 2012. Fossil Fruits and Seeds of the Middle Eocene Messel biota, Germany. *Abhandlungen der Senckenberg Gesellschaft für Naturforschung*, 570: 1-251.
- Coxall, H.K., Wilson, P.A., Pälike, H., Lear, C.H. and Backman, J., 2005. Rapid stepwise onset of Antarctic glaciation and deeper calcite compensation in the Pacific Ocean. *Nature*, 433(7021): 53-57.
- DeConto, R.M. and Pollard, D., 2003. Rapid Cenozoic glaciation of Antarctica induced by declining atmospheric CO<sub>2</sub>. *Nature*, 421(6920): 245-249.

- Dietrich, J., 2012. Phytostratigraphie, Paläoökologie und Taphonomie einer eozänen Blätterflora aus dem Tagebau Profen (Sachsen-Anhalt). Technische Universität Bergakademie Freiberg, Freiberg, 1-107 pp.
- Dolph, G.E. and Dilcher, D.L., 1980. Variation in leaf size with respect to climate in the tropics of the Western Hemisphere. *Bulletin of the Torrey Botanical Club*, 107(2): 154-162.
- Doria, G., Royer, D.L., Wolfe, A.P., Fox, A., Westgate, J.A. and Beerling, D.J., 2011. Declining atmospheric CO<sub>2</sub> during the late middle Eocene climate transition. *American journal of Science*, 311(1): 63-75.
- Eissmann, L., 1994. Leitfaden der Geologie des Präquartärs im Saale-Elbe-Gebiet. *Altenburger Naturwissenschaftliche Forschungen*, 7: 11-53.
- Eldrett, J.S., Harding, I.C., Firth, J.V. and Roberts, A.P., 2004. Magnetostratigraphic calibration of Eocene–Oligocene dinoflagellate cyst biostratigraphy from the Norwegian–Greenland Sea. *Marine Geology*, 204(1): 91-127.
- Ellenberg, H., 1975. Vegetationsstufen in perhumiden bis ariden Bereichen der tropischen Anden. *Phytocoenologica*, 2(3-4): 368-387.
- Engelhardt, H., 1922. Die alttertiäre Flora von Messel bei Darmstadt. *Abhandlungen der Hessischen Geologischen Landesanstalt Darmstadt*, 7(4): 17-128.
- Farquhar, G.D., Caemmerer, S.v. and Berry, J.A., 1980. A biochemical model of photosynthetic CO<sub>2</sub> assimilation in leaves of C<sub>3</sub> leaves. *Planta*, 149(1): 78-90.
- Farquhar, G.D., O’Leary, M.H. and Berry, J.A., 1982. On the relationship between carbon isotope discrimination and intercellular carbon dioxide concentration in leaves. *Functional Plant Biology*, 9(2): 121-137.
- Farquhar, G.D., Ehlenringer, J.R. and Hubick, K.T., 1989. Carbon isotope discrimination and photosynthesis. *Annual Review of Plant Physiology*, 40(1): 503-537.
- Farquhar, G.D., O’Leary, M.H. and Berry, J.A., 1982. On the relationship between carbon isotope discrimination and intercellular carbon dioxide concentration in leaves. *Functional Plant Biology*, 9(2): 121-137.
- Felder, M. and Harms, F.J., 2004. Lithologie und genetische Interpretation der vulkanosedimentären Ablagerungen aus der Grube Messel anhand der Forschungsbohrung Messel 2001 und weiterer Bohrungen. *Courier Forschungsinstitut Senckenberg*, 252: 151-203.

- Ferdani, F., 2014. Obereozäne Floren aus dem zentralen Weißelsterbecken (Mitteldeutschland) und ihre paläoökologische Position. *Altenberger Naturwissenschaftliche Forschungen*, 16: 1-115.
- Ferguson, D.K., 2005. Plant Taphonomy: Ruminations on the Past, the Present, and the Future. *Palaios*, 20(5): 418-428.
- Fischer, O., 1990. Blätter-Floren aus mitteleozänen Sedimenten des südlichen Weißelster Beckens (Profen und Scheiplitz). Humboldt-Universität Berlin; Museum für Naturkunde, Berlin, pp. 1-118.
- Francis, J.E., Marensi, S., Levy, R., Hambrey, M., Thorn, V.C. and Mohr, B., 2009. From Greenhouse to Icehouse - The Eocene/Oligocene in Antarctica. *Developments in Earth & Environmental Sciences*, 8: 309-368.
- Frey, E., Munk, W., Böhme, M., Morlo, M. and Hensel, M., 2010. First creodont carnivore from the Rupelian Clays (Oligocene) of the Clay Pit Unterfeld at Rauenberg (Rhein-Neckar-Kreis, Baden-Württemberg): *Apterodon rauenbergensis* n.sp. *Kaupia*, 17(1): 107-113.
- Gaertner, H.-R.v., Walther, H.W., Weber, H.S. and Voss, H.-H., 1971. The International Geological Map of Europe and the Mediterranean Region. United Nations Educational, Scientific and Cultural Organization (UNESCO) and the Commission for the Geological Map of the World (CMGW), pp. 2 sheets.
- Galmés, J., Flexas, J., Savé, R. and Medrano, H., 2007. Water relations and stomatal characteristics of Mediterranean plants with different growth forms and leaf habits: response to water stress and recovery. *Plant and Soil*, 290(1-2): 139-155.
- Gastaldo, R.A., Ferguson, D.K., Walther, H. and Rabold, J.M., 1996. Criteria to distinguish parautochthonous leaves in Tertiary alluvial channel-fills. *Review of Palaeobotany and Palynology*, 91(1): 1-21.
- Gastaldo, R.A., Riegel, W., Püttmann, W., Linnemann, U.G. and Zetter, R., 1998. A multidisciplinary approach to reconstruct the Late Oligocene vegetation in central Europe. *Review of Palaeobotany and Palynology*, 101(1): 71-94.
- Gee, C.T., 2005. The Genesis of Mass Carpological Deposits (Bedload Carpodeposits) in the Tertiary of the Lower Rhine Basin, Germany. *Palaios*, 20(5): 463-478.
- Gibbard, P.L. and Lewin, J., 2016. Filling the North Sea Basin: Cenozoic sediment sources and river styles. *Geologica Belgica*, 19(3-4): 201-217.

- Givnish, T., 1979. On the adaptive significance of leaf form. *Topics in plant population biology*: 375-407.
- Givnish, T.J., 1986. Optimal stomatal conductance, allocation of energy between leaves and roots, and the marginal cost of transpiration. In: T.J. Givnish (Editor), *On the Economy of Plant Form and Function*. Cambridge University Press, Cambridge.
- Glinka, U. and Walther, H., 2003. *Rhodomyrtophyllum reticulosum* (ROSSM.) KNOBLOCH & KVAČEK - ein bedeutendes eozänes Florenelement im Tertiär Mitteleuropas. *Feddes Repertorium*, 114(1-2): 30-55.
- Goth, K., Suhr, P. and Schulz, R., 2003. Zwei Forschungsbohrungen in das verdeckte Maar von Baruth (Sachsen). *Zeitschrift für Angewandte Geowissenschaften*, 1: 9-17.
- Greenwood, D.R., 1991. The taphonomy of plant macrofossils. In: S.K. Donovan (Editor), *The Processes of Fossilization*. Columbia University Press, New York, pp. 141-169.
- Greenwood, D.R. and Wing, S.L., 1995. Eocene continental climates and latitudinal temperature gradients. *Geology*, 23(11): 1044-1048.
- Greenwood, D.R., Scarr, J.M. and Christophel, D.C., 2003. Leaf stomatal frequency in the Australian tropical rainforest tree *Neolitsea dealbata* (Lauraceae) as a proxy measure of atmospheric pCO<sub>2</sub>. *Palaeogeography, Palaeoclimatology, Palaeoecology*, 196: 375-393.
- Greenwood, D.R., 2005. Leaf Margin Analysis: Taphonomic Constraints. *Palaios*, 20(5): 498-505.
- Grein, M., Roth-Nebelsick, A. and Wilde, V., 2010. Carbon isotope composition of middle Eocene leaves from the Messel pit, Germany. *Palaeodiversity*, 3: 1-7.
- Grein, M., Konrad, W., Wilde, V., Utescher, T. and Roth-Nebelsick, A., 2011a. Reconstruction of atmospheric CO<sub>2</sub> during the early middle Eocene by application of a gas exchange model to fossil plants from the Messel Formation, Germany. *Palaeogeography, Palaeoclimatology, Palaeoecology*, 309(3-4): 383-391.
- Grein, M., Utescher, T., Wilde, V. and Roth-Nebelsick, A., 2011b. Reconstruction of the middle Eocene climate of Messel using paleobotanical data. *Neues Jahrbuch für Geologie und Paläontologie, Abhandlungen*, 260(3): 305-318.
- Grein, M., Oehm, C., Konrad, W., Utescher, T., Kunzmann, L. and Roth-Nebelsick, A., 2013. Atmospheric CO<sub>2</sub> from the late Oligocene to early Miocene based on photosynthesis data and fossil leaf characteristics. *Palaeogeography, Palaeoclimatology, Palaeoecology*, 374: 41-51.

- Grimm, G.W. and Denk, T., 2010. The reticulate origin of modern plane trees (*Platanus*, Platanaceae): a nuclear marker puzzle. *Taxon*, 59(1): 134-147.
- Grimm, G.W. and Denk, T., 2012. Reliability and resolution of the coexistence approach - Revalidation using modern-day data. *Review of Palaeobotany and Palynology*, 172: 33-47.
- Grimm, G.W., Bouchal, J.M., Denk, T. and Potts, A., 2016. Fables and foibles: A critical analysis of the Palaeoflora database and the Coexistence Approach for palaeoclimate reconstruction. *Review of Palaeobotany and Palynology*, 233(216-235).
- Grimm, G.W. and Potts, A.J., 2016. Fallacies and fantasies: the theoretical underpinnings of the Coexistence Approach for palaeoclimate reconstruction. *Climate of the Past*, 12: 611-622.
- Grimm, K.I., Grimm, M.C., Köthe, A. and Schindler, T., 2002. Der "Rupelton" (Rupelium, Oligozän) der Tongrube Bott-Eder bei Rauenberg (Oberrheingraben, Deutschland). *Courier Forschungsinstitut Senckenberg*, 237: 229-253.
- Grimm, K.I. and Grimm, M.C., 2003. Geologischer Führer durch das Mainzer Tertiärbecken. In: K.I. Grimm, M.C. Grimm, F.O. Neuffer and H. Lutz (Editors), *Die fossilen Wirbellosen des Mainzer Tertiärbeckens. Teil 1-1. Mainzer Naturwissenschaftliches Archiv, Beiheft, Mainz*, pp. 1-158.
- Grimm, K.I. and Hottenrott, M., 2011. Erdgeschichtlicher Überblick. In: D.S. Kommission (Editor), *Stratigraphie von Deutschland IX. Tertiär, Teil 1. Schriftenreihe der Deutschen Gesellschaft für Geowissenschaften, Hannover*, pp. 31-41.
- Grimm, K.I., Radtke, G., Köthe, A., Reichenbacher, B., Schwarz, J., Martini, E., Kadolsky, D., Hottenrott, M. and Franzen, J.L., 2011. Regionale Biostratigraphie. In: D.S. Kommission (Editor), *Stratigraphie von Deutschland IX: Tertiär, Teil 1: Oberrheingraben und benachbarte Tertiärgebiete. Schriftenreihe der Deutschen Gesellschaft für Geowissenschaften*, pp. 43-56.
- Grubb, P.J., 1998. A reassessment of the strategies of plants which cope with shortages of resources. *Perspectives in Plant Ecology*, 1(1): 3-31.
- Grunert, P., Harzhauser, M., Rögl, F., Sachsendorfer, R., Gratzer, R., Soliman, A. and Piller, W.E., 2010. Oceanographic conditions as a trigger for the formation of an Early Miocene (Aquitanian) *Konservat-Lagerstätte* in the Central Paratethys Area. *Palaeogeography, Palaeoclimatology, Palaeoecology*, 292(3): 425-442.
- Haworth, M., Heath, J. and McElwain, J.C., 2010. Differences in the response sensitivity of stomatal index to atmospheric CO<sub>2</sub> among four genera of Cupressaceae conifers. *Annals of Botany*, 105: 411-418.



- Haworth, M., Elliot-Kingston, C. and McElwain, J.C., 2013. Co-ordination of physiological and morphological response of stomata to elevated CO<sub>2</sub> in vascular plants. *Oecologia*, 171(1): 71-82.
- Heer, O., 1855-1859. *Flora Tertiaria Helvetiae*, 3. Wintherthur.
- Hennig, D. and Kunzmann, L., 2013. Taphonomy and vegetational analysis of a late Eocene flora from Schleenhain (Saxony, Germany). *Geologica Saxonica*, 59: 75-87.
- Hetherington, A.M. and Woodward, F.I., 2003. The role of stomata in sensing and driving environmental change. *Nature*, 424(6951): 901-908.
- Heydt, A.v.d. and Dijkstra, H.A., 2006. Effect of ocean gateways on the global ocean circulation in the late Oligocene and early Miocene. *Paleoceanography*, 21(1): 1-18.
- Hren, M.T., Sheldon, N.D., Grimes, S.T., Collinson, M.E., Hooker, J.J., Bugler, M. and Lohmann, K.C., 2013. Terrestrial cooling in Northern Europe during the Eocene-Oligocene transition. *Proceedings of the National Academy of Sciences* 110(19): 7562-7567.
- Hyland, E.G. and Sheldon, N.D., 2013. Coupled CO<sub>2</sub>-climate response during the Early Eocene Climatic Optimum. *Palaeogeography, Palaeoclimatology, Palaeoecology*, 369: 125-135.
- Ivany, L.C., Patterson, W.P. and Lohmann, K.C., 2000. Cooler winters as a possible cause of mass extinctions at the Eocene/Oligocene boundary. *Nature*, 407(6806): 887-890.
- Jacques, F.M.B., Su, T., Spicer, R.A., Xing, Y., Huang, Y., Wang, W. and Zhou, Z., 2011. Leaf physiognomy and climate: Are monsoon systems different? *Global and Planetary Change*, 76(1): 56-62.
- Jurke, B., 2016. Möglichkeiten und Grenzen der Anwendbarkeit von Stomatadichte in Abhängigkeit der Blattmorphometrie für paläoklimatische Aussagen am Beispiel *Rhodomyrtophyllum* (Obereozän, Mitteldeutschland), Technische Universität Bergakademie Freiberg, Freiberg, 1-33 pp.
- Kennedy, E.M., Arens, N.C., Reichgelt, T., Spicer, R.A., Spicer, T.E.V., Stranks, L. and Yang, J., 2014. Deriving temperature estimates from Southern Hemisphere leaves. *Palaeogeography, Palaeoclimatology, Palaeoecology*, 412: 80-90.
- Kennett, J.P., 1977. Cenozoic evolution of Antarctic glaciation, the circum-Antarctic Ocean, and their impact on global paleoceanography. *Journal of Geophysical Research*, 82(27): 3843-3860.
- Khan, M.A., Spicer, R.A., Bera, S., Ghosh, R., Yang, J., Spicer, T.E., Guo, S., Su, T., Jacques, F. and Grote, P., 2014. Miocene to Pleistocene floras and climate of the Eastern Himalayan

- Siwaliks, and new palaeoelevation estimates for the Namling–Oiyug Basin, Tibet. *Global and Planetary Change*, 113: 1-10.
- Knobloch, E., Konzalová, M. and Kvaček, Z., 1996. Die obereozäne Flora der Staré Sedlo-Schichtenfolge in Böhmen (Mitteleuropa). *Rozpravy Českého geologického ústavu*, 49: 1-260.
- Konrad, W., Roth-Nebelsick, A. and Grein, M., 2008. Modelling stomatal density response to atmospheric CO<sub>2</sub>. *Journal of Theoretical Biology*, 253(4): 638-658.
- Köppen, W., 1936. Das geographische System der Klimate. In: W. Köppen and G. Geiger (Editors), *Handbuch der Klimatologie*. Gebrüder Borntraeger, Berlin, pp. 1-44.
- Kouwenberg, L.L., McElwain, J.C., Kürschner, W., Wagner, F., Beerling, D.J., Mayle, F.E. and Visscher, H., 2003. Stomatal frequency adjustment of four conifer species to historical changes in atmospheric CO<sub>2</sub>. *American Journal of Botany*, 90(4): 610-619.
- Kovach, W.L. and Spicer, R.A., 1995. Canonical Correspondence Analysis of Leaf Physiognomy: a Contribution to the Development of a New palaeoclimatological Tool. *Palaeoclimates*, 2: 125-138.
- Kovar-Eder, J., 2016. Early Oligocene plant diversity along the Upper Rhine Graben: The fossil flora of Rauenberg, Germany. *Acta Palaeobotanica*, 56(2): 329-440.
- Kovar-Eder, J. and Kvaček, Z., 2007. The integrated plant record (IPR) to reconstruct Neogene vegetation: The IPR-vegetation analysis. *Acta Palaeobotanica*, 47(2): 391-418.
- Kovar, J., 1982. Eine Blätter-Flora des Egerian (Ober-Oligozän) aus marinen Sedimenten der Zentralen Paratethys im Linzer Raum (Österreich). *Beiträge zur Paläontologie von Österreich*, 9: 1-209.
- Krumbiegel, G., Schwarzenholz, W., Rüffle, L. and Barthel, M., 1976. Allgemeine Problemstellung und Situation der ober- und mitteleozänen Floren des Geiseltales. In: M. Barthel (Editor), *Eozäne Floren des Geiseltales*. Abhandlungen des Zentralen Geologischen Instituts, Berlin, pp. 11-46.
- Krutzsch, W., Blumenstengel, H., Kiesel, Y. and Rüffle, L., 1992. Paläobotanische Klimagliederung des Alttertiärs (Mitteleozän bis Oberoligozän) in Mitteldeutschland und das Problem der Verknüpfung mariner und kontinentaler Gliederungen (klassische Biostratigraphien-paläobotanisch-ökologische Klimastratigraphie-Evolutions-Stratigraphie der Vertebraten). *Neues Jahrbuch für Geologie und Paläontologie Abhandlungen*, 186(1-2): 137-253.

- Krutzsch, W., 2000. Stratigraphische Tabelle Oberoligozän und Neogen (marin-kontinental). Berliner Geowissenschaftliche Abhandlungen E, 34: 153-165.
- Krutzsch, W., 2008. Die Bedeutung der fossilen Pollengattung *Mediocolpopollis* KRUTZSCH 1959 (fam. Santalaceae) für die Gliederung des Obereozäns im mitteldeutschen Ästuar. Hallesches Jahrbuch für Geowissenschaften, 25: 1-103.
- Krutzsch, W., 2011. Stratigrafie und Klima des Paläogens im Mitteldeutschen Ästuar im Vergleich zur marinen nördlichen Umrahmung. Zeitschrift der deutschen Gesellschaft für Geowissenschaften, 162(1): 19-46.
- Kunzmann, L., 2012. Early Oligocene riparian and swamp forests with a mass occurrence of *Zingiberoideophyllum* (extinct Zingiberales) from Saxony, central Germany. Palaios, 27(11): 765-778.
- Kunzmann, L. and Walther, H., 2007. A noteworthy plant taphocoenosis from the Lower Oligocene Haselbach member (Saxony, Germany) containing *Apocynophyllum neriifolium* Heer. Acta Palaeobotanica, 47(1): 145-161.
- Kunzmann, L. and Walther, H., 2012. Early Oligocene plant taphocoenoses of the Haselbach megafloral complex and the reconstruction of palaeovegetation. Palaeobiodiversity and Palaeoenvironments, 92(3): 295-307.
- Kunzmann, L., Kvaček, Z., Teodoridis, V., Müller, C. and Moraweck, K., 2016. Vegetation dynamics of riparian forest in central Europe during the late Eocene. Palaeontographica, Abteilung B, 295(1-3): 69-89.
- Kürschner, W.M., Kvaček, Z. and Dilcher, D.L., 2008. The impact of Miocene atmospheric carbon dioxide fluctuations on climate and the evolution of terrestrial ecosystems. PNAS, 105(2): 449-453.
- Kvaček, Z., 1994. Connecting links between the Arctic Palaeogene and European Tertiary floras. In: M.C. Boulter and H.C. Fisher (Editors), Cenozoic Plants and Climates of the Arctic. NATO ASI Series, London, pp. 251-266.
- Kvaček, Z., 2004. Revisions to the Early Oligocene flora of Flörsheim (Mainz Basin, Germany) based on epidermal anatomy. Senckenbergiana lethaea, 84(1-2): 1-73.
- Kvaček, Z., 2007. Do extant nearest relatives of thermophile European Cenozoic plant elements reliably reflect climatic signal? . Palaeogeography, Palaeoclimatology, Palaeoecology, 253: 32-40.
- Kvaček, Z., 2008. Whole-plant reconstructions in fossil angiosperm research. International Journal of Plant Sciences, 169(7): 918-927.

- Kvaček, Z., 2010. Forest flora and vegetation of the European early Palaeogene - a review. *Bull. Geosci.*, 85(1): 3-16.
- Kvaček, Z. and Walther, H., 1989. Revision der mitteleuropäischen tertiären Fageceen nach blattepidermalen Charakteristiken, III. Teil *Dryophyllum* DEBEY ex SAPORTA und *Eotrigonobalanus* WALTHER & KVAČEK gen. nov. *Feddes Repertorium*, 100(11-12): 575-601.
- Kvaček, Z. and Walther, H., 1998. The Oligocene Volcanic Flora of Kundratice near Litoměřice, České Středohoří Volcanic Complex, Czech Republic: A Review. *Acta Musei Nationalis Pragae Series B – Historia Naturalis*, 54(1-2): 1-42.
- Kvaček, Z. and Walther, H., 2001. The Oligocene of Central Europe and the development of forest vegetation in space and time based on megafossils. *Palaeontographica Abteilung B*, 259(1-6): 125-148.
- Kvaček, Z. and Walther, H., 2004. Oligocene flora of Bechlechovice at Dečín from the neovolcanic area of the České středohoří Mountains, Czech Republic. *Acta Musei Nationalis Pragae Series B – Historia Naturalis*, 60(1-2): 1-60.
- Kvaček, Z. and Manchester, S.R., 2004. Vegetative and reproductive structure of the extinct *Platanus neptuni* from the Tertiary of Europe and relationships within the Platanaceae. *Plant Systematics and Evolution*, 244(1): 1-29.
- Kvaček, Z., Kováč, M., Kovar-Eder, J., Dolakova, N., Jechorek, H., Parashiv, V., Kováčová, M. and Sliva, L., 2006. Miocene evolution of landscape and vegetation in the Central Paratethys. *Geologica Carpathica*, 57(4): 295-310.
- Kvaček, Z. and Teodoridis, V., 2011. The late Eocene flora of Kučlín near Bílina in North Bohemia revisited. *Acta Musei Nationalis Pragae Series B – Historia Naturalis*, 67(3-4): 83-144.
- Kvaček, Z., Teodoridis, V., Mach, K., Přikryl, T. and Dvořák, Z., 2014. Tracing the Eocene-Oligocene transition: a case study from North Bohemia. *Bulletin of Geoscience*, 89(1): 21-66.
- Lear, C.H., Bailey, T.R., Pearson, P.N., Coxall, H.K. and Rosenthal, Y., 2008. Cooling and ice growth across the Eocene-Oligocene transition. *Geology*, 36(3): 251-254.
- Lenz, O.K., Wilde, V. and Riegel, W., 2011. Short-term fluctuations in vegetation and phytoplankton during the Middle Eocene greenhouse climate: a 640-kyr record from the Messel oil shale (Germany). *International Journal of Earth Sciences*, 100(8): 1851-1874.

- Lenz, O.K., Wilde, V. and Riegel, W., 2014. Palynology as a High-Resolution Tool for Cyclostratigraphy in Middle Eocene Lacustrine Sediments: The Outstanding Record of Messel (Germany), STRATI 2013. Springer, pp. 113-117.
- Mach, K. and Dvořák, Z., 2011. Geology of the site Kučlín, the Trupelník Hill. Acta Musei Nationalis Pragae Series B – Historia Naturalis, 67(3): 77-82.
- Mai, D.H., 1967. Die tertiären Arten von *Trigonobalanus* FORMAN (Fagaceae) in Europa. Jahrbuch der Geologie, Berlin, 3: 381-409.
- Mai, D.H., 1981. Entwicklung und klimatische Differenzierung der Laubwaldflora Mitteleuropas im Tertiär. Flora, 171: 525-582.
- Mai, D.H., 1995. Tertiäre Vegetationsgeschichte Europas: Methoden und Ergebnisse. Spektrum Akademischer Verlag, Heidelberg, Germany.
- Mai, D.H., 1997. Die oberoligozänen Floren am Nordrand der Sächsischen Lausitz. Palaeontographica Abteilung B, 244: 1-124.
- Mai, D.H. and Walther, H., 1978. Die Floren der Haselbacher Serie im Weißelster-Becken (Bezirk Leipzig, DDR). Abhandlungen des Staatlichen Museums für Mineralogie und Geologie zu Dresden, 28: 1-200.
- Mai, D.H. and Walther, H., 1983. Die fossilen Floren des Weißelster-Beckens und seiner Randgebiete. Hallesches Jahrbuch für Geowissenschaften, 8: 59-74.
- Mai, D.H. and Walther, H., 1985. Die obereozänen Floren des Weißelster-Beckens und seiner Randgebiete. Abhandlungen des Staatlichen Museums für Mineralogie und Geologie zu Dresden 33: 5-176.
- Mai, D.H. and Walther, H., 1991. Die oligozänen und untermiozänen Floren NW-Sachsens und des Bitterfelder Raumes. Abhandlungen des Staatlichen Museums für Mineralogie und Geologie zu Dresden, 38: 1-230.
- Mai, D.H. and Walther, H., 2000. Die Fundstellen eozäner Floren des Weißelster-Beckens und seiner Randgebiete. Altenburger Naturwissenschaftliche Forschungen, 13: 1-59.
- Maxwell, E.E., Alexander, S., Bechly, G., Eck, K., Frey, E., Grimm, K., Kovar-Eder, J., Mayr, G., Micklich, N., Rasser, M., Roth-Nebelsick, A., Salvador, R.B., Schoch, R.R., Schweigert, G., Stinnesbeck, W., Wolf-Schwenninger, K. and Ziegler, R., 2016. The Rauenberg fossil Lagerstätte (Baden-Württemberg, Germany): A window into early Oligocene marine and coastal ecosystems of Central Europe. Palaeogeography, Palaeoclimatology, Palaeoecology, 463: 238-260.

- McElwain, J.C. and Chaloner, W.G., 1996. The Fossil Cuticle as a Skeletal Record of Environmental Change. *Palaios*, 11: 376-388.
- McElwain, J.C., Montañez, I., White, J.D., Wilson, J.P. and Yiotis, C., 2016. Was atmospheric CO<sub>2</sub> capped at 1000ppm over the past 300 million years? *Palaeogeography, Palaeoclimatology, Palaeoecology*, 441: 653-658.
- McInerney, F.A. and Wing, S.L., 2011. The Paleocene-Eocene Thermal Maximum: A perturbation of Carbon Cycle, Climate, and Biosphere with Implications for the Future. *Annual Review of Earth and Planetary Sciences*, 39: 489-516.
- Mertz, D.F. and Renne, P.R., 2005. A numerical age for the Messel fossil deposit (UNESCO World Heritage Site) derived from <sup>40</sup>Ar/<sup>39</sup>Ar dating on a basaltic rock fragment. *Courier Forschungsinstitut Senckenberg*, 255: 67.
- Micklich, N. and Hildebrandt, L.H., 2010. Emergency excavation in the Grube Unterfeld (Frauenweiler) clay pit (Oligocene, Rupelian; Baden-Württemberg, S Germany): new records and palaeoenvironmental information. *Kaupia*, 17(1): 3-21.
- Moraweck, K., 2013. Fossile Floren als Klimaindikatoren: Quantitative Paläoklimarekonstruktion für das Obereozän des Weißelsterbeckens, Technische Universität Dresden, Dresden, 1-98 pp.
- Moraweck, K., Uhl, D. and Kunzmann, L., 2015. Estimation of late Eocene (Bartonian-Priabonian) terrestrial palaeoclimate: Contribution from megafloreal assemblages from central Germany. *Palaeogeography, Palaeoclimatology, Palaeoecology*, 433: 247-258.
- Moraweck, K., Grein, M., Konrad, W., Kovar-Eder, J., Kvaček, J., Neinhuis, C., Roth-Nebelsick, A., Stiller, S., Streubig, M., Traiser, C., Utescher, T. and Kunzmann, L., in review. Leaf traits of extinct *Platanus neptuni* (Platanaceae): indicators for palaeoenvironment and reliable palaeoclimatic and palaeoatmospheric proxies? *Review of Paleobotany and Palynology*.
- Mosbrugger, V., 1999. The nearest living relative method. In: T.P. Jones and N.P. Rowe (Editors), *Fossil Plants and Spores: Modern Techniques*. Geological Society, London, pp. 261-265.
- Mosbrugger, V. and Schilling, H.-D., 1992. Terrestrial palaeoclimate in the Tertiary: a methodological critique. *Palaeogeography, Palaeoclimatology, Palaeoecology*, 99: 17-29.

- Mosbrugger, V. and Utescher, T., 1997. The coexistence approach - a method for quantitative reconstruction of Tertiary terrestrial palaeoclimate data using plant fossils. *Palaeogeography, Palaeoclimatology, Palaeoecology*, 134: 61-86.
- Mosbrugger, V. and Utescher, T., 1997-2016. PALAEOFLORE - Data base for palaeoclimate reconstructions using the Coexistence Approach. <http://www.palaeoflora.de>.
- Mosbrugger, V., Utescher, T. and Dilcher, D. L. 2005. Cenozoic continental climatic evolution of Central Europe. *PNAS*, 102(42): 14964-14969.
- Müller, C., 2014. Paläoklima und Paläovegetation im Obereozän Mitteldeutschlands am Beispiel einer Flora aus dem Tagebau Borna-Ost (Sachsen), Technische Universität Bergakademie Freiberg, Freiberg, 1-94 pp.
- Müller, C., 2016. Pflanzen-Insekten-Interaktionen innerhalb der späteozänen Profen Flora (Sachsen-Anhalt) und ihre paläoökologische Interpretation, Technische Universität Bergakademie Freiberg, Freiberg, 1-75 pp.
- Nicotra, A.B., Leigh, A., Boyce, C.K., Jones, C.S., Niklas, L.J., Royer, D.L. and Tsukaya, H., 2011. The evolution and functional significance of leaf shape in the angiosperms. *Functional Plant Biology*, 38(7): 535-552.
- Nobel, P.S., 1999. *Physicochemical and environmental plant physiology*. Academic Press, San Diego.
- Oschmann, W., 2016. *Evolution der Erde*. Haupt-Verlag, 1-383 pp.
- Pearson, P.N., Gavin, N., Foster, L. and Wade, B.S., 2009. Atmospheric carbon dioxide through the Eocene-Oligocene transition. *Nature*, 461(7267): 1110-1113.
- Peel, M.C., Finlayson, B.L. and McMahon, T.A., 2007. Updated world map of the Köppen-Geiger climate classification. *Hydrology and Earth System Sciences discussions*, 4(2): 439-473.
- Peppe, D.J., Royer, D.L., Cariglino, B., Oliver, S.Y., Newman, S., Leight, E., Enikolopov, G., Fernandez-Burgos, M., Herrera, F., Adams, J.M., Correa, E., Currano, E.D., Erickson, J.M., Hinojosa, L.F., Hoganson, J.W., Iglesias, A., Jaramillo, C.A., Johnson, K.R., Jordan, G.J., Kraft, N.J.B., Lovelock, E.C., Lusk, C.H., Niinemets, Ü., Peñuelas, J., Rapson, G., Wing, S.L. and Wright, I.J., 2011. Sensitivity of leaf size and shape to climate: global patterns and paleoclimate applications. *New Phytologist*, 190(3): 724-739.

- Poole, I. and Kürschner, W.M., 1999. Stomatal density and index: the practice. In: T.P. Jones and N.P. Rowe (Editors), *Fossil Plants and Spores: modern techniques*. Geological Society, London, pp. 257-260.
- Prothero, D.R., 1994. The late Eocene-Oligocene extinctions. *Annual Review of Earth and Planetary Sciences*, 22(1): 145-165.
- Quan, C., Liu, Y.-S. and Utescher, T., 2012. Paleogene temperature gradient, seasonal variation and climate evolution of northeast China. *Palaeogeography, Palaeoclimatology, Palaeoecology*, 313-314: 150-161.
- Rascher, J., Escher, D., Fischer, J., Dutschmann, U. and Kästner, S., 2005. *Geologischer Atlas Tertiär Nordwestsachsen 1: 250 000*. Sächsisches Landesamt für Umwelt und Geologie, Dresden, 1-16 pp.
- Rascher, J., Escher, D. and Fischer, J., 2008. Zur stratigraphischen Gliederung des obereozänen Hauptflözkomplexes (Thüringer und Bornauer Hauptflöz) in der Leipziger Bucht. *Zeitschrift der deutschen Gesellschaft für Geowissenschaften*, 159(1): 105-116.
- Ricklefs, R.E., 2008. *The Economy of Nature*. W. H. Freeman and Company, New York.
- Rögl, F., 1999. Short Note. Mediterranean and Paratethys. Facts and Hypotheses of an Oligocene to Miocene Paleogeography (Short Overview). *Geologica Carpathica*, 50(4): 339-349.
- Röhl, U., Westerhold, T., Bralower, T.J. and Zachos, J.Z., 2007. On the duration of the Paleocene-Eocene Thermal Maximum (PETM). *Geochemistry, Geophysics, Geosystems*, 8(12): 1-13.
- Roth-Nebelsick, A., 2005. Reconstructing atmospheric carbon dioxide with stomata: possibilities and limitations of a botanical pCO<sub>2</sub>-sensor. *Trees*, 19(3): 251-265.
- Roth-Nebelsick, A., Utescher, T., Mosbrugger, V., Diester-Haass, L. and Walther, H., 2004. Changes in atmospheric CO<sub>2</sub> concentrations and climate from the Late Eocene to Early Miocene: palaeobotanical reconstruction based on fossil floras from Saxony, Germany. *Palaeogeography, Palaeoclimatology, Palaeoecology*, 205: 43-67.
- Roth-Nebelsick, A., Grein, M., Utescher, T. and Konrad, W., 2012. Stomatal pore length change in leaves of *Eotrigonobalanus furcinervis* (Fagaceae) from the Late Eocene to the Latest Oligocene and its impact on gas exchange and CO<sub>2</sub> reconstruction. *Review of Palaeobotany and Palynology*, 174: 106-112.
- Roth-Nebelsick, A., Oehm, C., Grein, M., Utescher, T., Kunzmann, L., Friedrich, J.-P. and Konrad, W., 2014. Stomatal density and index of *Platanus neptuni* leaf fossils and



- their evaluation as a CO<sub>2</sub> proxy for the Oligocene. *Review of Palaeobotany and Palynology*, 206: 1-9.
- Roth-Nebelsick, A., Grein, M., Traiser, C., Kunzmann, L., Kovar-Eder, J., Kvaček, J. and Neinhuis, C., 2017. Functional leaf traits and leaf economics in the Paleogene - A case study for central Europe. *Palaeogeography, Palaeoclimatology, Palaeoecology*, 472: 1-14.
- Royer, D.L., 2001. Stomatal density and stomatal index as indicators of paleoatmospheric CO<sub>2</sub> concentration. *Review of Palaeobotany and Palynology*, 114(1): 1-28.
- Royer, D.L., 2012. Climate reconstruction from leaf size and shape: new developments and challenges. In: Ivany, L. C. and Huber, B. T. (Editor), *Reconstructing Earth's Deep-Time Climate - The State of the Art in 2012*. The Palaeontological Society Papers, pp. 195-212.
- Royer, D.L., Wing, S.L., Beerling, D.J., Jolley, D.W., Koch, P.L., Hickey, L.J. and Berner, R.A., 2001. Paleobotanical Evidence for Near present-Day Levels of Atmospheric CO<sub>2</sub> During Part of the Tertiary. *Science*, 292(5525): 2310-2313.
- Royer, D.L., Wilf, P., Janesko, D.A., Kowalski, E.A. and Dilcher, D.L., 2005. Correlations of climate and plant ecology to leaf size and shape: potential proxies for the fossil record. *American Journal of Botany*, 92(7): 1141-1151.
- Royer, D.L., Sack, L., Wilf, P., Lusk, C.H., Jordan, G.J., Niinemets, Ü., Wright, I.J., Westoby, M., Carglino, B., Coley, P.D., Cutter, A.D., Johnson, K.R., Labandeira, C.C., Moles, A.T., Palmer, M.B. and Valladares, F., 2007. Fossil leaf economics quantified: calibration, Eocene case study, and implications. *Palaeobiology*, 33(4): 574-589.
- Rüffle, L. and Jähnichen, H., 1976. Die Myrtaceen im Geiseltal und einigen anderen Fundstellen des Eozäns. In: M. Barthel (Editor), *Eozäne Floren des Geiseltales*. Abhandlungen des Zentralen Geologischen Instituts, Berlin, pp. 308-335.
- Rüffle, L. and Litke, R., 2000. Ergänzungen zur Eozän-Flora des Geiseltales, Deutschland, und einiger weiterer Eozän-Fundstätten. *Feddes Repertorium*, 111(7-8): 449-463.
- Rupp, R. and Ćorić, S., 2012. Zur Ebelsberg-Formation. *Jahrbuch der Geologischen Bundesanstalt*, 152: 67-100.
- Sack, L. and Scoffoni, C., 2013. Leaf venation: structure, function, development, evolution, ecology and applications in the past, present and future. *New Phytologist*, 198: 983-1000.

- Spicer, R.A., 1981. The Sorting and Deposition of Allochthonous Plant Material in a Modern Environment at Silwood Lake, Silwood Park, Berkshire, England. Geological Survey Professional Papers, 1143: 1-77.
- Spicer, R.A., 2009. CLAMP: Climate Leaf Analysis Multivariate Program. The Open University, <http://clamp.ibcas.ac.cn>.
- Spicer, R.A., Bera, S., Bera, S.D., Spicer, T.E.V., Srivastava, G., Mehrotra, R., Mehrotra, N. and Yang, J., 2011. Why do foliar physiognomic climate estimates sometimes differ from those observed? Insights from taphonomic information loss and a CLAMP case study from the Ganges Delta. *Palaeogeography, Palaeoclimatology, Palaeoecology*, 302: 381-395.
- Standke, G., 2008. Paläogeografie des älteren Tertiärs (Paleozän bis Untermiozän) im mitteldeutschen Raum. *Zeitschrift der deutschen Gesellschaft für Geowissenschaften*, 159(1): 81-103.
- Standke, G., Escher, D., Fischer, J. and Rascher, J., 2010. Das Tertiär Nordwestsachsens - Ein geologischer Überblick. Sächsisches Landesamt für Umwelt, Landwirtschaft und Geologie, Freiberg, 1-157 pp.
- Steinthorsdottir, M., Porter, A.S., Holohan, A., Kunzmann, L., Collinson, M. and McElwain, J.C., 2016. Fossil plant stomata indicate decreasing atmospheric CO<sub>2</sub> prior to the Eocene-Oligocene boundary. *Climate of the Past*, 12(2): 439-454.
- Sturm, M., 1971. Die eozäne Flora von Messel bei Darmstadt. I Lauraceae. *Palaeontographica Abteilung B*, 134(1): 1-60.
- Su, T., Xing, Y.-W., Liu, Y.-S., Jacques, F.M.B., Chen, W.-Y., Huang, Y.-J. and Zhou, Z.-K., 2010. Leaf Margin Analysis: A new equation from humid to mesic forests in China. *Palaios*, 25: 234-238.
- Suhr, P., 2003. The Bohemian Massif as a catchment area for the NW European Tertiary Basin. *Geolines*, 15: 147-159.
- Suhr, P. and Goth, K., 2008. Tertiäre Maare. In: W. Pälchen and H. Walter (Editors), *Geologie von Sachsen*. Schweizerbarth, Stuttgart, pp. 484-486.
- Taylor, T.N., Taylor, E.L. and Krings, M., 2009. *Paleobotany - The Biology and Evolution of Fossil Plants*. Academic Press, 1-1230 pp.
- Teodoridis, V., Kvaček, Z. and Uhl, D., 2009. Late Neogene palaeoenvironment and correlation of the Sessenheim-Auenheim floristic complex (Alsace/France). *Palaeodiversity*, 2: 1-17.

- Teodoridis, V., Mazouch, P., Spicer, R.A. and Uhl, D., 2011. Refining CLAMP – Investigations towards improving the Climate Leaf Analysis Multivariate Program. *Palaeogeography, Palaeoclimatology, Palaeoecology*, 299: 39-48.
- Teodoridis, V., Kvaček, Z., Zhu, H. and Mazouch, P., 2012. Vegetational and environmental analysis of the mid-litudinal European Eocene sites and their possible analogues in Southeastern Asia. *Palaeogeography, Palaeoclimatology, Palaeoecology*, 333: 40-58.
- Teodoridis, V. and Kvaček, Z., 2015. Palaeoenvironmental evaluation of Cainozoic plant assemblages from the Bohemian Massif (Czech Republic) and adjacent Germany. *Bulletin of Geosciences*, 90(3): 695-720.
- Traiser, C., Klotz, S., Uhl, D. and Mosbrugger, V., 2005. Environmental signals from leaves - a physiognomic analysis of European vegetation. *New Phytologist*, 166: 465-484.
- Traiser, C., Roth-Nebelsick, A., Lange, J. and Eder, J., 2015. MORPHYLL - database for acquisition of ecophysiologically relevant morphometric data of fossil leaves. Version 1.0, <http://www.morphyll.naturkundemuseum-bw.de>.
- Traiser, C., Roth-Nebelsick, A., Grein, M., Kovar-Eder, J., Kunzmann, L., Moraweck, K., Lange, J., Kvaček, J., Neinhuis, C., Folie, A., Franceschi, D.D., Kroh, A., Mohr, B., Prestianni, C., Poschmann, M. and Wuttke, M., in review. MORPHYLL - a database of fossil leaves and their morphological traits. *Palaeontologia Electronica*.
- Uhl, D., 2006. Fossil plants as palaeoenvironmental proxies - some remarks on selected approaches. *Acta Palaeobotanica*, 46(2): 87-100.
- Uhl, D., 2014. Variability of selected leaf traits in European beech (*Fagus sylvatica*) in relation to climatic factors - some implications for palaeoenvironmental studies. *Phytologica Balcanica*, 20(2-3): 145-153.
- Uhl, D., Mosbrugger, V., Bruch, A. and Utescher, T., 2003. Reconstructing palaeotemperatures using leaf floras – case studies for a comparison of leaf margin analysis and the coexistence approach. *Review of Palaeobotany and Palynology*, 126: 49-64.
- Uhl, D., Klotz, S., Traiser, C., Thiel, C., Utescher, T., Kowalski, E. and Dilcher, D.L., 2007. Cenozoic paleotemperatures and leaf physiognomy - A European perspective. *Palaeogeography, Palaeoclimatology, Palaeoecology*, 248: 24-31.
- Utescher, T., Bruch, A., Erdai, B., François, L., Ivanov, D., Jacques, F.M.B., Kern, A.K., Liu, Y.-S.C., Mosbrugger, V. and Spicer, R.A., 2014. The Coexistence Approach – Theoretical

- background and practical considerations of using plant fossils for climate quantification. *Palaeogeography, Palaeoclimatology, Palaeoecology*, 410: 58-73.
- Utescher, T., Bondarenko, O.V. and Mosbrugger, V., 2015. The Cenozoic Cooling - continental signals from the Atlantic and Pacific side of Eurasia. *Earth and Planetary Science Letters*, 415: 121-133.
- Vassio, E. and Martinetto, E., 2012. Biases in the frequency of fruits and seeds in modern fluvial sediments in northwestern Italy: The key to interpreting analogous fossil assemblages. *Palaios*: 779-797.
- Walter, R., 2014. *Erdgeschichte. Die Geschichte der Kontinente, der Ozeane und des Lebens*, 5. Schweizerbart, Stuttgart, 1-383 pp.
- Walther, H., 1976. Strukturbietende Blattreste aus dem Tertiär des Weißelster-Beckens. *Abhandlungen Staatliches Museum für Mineralogie und Geologie Dresden*, 25: 65-111.
- Walther, H., 1999. Die Tertiärflora von Kleinsaubernitz bei Bautzen. *Palaeontographica Abteilung B*, 249: 1-169.
- Walther, H. and Kvaček, Z., 2007. Seifhennersdorf: A window on early Oligocene volcanic ecosystems. *Acta Musei Nationalis Pragae Series B – Historia Naturalis*, 63(2-4): 69-215.
- Westoby, M., Falster, D.S., Moles, A.T., Vesk, P.A. and Wright, I.J., 2002. Plant ecological strategies: some leading dimensions of variation between species. *Annual Review of Ecology and Systematics*, 33(1): 125-159.
- Wilde, V., 1989. *Untersuchungen zur Systematik der Blattreste aus dem Mitteleozän der Grube Messel bei Darmstadt (Hessen, Bundesrepublik Deutschland)*. Courier Forschungsinstitut Senckenberg, 115: 1-213.
- Wilde, V., 2004. Aktuelle Übersicht zur Flora aus dem mitteleozänen "Ölschiefer" der Grube Messel bei Darmstadt (Hessen, Deutschland). *Courier Forschungsinstitut Senckenberg*, 252: 109-114.
- Wilf, P., 1997. When are leaves food thermometers? A new case study for Leaf Margin Analysis. *Paleobiology*, 23: 373-390.
- Wilf, P., Wing, S.L., Greenwood, D.R. and Greenwood, C.L., 1998. Using fossil leaves as paleoprecipitation indicators: An Eocene example. *Geology*, 26: 203-206.

- Wing, S.L. and Greenwood, D.R., 1993. Fossils and fossil climate: the case for equable continental interiors in the Eocene. *Royal Society of London Philosophical Transactions, series B*, 341: 243-252.
- Wolfe, J.A., 1979. Temperature parameters of humid to mesic forests of eastern Asia and their relation to forests of other areas of the Northern Hemisphere and Australasia. *Geological Professional Paper*, 1106(1-37).
- Wolfe, J.A., 1993. A method of obtaining climatic parameters from leaf assemblages. US Government Printing Office, 2040-2041: 1-70.
- Wolfe, J.A. and Spicer, R.A., 1999. Fossil leaf character states: multivariate analysis. In: T.P. Jones and N.P. Rowe (Editors), *Fossil plants and spores: modern techniques*. Geological Society of London, London, pp. 233-239.
- Woodward, F.I., 1987. Stomatal numbers are sensitive to increase in CO<sub>2</sub> concentration from pre-industrial levels. *Nature*, 327: 617-618.
- Woodward, F.I. and Bazzaz, F.A., 1988. The Response of Stomatal Density to CO<sub>2</sub> Partial Pressure. *Journal of Experimental Botany*, 39(209): 1771-1781.
- Wright, I.J., Reich, P.B., Westoby, M., Ackerly, D.D., Baruch, Z., Bongers, F., Cavender-Bares, J., Chapin, T., Cornelissen, J.H.C., Diemer, M., Flexas, J., Garnier, E., Groom, P.K., Gulias, J., Hikosaka, K., Lamont, B.B., Lee, T., Lee, W., Lusk, C., Midgley, J.J., Navas, M.-L., Niinemets, Ü., Oleksyn, J., Osada, N., Poorter, H., Poot, P., Prior, L., Pyankov, V.I., Roumet, C., Thomas, S.C., Tjoelker, M.G., Veneklaas, E.J. and Villar, R., 2004. The worldwide leaf economics spectrum. *Nature*, 428(6985): 821-827.
- Yang, J., Spicer, R.A., Spicer, T.E.V. and Li, C.-S., 2011. 'CLAMP Online': a new web-based palaeoclimate tool and its application to the terrestrial Paleogene and Neogene of North America. *Palaeobiodiversity and Palaeoenvironments*, 91(3): 163-183.
- Zachos, J., Pagani, M., Sloan, L., Thomas, E. and Billups, K., 2001. Trends, Rhythms, and Aberrations in Global Climate 65 Ma to Present. *Science*, 292(5517): 686-693.
- Zachos, J.C., Dickens, G.R. and Zeebe, R.E., 2008. An early Cenozoic perspective on greenhouse warming and carbon-cycle dynamics. *Nature*, 451(17): 279-283.
- Zhang, Y.G., Pagani, M., Liu, Z., Bohaty, S.M. and DeConto, R., 2013. A 40-million year history of atmospheric CO<sub>2</sub>. *Philosophical Transactions of the Royal Society A*, 371(2001): 1-20.

## Publications and presentations

### Publications (both submitted and printed)

Traiser, C., Roth-Nebelsick, A., Grein, M., Kovar-Eder, J., Kunzmann, L., **Moraweck, K.**, Lange, J., Kvaček, J., Neinhuis, C., Folie, A., Franceschi, D.D., Kroh, A., Mohr, B., Prestianni, C., Poschmann, M. and Wuttke, M., in review. MORPHYLL - a database of fossil leaves and their morphological traits. *Palaeontologia Electronica*.

**Moraweck, K.**, Grein, M., Konrad, W., Kovar-Eder, J., Kvaček, J., Neinhuis, C., Roth-Nebelsick, A., Stiller, S., Streubig, M., Traiser, C., Utescher, T., Kunzmann, L., in review. Leaf traits of extinct *Platanus neptuni* (Platanaceae): indicators for palaeoenvironment and reliable palaeoclimatic and palaeoatmospheric proxies? *Review of Palaeobotany and Palynology*.

Roth-Nebelsick, A., Grein, M., Traiser, C., **Moraweck, K.**, Kunzman, L., Kovar-Eder, J., Kvaček, J., Stiller, S., Neinhuis, C., 2017. Functional leaf traits and leaf economics in the Paleogene - A case study for Central Europe. *Palaeogeography, Palaeoclimatology, Palaeoecology* 472:1-14.

Kunzmann, L., Kvaček, Z., Teodoridis, V., Müller, C., **Moraweck, K.**, 2016. Events between the Mid-Eocene Climatic Optimum and the Eocene-Oligocene Transition as reflected in vegetation dynamics of riparian forest in central Europe during late Eocene. – *Palaeontographica* 295(1-3): 69-89.

**Moraweck, K.**, Uhl, D., Kunzmann, L., 2015. Estimation of late Eocene (Bartonian-Priabonian) terrestrial palaeoclimate: contributions from megafloral assemblages from central Germany. – *Palaeogeography, Palaeoclimatology, Palaeoecology* 433: 247–258.

---

**Conference Abstracts (published / unpublished; only own contributions)**

**Moraweck, K.**, Jurke, B., Schneider, J. W., Kunzmann, L. (2016): Methods to detect adaptation strategies of fossil leaves to paleoclimatic and paleoenvironmental changes traced on cuticles. – 25<sup>th</sup> International Workshop on Plant Taphonomy, Bonn, 25.-26.11.2016.

**Moraweck, K.**, Grein, M., Konrad, W., Kovar-Eder, J., Kunzmann, L., Kvacek, J., Neinhuis, Ch., Roth-Nebelsick, A., Stiller, S., Streubig, M., Traiser, Ch. (2016): Adaptations of fossil leaves to paleoclimatic and paleoenvironmental change during the Paleogene. – XIV. International Palynological Congress / X. International Organisation of Palaeobotany Conference, Salvador de Bahía, Brasilien, 23.-28.10.2016

**Moraweck, K.**, Grein, M., Konrad, W., Kovar-Eder, J., Kunzmann, L., Kvacek, J., Neinhuis, Ch., Roth-Nebelsick, A., Stiller, S., Streubig, M., Traiser, Ch. (2016): Adaptations of fossil leaves to paleoclimatic and paleoenvironmental change during the Paleogene. – 87. Jahrestagung der Paläontologischen Gesellschaft, Dresden, Germany, 11.-16.09.2016.

**Moraweck, K.**, Grein, M., Konrad, W., Kovar-Eder, J., Kvaček, J., Kunzmann, L., Neinhuis, C., Roth-Nebelsick, A., Stiller, S., Streubig, M., Traiser, C. (2015): Connecting micro- and macromorphology: problems and possibilities. – 24<sup>th</sup> International Workshop on Plant Taphonomy, Stuttgart, 26.-27.11.2015.

**Moraweck, K.**, Grein, M., Konrad, W., Kovar-Eder, J., Kunzmann, L., Kvaček, J., Roth-Nebelsick, A., Neinhuis, Ch., Stiller, S., Streubig, M., Traiser, Ch. (2015): Quantitative approach to detect adaptations of fossil leaves to paleoenvironmental change. – Sino-German meeting “The Yunnan Biodiversity Hotspot – Its history and future threats, Kunming, VR China, 05.-09.08.2015.

**Moraweck, K.** & Kunzmann, L. (2014): Palaeoclimate reconstruction within the Palaeogene using fossil plants. – *Geologica saxonica* 60 (2): 305–306.

**Moraweck, K.**, Grein, M., Konrad, W., Kovar-Eder, J., Kunzmann, L., Kvaček, J., Neinhuis, C., Roth-Nebelsick, A., Streubig, M., Traiser, C. (2014): How does leaf morphology reflect

palaeoclimate conditions? A quantitative approach tracing terrestrial climate conditions during the Palaeogene. – Rend. Online Soc. Geol. It. 31: 153–154.

**Moraweck, K.**, Grein, M., Konrad, W., Kovar-Eder, J., Kunzmann, L., Kvaček, J., Neinhuis, C., Roth-Nebelsick, A., Streubig, M., Traiser, C. (2014): How does leaf morphology reflect palaeoclimate conditions? A quantitative approach tracing terrestrial climate conditions during the Palaeogene. – IX. European Palaeobotanical Palynological Conference 2014, Padua, Italien.

**Moraweck, K.**, Kunzmann, L., Uhl, D. (2014): Tracing palaeoclimate conditions by fossil leaves - A quantitative approach using leaf morphology. – SDGG 85.

**Moraweck, K.** & Kunzmann, L. (2014): Plants as palaeoclimate proxies – Glimpses behind the scene. – 23. International Workshop on Plant Taphonomy, Berlin, Deutschland.

**Moraweck, K.**, Kunzmann, L., Uhl, D., Kleber, A. (2013): Palaeoclimate reconstruction within the Eocene in central Germany using fossil plants. – EGU [European Geoscience Union], Wien, Österreich.



## Eigenständigkeitserklärung

Hiermit versichere ich, dass ich die vorliegende Arbeit selbstständig und ohne Benutzung anderer als der angegebenen Hilfsmittel angefertigt habe; die aus fremden Quellen direkt oder indirekt übernommenen Gedanken sind als solche kenntlich gemacht. Die Arbeit ist bisher weder im Inland noch im Ausland in gleicher oder ähnlicher Form einer anderen Prüfungsbehörde vorgelegt. Die Bestimmungen der Promotionsordnung sind mir bekannt.

Radebeul, 17.02. 2017

Karolin Moraweck